

Development of novel toxin-like drugs that target malaria parasite motility

Swapna Johnson
M.Sc. (Hons)

*A thesis submitted in total fulfilment
of the requirements for the degree of*

Doctor of Philosophy
in
Chemistry

by creative work



LA TROBE UNIVERSITY
AUSTRALIA

School of Molecular Science
College of Science, Health and Engineering
La Trobe University
Victoria, 3086
Australia

February 2016

Table of Contents

Table of Contents	i
Abbreviations	vi
Acknowledgements	x
Abstract	xii
Statement of Authorship	xiii
Conference Presentations	xiv
Chapter 1: Introduction	1
1.1 Malaria	1
1.2 Treatment methods and their challenges	2
1.3 Challenges to current treatment methods	4
1.4 Novel anti-malarials from natural products.....	5
1.5 Actin	7
1.5.1 Difference between human and <i>Plasmodium</i> actin	9
1.5.2 Actin-dependent gliding.....	11
1.5.3 Actin binding in malaria	13
1.5.4 Apicomplexan actin regulators	13
1.6 Actin binding compounds	16
1.6.1 Compounds that prevent filament formation	16
1.6.1.1 ATP binding cleft-targeting compounds	17
1.6.1.2 Barbed end targeting compounds.....	19
1.6.1.3 Mechanism	25
1.6.2 Filament Stabilising Compounds	25
1.6.2.1 Mechanism	29
1.7 Thesis overview and aims	29

1.8 References	31
Chapter 2: Molecular modelling studies on actin inhibition.....	35
2.1 Molecular modelling	35
2.2 Homology modelling.....	35
2.3 Molecular dynamics	36
2.4 Results and discussion.....	36
2.4.1 Comparison of the binding sites of the human and the <i>Plasmodium</i> actin	38
2.5 Conclusion.....	40
2.6 References	41
Chapter 3: Efforts towards the total synthesis of latrunculin derivatives	42
3.1 Introduction	42
3.2 Results and Discussion.....	46
3.2.1 Synthesis of Fragment 1.....	47
3.2.2 Synthesis of Fragment 2.....	53
3.2.3 Synthesis of Fragment 3.....	57
3.2.3.1 Synthesis of 5-bromopent-2-yne	58
3.2.3.2 Synthesis of pent-3-yn-1-ylmagnesium bromide (3.047)	60
3.2.4 Coupling of the Fragments.....	62
3.2.5 The S _N 2 approach.....	68
3.2.5.1 Triflate formation.....	68
3.2.5.2 Mesylate formation	69
3.2.5.3 Tosylate formation	71
3.2.5.4 Mitsunobu reactions.....	71
3.2.6 Esterification	74
3.2.6.1 Activated ester.....	74
3.2.6.2 Acid halide method	76
3.2.7 Synthesis of saturated latrunculin derivative (3.096) via saturated acid (3.095)	81
3.2.7.1 EDCI Coupling	83

3.2.7.2 Alkyne Metathesis.....	84
3.2.8 Synthesis of aromatic latrunculin derivative (3.113) via aromatic acid (3.111)	89
3.2.8.1 Synthesis of aromatic acid (3.111).....	90
3.2.8.1.1 Grignard method	90
3.2.8.1.2 Negishi Coupling	97
3.2.8.1.3 Lithium-halogen exchange.....	99
3.2.8.1.4 Boronic acid method	100
3.3 Conclusion.....	101
3.4 References	103
Chapter 4: Truncated latrunculin analogues	107
4.1 Introduction	107
4.2 Synthesis of the new core.....	109
4.2.1 Method A	110
4.2.1.1 Synthesis of the building blocks (3.007 and 4.002)	110
4.2.1.2 Aldolisation and ring closure	113
4.2.2 Method B -Alternative synthesis of the core.....	121
4.2.2.1 Synthesis of the building blocks (4.011 and 4.012)	121
4.2.2.2 Alkene metathesis	124
4.3 Synthesis of truncated analogues of latrunculin.....	127
4.3.1 R ¹ Modifications	128
4.3.1.1 R ¹ Modifications with Ester linkage	128
4.3.1.1.1 Fatty acid derivatives	129
4.3.1.1.2 Heteroaromatic acid derivatives.....	130
4.3.1.1.3 Benzoate derivatives	130
4.3.1.2 Ketone based R ¹ modification.....	137
4.3.1.2.1 Hydrazone derivatives.....	146
4.3.1.2.2 Amine derivatives	151
4.4 Biological studies of the R ¹ modified analogues	153
4.4.1 <i>P. falciparum</i> growth inhibition assay	153

4.4.2 SAR interpretation of the synthesised truncated latrunculin analogues.....	153
4.4.3 Studies on <i>Toxoplasma gondii</i>	157
4.4.4 Pyrene Fluorescence assays	161
4.4.5 Cytotoxicity Assay	162
4.5 Conclusion.....	164
4.6 References	165
Chapter 5: Further exploration of the truncated latrunculin analogues.	167
5.1 Introduction	167
5.2 Piperidine derivatives	167
5.3 Expansion of the THP ring.....	172
5.4 R ² Modification	173
5.5 R ³ modifications	179
5.5.1 Deprotection of PMB group.....	185
5.6 R ⁴ Modification	187
5.7 Aromatic analogues.....	194
5.8 SAR interpretation of the synthesised truncated latrunculin analogues.....	197
5.8.1 SAR for R ² modified analogues and analysis of the results observed	197
5.8.2 SAR for R ³ modified analogues and analysis of the results observed	199
5.8.3 SAR for R ⁴ modified analogues and analysis of the results observed	200
5.9 SAR for the aromatic analogues and analysis of the results observed.....	201
5.10 Computational studies to understand the SAR.....	202
5.11 Conclusion.....	205
5.12 References	206
Chapter 6. Conclusion and Future directions.....	207
6.1 Conclusion.....	207
6.2 Future work	208
Chapter 7. Experimental	211
7.1 General experimental	211

7.2 General procedures	212
7.3 Chapter 3 compounds	215
7.4 Chapter 4 compounds	228
7.5 Chapter 5 compounds	249
7.6 References	276

Abbreviations

°C	degrees centigrade
3D	3-dimensional
Å	Angstrom
ACT	Artemisinin Combination Therapy
ADP	adenosine diphosphate
aq.	aqueous
Arg	arginine
Asn	asparagine
Asp	aspartic acid
ATP	adenosine triphosphate
BAIB	(diacetoxyiodo)benzene
BEMP	<i>tert</i> -butyliminotris(pyrrolidino)phosphorane
Boc	<i>tert</i> -butoxycarbonyl
CAN	cerium ammonium nitrate
CAP	cyclase-associated protein
cat.	catalytic
CC ₅₀	half-maximal cytotoxic concentration
CSA	(±) camphorsulfonic acid
DBU	1,8-diazabicycloundec-7-ene
DCC	1,3-dicyclohexylcarbodiimide
DCE	dichloroethane
DCM	dichloromethane
DDQ	2,3-dichloro-5,6-dicyano-1,4-benzoquinone

DEAD	diethyl azodicarboxylate
DIAD	diisopropyl azodicarboxylate
DIPEA	<i>N,N</i> -diisopropylethylamine
DMAP	4-(dimethylamino)pyridine
DMB	3,4-dimethoxybenzyl
DMEM	Dulbecco's Modified Eagle Medium
DMP	Dess–Martin periodinane
DMPU	1,3-dimethyl-3,4,5,6-tetrahydro-2-pyrimidinone
DMSO	dimethyl sulfoxide
EC ₅₀	effector concentration for half-maximum response
EDCI	1-ethyl-3-(3-dimethylaminopropyl) carbodiimide
EGTA	ethylene glycol tetraacetic acid
eq.	equivalents
FACS	Fluorescence Activated Cell Sorting
FBS	Fetal Bovine Serum
GIA	<i>P.falciparum</i> growth inhibition assay
Glu	glutamic acid
h	hour
HEK293	human embryonic kidney 293
HepG2	hepatocellular carcinoma cells
HFF	Human Foreskin Fibroblasts
Hoveyda-Grubbs' II	Hoveyda-Grubb's Catalyst 2 nd Generation
HPLC	High Performance Liquid Chromatography
HRMS	High Resolution Mass Spectrometry
HTPBS	Human Tonicity Phosphate-Buffered Saline
IBX	2-iodobenzoic acid

Ile	isoleucine
<i>J</i>	coupling constant
KHMDS	potassium bis(trimethylsilyl)amide
KSCN	potassium thiocyanate
LCMS	Liquid Chromatography-Mass Spectrometry
LiHMDS	lithium hexamethyldisilazide
Lys	lysine
M	molarity
Met	methionine
MF	microfilament
mg	milligram
min	minutes
NMP	<i>N</i> -methyl-2-pyrrolidone
NMR	Nuclear Magnetic Resonance
PBS	Phosphate Buffered Saline
Pd(dppf)Cl ₂	[1,1'-bis(diphenylphosphino)ferrocene]dichloropalladium(II)
<i>Pf</i>	<i>Plasmodium falciparum</i>
PMB	paramethoxybenzyl
Pro	proline
RBC	red blood cells
room temp.	room temperature
rt	retention time
SAR	Structure Activity Relationship
SIBX	stabilized 2-iodobenzoic acid
TBAB	tetrabutylammonium bromide
TBAF	tetrabutylammonium fluoride

TBS	<i>tert</i> -butyldimethylsilyl
TBSCl	<i>tert</i> -butyldimethylsilyl chloride
TBTU	<i>O</i> -(benzotriazol-1-yl)- <i>N,N,N',N'</i> -tetramethyluronium tetrafluoroborate
TEMPO	(2,2,6,6-tetramethylpiperidin-1-yl)oxidanyl
<i>tert</i> -	tertiary
TFA	tetrafluoroacetic acid
TFFH	tetramethylfluoroformamidinium hexafluorophosphate
THF	tetrahydrofuran
THP	tetrahydropyran
Thr	threonine
TLC	thin layer chromatography
Tyr	tyrosine
WHO	World Health Organization

Acknowledgements

PhD is a stretch of faith, and everyone who has known me closely these 4 years would realise that where I stand now is no less than a miracle. This journey has challenged and strengthened my faith in Jesus – May all glory be to him.

I would like to thank my supervisors Prof. Brian Smith, Prof. Jonathan Baell and Dr. Seb Marcuccio who have mentored me throughout these four years.

To Brian for giving me the opportunity to do a PhD under his guidance. For having faith in me and giving me every possible support and guidance. To Jonathan for his constant encouragement, understanding and support throughout my PhD. Thank you also for being so approachable, sympathetic and funny, which made this journey less daunting. To Seb for his advice and insights to this project whenever possible.

To Dr. Jake Baum for envisaging this project and for his positive outlook even when things did not work out as expected. I would also like to thank his team for running the pyrene fluorescence assays. To Dr. David Wilson for chairing my panel meeting.

To my ‘colleague’ Dr. Raphaël Rahmani who has taught me almost everything I know in organic synthesis. I cannot thank you enough for your guidance and advice on this project, but more so for your patience, time, encouragement and good will for me. You have been way more than a colleague to me - thank you.

Thanks to all the collaborators who have contributed towards this project. To Dr. James Beeson and Dr. Damien Drew (Burnet Institute) for running the GIA assays, to Dr. Chris Tonkin and Melanie Williams (WEHI, Melbourne) for running the assays on *Toxoplasmodium* parasites. To Dr. Johnny Huang (University of Queensland) for running the cytotoxicity assays. To Dr. Robert Gable (Melbourne University) for his X-ray crystallographic work.

To Dr. Jason Dang for the technical guidance. To Dr. Jason Dutton for arranging the glove-box.

I would like to thank all the Baell lab members both past present for making these four years such a memorable experience. Noel Pitcher (Noleee), Sunil Banga, Lisa Barbaro (sparkly), Andrew Tang (See-va 2), Mathilda Mesnard, Camille Lallemand, Natacha Traffet, Tamir Dingjan, Julia Beveridge, Thuy Le, Jephthah Odiba, Alfred Wong, Dr. Nghi Nguyen (Jonny), Dr. Silvia Teguh (See-va), Dr. Ryan Brady (Brandy), Dr. Jitendra Harjani (Jitu), Dr. David Leaver, Dr. Daniel Priebbenow, Dr. Yuezhou Zhang, Dr. Da-Hua Shi, Dr. Aaron DeBono (Skinny boy) and Kung Ban.

Each of you have helped, loved and supported me in your own ways for which I am sincerely grateful.

To Lori Ferrins (lolly) and Ben Cleary (custard boy) who started the journey of PhD with me. Lori, your friendship has been one of the best things that has happened to me, in the past 4 years. Thank you for putting up with my craziness and my all year Christmas carols, and mostly thank you for being there for me 'whenever' I needed you. Ben, thanks for being such a dependable, helpful and supporting person. It was a pleasure to work with you and I am glad we made it without the west gate.

To all my friends at La Trobe University, especially the Smith lab members and my friend Isabella Lobo, who made me feel welcome every time I worked there. To Dr. Phil Bergen and Dr. Martina Kocan for their encouragement and support.

To all my friends who add so much colour to my life by their love and presence.

To my dad - my pillar of strength, whose dream is this PhD. To my mum - my constant inspiration. I thank you both for all the sacrifices you have made, to enable me to reach this far.

To my husband, Johnson who taught me to aim high, be ambitious and reach my potential. Thank you for your constant love, encouragement, understanding and sacrifices throughout this time. To my son, Kevin who endured the biggest sacrifice of my time without complaining. Your smile is what kept me going. I love you.

Abstract

Malaria is one of the most significant infectious diseases affecting the human population. It is caused by *Plasmodium* parasites and is transmitted by mosquitos. In spite of existing drugs, malaria remains unconquered due to the growing resistance of the parasite. The World Health Organisation (WHO) reported 214 million cases of malaria in 2015.

Actin is an abundant protein found in eukaryotic cells that can reversibly polymerize between monomeric and filamentous states. Malarial parasites employ actin dynamics to invade host cells known as ‘gliding motility’. Thus, if actin dynamics are disrupted, the parasites can no longer glide and cause disease, making actin inhibitors of great interest as potential therapeutics to combat malaria.

Many natural products belonging to the macrolide family, such as the latrunculins, are known to bind to actin thereby disrupting its function. Computational analysis revealed that sequence similarity between malarial actin and human actin is high enough to render homology modelling meaningful, but low enough to allow for selectivity.

In the first part of this thesis, we look at the efforts towards the synthesis of latrunculin analogues and the numerous challenges involved in the synthesis of such complex natural products. The latter part of this thesis describes the design and synthesis of a library of truncated latrunculin analogues by retaining the key pharmacophores. Biological studies led to the identification of lead compounds with low micromolar activity against *Plasmodium* and *Toxoplasma* parasites, and which were significantly less toxic towards mammalian cells.

Although a parasite actin binding assay was not able to be accessed, computational studies on one of the most potent truncated latrunculin analogues, led to a model where Structure-Activity Relationships were able to be logically accounted for. This was used as further evidence that the antiparasitic activity of the compounds reported herein was plausibly linked to binding to parasite actin. It is anticipated that this work could pave way to the development of more potent and selective actin inhibitors for malaria.

Statement of Authorship

"Except where reference is made in the text of the thesis, this thesis contains no material published elsewhere or extracted in whole or in part from a thesis submitted for the award of any other degree or diploma. No other person's work has been used without due acknowledgment in the main text of the thesis. This thesis has not been submitted for the award of any degree or diploma in any other tertiary institution."

Swapna Johnson

February 2016

Conference Presentations

- 40th Annual Synthesis Symposium, Bio21, University of Melbourne, December 2015- Oral Presentation.
- RACI Medicinal Chemistry and Chemical Biology One Day Symposium, Monash University, September 2015- Poster Presentation.
- Frontiers meeting in Medicinal Chemistry (FMC 2015), Antwerp, Belgium, 14-16 September, 2015 - Poster Presentation.
- EFMC-YMCS 2015, Antwerp, Belgium, 17 September, 2015 - Poster Presentation.
- RACI National Congress, Adelaide, Dec 2014 - Oral Presentation.
- 38th Annual synthesis symposium, Bio21, University of Melbourne, December 2013 – Poster Presentation.
- 8th Annual postgraduate research symposium, Monash University, November 2013 – Poster Presentation.
- CTx Symposium, Monash University, October 2013 – Poster presentation.
- 37th Annual synthesis symposium, Bio21, University of Melbourne, December 2012 – Poster Presentation.
- Fragment Based Drug Discovery Symposium, Monash University, November 2012 – Poster Presentation.
- 7th Annual postgraduate research symposium, Monash University, September 2012 – Poster Presentation.

Chapter 1: Introduction

1.1 Malaria

Malaria is one of the most significant infectious diseases affecting human populations, it is caused by *Plasmodium* parasites and is transmitted by female *Anopheles* mosquitoes [1-4]. The World Health Organisation (WHO) reported 214 million cases of malaria in 2015 [5]. Although a number of drugs are available which can effectively treat malaria, the growing resistance of the parasites to these existing drugs is the global burden [6]. Also, our knowledge of the parasite biology at the molecular level is restricted by the complexity of the parasite life cycle [1].

Malaria is caused by unicellular obligate intracellular protozoan parasites belonging to the genus *Plasmodium* - a member of phylum apicomplexa which include the etiological agents of several important diseases of both humans and animals [7]. This includes toxoplasmosis [4], cryptosporidiosis [8] and theileriosis, which inflicts huge economic losses to cattle herders in the tropics [9]. The 5 species of the *Plasmodium* parasites known to cause infection in humans are *Plasmodium falciparum*, *Plasmodium vivax*, *Plasmodium ovale*, *Plasmodium malariae* and *Plasmodium knowlesi* of which *Plasmodium falciparum* is known to be the most lethal species [10].

The life cycle of the malaria parasite is quite complex as illustrated in **Figure 1.01**. It can be seen that the lifecycle of the parasite can be broken down into four stages, namely the liver stage, the blood or erythrocyte stage, the transmission stage and the mosquito stage [10]. The mosquito transfers the parasite at the sporozoite stage to the mammal during a blood meal. The sporozoite, carried by the blood stream, infects liver hepatocytes where they transform into schizonts, which are multi-nucleated infected cells containing tens of thousands of daughter cells (the liver stage) [11]. After parasite's growth and multiplication, the infected hepatocytes ruptures, releasing the daughter merozoites. Each merozoite then invades a red blood cell (RBC) and continues development through multiple rounds of erythrocyte infection (the blood stage). At the end of a ~ 48 h developmental cycle, each infected RBC ruptures, releasing 20 or more merozoites, each of which initiates a new erythrocytic cycle. Some of these merozoites switch from their developmental pathway to become sexual stages known as the gametocytes. Ingestion of a blood meal containing gametocytes by a mosquito (transmission stage) liberates the sexual stages from the RBCs, which fertilize to form a diploid zygote inside the mosquito. The zygote then rapidly transforms into a motile ookinete which penetrates the midgut epithelium and transforms into an oocyst which

generates 5,000-10,000 haploid sporozoites in 5-15 days. These sporozoites get liberated into the body cavity of mosquito (the mosquito stage). The sporozoites are then carried to the salivary gland by hemolymph where they await transmission via the next mosquito blood meal [1].

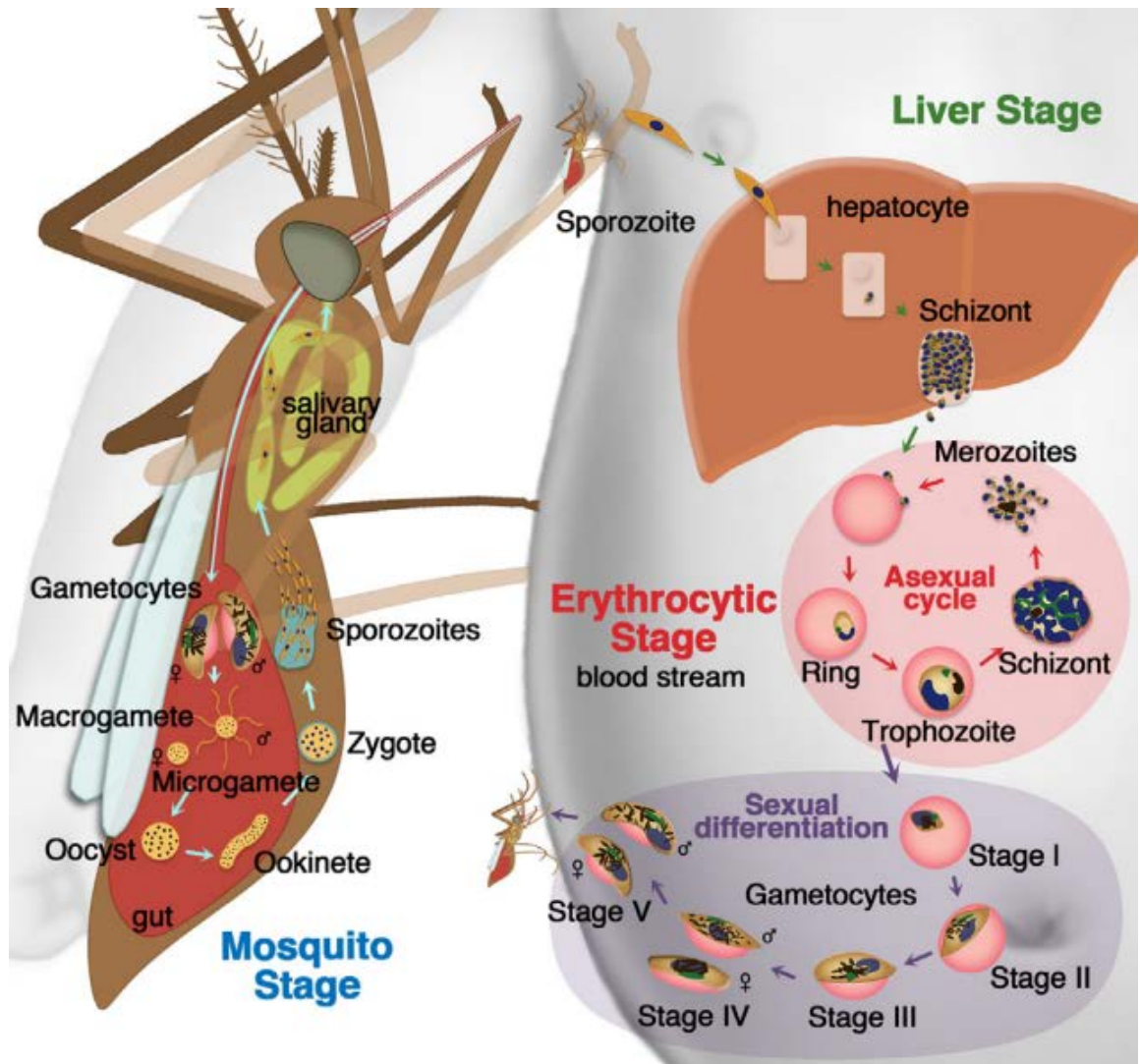


Figure 1.01: The life cycle of *Plasmodium* parasites inside humans and the mosquito [10].

It should be noted that the blood stage of the parasite is the primary focus of drug development so as to alleviate the symptoms, however in recent times the focus has also shifted to develop drugs that target the liver stage and the transmission stage so as to prevent relapses and protect other humans respectively which would be crucial for eradicating malaria [10].

1.2 Treatment methods and their challenges

Artemisinin is a highly potent anti-malarial which was extracted from *Artemisia annua L.* in the 1970s [12]. Pharmacologist, Youyou Tu was awarded the Lasker prize in 2011 and the Nobel Prize

in 2015 for the development of artemisinin. Currently the WHO recommends, artemisinin in combination with other drugs (Artemisinin Combination Therapy, ACT) as the first line therapy for uncomplicated *Plasmodium falciparum* infection [13]. The use of ACT is more effective in combating resistance and also reduces the number of therapies required (from seven to three). The five combinations include: artemether - lumefantrine, artesunate - amodiaquine, artesunate - mefloquine, artesunate - sulfadoxine-pyrimethamine, and dihydroartemisinin - piperaquine [13]. Artemisinin is a sesquiterpene lactone, and contains a 1, 2, 4- trioxane moiety, which also forms an endoperoxide bridge as shown in **Figure 1.02**. Once inside the parasite, this endoperoxide bridge is believed to undergo iron mediated cleavage producing radicals which results in inhibition of the parasite's growth [14, 15].

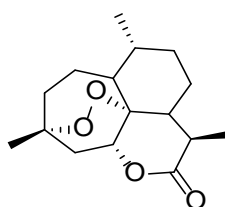


Figure 1.02: Structure of artemisinin.

Atovaquone, commercially available as Malarone® (GlaxoSmithKline) is a combination tablet of atovaquone and proguanil, and was the most prescribed malaria drug between 2005 and 2009 in Australia [16]. Atovaquone (**Figure 1.03**) is a naphthoquinone with a similar structure to ubiquinone and is known to affect the parasite's mitochondria [17].

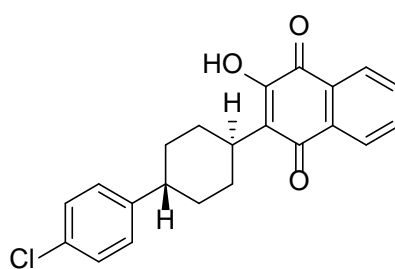


Figure 1.03: Structure of atovaquone.

Another treatment option for malaria is quinine (**Figure 1.04**), which was the first anti-malarial to be reported. Quinine was the main drug used in malaria treatment until 1920, after which its synthetic derivatives such as chloroquine, amodiaquine and mefloquine were introduced. These days quinine is usually reserved for second line treatment in severe *P. falciparum* infection or first line treatment, alongside clindamycin, during the first trimester of pregnancy [13].

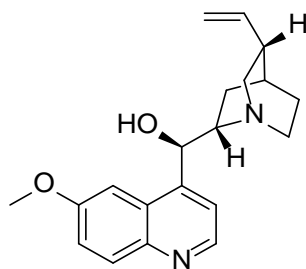


Figure 1.04: Structure of quinine.

1.3 Challenges to current treatment methods

Although there have been significant breakthroughs in the development of anti-malarial drugs, the disease still remains uncontrolled and fatal due to the parasite's continual development of resistance to the existing drugs which also results in non-resolution of symptoms, recrudescence and ultimately treatment failure [18]. **Figure 1.05** illustrates the timeline of the discovery of some of the anti-malarials and the time of their associated incidence of resistance [3]. As can be seen from **Figure 1.05**, the first line of treatment, quinine was effective for a long time before the emergence of resistance. However the more recent drugs such as pyrimethamine and atovaquone developed resistance almost as soon as they were introduced. It can also be seen that ACTs is currently our last line of defence against resistance [3].

In order to address this crucial issue of growing resistance, many strategies have been enforced to control the spread and severity of malaria. This includes preventive measures such as mosquito nets and treatment of water bodies [19], improvement of prescribing habits and therapeutic protocols and the use of combination therapies such as ACT [18, 20].

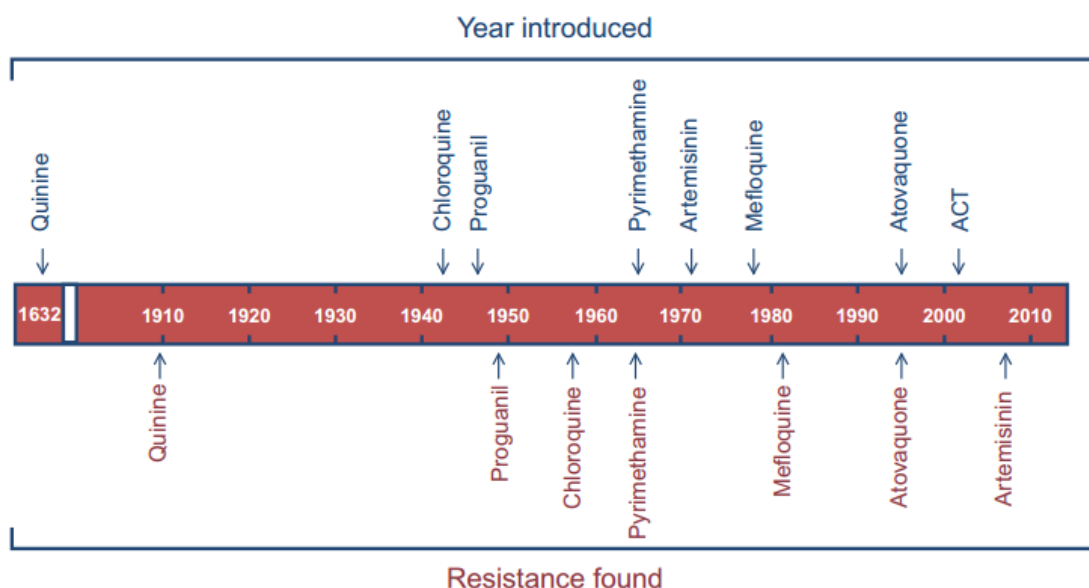


Figure 1.05: A comparison of the year of introduction of a new anti-malarial and the year of its emergence of resistance [3].

1.4 Novel anti-malarials from natural products

In addition to all the above mentioned approaches to control malaria, there has been extensive studies into the development of novel anti-malarials through drug discovery and also modifying the existing therapies to combat resistance [18]. The generally accepted criteria for any new anti-malarial are the following:

1. Should be potent against the parasite's blood stage.
2. Be active against drug resistant parasites.
3. Be free from any intrinsic safety liabilities such as cytotoxicity, genotoxicity and/ or cardiotoxicity.
4. The pharmacokinetic properties should be compatible with once daily oral dosing [21].

The disease-specific criteria for hits and leads for malaria according to the Global Health Innovative Technology Fund, recommends a validated hit to have a cellular potency of $EC_{50} < 1\mu M$ for sensitive and multiple resistant strains of *Plasmodium* and greater than 10-fold selectivity between the CC_{50} for the mammalian cell line and the EC_{50} for *Plasmodium* parasites [22]. The recommended cellular potency for an early lead is $EC_{50} < 100nM$ for sensitive and multidrug-resistant strains of *Plasmodium* parasites and a 100-fold selectivity between the CC_{50} for the mammalian cell line and the EC_{50} for *Plasmodium* parasites [22]. A lead should also be able to eradicate 90% of the target pathogen with less than 50 mg per kg in four doses over 4 days [22].

Natural products have been a reliable source of new drug candidates for many years and have led to the successful development of many drugs such as artemisinin, quinine and lapachol [20, 23]. Quinine was one of the first natural products used for the treatment of malaria, isolated from the cinchona tree bark; and led to the subsequent development of other chemotherapies for malaria including chloroquine, amodiaquine and mefloquine [24]. Naphthoquinone lapichol was another natural product found in tree bark which directed the selection of lapinone, which led to the discovery of atovaquone – an active ingredient in current prophylactics for malaria [23]. Artemisinin is a natural product based drug initially isolated from *Artemisia annua*, a wormwood [4, 20].

However, in spite of all these success stories, natural product drug discovery suffers from issues such as the unrealistic expectations of big pharma companies to produce “blockbuster drugs” with more than \$1 billion in annual sales and also the technical difficulties associated with identifying new compounds with desirable activity [25]. Other issues include unreliability of source and the complexity of the isolated bioactive substance [18]. The undesired physiochemical properties such as insolubility and instability add to the complexity of making these compounds as drug leads [18, 25]. There has been increasing realisation in recent times that these issues can however be addressed by the use of modern biotechnological advances, genomic studies and the use of molecular modelling, docking and other computer-aided drug discovery [18, 26].

Another useful approach to have is the development of natural product compound libraries and databases [27], which could be screened to identify an initial hit which upon employment of medicinal chemistry and Structure-Activity Relationship (SAR) studies could lead to the discovery of a lead compound. One such example is the development of the anti-malarial NITD609 which belong to the spirotetrahydro- β -carboline or the spiroindolones class of compounds and demonstrates nanomolar potency against *Plasmodium falciparum* and *Plasmodium vivax* in clinical studies [18, 28-30]. **Figure 1.06** shows the structure of NITD609.

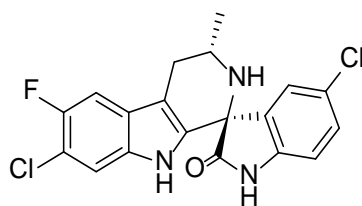


Figure 1.06: Structure of NITD609 [18].

Thus with the recent advances, natural product drug discovery can still be one of the efficient ways to find a hit compound which with appropriate use of medicinal chemistry could pave the way towards the identification of a lead compound for malaria.

1.5 Actin

Actin is one of the most abundant proteins found in all eukaryotic cells, and a large number of cellular functions depend on its ability to reversibly polymerize into long flexible filaments [31].

Figure 1.07 illustrates the dynamics of actin turnover. These actin filaments together with the molecular motor myosin drive many dynamic functions such as cell locomotion, division and growth; also, their interaction with membrane-associated proteins helps eukaryotic cells in adhesion to other cells or substrates, and in retaining their shape and mechanical strength [31].

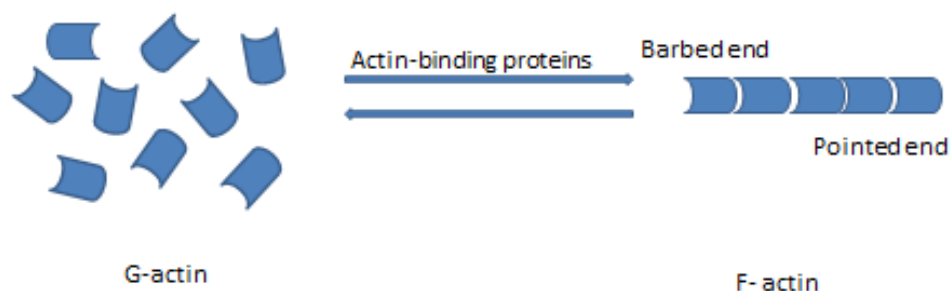


Figure 1.07: Schematic representation of the dynamic equilibrium between G-actin and F-actin controlled by actin binding proteins.

Actin essentially exists in two forms, that is, the monomeric globular or G-actin, and the polymeric filamentous F-actin as illustrated in **Figure 1.08** [32, 33]. G actin is 43-kDa in size and is comprised of four lobes or subdomains D1-D4 which supports a prominent DNase I binding loop and a hydrophobic cleft [34]. The deep cleft between subdomains D2 and D4 binds adenosine triphosphate (ATP) along with Mg^{2+} [31]. It has been suggested that the nucleotide binding cleft

can exist in two states, open and closed - of which the closed state is most stable when ATP is bound (adenosine diphosphate (ADP) -bound state favours a more open conformation of the cleft) as demonstrated by metadynamic simulations [32]. G-actin self-assembles into F-actin under physiological conditions to form a long double-stranded helical polymer such that the position of each monomer is related to the preceding one by a translation of ~ 27.5 Å and a rotation of $\sim -166^\circ$, giving the right-handed helical twist characteristic of the filament [31]. During the conversion of G-actin to F-actin, the tightly bound ATP is hydrolysed so as to slowly release P_i - thus the protomers of F-actin contain tightly bound ATP, ADP or ADP- P_i [32].

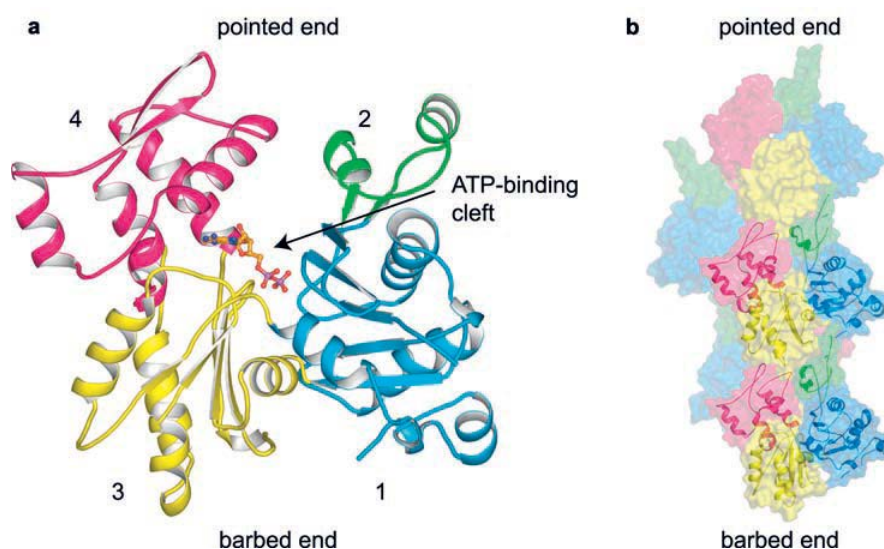


Figure 1.08: Structure of monomeric and filamentous actin. a) The ribbon represents the monomeric actin with the bound nucleotide in stick representation. b) Model of actin filament comprised of five monomers. [31]

Actin monomer polymerization is mediated by nucleotide hydrolysis which subsequently leads to the formation of a 5-9 nm diameter two-stranded helical structures known as actin microfilaments (MFs) [33]. The polymerization involves head to tail interactions, with the end comprising subdomains D1 and D3 the barbed or plus end, while the other end is the pointed or minus end [31]. The monomer addition at each end is asymmetric with the barbed end elongating five to ten times faster than the pointed end. The asymmetry in the rate of elongation may be due to conformational changes in subdomain D2 as a result of ATP hydrolysis by the monomer after addition into the filament [31]. This asymmetry leads to increased dissociation at the pointed end where the ADP accumulates due to weakening of intermolecular interactions there [31]. The barbed end on the other hand is continuously added to with ATP- bound actin monomers [31]. This fundamental process of actin filament dynamics, that is polymerization at one end and simultaneous depolymerisation at

the other end, is termed ‘treadmilling’ and provides a functional target for many actin-binding natural products [31, 35].

In mammalian cells, actin has six isoforms comprising two skeletal, two cardiac and two non-muscle [33]. It is understood that actin MFs have the ability to assemble and disassemble according to the cell’s needs, with their dynamism allowing the cell to respond to complex stimuli [33]. Actins can be grouped into two classes according to the N-terminal processing, namely Class I actin and Class II actin [36]. Non-muscle actins usually comprise the Class I actin and are processed from a primary sequence of Met-X-actin to acetyl-X-actin, where X is an acidic amino acid. Class II actin on the other hand comprise the vertebrate skeletal muscle actin that are processed from Met-Cys-X-actin to acetyl-X-actin. The second amino acid residue on the latter is mostly a highly conserved cysteine or rarely a glycine or alanine [36].

1.5.1 Difference between human and *Plasmodium* actin

Apicomplexan actins are quite different from the mammalian actins both in sequence and function [37]. The malaria parasite actins, actin I and actin II, share 82 and 76% identity with their vertebrate counterparts, and most of the differences are non-conservative amino acid changes [38]. **Figure 1.09** shows the sequence comparison of *Plasmodium falciparum* II (*PfII*) and Human alpha actin (showing 76% identity). The high level of sequence similarity suggests that comparative modelling of the *PfII* actin based on the human actin structure should provide a model suitable for use in drug design and development. That is, sequence similarity is high enough to render homology modelling meaningful but low enough to allow for selectivity.

Pf	3	EEAVALVVDNGSGMVKSGLAGDDAPKCVFPSPVGRPKMPNIMIGMEQKEC	52
Hs	5	DETTALVCDNGSGLVKAGFAGDDAPRAVFPSPVGRPRHQGVMMGMGQKDS	54
Pf	53	YVGDEAQNKRGILTLYPIEHGIVTNWDDMEKIWHHTFYNELRVSPREEHP	102
Hs	55	YVGDEAQSKRGILTLYPIEHGIITNWDDMEKIWHHTFYNELRVAPREEHP	104
Pf	103	VLLTEAPLNPKTNREKMTQIMFETFDVPAMYVSIQAILSLYASGRRTTGIV	152
Hs	105	TLLTEAPLNPKANREKMTQIMFETFNVPAMYVAIQAVLSLYASGRRTTGIV	154
Pf	153	LDSGDGVSHTVPIYEGYVLPHAINRIDMAGRDLYHMMKWFTERTGHTFTT	202
Hs	155	LDSGDGVTHNVPIYEGYALPHAIMRLDLAGRDLYLMLKILTERGYSFVT	204
Pf	203	TAEREIVRDIKEKLCYIAMDYDEELKRSEEHSDEIEEYELPDGNLITVG	252
Hs	205	TAEREIVRDIKEKLCYVALDFENEMATAAS-SSSLEKSYELPDGQVITIG	253
Pf	253	SERFRCPEALFNPTLIGRECPGLHITAYQSIMKCDIDIRKELYNIVLSG	302
Hs	254	NERFRCPETLFQPSFIGMESAGIHETTYNSIMKCDIDIRKDLYANNVMSG	303
Pf	303	GTTMYNNIGERLTKEMTNLAPSSMKIKVIAPPERKYSVWIGGSILSSLST	352
Hs	304	GTTMYPGIADRMQKEITALAPSTMKIKIAPPERKYSVWIGGSILASLST	353
Pf	353	FQQMWITKEEYEDSGPSIVHRKCF	376
Hs	354	FOOMWITKOEYDEAGPSIVHRKCF	377

Figure 1.09: Comparison of amino acid sequence of *Pf* actin II and human Alpha actin from a ClustalW alignment. An | (vertical bar) indicates a position of residue conservation; a : (colon) indicates conservation between groups of strongly similar properties –(scoring > 0.5 in the Gonnet PAM 250 matrix); a . (period) indicates conservation between groups of weakly similar properties (scoring ≤ 0.5 in the Gonnet PAM 250 matrix).

A study on the comparison of the apicomplexan and mammalian actin models revealed that most amino acid changes are limited to the monomer surface suggesting that although the overall structures are quite similar, actin-actin or actin-actin binding proteins interactions may be dramatically affected by the surface differences [34]. For example, the DNase I binding (D) loop in particular is very divergent [34].

Plasmodium falciparum, the agent responsible for the most virulent form of human malaria, expresses two types of actins, *Pf*ACTI and *Pf*ACTII [37]. Of these, *Pf*ACTI is expressed throughout the life cycle of the parasite while the *Pf*ACTII is mainly expressed during the sexual stage of the parasite [37]. One of the key features of the *Plasmodium* actin is that the filaments formed are very short [36, 37, 39] (approximately 100nm [36]). Recent studies have also shown that actin across

apicomplexan parasites primarily exist in monomeric (unpolymerized) state as evidenced by the absence of filamentous actin in the cytosol. This is due to the unusual instability of the apicomplexan actin filament compared with the conventional actin filaments [37, 39].

A study on the amino acid sequence of apicomplexan actin compared with that of selected vertebrates revealed large differences between the two [36]. Residues in the region 34-68 which are involved in the monomer-monomer contacts in F-actin, are considered to be one of the most divergent regions in *Pf*ACT I with sequence differences at nine positions [36]. For example, the histidine at position 40, which is believed to interact with 167 glutamic acid of an adjacent monomer via a hydrogen bond, is replaced by an asparagine in *P. falciparum* [36]. Studies have shown that the modification of this histidine can inhibit polymerization. Likewise, glutamine at position 41 (known to interact with adjacent monomer's lysine 113) is replaced by proline. Modification of glutamine 41 is known to increase the rate of polymerization and decrease critical concentration. The amino acids glycine and glutamine at positions 48 and 49, respectively, are replaced by glutamic acid in parasite actin. Other differences include replacement of tyrosine 53 by phenylalanine and serine 60 by tyrosine. Tyrosine 53, although not a part of the actin-actin interface, is thought to stabilize the loop composed of residues 40-50 [36].

Further investigation into the instability of the actin filaments in parasites has revealed that actin dynamics within the apicomplexan cell is very different from the other species. For example, the monomer-monomer interactions which usually stabilize the filaments are different therefore imparting parasite actin with its inherent instability [37]. The inter-strand actin filament contact in the 34-68 region is weakened due to the corresponding large amino acid difference in actin there [36]. Methylation of histidine 73 decreases fragmentation of actin filaments – the absence of this methylation in parasite actin results in increased instability [36].

Experimentally it has been shown that high concentrations of the mushroom toxin phalloidin can stabilize these short actin filaments *in vitro* leading to the formation of long stable filaments [37]. Actin stabilization has also been achieved in *Toxoplasma gondii* by reversing two key residues on the actin molecule [37]. Interestingly, this acquired stability leads to disruption of gliding in *T. gondii*, suggesting that the short and dynamic nature of the parasite's actin filament is an important adaptation for motility [37].

1.5.2 Actin-dependent gliding

Apicomplexan parasites are quite small in size and therefore are not able to drift using inertia and instead must crawl along the substrate as they tunnel into the host tissues and cells [8]. This mechanism of transport overcomes several challenges such as controlling direction, adhesion to

substrate, power generation and release from the substratum in order to move forward [8]. Although apicomplexan species adapt specifically to various hosts in order to target tissues, they are known to share common cell architecture and mode of locomotion [7]. This mode of locomotion is neither with the use of cilia or flagella nor the actin assembly driven by Arp 2/3 complex; instead, these parasites use a distinctive locomotive mechanism known as gliding which involves actin filament nucleation and polymerisation combined with an internally anchored myosin motor [40].

The motile invasive forms of the parasite are known as ‘zoites’ and have an apical morphology which determines the direction of parasite’s movement [34]. Gliding relies on a conserved molecular machinery that governs all apicomplexan cell motility and host cell invasion [7, 41]. The actomyosin motor is secured to the inner membrane complex in the supra-alveolar space beneath the outer plasma membrane of the parasite [7]. Although the exact mechanism of actin-based gliding is not clearly known, it is believed that the filamentous actin lying within the supra-alveolar space forms the key rigid support upon which the motor consisting of a single headed myosin bears in order to create the rearward traction force necessary for the motility [7, 40]. This mechanism is illustrated in **Figure 1.10**. In other words, the actins form a short, dynamic filament bridge which connects the extracellular environment via the cytoplasmic tail of transmembrane-bound adhesins (from the TRAP family of proteins) secreted onto the parasite surface with the myosin motor [40]. These adhesins bind to the host surface and are driven rearward by the myosin via the actin filament, thereby propelling the parasite over the cell substratum or actively penetrating target cells [40]. The directionality of the parasite is according to the orientation of the filaments [36]. Two proteins, TREP, a transmembrane protein, and TRAP, a substrate interacting surface protein, are examples of surface adhesins that are essential for the gliding of the parasite in the sporozoite stages specifically [41, 42].

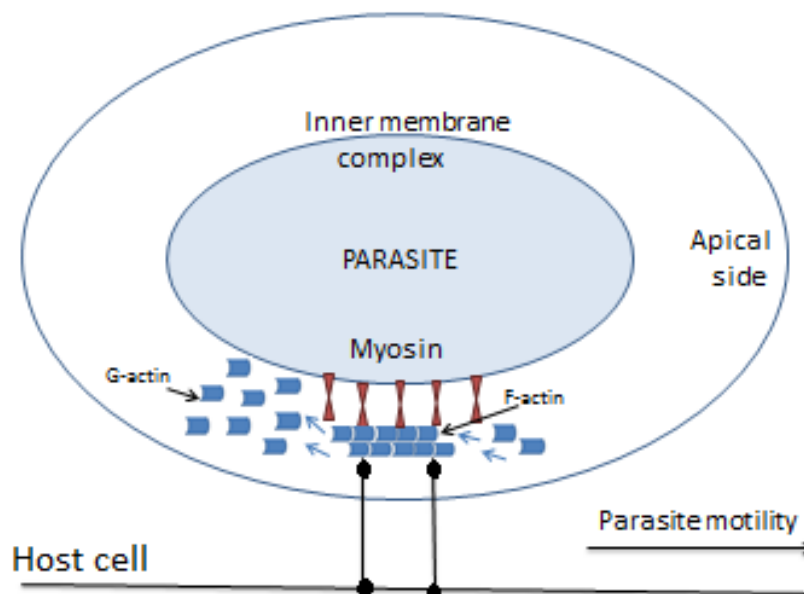


Figure 1.10: Model showing apicomplexan gliding motility (adapted from [36]).

1.5.3 Actin binding in malaria

Various studies have shown that *Plasmodium* actin differs from human actin in filament length, stability, turnover and propensity to form filaments [36]. Furthermore, reviews on the structural analysis of the interaction between actin binding cytotoxins reveal that several binding sites defined in mammalian actin are located in areas of sequence difference between the human and *Plasmodium* actin [31]. Thus, compounds that selectively target these sites, with a preference for residues characterising the *Plasmodium* actin over the human actin monomer could be used to selectively target parasite actin-dependent processes arresting gliding and invasion and, as such, being a potent therapeutic approach to stopping *Plasmodium* parasite disease.

1.5.4 Apicomplexan actin regulators

Actin binding proteins can be broadly classified on the basis of their effect on the actin monomer or filament, such as sequestering, severing, capping or nucleation [31]. **Figure 1.11** illustrates the different types of actin binding compounds and their effect on actin. In addition to these, there are also proteins which play dual roles such as sever and cap the actin filaments [31].

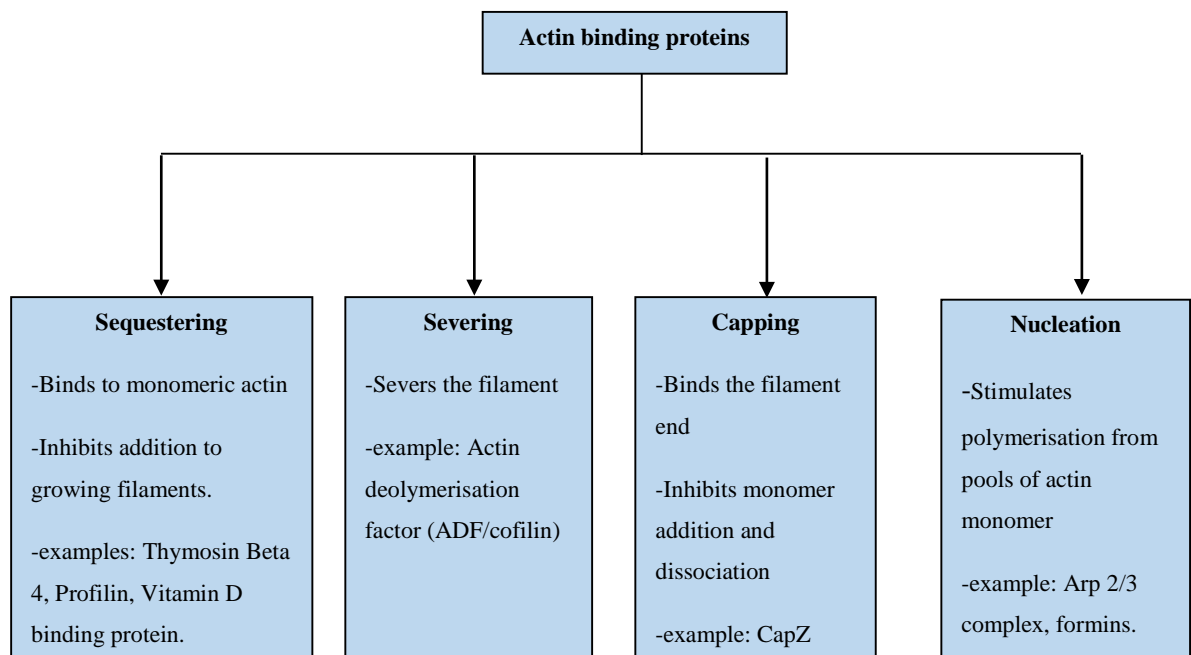


Figure 1.11: The different types of actin regulators and their functions.

It has been observed that the formation of F-actin in most eukaryotic organisms is governed by nearly 150 actin regulators, while in apicomplexa they are limited to very few in number [43]. The parasites of the apicomplexan family, lack many of the genes that code for the actin regulatory factors such as the Arp2/3 complex, as well as cross-linking, branching and nucleation promoting factors including WASp and WH2-domain [44], consistent with the absence of branched and elongated actin containing structures in apicomplexan cells [45]. Interestingly, even with this reduced cohort of actin regulators, apicomplexan parasites undergo fast (1-3 $\mu\text{m/s}$) actin dependent motility and host cell invasion [44]. Of the actin regulators present, apicomplexan parasites are known to contain formins and coronins, actin filament binding proteins, along with profilin, actin-depolymerizing factor/cofilin and Srv2/cyclase-associated protein (CAP), each of which are actin monomer binding proteins [34].

a) Formin

Formins are a family of proteins which help actin nucleate into unbranched filaments [40]. *P. falciparum* expresses two very large (>300 kDa) formin-like proteins, namely *Pf*Formin 1 and *Pf*Formin 2, that cluster into two different families, each playing a conserved role in actin regulation [40]. It has been shown that *Pf*Formin 2 has cytoplasmic localization [44] while *Pf*Formin 1 may localize to the parasite-erythrocyte tight junction during RBC invasion, a location coinciding with the predicted site of the activated actomyosin motor in the invading malaria parasite [40]. Compared

with other formins, *Pf*Formins lack the GTPase-binding and diaphanous auto-regulatory domains [44].

b) Coronin

Coronin is a highly conserved eukaryotic actin regulator known to be present in apicomplexa [46]. Coronin (an ortholog of the WD40-repeat containing protein) is the only candidate for F-actin bundling in the apicomplexan parasite [44]. Apicomplexan coronins lack the microtubule-binding domain of canonical coronins, but do, however, possess the majority of the residues essential for actin interaction in yeast [44]. Thus, it is assumed that coronin stabilizes F-actin scaffolds in the parasite [44].

c) Profilin

Profilin is a small actin binding protein that binds actin monomers [34], thereby sequestering them and making pools of actin monomer available for polymerization [44]. This facilitation of polymerization at the barbed end is achieved by recharging ADP-actin monomer with ATP [34]. It is assumed that profilin is an important co-regulator in formin-mediated elongation of actin filaments and appears to be present during the asexual stages in *P. falciparum* [40]. Apicomplexa encode a profilin-like protein that is believed to be involved in nucleotide re-loading [44]. Interestingly, expression of *P. falciparum* profilin (*Pf*PRF) peaks with that of *Pf*Formin1 and dips with the peak in the expression of *Pf*Formin2 [40].

d) Actin depolymerisation factors (ADF)

ADFs are MF turnover modulating G and F actin binding proteins belonging to the ADF/cofilin superfamily [44] and play their role in actin-filament turnover by monomer sequestration, pointed end depolymerisation and filament severing [34]. All apicomplexan parasites are known to code for at least one of the ADF genes; *Plasmodium* codes for two genes, namely ADF1 and ADF2 [44]. ADF1 is essential during the pathogenic RBC stages of infection while ADF2 influences only the sexual stages of the parasite [44]. Conventional mammalian ADFs and *Plasmodium* ADFs differ in several aspects. For example, as opposed to mammalian ADF/cofilin proteins, which are capable of depolymerisation or severing [34] and inhibit nucleotide exchange, *Pf*ADF1 has been shown to be a stimulator of nucleotide exchange (more like a profilin), is a weak actin sequester [44] and doesn't bind stably to filaments [46]. *Pf*ADF1 has also been shown to be a definitive severer of actin filaments [46].

e) CAP and capping proteins

CAPs are evolutionarily conserved actin regulators which consist of an N-terminal adenylate cyclase binding domain, a central proline-rich segment, and a C-terminal actin binding domain [9]. The apicomplexan parasites possess a (CAP)/Srv2 capping protein homolog which has only the C-terminal actin binding domain [9]. Their primary role is thought to be to sequester actin monomers, although the ortholog in the mouse malaria parasite *P. berghei* has surprisingly been shown to be non-essential during asexual development of the parasite [46]. Capping proteins (not to be confused with CAP), made up by an alpha and beta subunit bind to the filament's barbed end and thereby prevent monomer addition and dissociation [31].

1.6 Actin binding compounds

Other than the actin binding proteins found within the organism, there are a large number of natural products known to bind to actins thereby altering their polymerization or activity, and are therefore cytotoxic. The sources of these compounds include terrestrial plants, fungi, bacteria, marine sponges, nudibranchs and algae [47, 48]. Interestingly, many of these actin targeting cytotoxins are from the macrolide family and have a characteristic primarily hydrophobic core associated with stereochemically complex side groups [31, 47]. Each compound has a specific target site on the actin molecule, often disrupting G-actin's ability to form filaments, destabilizing the growing filament or stabilising the filament preventing disassembly [31]. Three major classes of these actin binding compounds that have been the focus of extensive interest are the latrunculins, cytochalasins and jasplakinolide derivatives [33].

1.6.1 Compounds that prevent filament formation

The binding of certain compounds can block or destabilize actin filaments. This is generally achieved by binding to either the ATP-binding cleft or the barbed end of the actin monomer [31]. The F-actin destabilizing compounds can be sequestering compounds which help actin monomers to passively dissociate from the filament, or the severing compounds which bind to the filament and disrupt the interaction between adjacent monomers [31]. The compounds that prevent filament formation can be broadly classified into ATP binding cleft targeting compounds and the barbed end targeting compounds.

1.6.1.1 ATP binding cleft-targeting compounds

a) Latrunculins. Latrunculins are unique macrolides initially isolated from the marine sponge *Negombata magnifica* found in the red sea [31, 49]. It was observed that when squeezed this sponge secreted a reddish fluid which is toxic to fish [49]. Later studies revealed the presence of 14- and 16-membered lactones in the fluid with a unique 2-thiazolidinone moiety [49]. Later it was discovered that these macrolides can also be found in taxonomically unrelated organisms suggesting that symbiotic microbes could be the actual producer of these interesting secondary metabolites [49]. To date, eight types of latrunculins have been isolated from different sponges [31, 47]. Latrunculin A, B (**Figure 1.12**) and their various derivatives have been successfully synthesised [50]. Latrunculins in addition to being ichthyotoxic are also cytotoxic to tumor cells and have antiviral properties as well [49].

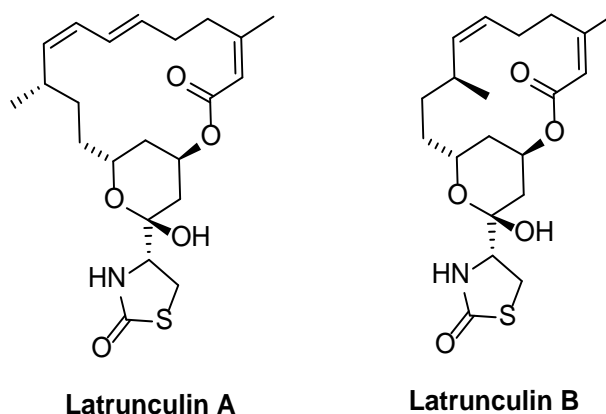


Figure 1.12: Structure of latrunculin A and B.

The cytotoxicity of latrunculins is due to their ability to bind to the actin monomer in a 1:1 complex which is no longer capable of polymerizing into F-actin [51]. The latrunculins specifically bind above the ATP binding cleft between subdomains D2 and D4 of the actin monomer [31] and thereby sequester actin away from the free cytosolic pool in a fashion similar to that of monomer sequestering proteins [47]. Crystal structures of latrunculin A with rabbit muscle alpha actin monomer (PDB ID: 1ESV) shows that the 2-thiazolidinone group is inserted into a pocket lined by residues Tyr 69, Asp 157, Arg 183, Thr 186, Arg 206 and Arg 210 (as shown in **Figure 1.13**), where specific contacts involving the NH, OH, CO, and O-ester of latrunculin A are formed.

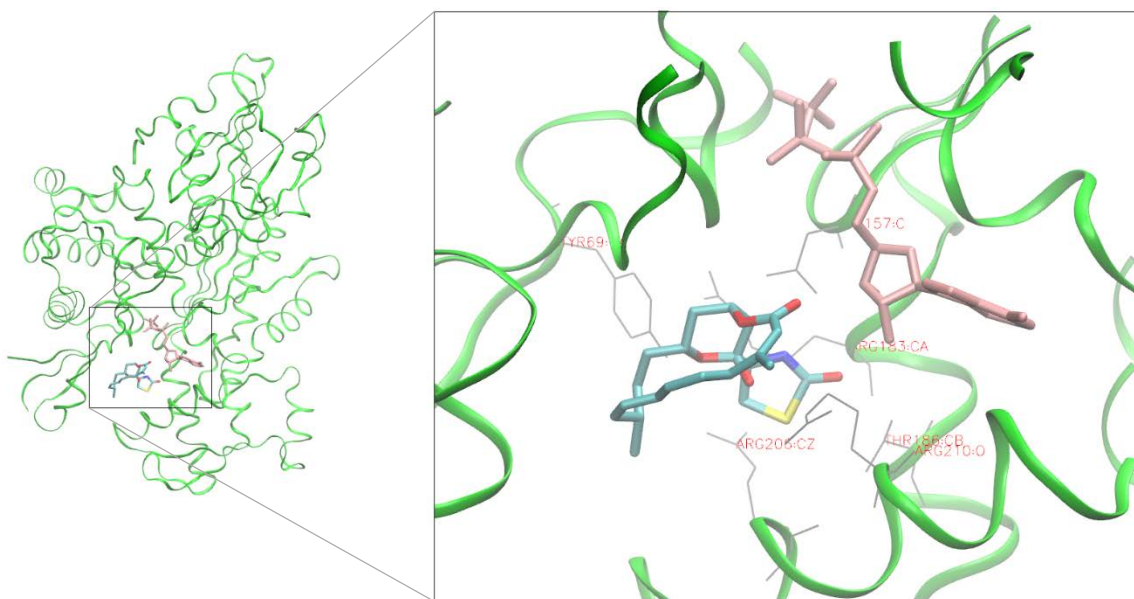


Figure 1.13: Image of rabbit muscle alpha actin bound to latrunculin A (tube) showing the pocket lined by Tyr 69, Asp 157, Arg 183, Thr 186, Arg 206 and Arg 210 (PDB ID: 1ESV). Latrunculin A is represented in tube form, the protein in ribbon form (green), the ATP in tube form (pink) and the interacting residues in stick form (grey).

Latrunculin B, which differs from latrunculin A only in the absence of two methylene carbon atoms on the macrocyclic ring, is slightly less toxic than latrunculin A [31]. In yeast and hamster fibroblast cell growth studies, latrunculin A demonstrated microfilament disrupting activity of 0.5-1.0 $\mu\text{g/mL}$ while latrunculin B had an activity ranging from 0.5-10.0 $\mu\text{g/mL}$ [52]. This difference in activity is probably due to the loss of hydrophobic interactions normally made by these two carbons and residue Gln59 in the latrunculin A-actin complex [31]. This suggests that the shape and size of the ring is also an important determinant in the overall binding affinity of these compounds with actin [31].

Latrunculins are also capable of depolymerizing the F-actin filaments [31]. This is thought to arise by latrunculin binding between subdomains D2 and D4 of the actin monomer, which acts as a wedge that restricts conformational changes required for stable interactions between actin monomer interfaces to form stable filaments, thereby sequestering the monomer from polymerization [31].

1.6.1.2 Barbed end targeting compounds

The barbed end targeting natural products are large in number with variable chemical structures. Compared to latrunculins, these toxins have larger and more diverse ring structures and a longer stereochemical side chain [31]. These compounds can be divided into seven classes as listed below.

- a) **Cytochalasins.** Cytochalasins belong to a family of fungal metabolites that mainly target the barbed end of F-actin with high affinity (equilibrium dissociation constant, $K_d \sim 2\text{nM}$) [53]. This binding partially inhibits the association and dissociation of actin monomers at the barbed end [53]. Depending on its structure, cytochalasin is classified into three groups, namely the 10-phenylcytochalasins (eg. cytochalasin A, B and D), the 10-indolylcytochalasins (eg. chaetoglobosin A and D), and the 10-isopropylcytochalasins (eg. aspochalasin B and D) [47]. Of the various effects cytochalasin has on actin cytoskeleton, the capping effect is the most prominent in which cytochalasin caps the barbed end of the actin filament and thus inhibits further monomer addition and elongation [47]. This leads to depolymerisation at the pointed end due to net loss of monomers [47]. At high concentrations, cytochalasin can also sever the actin filaments and sequester the actin monomers [47].

Structurally, cytochalasins are characterised by the presence of a 11- to 14-membered macrocyclic ring fused to a saturated isoindolone unit [54, 55] as shown in **Figure 1.14**. The first attempt to make the isoindolone unit was made by Joseph Auerbach and Steven M. Weinreb in 1975 employing an intramolecular Diels-Alder addition as the key step [55]. In 1999, Merifield and Thomas successfully synthesised cytochalasin D from methacrolein and (*E*)-but-2-enyl(diisopinocampheyl) borane in 26 steps [56].

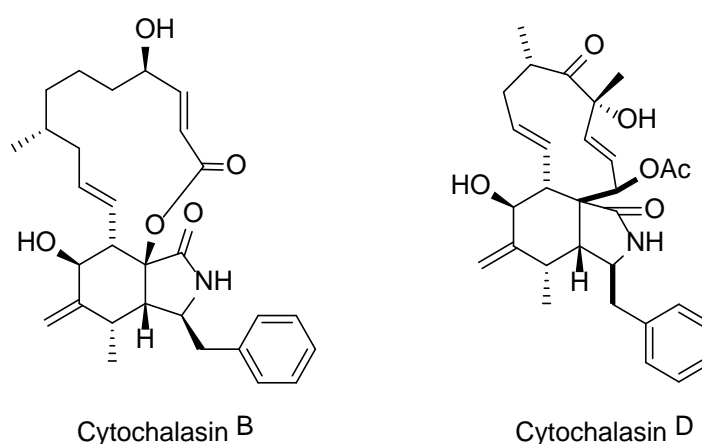


Figure 1.14: Structure of cytochalasin B and cytochalasin D.

- b) **Trisoxazole toxins.** There are more than 30 forms of these compounds isolated from pacific sponges and nudibranch egg masses. **Figure 1.15** shows the general structure of the trisoxazoles. Examples include mycalolides, ulapualides, kabiramides and halichondramides [31]. Mycalolide A has been synthesised from (*R*)-1,2,4 butanetriol and *tert*-butyl 3,4-epoxybutanoate which requires more than 40 steps [57]. Ulapualide A has

also been synthesised by Pattenden *et al.* using three starting materials namely, 3-benzyloxypropanal, (*R*)-2-benzyl-3-propionyl-2-oxazolidinone and Garner's aldehyde in 52 steps [58].

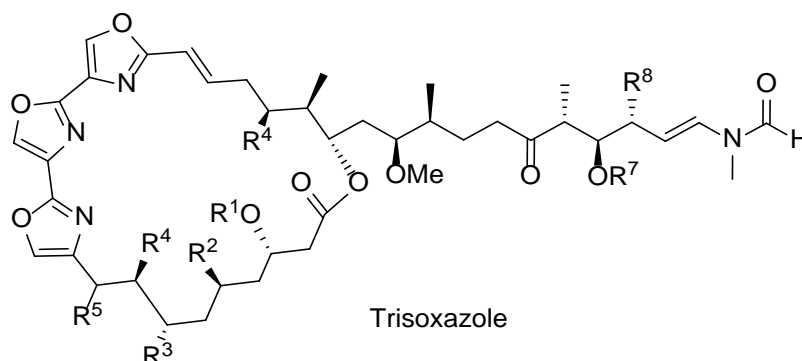


Figure 1.15: Structure of trisoxazole.

- c) **Reidispongiolides and sphinxolides.** These are closely related macrocyclic lactone isolated from New Caledonian marine sponges *Reidispongia coerulea* and *Neosiphonia superstes* [31, 59]. **Figure 1.16** represents the general structure of these compounds. They have high actin binding affinity and are cytotoxic against numerous human cancer cells [59]. Studies show that the presence of *N*-methyl-vinylformamide moiety at the terminus of the macrolide tail is essential for toxin potency [59]. The structure of actin bound to reidispongiolide A and C have been determined (PDB ID: 2ASM and 2ASP, respectively). The total synthesis of reidispongiolide A was achieved by Paterson *et al.* using ethyl ketones and an epoxide [60]. The crystal structure of sphinxolide B has also been determined (PDB ID: 2ASO).

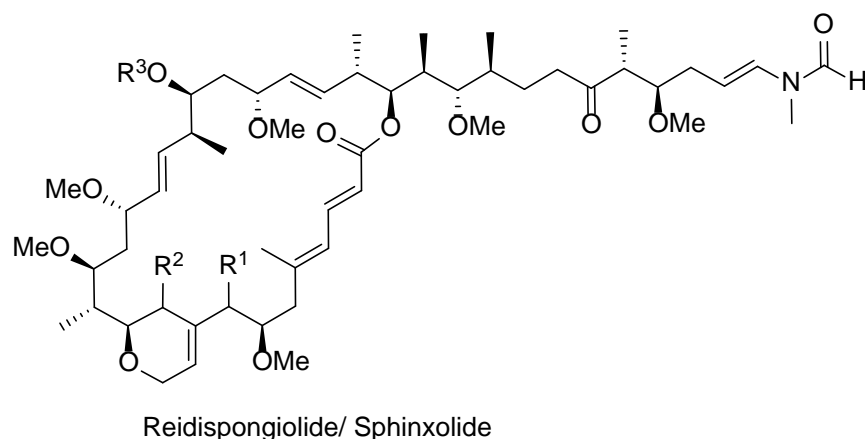


Figure 1.16: General structure of reidispongiolides or sphinxolides.

- d) **Aplyronines.** These compounds are isolated from the Pacific sea hare *Aplysia kurodai* and are structurally different from the other two macrolide primarily in the main chain of their ring structures [31]. To date only one total synthesis of aplyronine has been reported [61], although some second generation and fragment synthesis have recently been published [62, 63]. **Figure 1.17** shows the structure of aplyronines. The actin bound structure of these compounds has been determined (PDB ID: 1WUA).

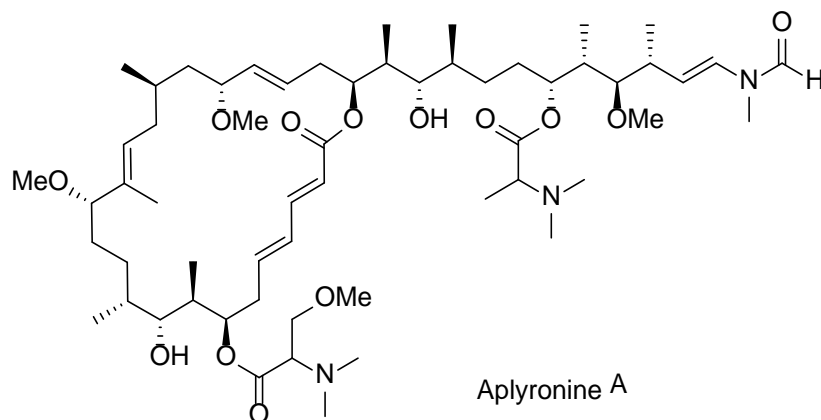


Figure 1.17: Structure of aplyronines.

- e) **Swinholide and misakinolide (bistheonellide).** These are dimeric lactone macrolides (as shown in **Figure 1.18**) isolated from the marine sponge *Theonella swinhoei* [31]. Swinholide A acts as actin polymerization inhibitor by sequestering the G actin by forming 1:2 complexes whereby the two actin monomers bound to the macrolide are no longer capable of participating in actin filament elongation or nucleation (PDB ID: 1YXQ) [64]. It is also involved in the severing of F-actin thereby catalysing depolymerisation [47, 64]. *In vitro* actin filament severing and polymerization assays indicate that the *N*-methyl-

vinylformamide moiety at the terminal of the macrolide tail of these compounds is necessary for toxicity [59]. Total synthesis of swinholides A has been achieved in less than 20 steps [65].

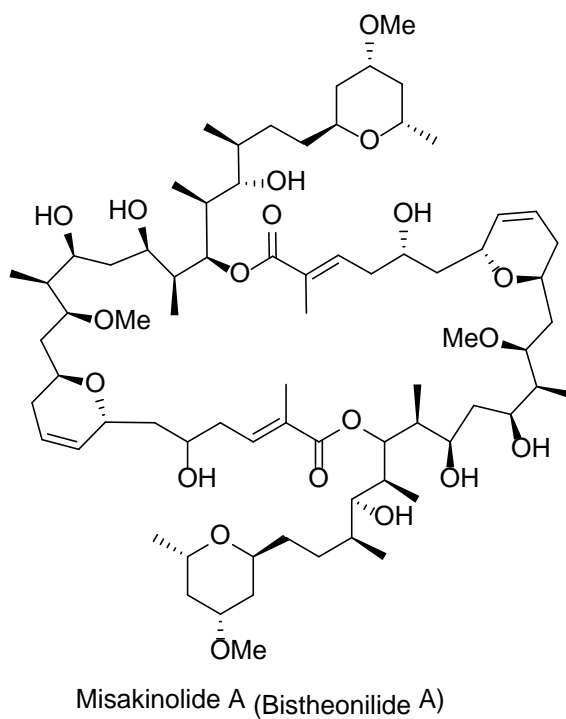
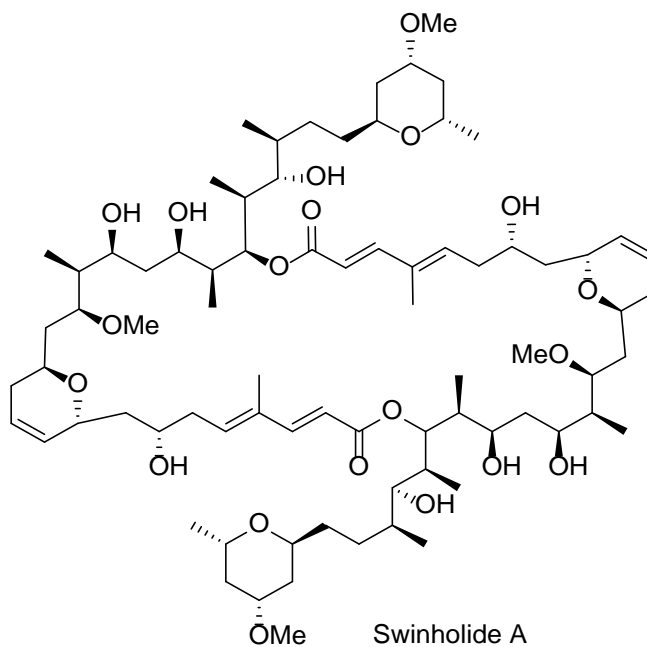


Figure 1.18: Structure of swinholide A and misakinolide A.

- f) **Scytophycins.** These macrolides (eg. tolytoxin) resemble monomeric versions of swinholide and are isolated from terrestrial cyanobacterium *Scytonema pseudohofmanni* [31]. **Figure 1.19** shows the structure of scytophycin.

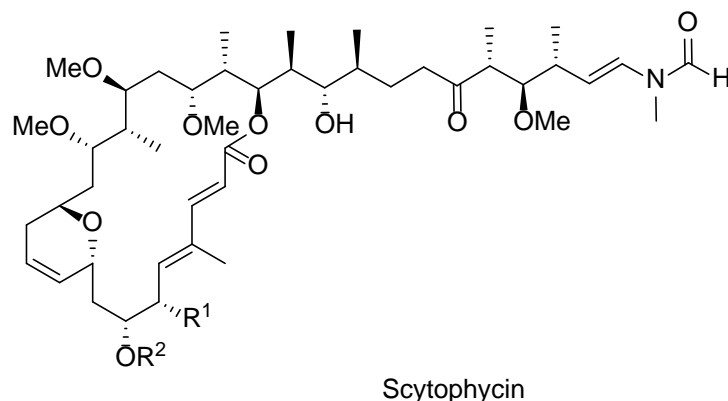


Figure 1.19: Structure of scytophycin.

- g) **Lobophorolide.** This is a recently identified 22-membered cyclic lactone isolated from the brown alga *Lobophora variegata* as shown in **Figure 1.20** [66]. Its crystal structure with actin has been determined (PDB ID: 3M6G).

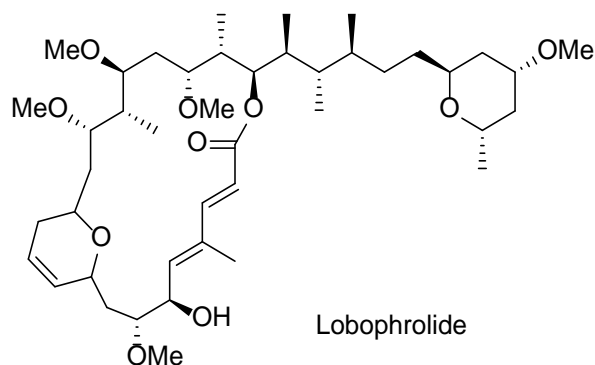
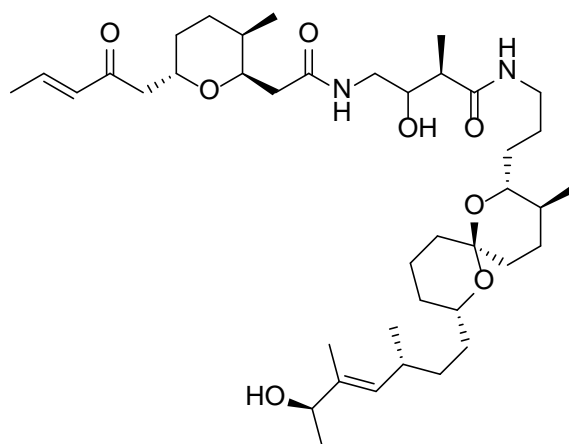


Figure 1.20: Structure of lobophorolide.

- h) **Bistramides.** These are a unique family of dilactam polyethers isolated from the marine ascidian *Lissoclinum bistratum* [31]. Recent studies have shown that these can target actin with high affinity, inhibit filament formation and promote filament disruption [31]. Bistramide A has been successfully synthesised using a dithiane, epoxide and allyl alcohol [67] and its crystal structure bound to actin has also been determined (PDB ID: 2FXU). **Figure 1.21** shows the structure of bistramide A.



Bistramide A

Figure 1.21: Structure of bistramide A.

1.6.1.3 Mechanism

Contrary to the ATP-binding pocket binding compounds, barbed end targeting compounds interact at the surface and are solvent exposed [31]. It is likely that the steric hindrance between the axial monomers of actin in the filament is responsible for destabilization of the filament [31]. That is, the position of the barbed end bound toxin can create a steric clash between the hydrophobic residues found in the DNase I binding loop of the lower monomer and the hydrophobic cleft separating the actin subdomains D1 and D3 of the axial upper monomer [31].

1.6.2 Filament Stabilising Compounds

A separate class of cytotoxic natural products that have been very useful in understanding actin filament assembly and organization are those that stably interact with the actin filament [31]. A cyclic depsipeptide is the common chemical feature of this class of compounds which refers to an oligomeric compound containing an amino acid group joined by a peptide bond and a carboxylic acid group joined by an ester bond [31]. There are six different families of these compounds as listed below.

- a) **Phalloidin.** It is isolated from the death cap mushroom *Amanita phalloides* and is considered to be the best actin filament stabilizing compound currently known [31]. Fluorescent derivatives of phalloidin have been used in microscopic studies of actin filament [68]. From the studies on phalloidin binding site on actin, it is understood that phalloidin interacts with three actin monomers simultaneously at three different binding sites [31]. It is believed that phalloidin binding between the loop containing residues 198–

201 of the lower actin subunit, and the loop of residues 73–75 and residue 179 of the diagonal subunit of actin, stabilizes the filament [31]. Phalloidin (**Figure 1.22**) has been synthesised by a solid phase approach by Anderson *et al.* in 2005 [69].

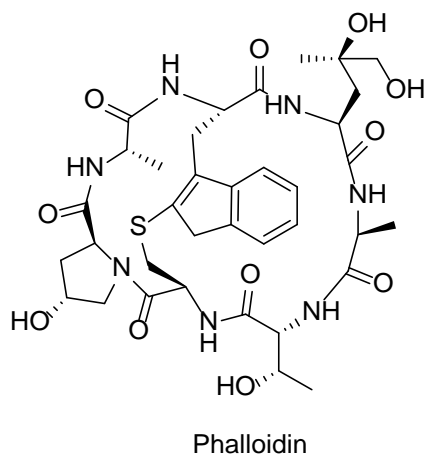


Figure 1.22: Structure of phalloidin.

- b) Jasplakinolide.** Jasplakinolide is isolated from marine sponge *Jaspis johnstoni* and is an actin filament stabilizer as well as potent polymerization inducer [31]. Although structurally different, they are functionally similar to phalloidin (**Figure 1.23**) and even competes with its binding site [31]. Jasplakinolide is an actin filament stabilising compound which when administered to the apicomplexan parasites leads to the formation of densely bundled mats of filament arranged in random orientation instead of forming neat parallel arrays of ordered short filaments [34]. Thus, after jasplakinolide treatment, the parasites lose directionality and are unable to invade [34]. Solid-phase based total synthesis of jasplakinolide by ring-closing metathesis was achieved by Tannert *et al.* [70].

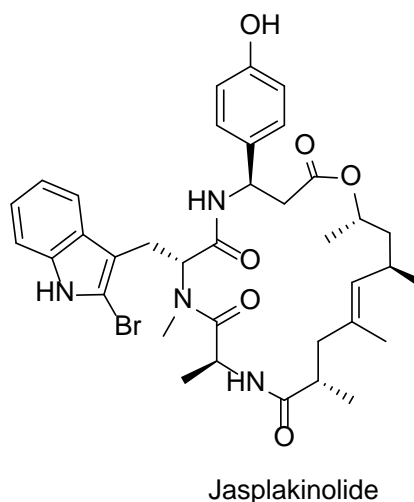


Figure 1.23: Structure of jasplakinolide.

- c) **Chondramides.** These 18-membered depsipeptides (**Figure 1.24**) are obtained from myxobacterium *Chondromyces crocatus* and are similar in structure to jasplakinolide [31]. Chondramide A has been synthetically prepared [71].

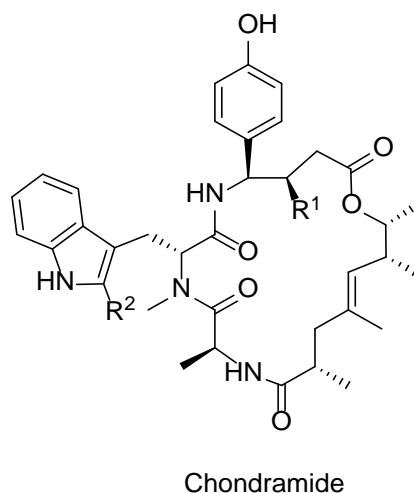
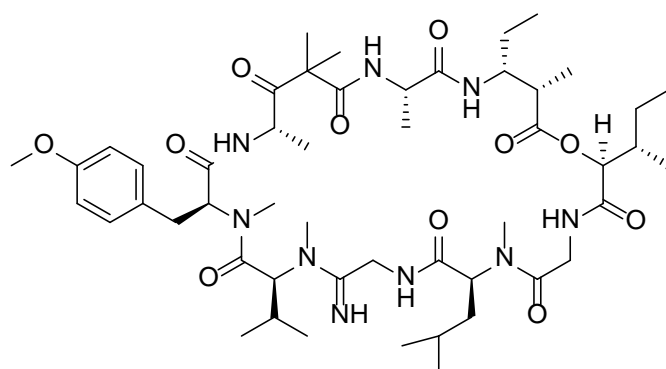


Figure 1.24: Structure of chondramide.

- d) **Dolastatin.** This family of cytotoxins isolated from the Indian Ocean Sea hare *Dolabella auricularia* are potent anti-cancer agents [31]. X-ray fibre diffraction studies have shown that dolastatin 11 (**Figure 1.25**) enhances filament stability by bridging the two long-pitch strands between subdomain D4 of one actin subunit and subdomain D1 of the diagonal subunit [31]. Although this mechanism is similar to that of phalloidin, studies have confirmed that the binding site of dolastatin is different to that of phalloidin [31]. Total

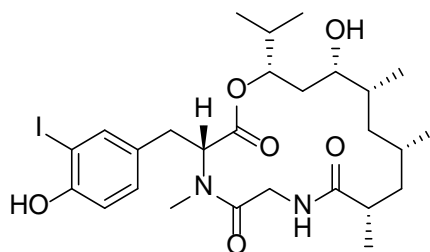
synthesis of dolastatin 10 has been achieved through ruthenium-catalyzed asymmetric hydrogenation [72].



Dolastatin 11

Figure 1.25: Structure of dolastatin 11.

- e) **Doliculide.** It is a 16-membered cyclic desipeptide (**Figure 1.26**) isolated from *D. auricularia* and its (-) isoform which has been synthesised in 2004 [73] exhibits activity identical to that of jasplakinolide [31].



(-)-Doliculide

Figure 1.26: Structure of doliculide.

- f) **Amphidinolides.** These are unique group of cytotoxic compounds isolated from *Amphidinium sp.* dinoflagellates that live off the coasts of Japan and the U.S. Virgin Islands [31]. Interestingly amphidinolide H (**Figure 1.27**) involves formation of a residue-specific covalent bond [31]. Synthesis of amphidinolide T2 was recently achieved by Li *et al.* [74].

The aim of this project is to investigate latrunculin analogues as tools to probe actin inhibition across the human and *Plasmodium* species and to help understand the key difference between them. This information will then be used to tailor a parasite specific actin inhibitor. Such compounds which specifically target parasite actin over host actin could be potent and safe antimalarial agents, stopping parasite motility and, as such, preventing disease.

1.8 References

1. Menard, R., The journey of the malaria sporozoite through its hosts: two parasite proteins lead the way. *Microbes and Infection*, 2000; 2: 633-642.
2. Cervantes, S., et al., High content live cell imaging for the discovery of new antimalarial marine natural products. *BMC Infect Dis*, 2012; 12.
3. Calderon, F., Wilson, D.M., and F.J. Gamo, Antimalarial drug discovery: recent progress and future directions. *Prog Med Chem*, 2013; 52: 97-151.
4. Hertweck, C., Natural products as source of therapeutics against parasitic diseases. *Angew Chem Int Ed*, 2015; 54: 14622 –14624.
5. World malaria report 2015. World Health Organisation (WHO), 2015.
6. Gelb, M.H., Drug discovery for malaria: a very challenging and timely endeavor. *Curr Opin Chem Biol*, 2007; 11: 440-445.
7. Angrisano, F., et al., A GFP-Actin reporter line to explore microfilament dynamics across the malaria parasite lifecycle. *Mol Biochem Parasit*, 2012; 182: 93-6.
8. Sibley, L.D., How apicomplexan parasites move in and out of cells. *Curr Opin Chem Biotech*, 2010; 21: 592-598.
9. Hliscs, M., et al., Structure and function of a G-actin sequestering protein with a vital role in malaria oocyst development inside the mosquito vector. *J Biol Chem*, 2010; 285: 11572-11583.
10. Biamonte, M.A., Wanner, J. and Le Roch, K.G., Recent advances in malaria drug discovery. *Bioorg Med Chem Lett*, 2013; 23: 2829-2843.
11. Prudencio, M., Rodriguez, A., and Mota, M.M., The silent path to thousands of merozoites: the *Plasmodium* liver stage. *Nat Rev Micro*, 2006; 4: 849-856.
12. Tu, Y., The discovery of artemisinin (qinghaosu) and gifts from Chinese medicine. *Nat Med*, 2011; 17: 1217-1220.
13. Guidelines for the treatment of malaria. Third edition, 2015.
14. Hartwig, C.L., et al., Accumulation of artemisinin trioxane derivatives within neutral lipids of *Plasmodium falciparum* malaria parasites is endoperoxide-dependent. *Biochem Pharmacol*, 2009; 77: 322-36.
15. del Pilar Crespo, M., et al., Artemisinin and a series of novel endoperoxide antimalarials exert early effects on digestive vacuole morphology. *Antimicrob Agents Ch*, 2008; 52: 98-109.
16. Leggat, P.A., Trends in antimalarial prescriptions in Australia 2002 to 2005. *J Travel Med*, 2008; 15: 302-306.
17. Fry, M. and Pudney, M., Site of action of the antimalarial hydroxynaphthoquinone, 2-[trans-4-(4'-chlorophenyl) cyclohexyl]-3-hydroxy-1,4-naphthoquinone. *Biochem Pharmacol*, 1992; 43: 1545-1553.
18. Guantai, E. and Chibale, K., How can natural products serve as a viable source of lead compounds for the development of new novel anti-malarials? *Malaria J*, 2011; 10: S2.
19. Boudova, S., et al., The prevalence of malaria at first antenatal visit in Blantyre, Malawi declined following a universal bed net campaign. *Malaria J*, 2015; 14: 422.
20. Mitchell, W., Natural products from synthetic biology. *Curr Opin Chem Biol*, 2011; 15: 505-515.
21. Tcherniuk, S., et al., Anti-malarial effect of semi-synthetic drug amitozynn. *Malaria J*, 2015; 14: 425.
22. Katsuno, K., et al., Hit and lead criteria in drug discovery for infectious diseases of the developing world. *Nat Rev Drug Discov*, 2015; 14: 751-758.
23. Wells, T., Natural products as starting points for future anti-malarial therapies: going back to our roots? *Malaria J*, 2011; 10: S3.
24. Anthony, M., et al., The global pipeline of new medicines for the control and elimination of malaria. *Malaria J*, 2012; 11: 316.
25. Li, J.W.-H. and Vederas, J.C., Drug Discovery and Natural Products: End of an Era or an Endless Frontier? *Science*, 2009; 325: 161-165.

26. Prachayasittikul, V., et al., Computer-Aided Drug Design of Bioactive Natural Products. *Curr Top Med Chem*, 2015; 15: 1780-800.
27. Lei, J. and Zhou, J., A Marine Natural Product Database. *J Chem Inf Comp Sci*, 2002; 42: 742-748.
28. Rottmann, M., et al., Spiroindolones, a new and potent chemotype for the treatment of malaria. *Science*, 2010; 329: 1175-1180.
29. Rottmann, M., et al., Spiroindolones, a potent compound class for the treatment of malaria. *Science*, 2010; 329: 1175-1180.
30. Yeung, B.K.S., et al., Spirotetrahydro β -Carbolines (Spiroindolones): A New Class of Potent and Orally Efficacious Compounds for the Treatment of Malaria. *J Med Chem*, 2010; 53: 5155-5164.
31. Allingham, J.S., Klenchin, V.A. and Rayment, I., Actin-targeting natural products: structures, properties and mechanisms of action. *Cell Mol Life Sci*, 2006; 63: 2119-2134.
32. Pivovarova, A.V., Khaitlina, S.Y. and Levitsky, D.I., Specific cleavage of the DNase-I binding loop dramatically decreases the thermal stability of actin. *Febs J*, 2010; 277: 3812-3822.
33. da Costa, S.R., Okamoto, C.T. and Hamm-Alvarez, S.F., Actin microfilaments et al. - the many components, effectors and regulators of epithelial cell endocytosis. *Adv Drug Deliver Rev*, 2003; 55:1359-1383.
34. Baum, J., et al., Regulation of apicomplexan actin-based motility. *Nat Rev Microbiol*, 2006; 4: 621-628.
35. Oda, T., et al., The nature of the globular- to fibrous-actin transition. *Nature*, 2009; 461: 550-550.
36. Schmitz, S., et al., Malaria parasite actin filaments are very short. *J Mol Biol*, 2005; 349: 113-125.
37. Skillman, K.M., et al., Evolutionarily Divergent, Unstable Filamentous Actin Is Essential for Gliding Motility in Apicomplexan Parasites. *Plos Pathog*, 2011; 7.
38. Wesseling, J.G., Smits, M.A. and Schoenmakers, J.G.G., Extremely Diverged Actin Proteins In *Plasmodium falciparum*. *Mol Biochem Parasit*, 1988; 30: 143-153.
39. Schmitz, S., et al., Malaria Parasite Actin Polymerization and Filament Structure. *J Biol Chem*, 2010; 285: 36577-36585.
40. Baum, J., et al., A malaria parasite formin regulates actin polymerization and localizes to the parasite-erythrocyte moving junction during invasion. *Cell Host Microbe*, 2008; 3: 188-198.
41. Combe, A., et al., TREP, a novel protein necessary for gliding motility of the malaria sporozoite. *Int J Parasitol*, 2009; 39: 489-496.
42. Siden-Kiamos, I., Pinder, J.C. and Louis, C., Involvement of actin and myosins in *Plasmodium berghei* ookinete motility. *Mol Biochem Parasit*, 2006; 150: 308-317.
43. Siden-Kiamos, I., Louis, C. and Matuschewski, K., Evidence for filamentous actin in ookinetes of a malarial parasite. *Mol Biochem Parasit*, 2012; 181:186-9.
44. Sattler, J.M., et al., Actin regulation in the malaria parasite. *Eur J Cell Biol*, 2011; 90: 966-971.
45. Morrisette, N.S. and Sibley, L.D., Cytoskeleton of apicomplexan parasites. *Microbiol Mol Biol R*, 2002; 66: 21-38.
46. Wong, W., et al., Minimal requirements for actin filament disassembly revealed by structural analysis of malaria parasite actin-depolymerizing factor 1. *P Natl Acad Sci USA*, 2011; 108: 9869-9874.
47. Kustermans, G., Piette, J. and Legrand-Poels, S., Actin-targeting natural compounds as tools to study the role of actin cytoskeleton in signal transduction. *Biochem Pharmacol*, 2008; 76: 1310-1322.
48. Pollard, T.D. and Cooper, J.A., Actin, a Central Player in Cell Shape and Movement. *Science*, 2009; 326: 1208-1212.
49. Kudrimoti, S., et al., Semisynthetic latrunculin B analogs: Studies of actin docking support a proposed mechanism for latrunculin bioactivity. *Bioorg Med Chem*, 2009; 17: 7517-7522.

50. Fuerstner, A., et al., Total syntheses of the actin-binding macrolides latrunculin A, B, C, M, S and 16-epi-latrunculin B. *Chem-Eur J*, 2007; 13: 115-134.
51. Fuerstner, A., et al., Latrunculin analogues with improved biological profiles by "diverted total synthesis": Preparation, evaluation, and computational analysis. *Chem-Eur J*, 2007; 13: 135-149.
52. Vilozny, B., et al., A New Dimension to the Biosynthetic Products Isolated from the Sponge *Negombata magnifica*. *J Nat Prod*, 2004; 67: 1055-1057.
53. Nair, U.B., et al., Crystal Structures of Monomeric Actin Bound to Cytochalasin D. *J Mol Biol*, 2008; 384: 848-864.
54. Vedejs, E., et al., Synthesis of the cytochalasin D isoindolone unit: solutions to the problem of regiochemistry in N-benzoylpyrrolinone Diels-Alder reactions. *J Org Chem*, 1982; 47: 1534-1546.
55. Auerbach, J. and Weinreb, S.M., Synthesis of the isoindolone nucleus of the cytochalasins. *J Org Chem*, 1975; 40: 3311-3312.
56. Merifield, E. and Thomas, E.J., Total synthesis of cytochalasin D: total synthesis and full structural assignment of cytochalasin O. *J Chem Soc Perk T 1*, 1999; 3269-3283.
57. Panek, J.S. and Liu, P., Total synthesis of the actin-depolymerizing agent (-)-mycalolide A: Application of chiral silane-based bond construction methodology. *J Am Chem Soc*, 2000; 122: 11090-11097.
58. Pattenden, G., et al., Total synthesis of (-)-ulapualide A, a novel tris-oxazole macrolide from marine nudibranchs, based on some biosynthesis speculation. *Org Biomol Chem*, 2008; 6: 1478-1497.
59. Allingham, J.S., et al., Structures of microfilament destabilizing toxins bound to actin provide insight into toxin design and activity. *P Natl Acad Sci USA*, 2005; 102: 14527-14532.
60. Paterson, I., et al., Total synthesis of (-)-reidispongiolide a, an actin-targeting marine macrolide. *Angew Chem Int Edit*, 2007; 46: 6167-6171.
61. Kigoshi, H., et al., Total Synthesis Of Aplyronine-A, A Potent Antitumor Substance Of Marine Origin. *J Am Chem Soc*, 1994; 116: 7443-7444.
62. Hong, W.P., et al., Synthesis of the C1-C20 and C15-C27 Segments of Aplyronine A. *Org Lett*, 2011; 13: 6342-6345.
63. Kobayashi, K., et al., Toward the Second Generation Synthesis of Aplyronine A: Stereocontrolled Assembly of the C1-C19 Segment by Using an Asymmetric Nozaki-Hiyama-Kishi Coupling. *Org Lett*, 2011; 13: 900-903.
64. Yeung, K.S. and Paterson, I., Actin-binding marine macrolides: Total synthesis and biological importance. *Angew Chem Int Edit*, 2002; 41: 4632-4653.
65. Nicolaou, K.C., et al., Total synthesis of swinholide A. *J Am Chem Soc*, 1996; 118: 3059-3060.
66. Blain, J.C., et al., Two Molecules of Lobophorolide Cooperate to Stabilize an Actin Dimer Using Both Their "Ring" and "Tail" Region. *Chem Biol*, 2010; 17: 802-807.
67. Yadav, J.S. and Chetia, L., Stereoselective total synthesis of bistramide A. *Org Lett*, 2007; 9: 4587-4589.
68. Schueler, H. and Matuschewski, K., Regulation of apicomplexan microfilament dynamics by a minimal set of actin-binding proteins. *Traffic*, 2006; 7: 1433-1439.
69. Anderson, M.O., Shelat, A.A. and Guy, R.K., A solid-phase approach to the phallotoxins: Total synthesis of [Ala⁷] -phalloidin. *J Org Chem*, 2005; 70: 4578-4584.
70. Tannert, R., et al., Solid-phase based total synthesis of Jasplakinolide by ring-closing metathesis. *Chem Commun*, 2009; 1493-1495.
71. Schmauder, A., Sibley, L.D. and Maier, M.E., Total Synthesis and Configurational Assignment of Chondramide A. *Chem-Eur J*, 2010; 16: 4328-4336.
72. Mordant, C., et al., Total synthesis of dolastatin 10 through ruthenium-catalyzed asymmetric hydrogenations. *Tetrahedron*, 2007; 63: 6115-6123.
73. Hanessian, S., Mascitti, V. and Giroux, S., Total synthesis of the cytotoxic cyclodepsipeptide (-)-doliculide: The "ester" effect in acyclic 1,3-induction of deoxypropionates. *P Natl Acad Sci USA*, 2004; 101: 11996-12001.

74. Li, H.M., et al., A Concise Total Synthesis of Amphidinolide T2. *Chem-Eur J*, 2010; 16: 11530-11534.

Chapter 2: Molecular modelling studies on actin inhibition

2.1 Molecular modelling

Molecular modelling involves the development of models of molecular systems, chemical reactions and other phenomena of interest to chemistry. These molecular models are useful to predict and understand properties and quantities that cannot be directly observed experimentally. However, it must be kept in mind that all the computer-generated simulations are based on certain assumptions and approximations, and therefore can only serve as a guide. In recent times, molecular modelling has attracted much attention due to its ability to lead structure guided drug design. Drug design with the understanding of target protein and the possible molecular interactions, help in predicting and understanding the origin of the binding affinity of ligands and also their various possible binding modes. Molecular modelling can also help to understand the differences between the protein residues of different species that leads to specificity in lead drug candidates.

2.2 Homology modelling

It is important to know the 3-dimensional (3D) structure of a protein in order to understand how it binds and interacts with ligands. We also need this information so that an appropriate model can be developed for the molecular dynamics (MD) studies. Such 3D structures are usually obtained by X-ray crystallography or NMR spectroscopy, and in the absence of known structures, one can employ homology modelling using similar protein structures to develop an appropriate model for the MD studies. The basis for homology modelling lies in the fact that the tertiary structure of a protein is more conserved than the amino acid sequence and that the number of stable folds possible at each level in the hierarchical structure of proteins is limited [1]. This implies that 3D structures of closely related homologous proteins can be used to model proteins of unknown tertiary structure [1]. There are various tools available for performing homology modelling such as the Swiss-model web server, Modeller software, 3D-JIGSAW server, CPHmodels server and FAMS server [2].

Since making a homology model involves the determination of a 3D structure of an unknown protein with respect to the known protein, it is important that the protein whose structure will be used as the template and the protein whose structure we wish to predict share a reasonable level of sequence similarity. There is a general consensus that a sequence similarity of at least 35% is

essential in order to develop a reliable model, although greater than 50% similarity leads to models with significantly increased reliability [3].

2.3 Molecular dynamics

MD is an essential element of computational chemistry where Newton's equations of motion are solved for a molecular system after allowing them to interact for a certain amount of time [4]. In other words, MD simulations involve the calculation of instantaneous forces and the consequential movements present in a chemical system [4]. Each particle within the system is considered to be a point mass in accordance with the Born-Oppenheimer approximation in order to increase the efficiency of such calculations.

MD simulations are crucial to the development of an understanding of the structure and function of biological macromolecules from their physical basis, particularly now that our understanding of such molecules has shifted from being one of relatively rigid structures to a more dynamic entity with internal motions and conformational changes [5]. Although computational studies are often not infallible on their own, they are extensively used to propose and test a hypothesis or to compare and confirm experimental data so as to improve the methodology. There are also many examples of computer assisted drug discovery such as cases where MD has revealed the flexibility of an otherwise unavailable binding site [6].

2.4 Results and discussion

The aim of this computational study was to determine the binding interactions of the human and *Plasmodium* actin with latrunculin like compounds. This understanding would help in the design and synthesis of latrunculin analogues with improved affinity and selectivity.

In order to create a homology model of human and *Plasmodium* actin, the first step was to identify a crystal structure of actin with latrunculin bound that would serve as the template. This was achieved by searching the Protein Data Bank (PDB). Although there are a number of crystal structures of actin available in the literature (PDB ID: 1ESV, 1IJJ, 2Q0U), the crystal structure with PDB ID: 2Q0U, a crystal structure of rabbit muscle actin with latrunculin B bound to it, was chosen as the template due to its high resolution [7].

On closer examination of the crystal structure (PDB ID: 2Q0U) it was found that histidine 73 was modified. According to Schmitz *et al.*, methylation of histidine is absent in *Plasmodium falciparum* actin I [8], from which we assumed that methylation of this histidine residue was irrelevant in this study.

Another issue to be resolved before commencing the homology modelling was to ascertain if the latrunculin binding affected the ‘form’ of actin. In other words, actin could be modelled in either its open or closed form, however, it was necessary to understand the impact of latrunculin binding on actin so as to model the correct form. Since the work by Allingham *et al.* (PDB ID: 2Q0U) does not mention which type was represented in the crystal structure, we compared this unknown crystal structure to a known open (PDB ID: 1HLU) [9] and a known closed form (PDB ID: 2BTF) [10]. This comparison was brought about by superimposing both the structures in the Visual Molecular Dynamics (VMD) program. It was revealed that the crystal structure in 2Q0U was in the same form as the crystal structure in 2BTF, thus the actin in PDB ID: 2Q0U is in its closed form.

The PSIPRED program [11] was used to predict the secondary structure of human and *Plasmodium* actin, and to determine the sequence alignment with the template structure. The sequence alignment was confirmed using ClustalW; the sequence alignment is shown in **Figure 2.01**.

The sequence identity between the *Plasmodium* and template sequences was found to be 82%, indicating that the homology model should be very reliable [3]. Surface exposed water molecules surrounding the actin protein were removed from the template, leaving only water molecules within the ligand binding region and those that were buried within the protein. Lastly, the template and the two sequences were used to generate the homology models using the modelling program ‘Modeller’ [12].

The lowest energy homology models of the human and the *Plasmodium* actin were superimposed using the VMD program to visually inspect the models. These models were then subjected to energy minimisation using the program ‘YASARA’ [13]. The simulation cell was defined to extend beyond 5 Å around all atoms, the cell boundaries were set to periodic and the cell filled with water. The YAMBER3 force field was used and the pressure was maintained at 1 bar. The energy-minimised models were then subjected to cell neutralisation and pKa prediction calculations followed by a very short MD simulation of 200 ps. The simulated models obtained were subjected to a final energy minimisation to obtain the models of latrunculin B bound to the human and *Plasmodium* actin. The models were again examined using VMD and the various interactions carefully studied.

could also be seen that the macrocycle is involved in hydrophobic interactions with the hydrophobic residues Pro 32 and Ile 34.

Only two residue differences were identified within 7 Å distance in the binding pocket of the human and the *Plasmodium* actin. The first difference is the replacement of Arg 206 in human actin with a Lys 207 in the *Plasmodium* actin, and the second difference is the replacement of Met 16 in human actin with an Asn 17 in the *Plasmodium* actin. While the ester carbonyl cannot form any hydrogen bonds with the Met 16 in the human actin, the *Plasmodium* actin can engage in hydrogen bonding between the ester carbonyl and Asn 17.

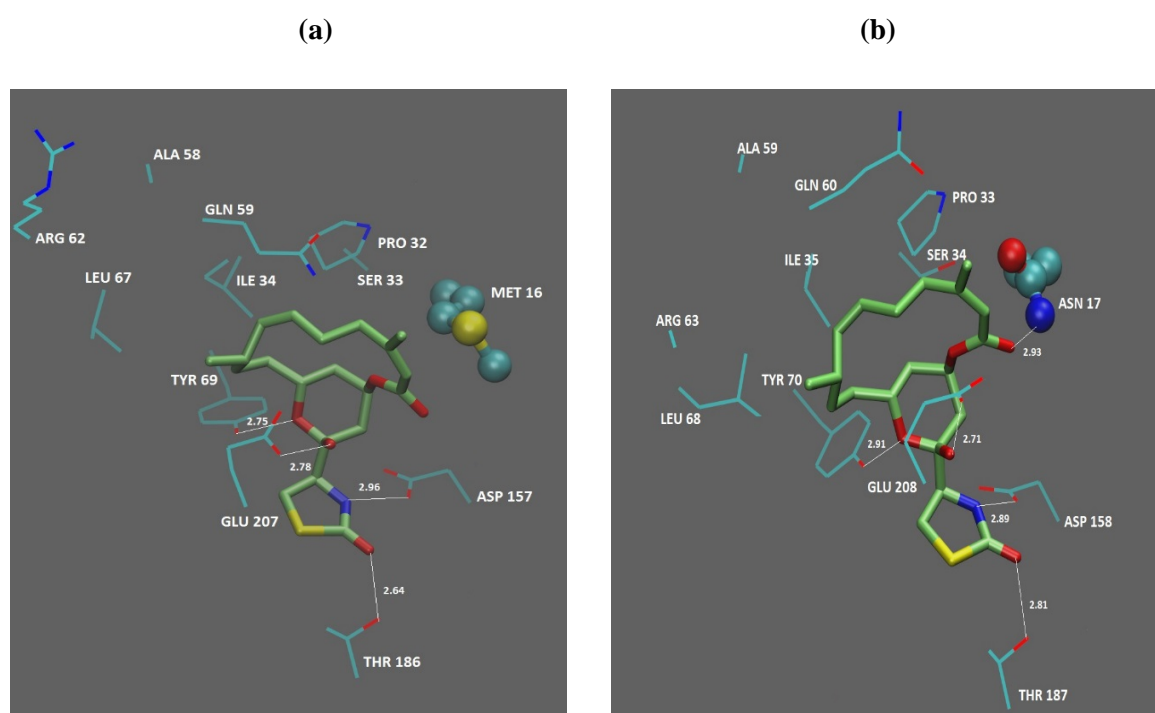


Figure 2.02: Image of latrunculin B bound with the (a) human actin model and (b) *Plasmodium* actin model. Latrunculin B is represented in tube form, the interacting protein residues in stick, and residues Met 16 (in human) and Asn 17 (in *Plasmodium*) in ball and stick. Hydrogen bonds between latrunculin B and the protein are indicated (Ångstrom).

Other interactions observed in the *Plasmodium* actin model are the hydrogen bonding between Glu 208 and the methoxyl group, between Thr 187 and the carbonyl of the thiazolidinone, between Tyr 70 and oxygen of the THP ring and between Asp 158 and the nitrogen of the thiazolidinone ring. As can be seen from **Figure 2.02**, these interactions are conserved in the human actin as well.

2.5 Conclusion

The substrate binding sites of human and *Plasmodium* actin are very similar, however, the few differences identified could be potentially explored to enhance selectivity. Another key feature identified from this computational study is that the key pharmacophores involved in latrunculin binding are within the thiazolidinone and the THP moiety, while the macrocycle is only involved in making hydrophobic interactions to stabilise the ligand in the binding pocket.

2.6 References

1. Sali, A. and Blundell, T.L., Definition of general topological equivalence in protein structures. A procedure involving comparison of properties and relationships through simulated annealing and dynamic programming. *J Mol Biol*, 1990; 212: 403-28.
2. Combet, C., et al., Geno3D: automatic comparative molecular modelling of protein. *Bioinformatics*, 2002; 18: 213-214.
3. Launay, G. and Simonson, T., Homology modelling of protein-protein complexes: a simple method and its possibilities and limitations. *BMC Bioinformatics*, 2008; 9: 427.
4. van Gunsteren, W.F. and Berendsen, H.J.C., *Computer Simulation of Molecular Dynamics: Methodology, Applications, and Perspectives in Chemistry*. Angew Chem Int Edit, 1990; 29: 992-1023.
5. Karplus, M. and McCammon, J.A., Molecular dynamics simulations of biomolecules. *Nat Struct Mol Biol*, 2002; 9: 788-788.
6. Adcock, S.A. and McCammon, J.A., Molecular Dynamics: Survey of Methods for Simulating the Activity of Proteins. *Chem Rev*, 2006; 106: 1589-1615.
7. Allingham, J.S., Miles, C.O. and Rayment, I., A structural basis for regulation of actin polymerization by pectenotoxins. *J Mol Biol*, 2007; 371: 959-70.
8. Schmitz, S., et al., Malaria parasite actin filaments are very short. *J Mol Biol*, 2005; 349: 113-125.
9. Chik, J.K., Lindberg, U. and Schutt, C.E. The Structure of an Open State of β -Actin at 2.65 Å Resolution. *J Mol Biol*, 1996; 263: 607-623.
10. Schutt, C.E., et al., The structure of crystalline profilin–beta-actin. *Nature*, 1993; 365: 810-816.
11. Jones, D.T., Protein secondary structure prediction based on position-specific scoring matrices. *J Mol Biol*, 1999; 292: 195-202.
12. Sali, A. and Blundell, T.L., Comparative protein modelling by satisfaction of spatial restraints. *J Mol Biol*, 1993; 234: 779-815.
13. Venselaar, H., et al., Protein structure analysis of mutations causing inheritable diseases. An e-Science approach with life scientist friendly interfaces. *BMC Bioinformatics*, 2010; 11: 1-10.

Chapter 3: Efforts towards the total synthesis of latrunculin derivatives

3.1 Introduction

Latrunculins are a class of natural products derived from the marine sponge species *Negombata magnifica* and are found in several forms such as latrunculin A, B, C, M and S [1]. Kashman *et al.* in 1980 isolated latrunculin A and latrunculin B (**Figure 3.01**), and characterized them by spectroscopic methods and X-ray diffraction [2, 3]. There has been recent interest in this class of natural products due to their ability to bind to G-actin and thereby preventing it from polymerising [1, 4-7].

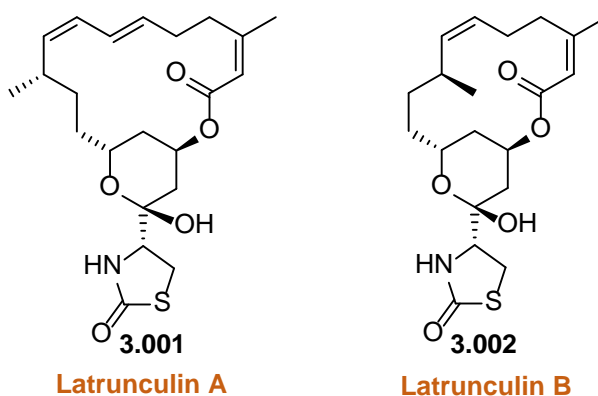


Figure 3.01: Structure of latrunculin A and latrunculin B.

The total synthesis of latrunculin B was first achieved by Smith *et al.* in 1986 [8]. **Figure 3.02** shows the retrosynthetic route followed by Smith *et al.*, which proposes the synthesis of both latrunculin A and B [8]. As can be seen from the figure, Mitsunobu macrolactonisation could be used to form the macrocycle and a Wittig olefination would construct the requisite Z-olefin in both latrunculin natural products. The cyclic ketal moiety **3.004** was accessed by an aldol reaction followed by an acid-mediated cyclisation sequence.

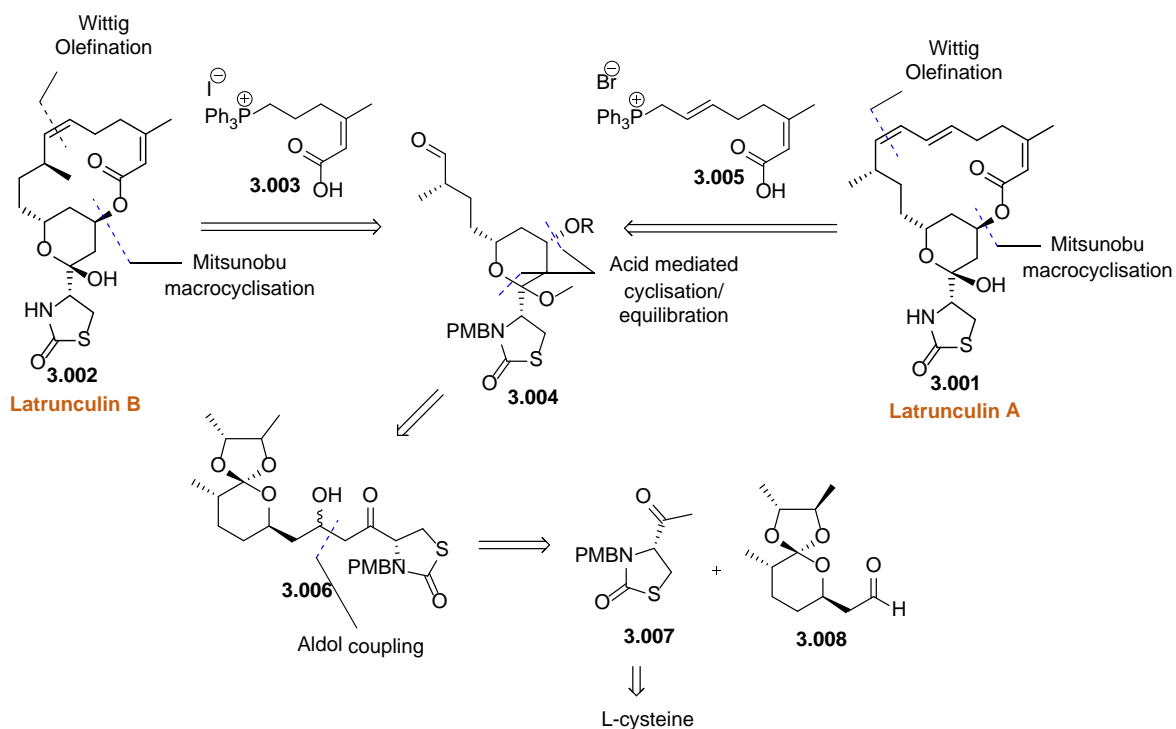


Figure 3.02: Smith's retrosynthetic scheme for the synthesis of latrunculin A and latrunculin B.

In 1990, White *et al.* reported the synthesis of latrunculin A as well as other latrunculin congeners [9, 10]. This scheme utilized a multicomponent reaction sequence developed in their lab to construct the northern hemisphere carbon skeleton in a single step. This involved employing the tandem dienolate addition/Wittig olefination one-pot protocol followed by Mitsunobu macrolactonisation to close the 16-membered lactone in 19 steps as shown in **Figure 3.03**.

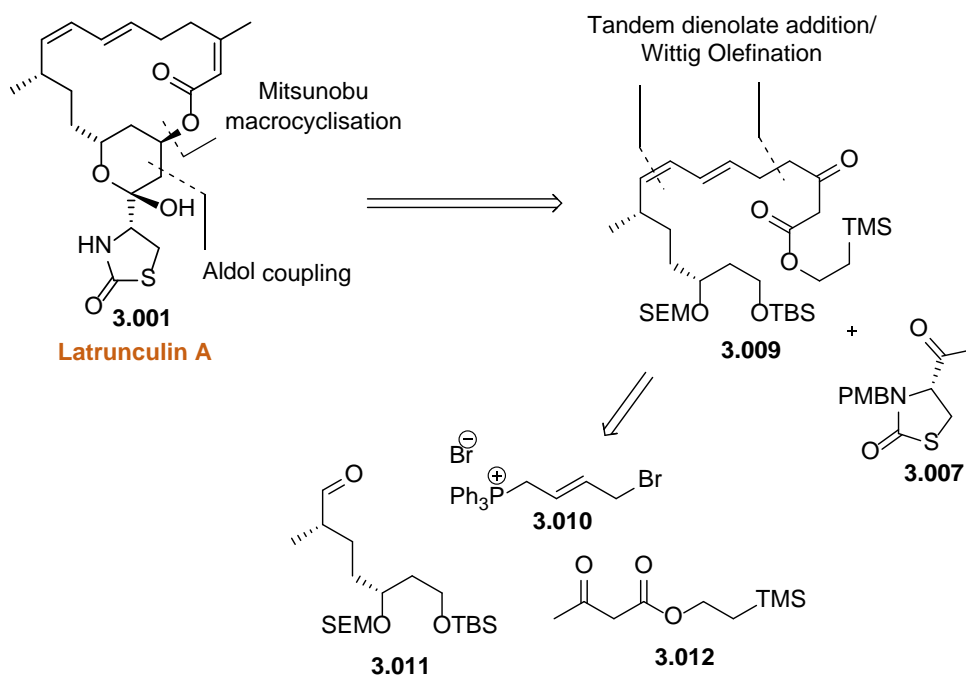


Figure 3.03: White's retrosynthetic analysis of latrunculin A.

In 1990, Smith *et al.*, also successfully synthesised latrunculin A [11] and in 2013, the same group described the total synthesis of (+)-18-*epi*-latrunculol A (**3.013**) [12]. For the synthesis of the (+)-18-*epi*-latrunculol A, late stage stereoinversion using Mitsunobu macrolactonization reaction was employed to form the 16-membered lactone as shown in the **Figure 3.04**. Carreira alkynylation was used to unite the alkyne **3.014** with the aldehyde **3.015** and a Seyferth-Gilbert homologation was employed to construct alkyne **3.014** from alcohol **3.016**. Alkene metathesis was used for the synthesis of the precursor **3.017** of the methoxy ketal.

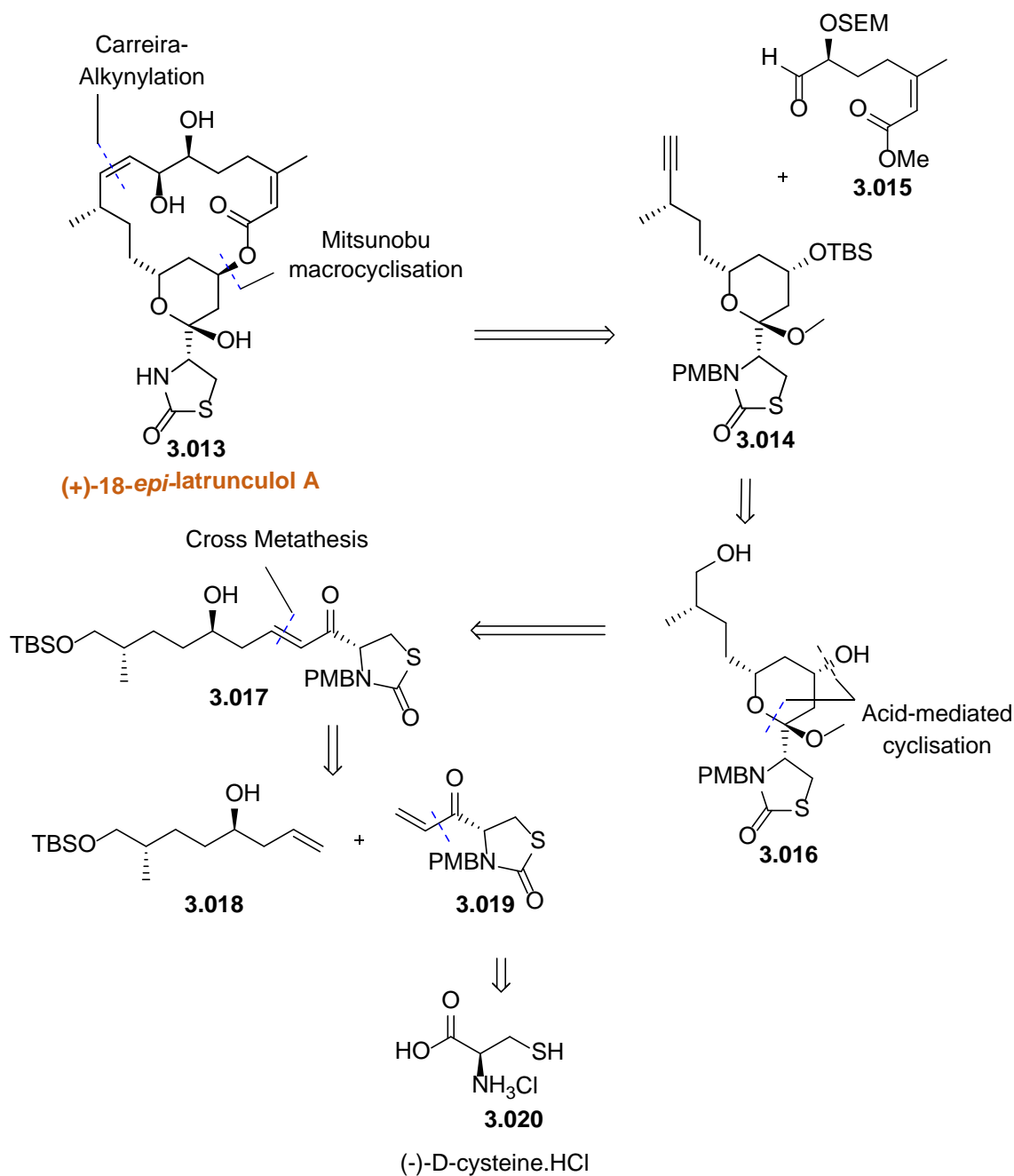


Figure 3.04: Smith's synthetic scheme for the synthesis of (+)-18-epi-latrunculol A.

Fürstner *et al.*, in 2007, also synthesised latrunculins and a number of synthetic derivatives [1, 6]. **Figure 3.05** shows the structure of naturally occurring latrunculin A (**3.001**), latrunculin B (**3.002**) and a synthetic latrunculin B derivative (**3.021**). Fürstner's work demonstrated that latrunculin A (**3.001**) was more potent than latrunculin B (**3.002**) in disrupting the actin microfilaments in NIH3T3 fibroblasts [6]; latrunculin A (**3.001**) reduced the percentage of viable cells by 20% at 1 μM concentration and resulted in 50% reduction at 5 μM concentration [6]. With latrunculin B (**3.002**), a concentration of 1 μM had no effect, while a 5 μM concentration caused 20% reduction

in the number of viable cells [6]. More interestingly, the synthetic latrunculin B derivative (**3.021**) was found to be as potent as latrunculin A [6].

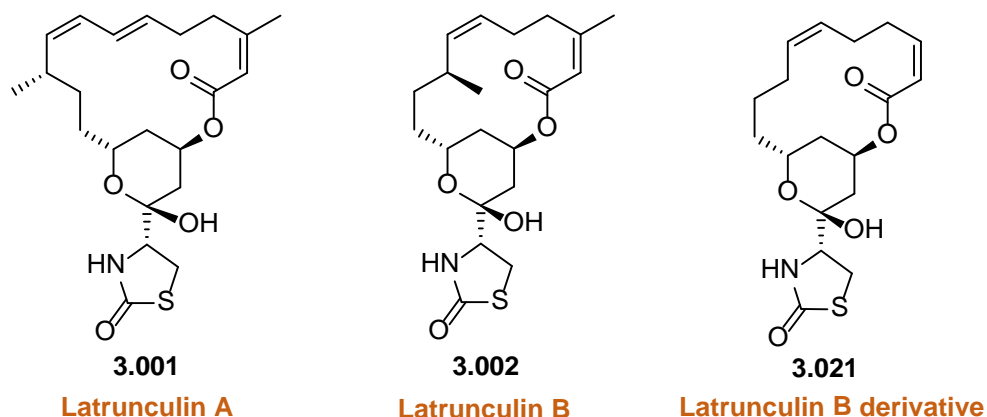


Figure 3.05: Structures of latrunculin A (**3.001**), latrunculin B (**3.002**) and latrunculin B derivative (**3.021**).

The aim of this thesis was to develop latrunculin based actin inhibitors with improved activity and selectivity for *Plasmodium* parasites. Synthesis of the latrunculin B derivative **3.021** was initially undertaken since it is as potent as the naturally occurring latrunculin A. It was also synthetically more accessible since the macrocyclic backbone was more relaxed as it lacked two methyl groups, of which one is chiral [6]. Once obtained, **3.021** could then be derivatised in order to study the SAR and selectivity profile around these compounds.

3.2 Results and Discussion

The latrunculin B derivative, **3.021**, is a complex molecule with a unique thiazolidinone moiety and a macrocyclic ring. In order to synthesise it, Fürstner envisioned a retrosynthetic route [1] (**Figure 3.06**) which proceeds via the synthesis of three building blocks which could then be assembled. The advantage of this scheme was its convergent nature which allowed for the synthesis of analogues easily. With the three main disconnections, as illustrated in **Figure 3.06**, the molecule could be broken down into the left side (Fragment 1) which would be connected to the southern part of the molecule (Fragment 2) using an aldol reaction; the right hand side of the molecule (Fragment 3) could then be introduced by an esterification with the alcohol of Fragments (1+2). Finally, alkyne metathesis could be employed in order to close the macrocycle, which after reduction of the triple

bond and deprotection of the functional groups would give the desired latrunculin B derivative **3.021**.

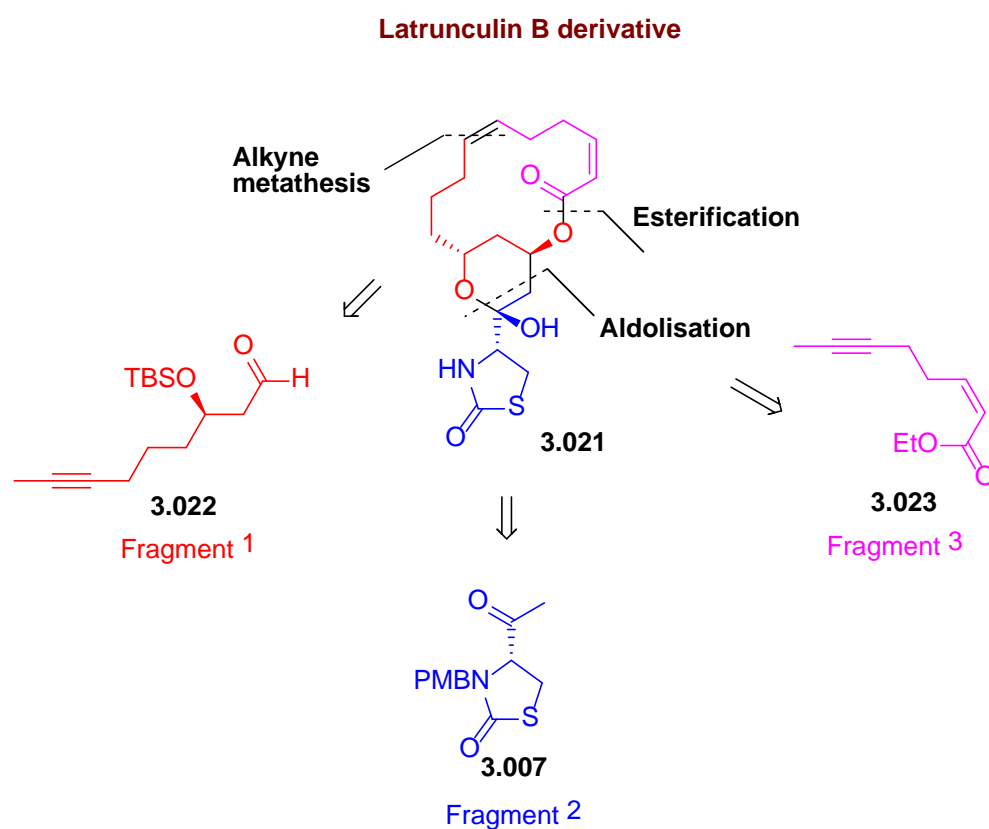


Figure 3.06: Fürstner's retrosynthetic pathway for the synthesis of the latrunculin B derivative **3.021** [1].

3.2.1 Synthesis of Fragment 1

Fragment 1 involved the synthesis of the left hand side of the latrunculin B derivative **3.021**. **Figure 3.07** shows the initial proposed pathway for the synthesis of Fragment 1. Fürstner started the synthesis of Fragment 1 from the aldehyde **3.026**. However, commercially available **3.026** was expensive and not readily available, therefore it was decided to synthesise it. For this, 5-hexyn-1-ol (**3.024**), was alkylated at the terminal alkyne to give the alcohol **3.025**, which was oxidised to the corresponding aldehyde (**3.026**).

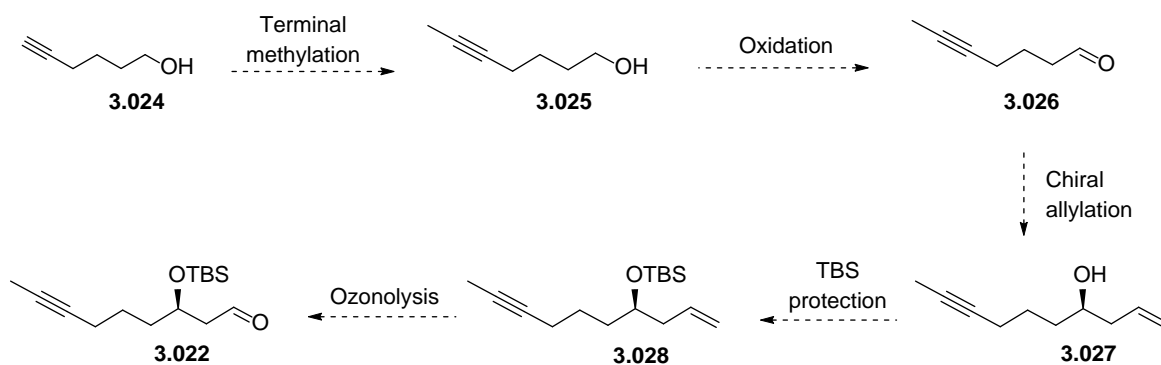


Figure 3.07: The proposed synthesis of Fragment 1 from 5-hexyn-1-ol **3.024**.

The alkylation could be achieved by deprotonating the alkyne using a strong base and then treating with iodomethane [13]. Since deprotonation of the alcohol would be a competing reaction in this case, 2.5 equivalents (eq.) of *n*-BuLi was used for deprotonation to ensure that both the alcohol and alkyne were deprotonated before the addition of 0.95 eq. of iodomethane so that only the terminal alkyne was methylated (since alkyne is more basic than the alkoxide). Nevertheless, it was difficult to obtain selectivity for the alkyne over the alcohol, and therefore this direct route was abandoned. It was decided to first protect the alcohol so that it could not interfere with the deprotonation, and then carry out the terminal alkylation as shown in the revised scheme in **Figure 3.08**.

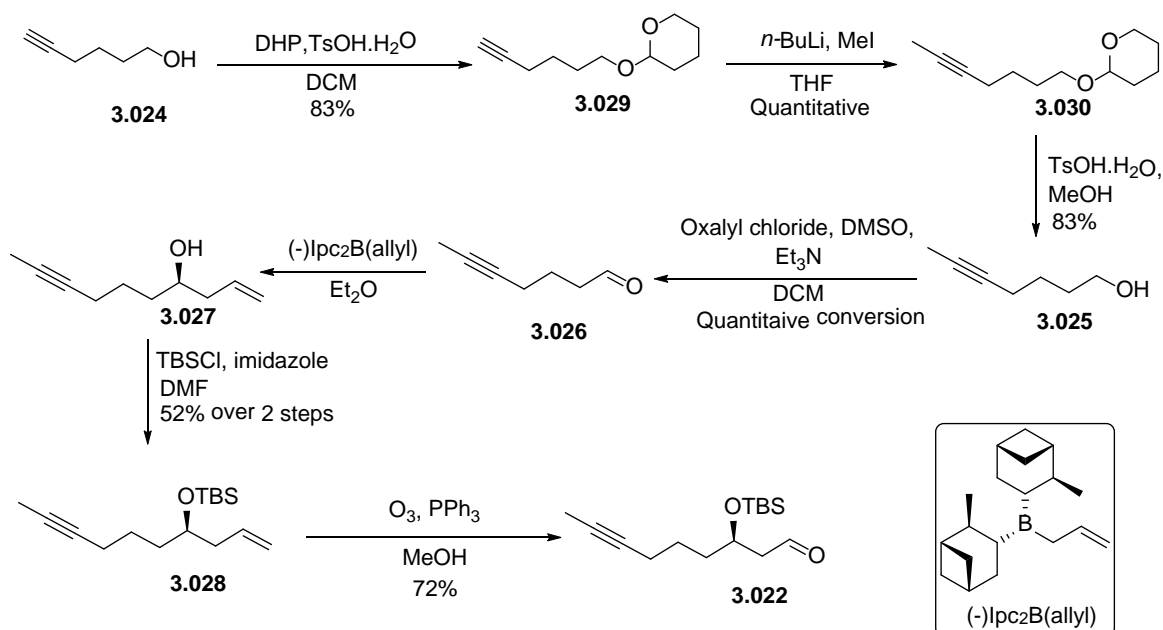


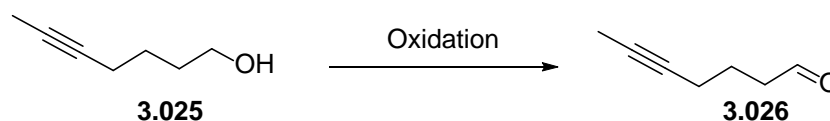
Figure 3.08: Revised scheme for the synthesis of Fragment 1, **3.022**.

Thus the alcohol **3.024**, was protected as a tetrahydropyran (THP) derivative using *p*-toluene sulfonic acid monohydrate and dihydropyran in DCM [14]. The THP protected compound **3.029** was then methylated as shown in **Figure 3.08**. Although this reaction led to the formation of the desired product, a few optimisations were required in order to obtain the product in higher yields. Firstly, the equivalents of *n*-BuLi and iodomethane were increased from 1.2 eq. to 1.5 eq. respectively, to ensure complete deprotonation and methylation. Secondly, after the addition of *n*-BuLi at -78°C and maintaining the reaction mixture at this temperature for 20 mins, the reaction was warmed to 0°C and maintained at 0°C for 1 h in order to obtain complete deprotonation of the alkyne. Once completely deprotonated, the reaction mixture was cooled back to -78°C, before iodomethane was added and stirred for 20 mins, followed by warming the reaction mixture to 0°C until the completion of the reaction. Failure to warm the reaction mixture to 0°C resulted in incomplete conversion resulting in a 1:1 mixture of the starting material (**3.029**) and the product (**3.030**). Once the terminal methylation was achieved, the THP protection was removed using *p*-toluene sulfonic acid monohydrate in methanol to obtain **3.025** in 83% yield [15].

The next step was to oxidise the alcohol **3.025** to the corresponding aldehyde **3.026**. Compound **3.026** was volatile and unstable and thus required a simple and clean method for its generation. Oxidation of alcohols to aldehydes can be achieved by various methods such as Parikh Doering oxidation [16], TEMPO- BAIB oxidation (TEMPO: (2,2,6,6-tetramethylpiperidin-1-yl)oxidanyl,

BAIB: bisacetoxyiodobenzene) [17] or Swern oxidation [18]. **Table 3.01** shows the various oxidation methods trialed for this conversion. The first attempt made was using Parikh Doering oxidation which employs dimethyl sulfoxide (DMSO) as the oxidant activated by the sulphur trioxide pyridine complex in the presence of triethylamine (**Table 3.01**, entry 1). TLC analysis after 2 h indicated that there was no more starting material left and therefore the reaction was quenched and a proton NMR of the crude was obtained. However, the proton NMR spectrum did not correspond to the product or the starting material indicating that the reaction had only led to the formation of undesirable products which could not be identified. Alternatively, TEMPO-BAIB oxidation [17] and Swern oxidation [18] were also trialed. The TEMPO-BAIB oxidation (**Table 3.01**, entry 2) resulted in formation of the product as evidenced by the proton NMR spectrum of the crude, however the reaction did not go to completion as there was starting material evident. The Swern oxidation on the other hand showed complete conversion by TLC analysis and proton NMR analysis and thus was the method of choice for this reaction (**Table 3.01**, entry 3). Due to the instability and volatility of the product, the aldehyde (**3.026**) formed was directly used for the next step without any purification.

Table 3.01: Attempted oxidation reactions for the conversion of alcohol **3.025** to the aldehyde **3.026**.



Entry	Reaction	Conditions	Comment
1	Parikh Doering	DMSO, SO ₃ .Py, Et ₃ N, DCM	Unidentified products
2	TEMPO-BAIB	TEMPO, BAIB, DCM	Incomplete conversion
3	Swern	Oxalyl chloride, DMSO, Et ₃ N, DCM	Complete conversion

The next step involved the allylation of the aldehyde **3.026** to form the chiral alcohol **3.027**, protecting the alcohol formed and then subjecting it to ozonolysis to obtain **3.022**, Fragment 1. Alternatively, it was also possible to use the Mukaiyama aldolisation [19, 20] using vinyloxysilane which would lead to the final aldehyde in one step. Although enantioselective Mukaiyama aldolisation reactions are known [21, 22], the conditions chosen were non-enantioselective since both the isomers formed could be potentially interesting for SAR studies.

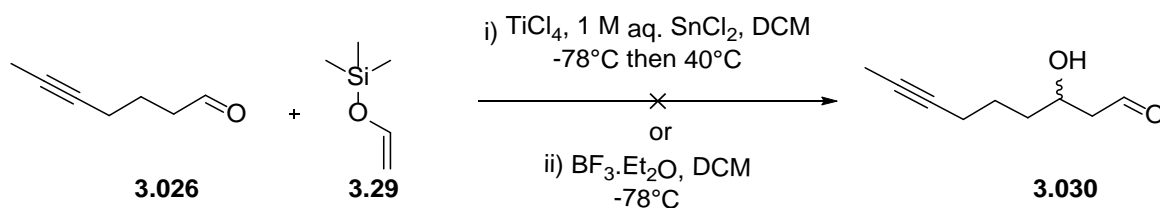


Figure 3.09: Attempted Mukaiyama aldolisation reactions under two different conditions [19, 20].

The Mukaiyama aldolisation was performed under two sets of reaction conditions as shown in **Figure 3.09** [19, 20]. In the first method involving titanium tetrachloride and 1 M aq. stannous chloride [20], the proton NMR of the crude mixture obtained indicated that the desired product was not formed, and instead the reaction had led to the formation of unidentifiable side products. With the second method involving $\text{BF}_3 \cdot \text{Et}_2\text{O}$ [19], the TLC analysis demonstrated the formation of new products however, the reaction did not go to completion. Again, the proton NMR of the crude mixture represented only the presence of undesired products.

Since both the attempts at the Mukaiyama aldolisation did not lead to the formation of the desired products, it was decided to follow Fürstner's scheme and allylate first and then ozonolyse [1]. Allylation can be achieved by several methods [23-25]. However in this particular case, a chiral alcohol needed to be introduced and therefore a chiral allylating agent namely (–)-B-allyldiisopinocampheylborane solution ((–)-Ipc₂B(allyl) borane solution) was used for this conversion as described by Fürstner [1, 26, 27].

The reaction is known as the Brown allylation [27] and proceeds through a Zimmerman-Traxler-type transition state as shown in **Figure 3.10**, the steric hindrance posed by the boron substituents compels the hydrogen of the aldehyde to take the axial position rather than the equatorial position and thus gives the desired configuration to the product.

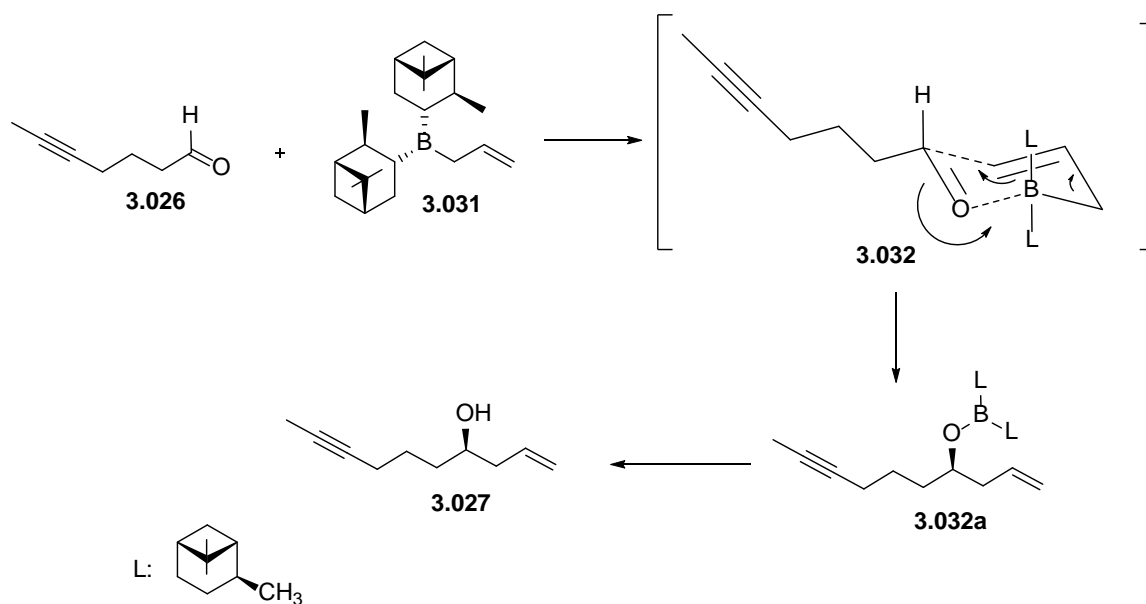


Figure 3.10: Mechanism for the Brown allylation showing the Zimmerman-Traxler-type transition state (**3.032**).

The alcohol **3.027** thus made was found to be slightly impure due to the presence of certain impurities which had the same polarity as the product and were co-eluting during the purification. The alcohol was used for the *tert*-butyldimethylsilyl (TBS) protection and was then purified at this stage. The TBS-protection using TBSCl and imidazole was carried out in DMF and resulted in compound **3.028** in 52% yield over 2 steps. The final step for the synthesis of Fragment 1 involved the conversion of the terminal alkene of compound **3.028** to an aldehyde. This involved breaking the C-C double bond and making a C-O bond and was achieved by an ozonolysis reaction in accordance with Fürstner's synthetic scheme. The product of the ozonolysis depends on the type of work up employed [28]. For example quenching with sodium borohydride gives alcohols, with peroxides the corresponding acids are obtained and with triphenylphosphine (PPh₃) the corresponding aldehyde/ketones are obtained as shown in **Figure 3.11**.

For this reaction, sudan red indicator was added to the TBS-protected compound **3.028** and cooled to -78°C. It was then treated with ozone until the colour of the sudan red indicator disappeared. The reaction mixture was then quenched with PPh₃ to obtain the aldehyde **3.022** in 72% yield.

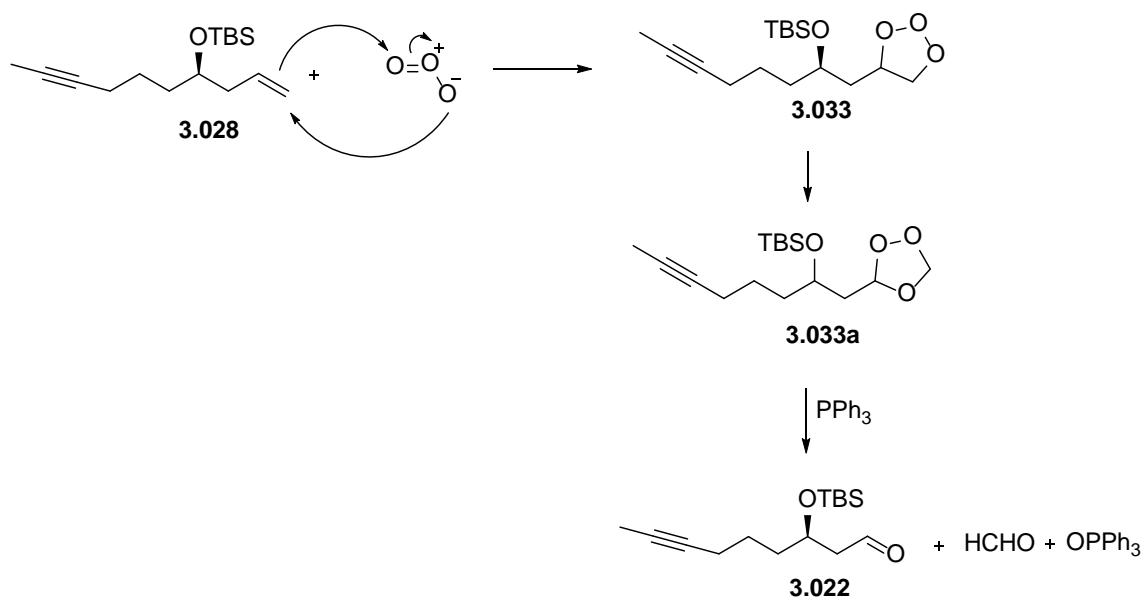


Figure 3.11: Mechanism of ozonolysis [28].

3.2.2 Synthesis of Fragment 2

Fragment 2 involved the synthesis of the ketone **3.007**. The synthesis was performed according to Fürstner's synthetic scheme and involved 4 steps as shown in **Figure 3.12**.

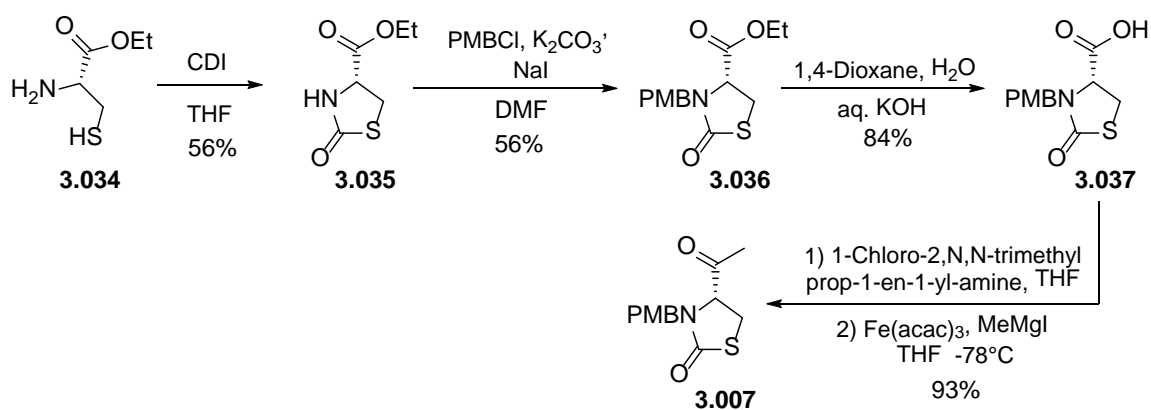


Figure 3.12: Synthetic scheme for the synthesis of Fragment 2.

Fragment 2 was chiral and the (*R*) isomer was required. Commercially available L-cysteine ethyl ester hydrochloride (**3.034**) was used as the starting material so as to have the desired stereochemistry. The first step involved a reaction with carbonyldiimidazole (CDI) in THF which

led to the formation of the five membered thiazolidinone ring in moderate yields. The mechanism of this ring formation using CDI is illustrated in **Figure 3.13**. The free amine of cysteine attacks the carbonyl carbon of CDI. This is followed by the subsequent attack of the sulfur on the same carbon, thereby closing the ring resulting in formation of compound **3.035** as shown in **Figure 3.13**.

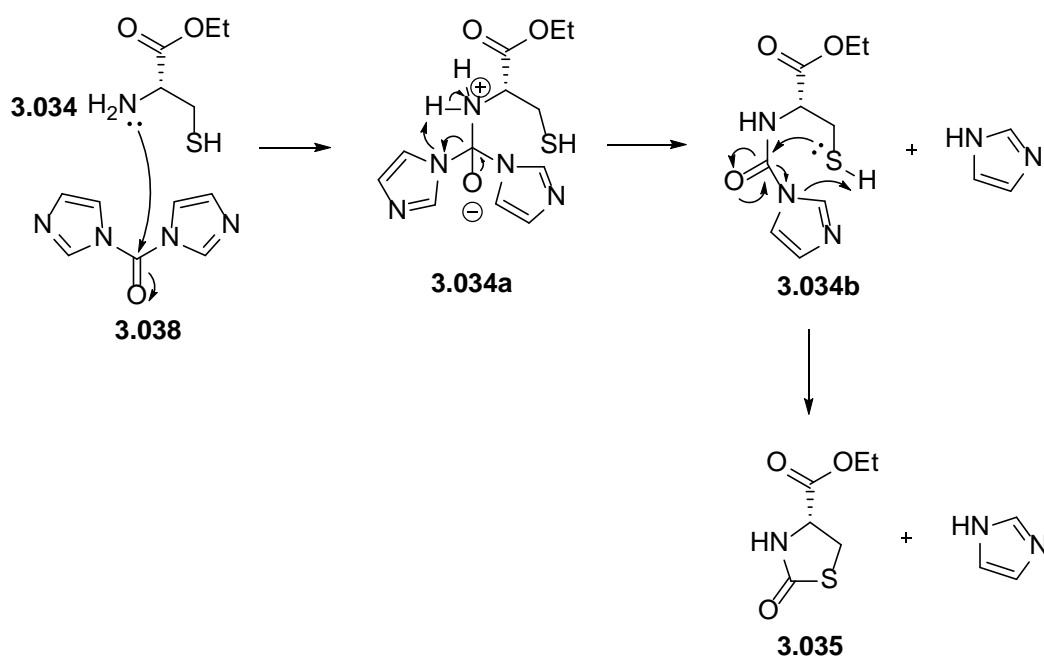


Figure 3.13: Mechanism showing the formation of the five membered ring from the L-cysteine derivative.

The nitrogen of compound **3.035** was then protected with *p*-methoxybenzyl chloride in order to avoid any reaction at this position in the subsequent steps. Being a chloro derivative, compound **3.040** (**Figure 3.14**) was not activated enough and therefore the reactivity was enhanced via an *in situ* Finkelstein reaction with sodium iodide, which produced the more reactive *p*-methoxybenzyl iodide, **3.041** which is much more reactive than the chloro derivative. As can be seen in **Figure 3.14**, only a catalytic amount of the iodine source is required for this reaction as the nucleophile is regenerated.

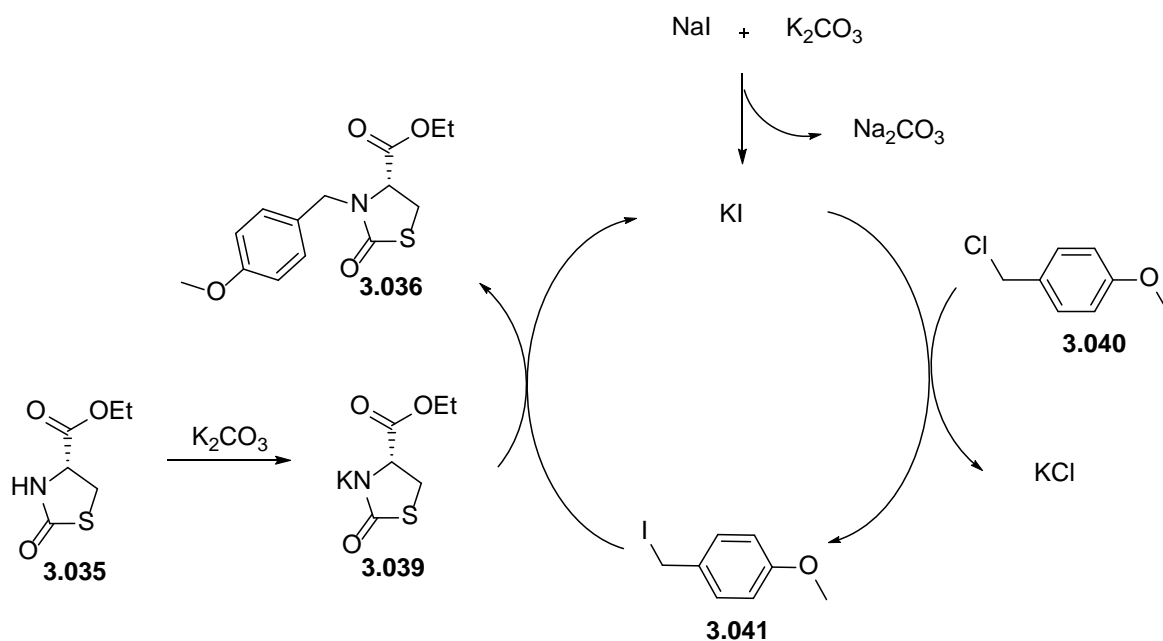


Figure 3.14: Mechanism for the Finkelstein reaction.

The next step was the saponification of the ester **3.036** to give the acid **3.037**. This reaction proceeded smoothly with the TLC analysis indicating completion of reaction within 1 h. The proton NMR spectrum indicated that the crude product was fairly clean and did not require any further purification.

The final step for the synthesis of Fragment 2 was the conversion of the acid **3.037** to the corresponding ketone **3.007**. For this, the acid **3.037** was first converted into the acyl chloride **3.044** and then treated with the methyl Grignard reagent to obtain the ketone **3.007**. For the conversion of the acid to the acyl chloride, Fürstner used 1-chloro-2,*N,N*-trimethyl prop-1-en-1-yl-amine **3.042** as the chlorinating agent (**Figure 3.15**). This reagent, although fairly expensive, works under neutral conditions thereby conserving the optical purity and also with good yields.

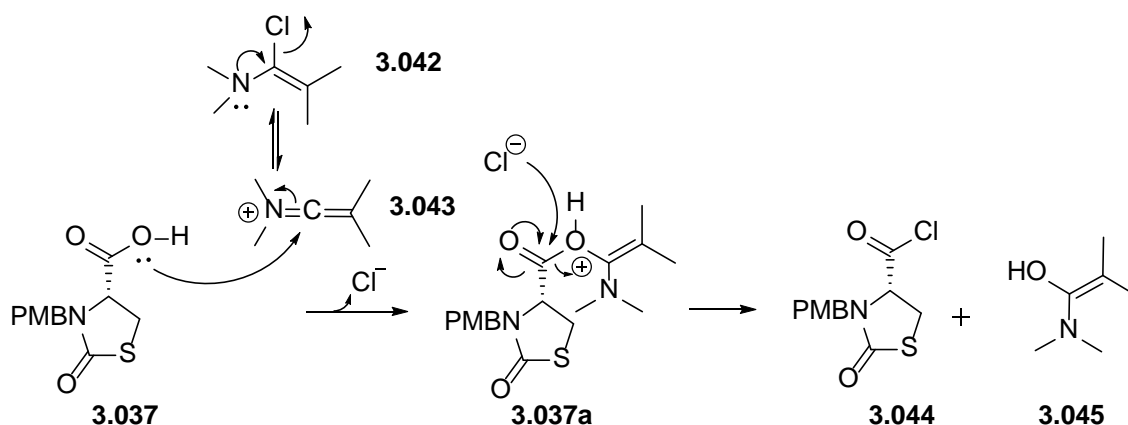


Figure 3.15: Mechanism for the formation of the acid chloride using the chlorinating agent 1-chloro-2,*N,N*-trimethyl prop-1-en-1-yl-amine **3.042**.

It was envisioned that the acid **3.037** could be chlorinated with oxalyl chloride [29], as this would be an economical and fast way of carrying out this reaction. However the yields were poor (22%). Another approach to this was to synthesise the acid fluoride [30] instead of the acid chloride. With this in mind, the fluorinating agent, tetramethylfluoroformamidinium hexafluorophosphate (TFFH) was employed. Analysis of the proton NMR of the crude mixture after work up did not indicate the presence of the desired product and therefore this approach was not pursued.

Fürstner had reported that the final conversion of the acid chloride **3.044** to the ketone **3.007** was more efficient when catalysed with the iron (III) acetylacetonate ($\text{Fe}(\text{acac})_3$) catalyst than when executed uncatalysed or with copper salts [31]. The mechanism for the iron catalysed cross couplings are shown in **Figure 3.16**. It was found that *N,N*-dimethylisobutyramide **3.045** (produced as the by-product during the acid chloride formation), co-elutes with the desired product during column chromatography. It was found that **3.045** was water soluble and was removed by successive washings with water.

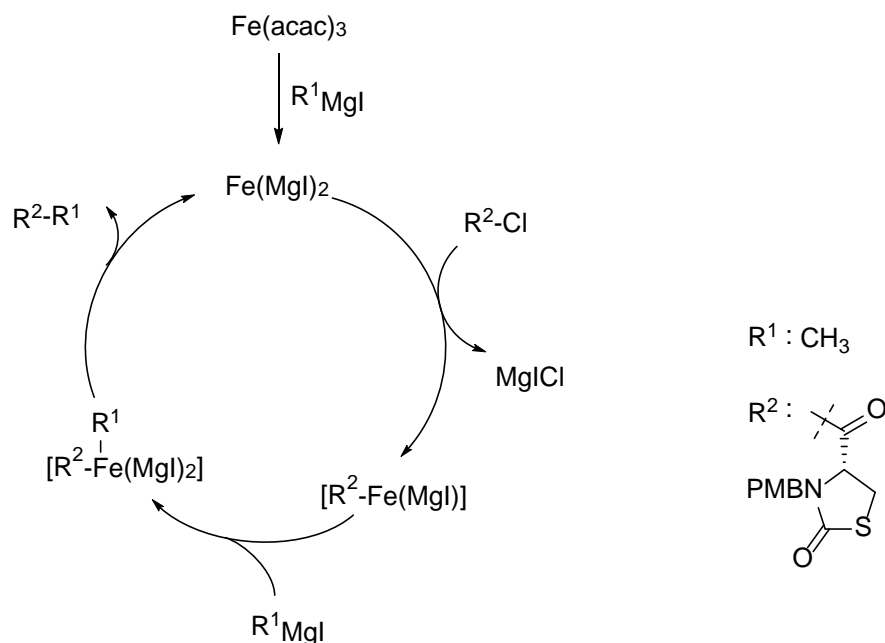


Figure 3.16: The catalytic cycle with $Fe(acac)_3$ which converts an acid chloride into a ketone.

3.2.3 Synthesis of Fragment 3

Fürstner synthesised Fragment 3 by the $Fe(acac)_3$ catalysed reaction of ethyl (Z)-3-chloroacrylate **3.046** and the Grignard reagent **3.047** and then hydrolysing the ester **3.048** to the corresponding acid **3.023** as shown in **Figure 3.17** [6].

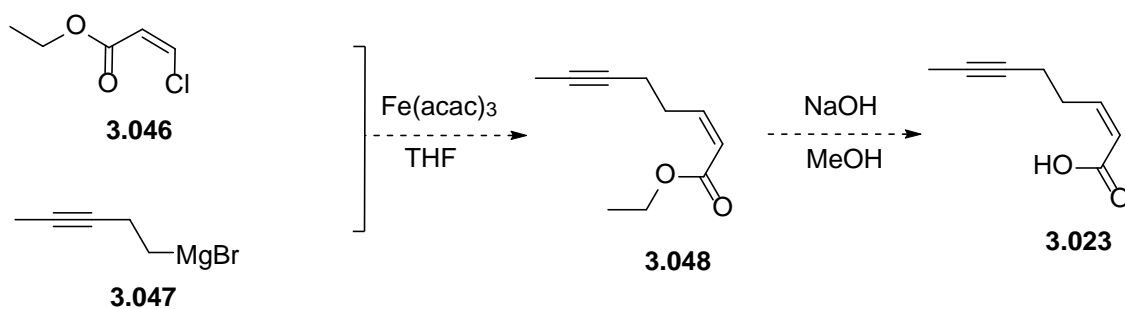


Figure 3.17: Fürstner's synthetic pathway for the synthesis of Fragment 3.

Synthesis of **3.046** has been described as treating ethyl propiolate **3.049** with lithium chloride and acetic acid under reflux conditions to obtain selective chlorination in the *cis* position [1]. However, the reaction was low yielding (15%) due to incomplete conversion and therefore needed

optimisation. The reaction was performed in a sealed tube and heated to 170°C which led to a considerable improvement in the yield (79%) as shown in **Figure 3.18**.

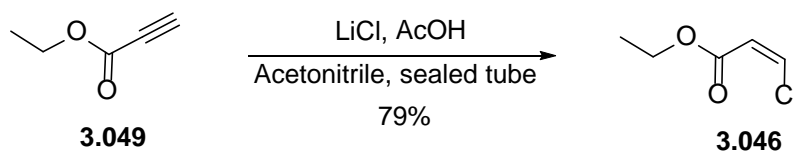


Figure 3.18: Synthesis of ethyl (Z)-3-chloroacrylate.

3.2.3.1 Synthesis of 5-bromopent-2-yne

Fürstner started the synthesis of the Grignard reagent **3.047** with 5-bromopent-2-yne **3.050**, however it was not commercially available and therefore it was necessary to synthesise it. Two different approaches were tried in order to obtain **3.047**.

The first approach was to start from 4-bromobut-1-yne **3.051** and then carry out a terminal alkylation as shown in **Figure 3.19**. For this, the terminal alkyne **3.051** would first be deprotonated with a base and then treated with iodomethane to install the methyl group.

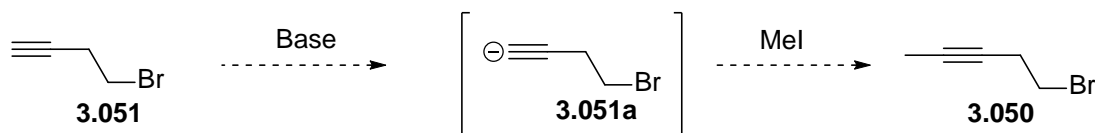


Figure 3.19: Proposed synthesis of 5-bromopent-2-yne **3.050** starting from 4-bromobut-1-yne **3.051**.

A range of different conditions were explored for this transformation as outlined in **Table 3.02**. Firstly, LDA was used as the base (**Table 3.02**, entry 1). It was found that the reaction did not go to completion as evidenced by TLC analysis and resulted in isolation of very little product. The conditions were optimised by stirring the starting material for 1 h at -78°C with LDA and then increasing the temperature to 0°C and maintaining this temperature for another 1 h. The same procedure was also repeated after the addition of iodomethane at -78°C. With this optimisation it was found that the yield of the product formed was improved as the proton NMR spectrum indicated a 1:1 mixture of the starting material and the product.

Secondly, *n*-BuLi was used as the base [32] (**Table 3.02**, entry 2). The procedure involved addition of 1.1 eq. of *n*-BuLi to a solution of starting material in THF at -78°C. The reaction mixture was stirred for 1 h at this temperature before being warmed to 0°C for 1 h. It was again cooled to -78°C when 1.5 eq. of iodomethane was then added and stirred for 1 h. The temperature was again raised to 0°C and maintained at that temperature until the completion of the reaction. TLC analysis indicated that the reaction had gone to completion as no starting material could be observed on the TLC plate, however after work up and extraction it was found that the reaction had led to the formation of an undesirable product since the proton NMR spectrum did not correspond to the desired product.

The third set of conditions used, involved isopropylmagnesium bromide as the base (**Table 3.02**, entry 3). Although the starting material still remained according to the TLC analysis, there were additional compounds present, indicative of the possible product formation. However after work up, the proton NMR spectrum revealed that none of the isolated products were the desired product.

Table 3.02: The conditions trialed for the synthesis of compound **3.050** from 4-bromo-1-butyne **3.051**.

Entry	Reagent/s	Observations
1	Diisopropylamine-Butyl lithium (LDA), THF	1:1 mixture of starting material and product
2	<i>n</i> -BuLi, THF	Undesired product
3	Isopropylmagnesium bromide, THF	Undesired product

Since none of the optimisations described above were ideal for the synthesis of **3.050**, it was decided to consider a different synthetic approach. The alternative route employed was using **3.052** as the starting material and converting the alcohol into the bromo group as shown in **Figure 3.20**.

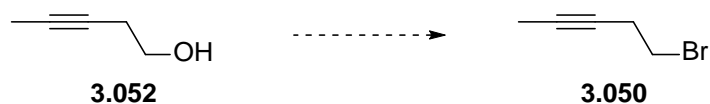


Figure 3.20: Proposed synthesis of 5-bromopent-2-yne **3.050** starting from pent-3-yn-1-ol **3.052**.

The first attempt with this approach was using the Appel reaction [33-35]. Classic Appel reaction conditions involve the conversion of an alcohol to a bromo group using PPh_3 and carbon tetrabromide [33]. The reaction produces the desired product along with two side products namely triphenylphosphine oxide and bromoform. Triphenylphosphine oxide can be removed by adding petroleum benzene to the reaction mixture causing it to precipitate. However, bromoform was difficult to remove using standard purification techniques such as column chromatography. Distillation was also attempted to remove the bromoform, however with the product and bromoform both being volatile and with similar boiling points (142.5°C and 149°C respectively), could not be separated.

It was therefore decided to explore another brominating agent (which would eliminate the formation of bromoform as a by-product) such as *N*-bromosuccinimide (NBS) [15]. TLC analysis of the reaction mixture when 1.1 eq. of NBS was used, indicated that the reaction had not gone to completion and therefore the reaction was repeated with an increased number of equivalents of NBS (1.3 eq.). TLC analysis indicated the complete consumption of starting material and addition of petroleum benzene led to the precipitation of the triphenylphosphine oxide side-product. This was followed by kugelrohr distillation to obtain the desired product in 55% yield as shown in **Figure 3.21**.

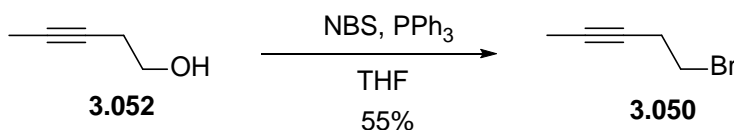


Figure 3.21: Synthesis of 5-bromopent-2-yne using NBS.

3.2.3.2 Synthesis of pent-3-yn-1-ylmagnesium bromide (**3.047**)

The synthesis of pent-3-yn-1-ylmagnesium bromide **3.047** has been described by Fürstner *et al.* using 5-bromopent-2-yne **3.050** as the starting material. However, it was observed that this Grignard formation was difficult and required careful optimisations as described below.

Initially, catalytic amount of iodine was added to magnesium in diethylether and stirred for 1 h. This was followed by addition of the starting material **3.050** as a solution in diethyl ether in order to initiate the reaction as evidenced by an exotherm. It was found that the reaction does not initiate under these conditions. The second attempt at making this Grignard reagent involved heating the reaction mixture to reflux for 2-4 h after the addition of the starting material. It was noticed that such heating did initialize the reaction (as the colour of the reaction mixture changed from brown to milky white), however, this initiation did not sustain for long as no further reaction took place and the magnesium metal was not consumed. Finally, heating the magnesium and iodine in diethyl ether to reflux and maintaining the reflux while the starting material **3.050** was being introduced was tried. It was observed that this procedure not only initiated the reaction but also helped sustain the reaction leading to a complete disappearance of magnesium (an evidence of the Grignard reagent formation). **Figure 3.22** shows the synthesis of the Grignard reagent **3.047**.

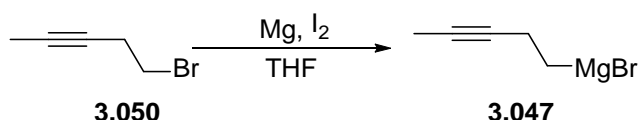


Figure 3.22: Synthesis of the Grignard **3.047**.

Once the Grignard reagent was formed, it was treated with ethyl (Z)-3-chloroacrylate **3.046** using Fe(acac)₃ as the catalyst to obtain ethyl (Z)-oct-2-en-6-ynoate **3.048**. The last step for the synthesis of Fragment 3 involved the hydrolysis of the ester **3.048** to form the desired acid **3.023** using NaOH and methanol in moderate yields (41%) as shown in **Figure 3.23**.

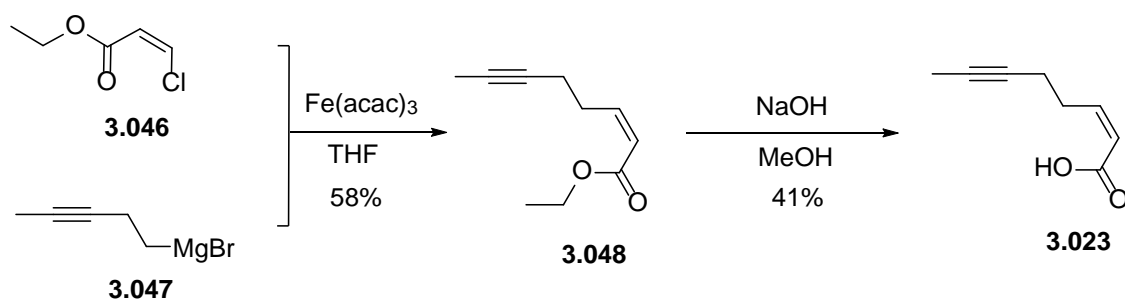


Figure 3.23: Synthesis of Fragment 3.

3.2.4 Coupling of the Fragments

Once the three fragments were synthesised, the next step was to couple them together. Fragments 1 (**3.022**) and 2 (**3.007**) were first joined using an aldol reaction. **Figure 3.24** shows the mechanism of the base induced aldol reaction. A Lewis acid (titanium tetrachloride) was initially added to the ketone (**3.053**) to activate the carbonyl group which then forms the titanium enolate **3.055** in the presence of the base *N,N*-Diisopropylethylamine (DIPEA). The enolate then reacts with the aldehyde **3.057** to form the product **3.058** as an aldol adduct.

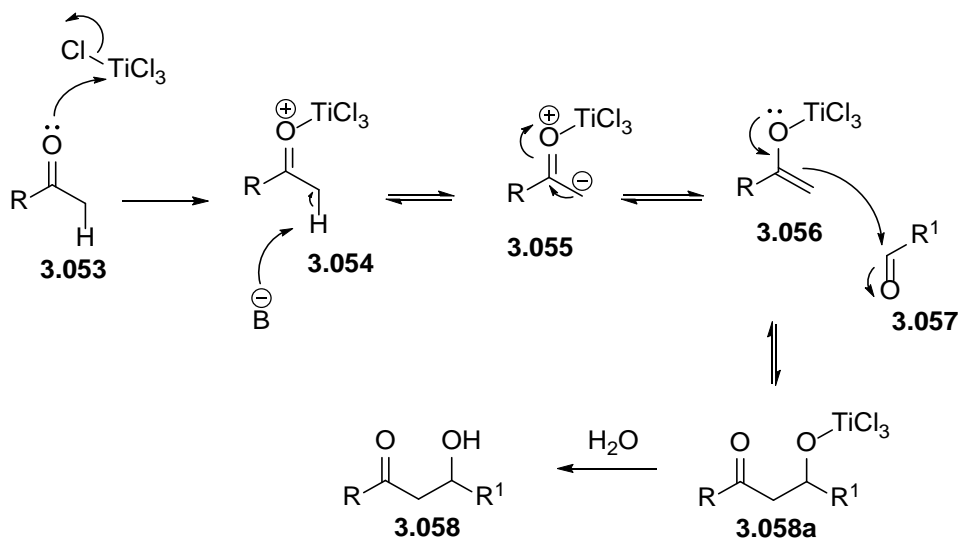


Figure 3.24: Mechanism of the aldol reaction [36].

Figure 3.25 shows the scheme followed for the formation of the aldol adduct, it should be noted that the aldol product was obtained as a mixture of the two diastereomers namely compound **3.059** and **3.060** in a 1.1:1 ratio with 86% overall combined yield. Although Fürstner had described these diastereomers to be separable at this stage, it was found that the two diastereomers had very similar

polarity and thus it was decided to carry them through as a mixture to the next step and separate them later. Thus, the crude material was used directly for the next step which involved the deprotection of the TBS group which leads to spontaneous ring closure forming the hemiacetals **3.061** and **3.062**.

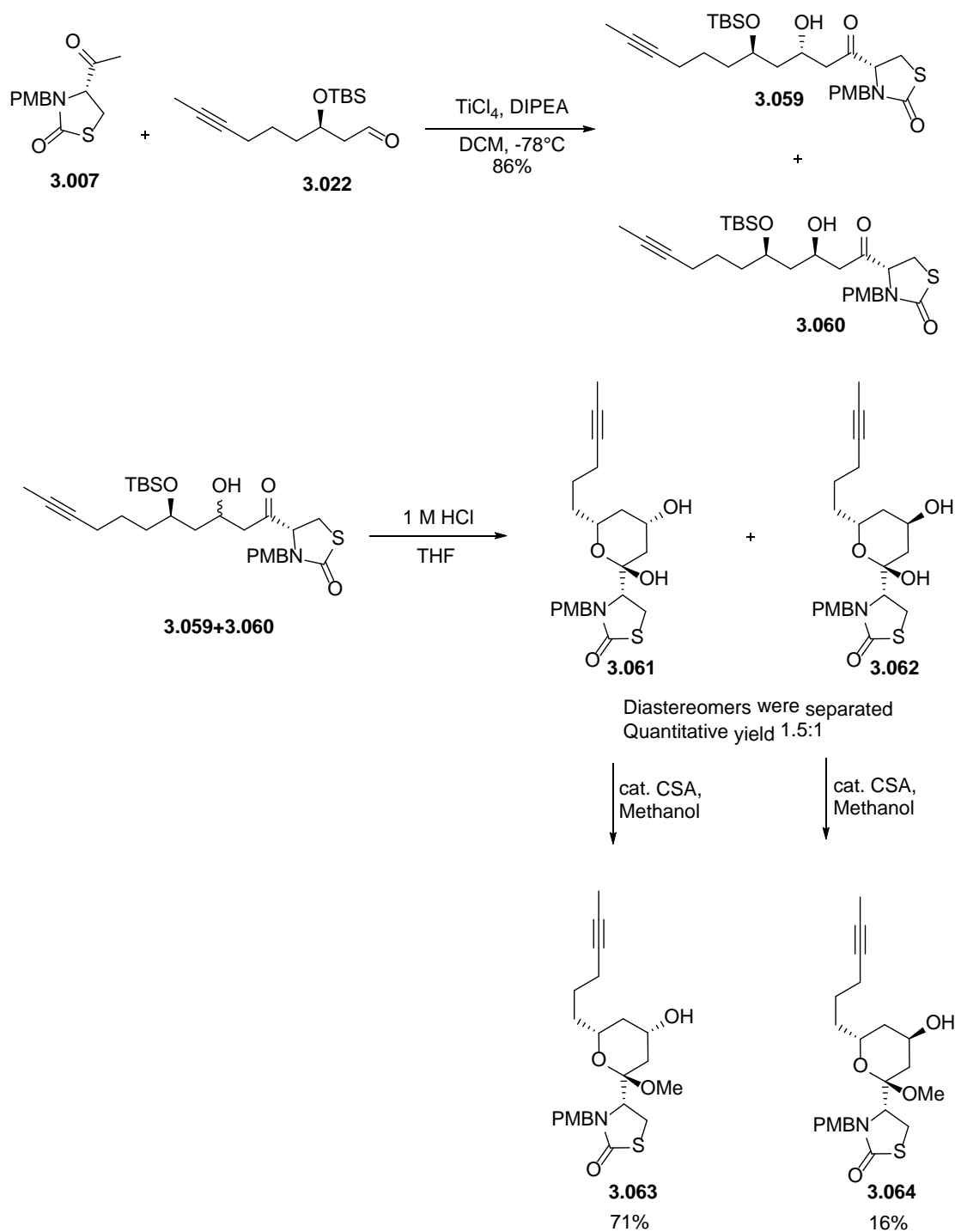


Figure 3.25: The coupling between Fragments 1 and 2.

Figure 3.26 illustrates the mechanism of spontaneous ring closure forming the hemiacetals **3.061** and **3.062**. It was found that the polarity of the two diastereomeric hemiacetals **3.061** and **3.062** were distinct and thus were easily separated by flash chromatography in a 1.5:1 ratio respectively.

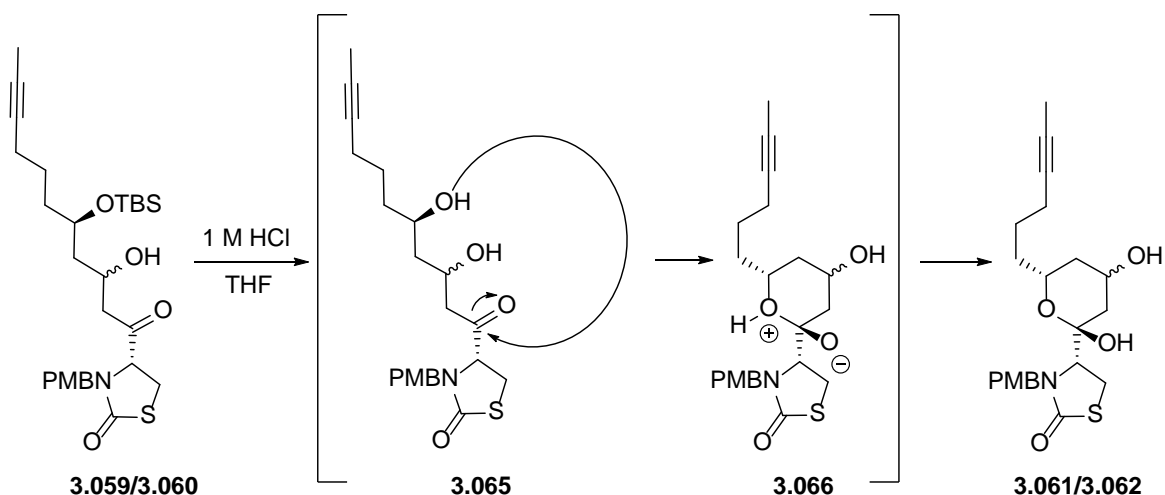


Figure 3.26: TBS-deprotection and spontaneous ring closure leading to the formation of the hemiacetals **3.061** and **3.062**.

The hemiacetals **3.061** and **3.062** were unstable as they have a tendency to ring open and eliminate a water molecule under acidic conditions to form the oxonium **3.068** as shown in **Figure 3.27**.

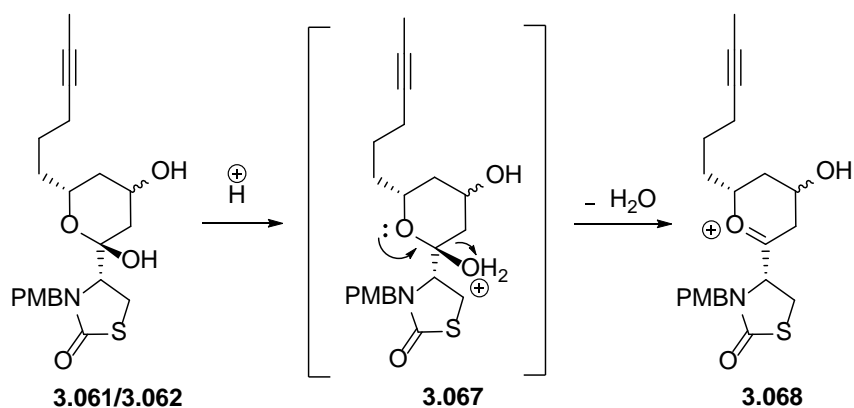


Figure 3.27: Mechanism of formation of oxonium under acidic conditions.

It was therefore chosen to convert the free hydroxyl group of these hemiacetals into a protected form so that they would be more stable. The hemiacetals were therefore separately treated with methanol and catalytic (±) camphorsulfonic acid (CSA) whereby the oxonium **3.068** was formed, and methanol adds to the oxonium to form the acetals **3.063** and **3.064**. Diastereomer **3.063** was the major isomer with 71% yield and **3.064** was the minor isomer with 16% yield (which aligns with Fürstner's findings [1]).

The next step involved the reaction between the acetals (**3.063** and **3.064**) and Fragment 3 (**3.023**). Although the reaction appears to involve a simple ester formation, there were two critical aspects to consider for this reaction as described below:

Firstly, the diastereomer **3.063** obtained in 71% yield was in the *S* configuration at the free hydroxyl position while the minor isomer **3.064** (16% yield), was in the *R* configuration. It should be noted that the final latrunculin B derivative (**3.021**) has the *R* configuration and it was therefore necessary to employ the esterification in such a fashion that the stereochemistry of **3.063** was reversed (such as with an S_N2 process so as to utilise the major diastereomer for the synthesis). Secondly it was important to be aware that Fragment 3 (**3.023**) contained a *cis* double bond. As such, care needed to be taken in order to implement esterification conditions such that the *cis* double bond did not isomerise.

The original attempt was in accordance with Fürstner's method and an S_N2 reaction was performed on the major diastereomer **3.063** via the triflate route as shown in **Figure 3.28** [1]. For this, the methyl acetal **3.063** was first converted into the triflate **3.069** using triflic anhydride and pyridine. The triflate thus formed was directly used to react with the sodium salt of Fragment 3, **3.070** (synthesised by refluxing **3.023** in THF with NaH). 15-Crown-5 ether was then added and stirred overnight. The TLC analysis indicated that the starting material was not consumed as was confirmed by the proton NMR spectrum of the crude mixture. The experiment was repeated however, the results described by Fürstner could not be reproduced.

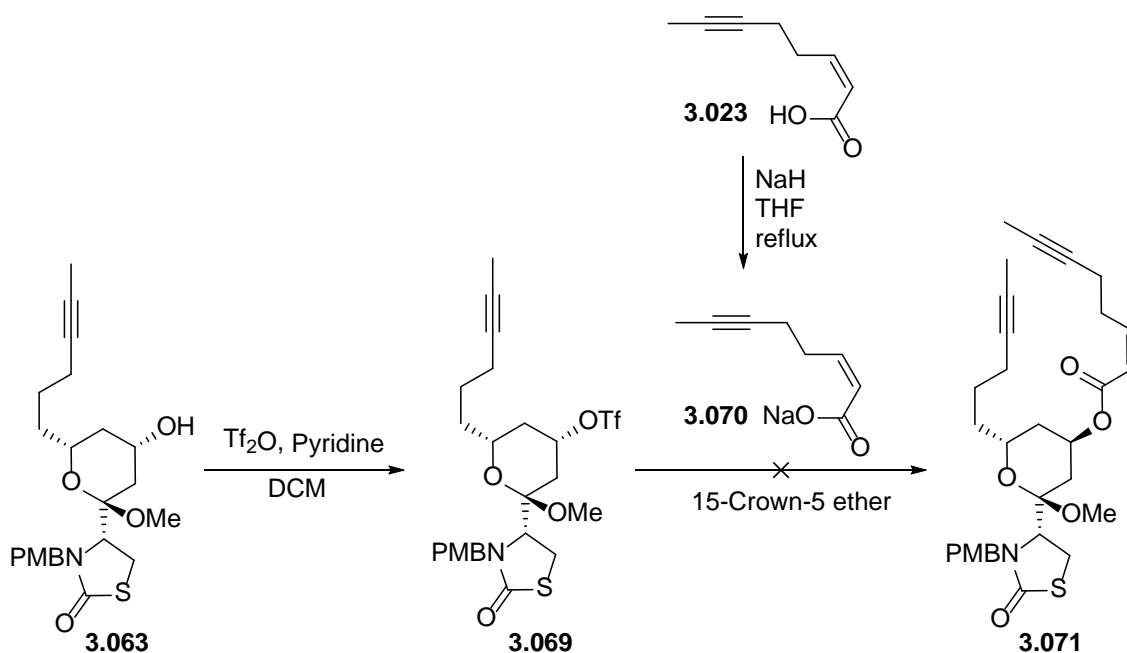


Figure 3.28: Attempted S_N2 type esterification reaction for the synthesis of the diyne **3.071**.

In order to explore the optimisations for this reaction and also to determine the best method for this conversion, it was necessary to do a number of trial reactions. Since the compounds made so far were results of long multi-step schemes, it was decided that the trial reactions would be performed on a model system in order to conserve these intermediates. With this in view, cyclohexanol was chosen as the model system for the acetals **3.063** and **3.064**, and cinnamic acid was chosen as the model acid for Fragment 3 (although cinnamic acid is a *trans* acid unlike **3.023**). The esterification on the model system (shown in **Figure 3.29**) should lead to the formation of the ester **3.074**.

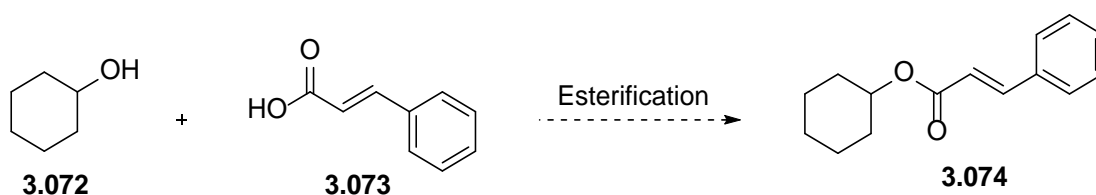


Figure 3.29: Attempts at esterification using the models substrates cyclohexanol and cinnamic acid to obtain the ester **3.074**.

The trials on the model system could be divided into two approaches namely the S_N2 approach and the esterification approach.

3.2.5 The S_N2 approach

The implementation of S_N2 reaction for the formation of the ester would be the preferred method for synthesis of the latrunculin B derivative (**3.021**) since it would enable the utilisation of the major diastereomers **3.063** by inverting the stereocentre during the reaction thereby forming the latrunculin derivative with the desired stereochemistry.

3.2.5.1 Triflate formation

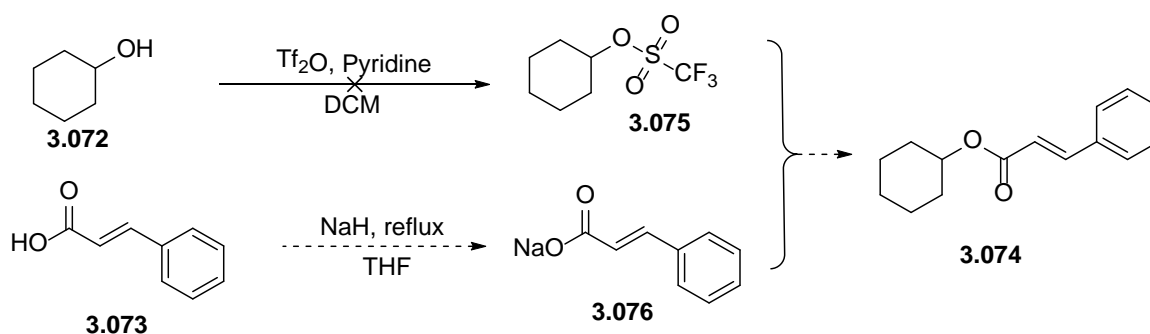


Figure 3.30: Proposed synthesis of ester **3.074** on the model system via the triflate formation method.

The first reaction trialed on the model system was the triflate formation as described by Fürstner. Once formed, the triflate **3.075** was treated with the sodium salt of cinnamic acid **3.076** as shown in **Figure 3.30**. The triflate formation was initially performed at 0°C; although the starting material was completely consumed, the isolated compound was not the desired product as evidenced by proton NMR analysis. Since the temperature can play a crucial role in such reactions [1], it was decided to repeat the reaction at a much lower temperature (-78°C) as this should avoid any undesirable side-reactions. The TLC analysis indicated that the starting material was completely consumed, however the desired product was not formed. The proton NMR spectrum only indicated formation of the some unknown product. Thus the triflate formation attempted at two different temperatures did not lead to the formation of the desired ester even with the model system.

3.2.5.2 Mesylate formation

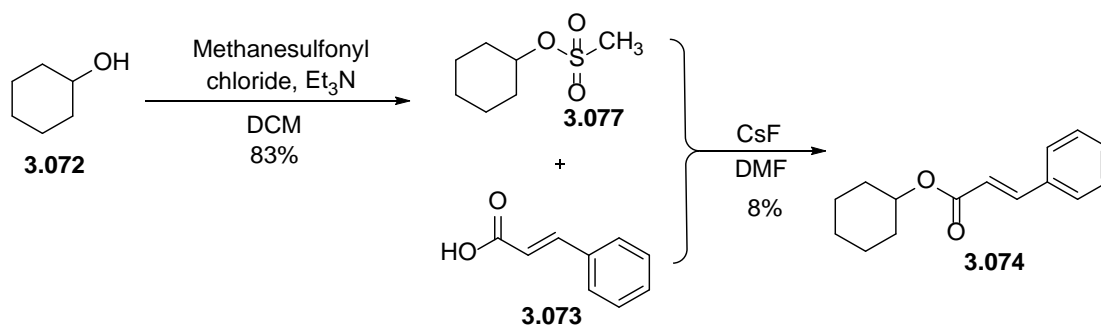


Figure 3.31: Synthesis of the ester **3.074** on the model system via mesylate formation.

Next, it was decided to attempt the same conversion using a mesylate instead of a triflate. It was hypothesised that mesylates being less reactive than triflates, would probably avoid side reactions (such as elimination reactions leading to formation of cyclohexene) and only lead to the desired product. Thus cyclohexanol was treated with methanesulfonyl chloride and triethylamine in DCM at 0°C to form the desired mesylate **3.077** in 83% yield [37]. The mesylate was then treated with cinnamic acid and cesium fluoride in DMF as shown in **Figure 3.31** [38]. The proton NMR analysis confirmed the presence of the desired product, however yield of the reaction was very low (8%) and therefore required optimisation. A summary of all of the optimisations trialed is shown in **Table 3.03**.

Table 3.03: Attempted optimisations for the mesylate method for esterification.

Entry	Acid equivalents	Temperature	Solvent	Additive	Time	Yield
1	5 eq.	90°C	DMF	CsF	8 h	8%
2	5 eq.	120°C	DMF	CsF	8 h	31% crude
3	2 eq.	120°C	DMF	CsF	8 h	39% crude
4	5 eq.	80°C	DCM	CsF	8 h	No reaction
5	5 eq.	80°C	Diethyl ether	CsF	8 h	No reaction
6	5 eq.	80°C	Acetonitrile	CsF	72 h	22% crude
7	5 eq.	120°C	Acetonitrile	CsF	72 h	34% crude
8	5 eq.	90°C	DMA	CsF	72 h	20% crude
9	5 eq.	60°C	THF	TBAF	46 h	trace

The first optimisation trialed involved increasing the temperature to 120°C (**Table 3.03**, entry 2). The TLC analysis displayed complete disappearance of the mesylate, however after extraction the crude material recovered was 31% which was far from ideal since it included the unreacted cinnamic acid. The effect of the number of equivalents of cinnamic acid was also studied. At 120°C with 2 eq. of cinnamic acid (**Table 3.03**, entry 3) the recovery of the crude product was 39% and so it was assumed that changing the equivalents of the acid did not improve the yield of the reaction.

Examination of the effect of the solvent on the yield of the reaction was also investigated (**Table 3.03**, entry 4, 5, 6 and 8). The reaction was repeated with four different solvents namely DCM, diethyl ether, acetonitrile and dimethyl acetamide (DMA) at 80°C. TLC analysis of the reactions in DCM and diethyl ether did not display formation of any new product. With acetonitrile, formation of a new product was visible by TLC analysis, however the reaction did not lead to completion even after stirring for 72 h. The proton NMR spectrum demonstrated the presence of the desired product however the yield of the crude product was still low at 22%. Given this result, the reaction in acetonitrile was repeated at 120°C (**Table 3.03**, entry 7) however it still did not lead to completion as evidenced by TLC analysis and the recovered yield of the crude product was 34%. The reaction with DMA (**Table 3.03**, entry 8) led to a 20% yield of the crude product.

The next optimisation attempted was using tetrabutylammonium fluoride (TBAF) (as a 1 M solution in THF) instead of CsF (**Table 3.03**, entry 8) since TBAF has been shown to bring about effective S_N2 reaction of acids and acid chlorides and therefore was a likely candidate for mesylates as well [39]. The TLC analysis indicated the formation of a new product, although the starting material was not entirely consumed. The proton NMR spectrum of the crude mixture showed the presence of very little product, some starting material and largely unknown impurities, thus this method was also not pursued further.

Despite all of the optimisations detailed in **Table 3.03**, the mesylate method was not ideal due to its poor yield and therefore other conditions needed to be trialed.

3.2.5.3 Tosylate formation

The next route considered, involved the conversion of the alcohol into the corresponding tosyl group which could then be treated with the acid to form the ester **3.074** as shown in **Figure 3.32**. Tosylation was achieved by treating cyclohexanol with *p*-toluenesulfonyl chloride, pyridine and DMAP in 82% yield [40]. The tosylate **3.078** was then treated with cinnamic acid, 1,8-diazabicycloundec-7-ene (DBU) and toluene at 80°C for 4 h. TLC analysis indicated the completion of the reaction however, as with the mesylation, the yield of this reaction was very poor (10%) and was not pursued further.

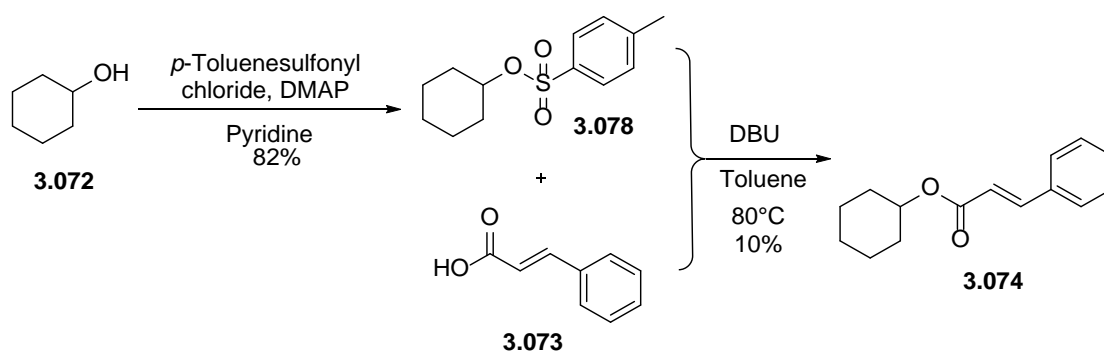


Figure 3.32: Synthesis of ester **3.074** on the model system via the tosylate formation method.

3.2.5.4 Mitsunobu reactions

The Mitsunobu reaction is one of the most widely used methods for coupling an alcohol and an acid using oxidising azo reagents such as diethyl azodicarboxylate (DEAD) or diisopropyl azodicarboxylate (DIAD) and a reducing phosphine such as PPh_3 [41-43]. The versatility,

stereospecificity and mild reaction conditions make Mitsunobu reactions very interesting in organic chemistry [41, 44]. The Mitsunobu reaction, if successful, would be of significance due to its nature to invert chiral alcohols during the reaction [44]. This would mean that the major isomer **3.063** could be utilised for the synthesis of the latrunculin derivative **3.021**. **Figure 3.33** illustrates the mechanism of a Mitsunobu reaction [41-43].

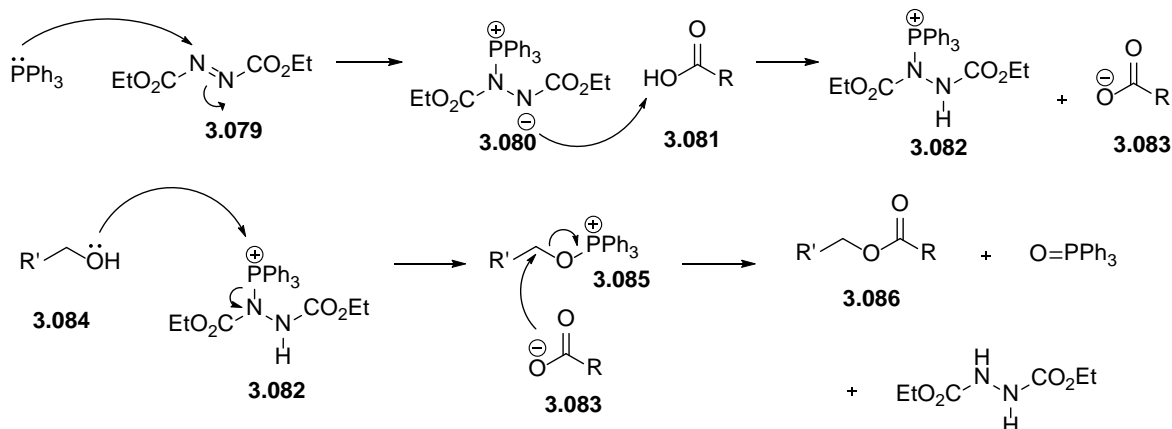


Figure 3.33: Mechanism of Mitsunobu reaction [41-43].

Firstly the PPh_3 adds to the azo reagent (DEAD) **3.079** to form the Morrison-Brunn-Huisgen betaine **3.080**, which being very reactive deprotonates the acid to form **3.082** as shown in **Figure 3.33**. The alcohol can then extract the PPh_3 group to form **3.085** intermediate which reacts with the deprotonated acid to form the ester **3.086** and triphenylphosphine oxide.

The first reaction was performed with cyclohexanol in toluene, to which cinnamic acid (4 eq.), PPh_3 (10 eq.) and DEAD (5 eq.) were successively added at room temperature. The TLC analysis after 8 h indicated consumption of the starting materials and led to the isolation of 33% of the desired product.

In order to optimise the conditions of the Mitsunobu reaction and obtain better yields, various trials were made as outlined in **Table 3.04**. Since only a moderate yield was obtained with DEAD (**Table 3.04**, entry 1), the Mitsunobu reactions were also performed with DIAD. The reaction with DIAD was performed at 0°C , however it failed to go to completion and only starting material was recovered (**Table 3.04**, entry 2). The DIAD was also added at room temperature and the reaction monitored for 96 h (**Table 3.04**, entry 3), yet the TLC analysis of both reactions with DIAD did not indicate the formation of any new product.

Table 3.04: Attempted optimisations for the Mitsunobu reaction.

Entry	Azo reagent	Comment	Yield
1	DEAD	Cinnamic acid (4 eq.), PPh ₃ (10 eq.) and DEAD (5 eq.).	33%
2	DIAD	DIAD, 0°C	Only starting material
3	DIAD	DIAD, room temp., 96 h	Only starting material
4	DIAD	Sonication (30 mins)	17%
5	DEAD	Changed order of addition, sonication (10 mins)	Only starting material
6	DEAD	Changed eq. of PPh ₃ (3.9 eq.) with respect to the acid (4 eq.)	30%
7	DEAD	Changed eq. of PPh ₃ with sonication (15 mins) and increased concentration (2.6 M)	28%

There has been literature evidence for the Mitsunobu reaction being carried out with sonication which works more efficiently than the conventional method [45]. Thus cinnamic acid, cyclohexanol and PPh₃ were taken and sonicated until everything dissolved and the solution becomes clear. DIAD was then slowly added while the solution was being sonicated. The reaction was further sonicated for 15 minutes (**Table 3.04**, entry 4). The TLC analysis indicated the formation of a new product, although the reaction still displayed the presence of the starting material. The reaction was stirred (without sonication) for a further 48 h at room temperature, however there was still no change by TLC analysis. The reaction was quenched and purified to isolate the desired product in 17%.

In order to rule out the effect of the order of addition of the reagents [46], it was decided to change the order of addition (**Table 3.04**, entry 5). Thus the acid and PPh₃ were dissolved in THF and sonicated at 25°C. During this sonication, DEAD was added dropwise and sonicated for a further 10 mins. Acid was then slowly introduced and sonicated for 15 mins. The reaction was then stirred for 12 h at 30°C. The TLC analysis after 12 h still revealed the presence of the starting material and therefore the temperature of the reaction was further increased to 40°C for 5 h. The reaction was then quenched and purified, however there was no product formation as only starting materials could be recovered.

Next it was decided to change the equivalents of the starting material and PPh₃ used with respect to each other, to study if this had any effect on the yield. Thus PPh₃ was used in slightly lower quantity (3.9 eq.) than the acid (4 eq.) (**Table 3.04**, entry 6). The addition of DEAD was also performed at 0°C to avoid any possible side reactions. The reaction was stirred for 8 h at room temperature and then at 40°C for 3 h. TLC analysis indicated formation of a new product and the reaction was quenched and purified to yield the desired product in a 30% yield.

In order to understand if changes in concentration and sonication could improve the yield, the above reaction was repeated with an increased concentration (from 0.12 M to 2.6 M) and sonication for 15 mins (**Table 3.04**, entry 7). The yield however dropped to 17% suggesting that a very high concentration was not ideal for this type of reaction. Since the best yield optimised with the model system was 30%, it was decided to explore esterification approach.

3.2.6 Esterification

The esterification approach was not the method of choice because it would only enable the use of the minor diastereomer **3.064** for the synthesis of the latrunculin B derivative. Nevertheless, in the light of the S_N2 approaches being non ideal, it was essential to explore these conditions to take the synthesis of latrunculin B derivative **3.021** forward.

3.2.6.1 Activated ester

Ester formation via an activated ester route is an established method [47, 48]. This method involves converting the acid into the corresponding activated ester which is a good leaving group and thus readily reacts with alcohols or amines to produce the desired ester or amide respectively. However, this method does not lead to inversion of the stereocenter and therefore only the minor isomer **3.064** could be employed for the synthesis of the latrunculin B derivative **3.021**. An aliphatic model system was explored as it would be better at mimicking the electronics in the acid required for the synthesis of the latrunculin derivative. As such, it was crotonic acid **3.087** that was chosen for this new model system. Various types of activated esters can be formed [47, 48], and in this study we employed the use of *N*-hydroxysuccinimide as was described by Kim, M *et al.* in 2009 [47] to produce **3.089** in 40% yield as shown in **Figure 3.34**.

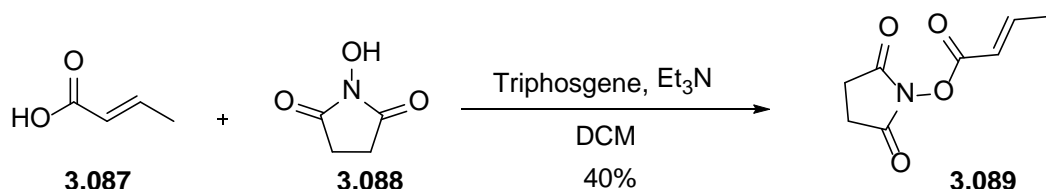
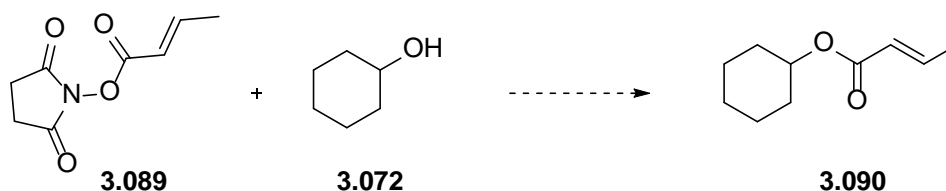


Figure 3.34: Synthesis of the activated ester **3.089**.

The activated ester **3.089** thus produced was then treated with cyclohexanol in 1,4-dioxane and heated to 60°C to effect the esterification. TLC analysis after 1 h indicated that no new product had formed. In order to bring about the esterification, the temperature was increased by 10°C every hour and the reaction was closely monitored by TLC. However, it was found that even at 100°C, there was no reaction. The reaction mixture was then transferred to a sealed tube and heated to 150°C. Heating to such high temperatures led to decomposition of the starting material by TLC analysis. **Table 3.05** outlines a number of conditions trialed for the synthesis of the desired ester.

Table 3.05: Optimisations undertaken for the synthesis of the ester **3.090** via an activated ester



Entry	Condition	Yield/ Comment
1	Heating 150°C (sealed tube)	Decomposition
2	DBU	3% desired product
3	DIPEA	Only starting materials
4	NaH	28% by proton NMR of the crude mixture

Initially exploration of the base in bringing about this reaction was undertaken. The addition of a base would make cyclohexanol a better nucleophile and promote the ester formation. Thus the previous experiment was repeated at 100°C with the non-nucleophilic base DBU (**Table 3.05**, entry 2). However, TLC analysis after 18 h indicated that only starting materials were present. Addition of a further equivalent of DBU and continuing the reaction for 12 h led to the formation of a new

product by TLC analysis, which was confirmed to be the desired ester by proton NMR analysis. However, the yield of the reaction was very poor at ~3%.

Since the introduction of a base led to product formation, a change in base was trialed. Thus the experiment was repeated with DIPEA (**Table 3.05**, entry 3) and NaH (**Table 3.05**, entry 4) as the base. The reaction with DIPEA did not lead to any product formation while the reaction with NaH led to product formation but the yield was still quite low (28% crude) and hence other conditions for the esterification were explored.

3.2.6.2 Acid halide method

Another approach trialed for this esterification was converting the acid into an acyl chloride and then coupling with cyclohexanol as shown in **Figure 3.35**. Both cinnamic acid and crotonic acid were used as substrates for these trials.

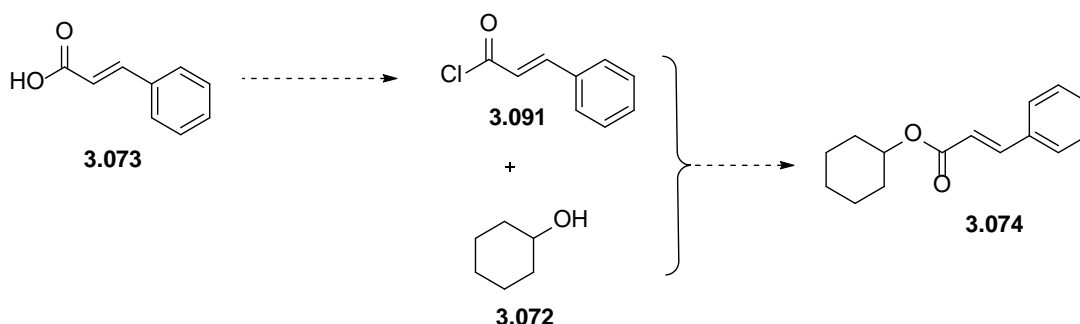


Figure 3.35: Attempted synthesis of the ester **3.074** using the acid chloride method.

There are many methods to synthesise acyl halides as reported in the literature [49-51], as such it was decided to trial a variety of conditions to see which would be most successful. **Table 3.06** outlines the various conditions employed in order to synthesise the acyl halides. Initially, cinnamic acid was treated with oxalyl chloride and catalytic DMF prior to the addition of cyclohexanol (**Table 3.06**, entry 1). Since cinnamic acid was the limiting reagent in this reaction, TLC was performed to visualise its disappearance. The TLC indicated that although some new products were being formed, the acid remained as was confirmed by proton NMR analysis of the crude mixture. Synthesis of the corresponding acid fluoride was also trialed by reaction of cinnamic acid using TFFH (**Table 3.06**, entry 2) [30], but this reaction did not produce any desired product as evidenced by the proton NMR of the crude mixture.

Table 3.06: Optimisations undertaken for the synthesis of the acid chloride.

Entry	Substrate	Condition	Comment
1	Cinnamic acid	Oxalyl chloride, cat. DMF, DCM	Trace amount of product formation
2		TFFH	No product formation
3	Crotonic acid	Oxalyl chloride, DMF, DCM	No product formation
4		TFFH	No product formation

Synthesis of the acid chloride via treatment with oxalyl chloride was repeated with crotonic acid as substrate, and then treated with cyclohexanol (**Table 3.06**, entry 3). The proton NMR spectrum did not indicate the production of the desired product. Synthesis of the acid fluoride [30] was also repeated with crotonic acid, however it did not lead to the desired product (**Table 3.06**, entry 4).

In order to identify whether it was the acid chloride formation that was not working or the coupling with cyclohexanol, it was decided to use commercially available crotonyl chloride instead of crotonic acid to study the coupling reaction. The cyclohexanol was also converted to the corresponding alkoxide before treating with the crotonyl chloride to make the reaction more feasible. **Table 3.07** shows the various attempts made at forming the ester starting from the commercial acid chloride. The alkoxide of cyclohexanol was made using two different bases, namely NaH (**Table 3.07**, entry 1) and DBU (**Table 3.07**, entry 2). Both the alkoxides were then individually treated with crotonyl chloride. The reaction with NaH as the base gave 21% of crude product and was not pursued further. The reaction with DBU led to a 51% yield of the crude mixture which on purification led to the isolation of 24% of the desired product. Thus it was inferred that synthesising the acid chloride did not lead to efficient product formation.

Table 3.07: The various conditions attempted at synthesising an ester starting from an acid chloride.

Entry	Acid chloride	Alcohol	Conditions	Comment
1	Crotonyl chloride	Alkoxide of cyclohexanol formed using NaH	-	21% crude
2		Alkoxide of cyclohexanol formed using DBU	-	24% desired product
3		Cyclohexanol	CuO, acetonitrile, 3 h, room temperature	44% desired product
4			CuO, acetonitrile, 12 h, reflux	74% desired product
5	Cinnamoyl chloride	Cyclohexanol	CuO, acetonitrile, 12 h, reflux	62% desired product

A literature search led to the work by Kim *et al.* in 2009, which described a mild and efficient method for the synthesis of amide bonds in the absence of a base [52]. They also showed that this method could also be used for the synthesis of esters [52]. Although this procedure mainly focuses on aromatic acid chlorides, there was one example with oleoyl chloride (non- conjugated alkyl chain with (Z) double bond) and cyclohexanol leading to 78% of the corresponding ester. Thus it was decided to try this method with crotonyl chloride. The procedure involved treating the acid chloride and the alcohol with CuO as shown in **Figure 3.36**.

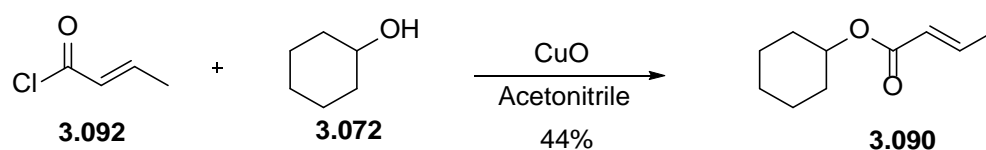


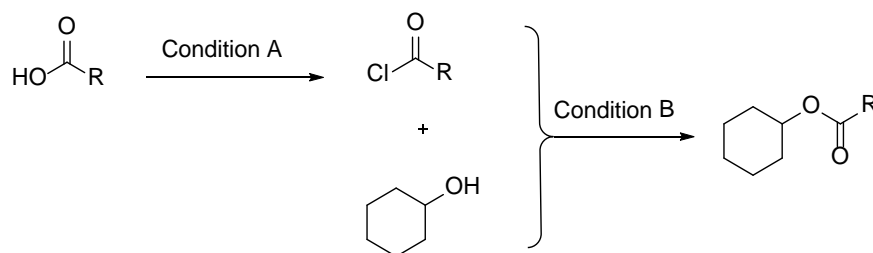
Figure 3.36: Synthesis of ester **3.090** using CuO.

Initially the starting materials were stirred with copper oxide in acetonitrile at room temperature for 3 h (**Table 3.08**, entry 2). This gave 44% of the desired product which looked promising. In an effort to further improve the yield, the reaction mixture was heated to reflux overnight. The increase in temperature and reaction time had a positive effect on the yield as it increased to 74% (**Table**

3.08, entry 4). The procedure was also repeated using cinnamoyl chloride as the starting material and this also gave the desired product in a 62% yield (**Table 3.08**, entry 5).

With this working method at hand, the synthesis needed to be established starting from the crotonic acid, which was first converted into the acid chloride using oxalyl chloride as described earlier and then treating with cyclohexanol using CuO in acetonitrile. However, the proton NMR spectrum of the crude mixture indicated that cyclohexanol was not consumed and no product was formed. From this it was clear that we needed to establish a method to synthesise the acid chloride. **Table 3.09** shows the different conditions chosen to bring about this transformation. Treating crotonic acid with thionyl chloride in pyridine and DCM (**Table 3.09**, entry 2) [53] was also not optimal as it only resulted in a 3% yield of product. The next method trialed was to use neat thionyl chloride under reflux conditions [54-56]. This method gave 58% of the crude cyclohexyl (*E*)-but-2-enoate, which was worth pursuing further. Since there was a possibility that the product could be slightly volatile, and hence show a lower yield, the same procedure was used with cinnamic acid and led to production of cyclohexyl cinnamate in 76% yield.

Table 3.09: Attempts at synthesising the ester by first converting the acid to the corresponding acid chloride and then treating with cyclohexanol using CuO.



Entry	Substrate acid	Condition A	Condition B	Comment
1	Crotonic acid	Oxalyl chloride, DMF, DCM	CuO, acetonitrile, 12 h, reflux	No product
2		SOCl ₂ , pyridine, DCM		<3% product
3		SOCl ₂ , reflux		58% product
4	Cinnamic acid	SOCl ₂ , reflux		76% product

The last issue to address before applying these conditions to the actual system, was to ensure that this method does not cause the double bond of the acid in Fragment 3 (**3.023**) to isomerise. This

was because Fragment 3 has a *cis* double bond which needed to be conserved from isomerising to the *trans* form.

The above procedure (Table 3.09, entry 4) was tried with Fragment 3, and it was found that the reaction worked with a 58% yield. However, upon examining the proton NMR spectrum, it was found that two products had been formed namely the *cis* and the *trans* isomers in 1:3 ratio respectively as shown in Figure 3.37. The *trans* isomer was found to be the major isomer, implying that the *trans* form was the thermodynamically preferred form for the acid under these conditions. Thus, although this method led to esterification occurring in a reasonable yield, the double bond of the acid was isomerised and therefore could not be employed for the actual synthesis of the natural product derivative.

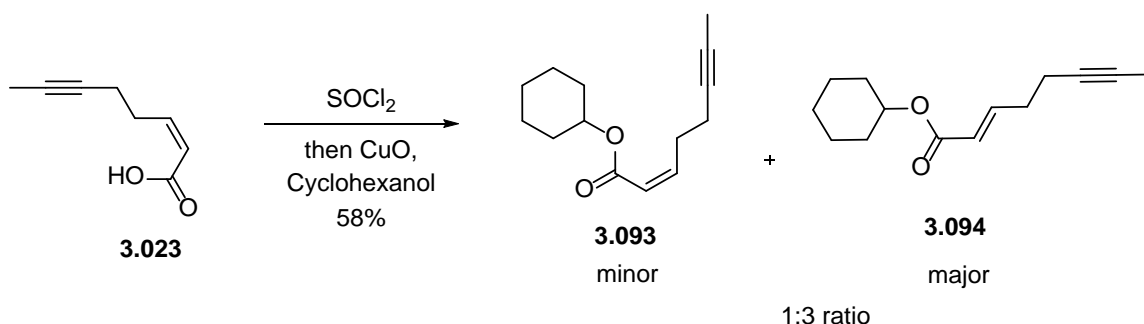


Figure 3.37: Esterification by forming the acid chloride followed by CuO coupling giving the ester in the *cis* and the *trans* form.

At this stage it was not known if the isomerisation of the double bond was during the acid chloride formation or the esterification (using CuO). In order to eliminate the isomerisation during the acid chloride formation, it was necessary to form the acid chloride under neutral conditions. Therefore it was decided to synthesise the acid chloride using 1-chloro-2,*N,N*-trimethyl prop-1-en-1-yl-amine (**3.042**) which is known to chlorinate under neutral conditions [1] and has also been used by Fürstner for the synthesis of Fragment 2 without leading to isomerisation of the chiral centre. The acid chloride thus synthesised was directly treated with cyclohexanol and CuO as shown in Figure 3.38. This procedure however led to the production of only the *trans* isomer as evidenced by the NMR spectrum of the crude mixture. This meant that the isomerisation of the double bond was occurring during the esterification reaction using CuO and therefore this method could not be used for esterification on the actual system.

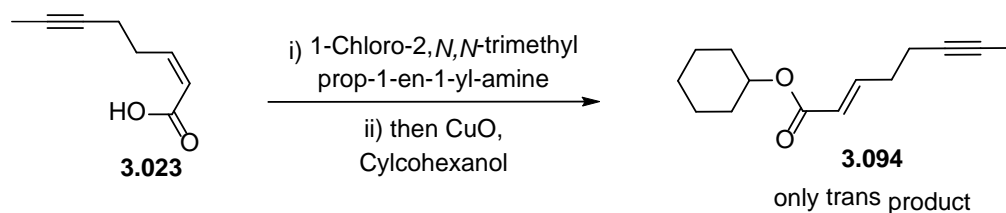


Figure 3.38: Synthesis of acid chloride using the 1-chloro-2,*N,N*-trimethyl prop-1-en-1-yl-amine followed by esterification using CuO leading to the formation of only the *trans* ester **3.094**.

Thus synthesis of latrunculin B derivative **3.021** was found to have numerous challenges which needed to be overcome. It was hoped that eliminating the *cis* double bond from Fragment 3 **3.023** might not only resolve the issue of *cis/trans* isomerisation, but may also enable the successful synthesis of a new latrunculin analogue that was still meaningful in terms of SAR.

3.2.7 Synthesis of saturated latrunculin derivative (**3.096**) via saturated acid (**3.095**)

In order to remove the problem of double bond isomerisation, it was decided to use the saturated acid (oct-6-ynoic acid) **3.095** instead of **3.023** and try and couple compound **3.064** using the CuO method. This change would lead to the synthesis of the new latrunculin derivative **3.096** as the final product (**Figure 3.39**) and not the initially targeted latrunculin B derivative **3.021**.

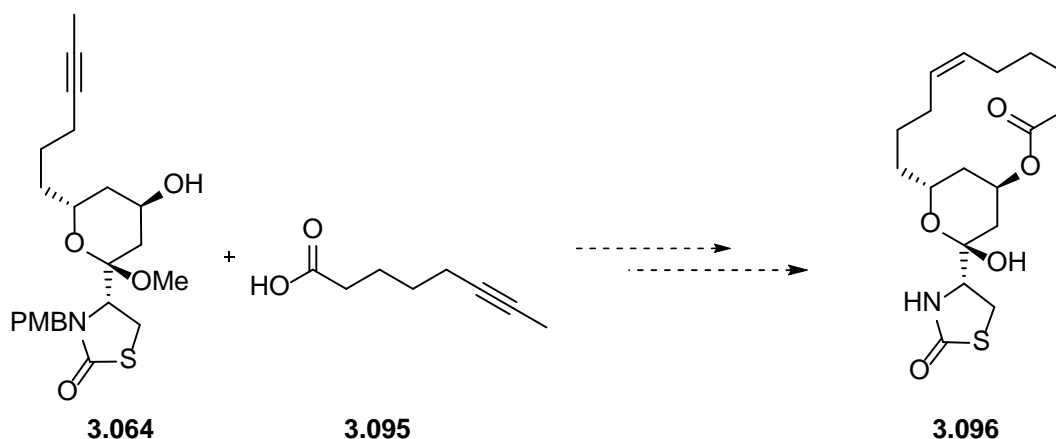


Figure 3.39: Proposed synthesis of new saturated latrunculin derivative **3.096** using the saturated acid **3.095**.

Oct-6-ynoic acid was prepared from the commercially available 6-heptynoic acid using LDA and iodomethane [57] and was then converted to the corresponding acid chloride **3.098** with thionyl chloride as shown in **Figure 3.40**. The acid chloride thus formed was then coupled with compound **3.063** using CuO. It should be noted that compound **3.063** was chosen for this esterification reaction, because as a test reaction it was not necessary to use the right diastereomer (**3.064**) at this stage. However, it was found that the CuO method did not give the desired product in this system. The isolated compounds of this reaction were only starting material and some undesired products. One of the isolated side products represented vinylic protons in the proton NMR spectrum suggesting that it might have been the result of elimination of water from the starting material. Thus, the CuO method could not be used for the actual system even with the saturated acid as the coupling partner. In other words, the CuO method which was identified to be the only promising reaction condition for the esterification reaction from our extensive study on model systems, failed on the actual system.

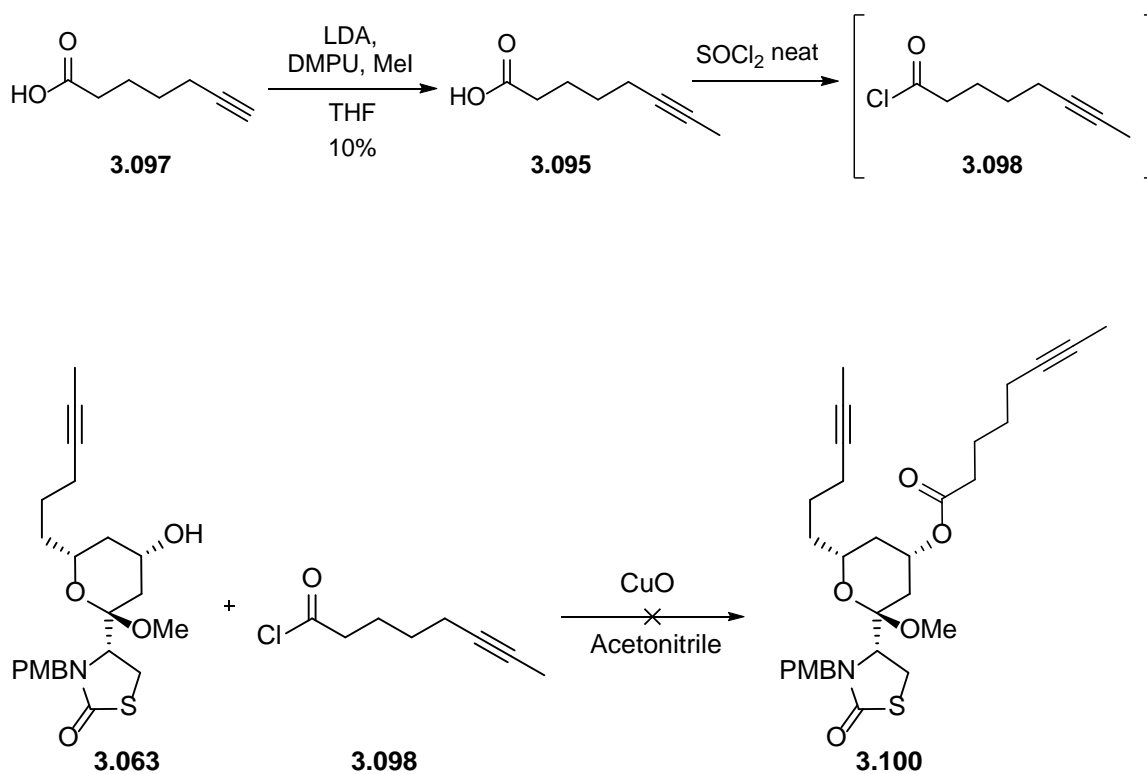


Figure 3.40: Synthesis of the saturated acid component (**3.095**) and the attempted esterification reaction on the actual system using the CuO method.

3.2.7.1 EDCI Coupling

Since the Fragment 3 **3.023** was changed to the saturated **3.095**, there was no longer any need to be concerned about the issue of isomerisation of the double bond. Thus the esterification could now be attempted without any restriction of the type of conditions used. Coupling using EDCI is a very straight forward way of generating an ester linkage [58, 59]. Thus the facile EDCI coupling was used to couple compound **3.063** with oct-6-ynoic acid to generate **3.100** in 63% yield as shown in the **Figure 3.41** [59]. The experiment was also repeated on the minor isomer (**3.064**) and led to formation of **3.101** in 47%.

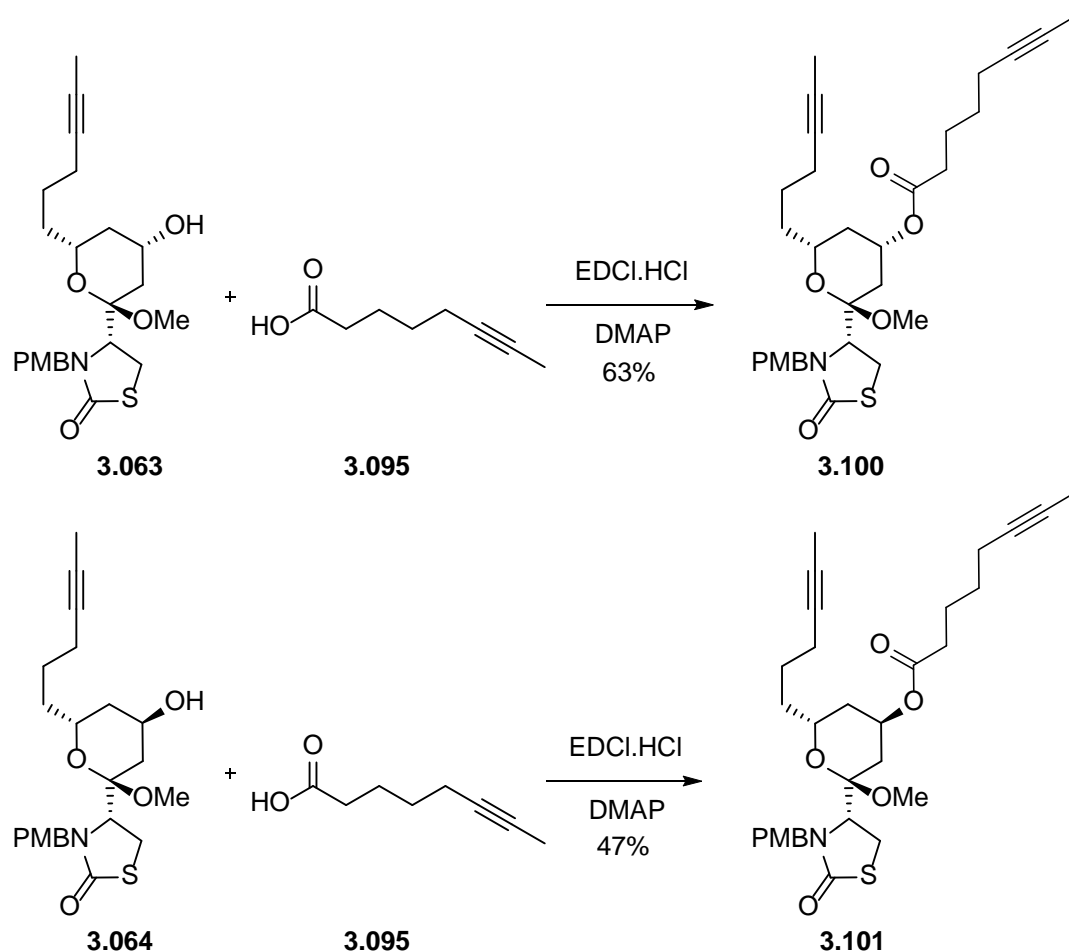


Figure 3.41: EDCI coupling of compounds **3.063** and **3.064** using the saturated acid **3.095**, leading to the formation of the corresponding esters **3.100** and **3.101**.

3.2.7.2 Alkyne Metathesis

Once the esters **3.100** and **3.101** were formed, the next step was to bring the two alkyne chains together using the alkyne metathesis reaction [1]. This would form the macrocycle which would then be reduced to the *Z* double bond and finally treated with CAN to deprotect the PMB and the acetal to form the latrunculin derivative **3.096** [1].

Alkyne metathesis originates from heterogeneous catalysis and is the reaction which involves breaking and making of C-C triple bonds [60, 61]. There are various types of alkyne metathesis such as the alkyne cross metathesis, ring closing alkyne metathesis (RCAM), ring-opening alkyne metathesis polymerisation and the acyclic diyne metathesis polymerisation [61]. In this study we would be employing the RCAM. The generally accepted mechanism of the alkyne metathesis is

shown in **Figure 3.42** [62]. It can be seen that the substrates go through a 4-membered transition state which rearranges and collapses to form the metathesis product.

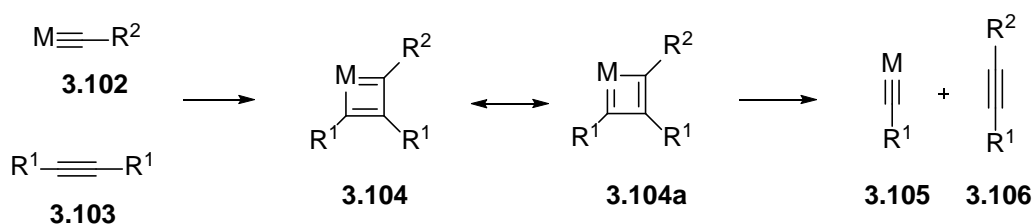


Figure 3.42: Mechanism of alkyne metathesis catalysed by metal alkylidynes [62].

The instability of many of the early alkyne metathesis catalysts, used to be a major hindrance in their use, since handling under rigorous inert conditions or using a glove box might not always be feasible. However, many of the modern catalysts are known to be more stable and some can even be activated *in situ* [62-64].

In this study we attempted the alkyne metathesis using two molybdenum catalysts as shown in **Figure 3.43**. Catalyst **3.109** was an air stable catalyst activated by heating to 80°C [64], while catalyst **3.108** was air sensitive and was therefore used under an argon glove box. Both of these catalysts were used on the ester **3.101** as it had the right stereochemistry required for the ring to form the desired latrunculin analogue **3.095** [1]. It was observed that the RCAM failed with both these catalyst systems as it only led to decomposition of the starting materials.

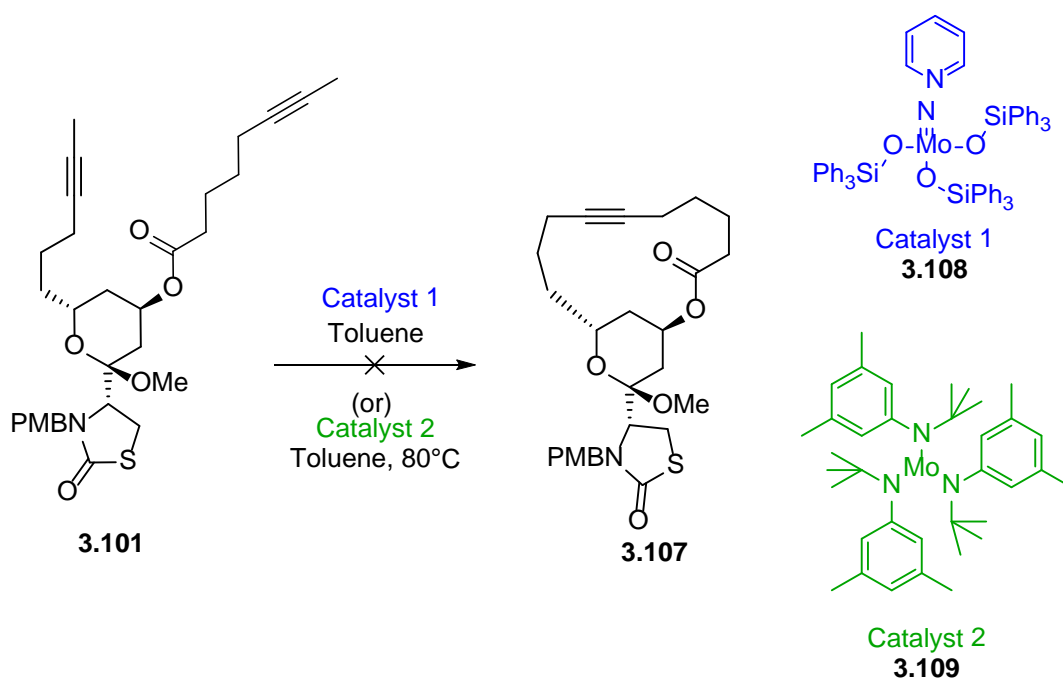


Figure 3.43: Attempted alkyne metathesis reaction on ester **3.101** using two different molybdenum catalysts **3.108** and **3.109**.

In order to rule out the possibility of the unreactivity of the alkyne metathesis as the reason for the failure of this reaction, it was decided to attempt reduction of the two alkyne chains to the corresponding alkenes and then proceed with the much more established alkene metathesis route to form the macrocycle as shown in **Figure 3.44** [65, 66]. This method would have the same number of steps as the alkyne metathesis since the reduction of the triple bond necessary for the synthesis of the latrunculin derivative would not be required anymore.

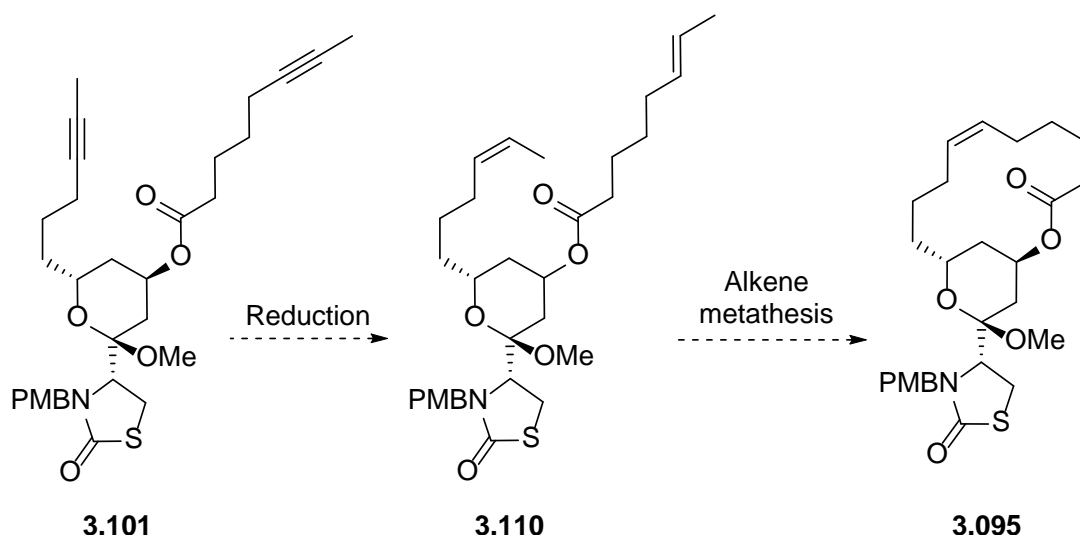


Figure 3.44: Proposed formation of the macrocycle by reducing the triple bond to double bond, followed by ring closing by using alkene metathesis.

With this in mind the reduction was explored as summarised in **Table 3.10**. The first attempt was to reduce using Lindlar catalyst in DCM (**Table 3.10**, entry 1) [1]. The reaction did not lead to reduction of the triple bond and only starting material could be recovered from this reaction. The second attempt employed the same conditions but changed the solvent to methanol (as alcohols are well reported solvent for hydrogenations [67, 68]) (**Table 3.10**, entry 2). This was also not successful, and only starting material could be recovered. The final attempt made at this reduction was using sodium borohydride, nickel(II)acetate and ethylenediamine (**Table 3.10**, entry 3). As with the other attempts, this reaction also did not yield the desired product and only the starting material was recovered. Thus it was understood that the reduction of the alkyne on compound **3.101** was not feasible under these conditions. In the interest of time, this approach was not pursued any further.

Table 3.10: Different conditions attempted for the reduction of the two alkyne groups of compound **3.101** to the corresponding alkene compound **3.110**.

Entry	Conditions	Comment
1	Pd/ CaCO ₃ , DCM, H ₂ gas	Only starting material was recovered
2	Pd/ CaCO ₃ , MeOH, H ₂ gas	
3	NaBH ₄ , Ni(OAc) ₂ , H ₂ gas Ethylenediamine, EtOH	

Another likely reason for the failure of the alkyne metathesis reaction could be the absence of the Z double bond in the saturated Fragment 3. In other words, the presence of the Z double bond may be essential in order to orientate the rest of the alkyne chain in the direction of the other alkyne, bringing the two alkyne chains close to each other. In the absence of such orientation (as in the case of the saturated Fragment 3), the two alkyne chains may be too far away and the metathesis conditions may not be forcing enough to bring them together so as to effect the bond formation.

Thus it is probably necessary to have a Z double bond to orient the rest of the alkyne chain of fragment 3 in a particular direction, however, the presence of the Z double bond meant that the esterification reaction was not feasible. In order to resolve both of these issues, it was decided to employ a phenyl ring fused at the Z double bond position instead, as shown in **Figure 3.45**.

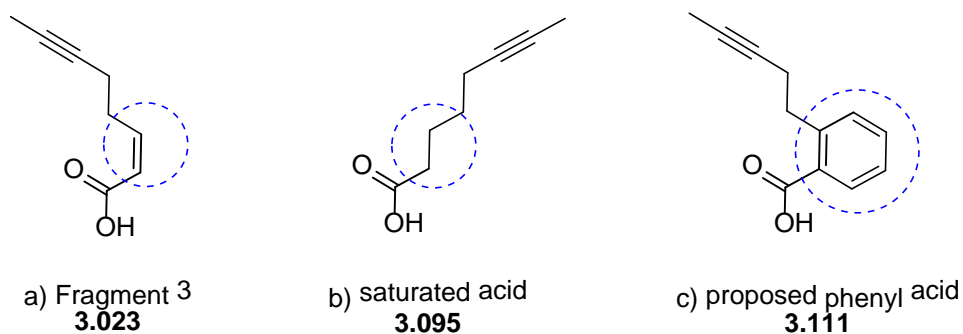


Figure 3.45: Various Fragment 3 used in this study: a) Fragment 3 (**3.023**), b) the saturated acid (**3.095**) and c) the proposed phenyl acid (**3.111**).

3.2.8 Synthesis of aromatic latrunculin derivative (**3.113**) via aromatic acid (**3.111**)

As it was observed that the presence of double bond within Fragment 3 was leading to problems like double bond isomerization when coupling, and it was noticed that the RCAM was difficult in the absence of the double bond constraint (as evidenced by the failure to ring close in the saturated analogue); it was logical to decide to have the constraint within a closed system so that the issue of double bond isomerization was omitted. With this in mind, it was decided that the aromatic latrunculin analogue **3.113** would be synthesised using the phenyl acid **3.111** as shown in **Figure 3.46**.

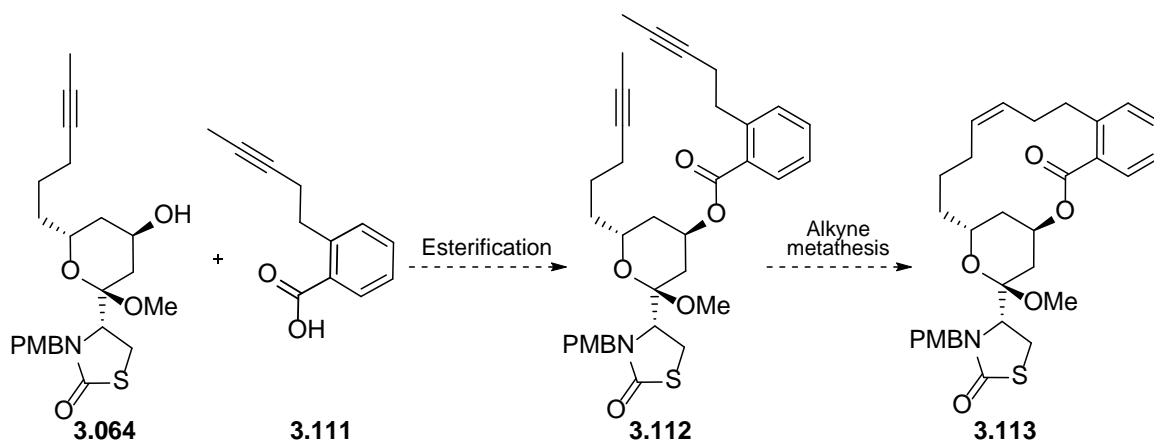


Figure 3.46: Proposed synthesis of aromatic latrunculin analogue **3.113**.

3.2.8.1 Synthesis of aromatic acid (**3.111**)

3.2.8.1.1 Grignard method

The first attempt was to synthesise the aromatic acid by following the same synthetic route as that used for the synthesis of Fragment 3 **3.023** [1]. **Figure 3.47** shows the synthetic scheme followed starting from 2-iodobenzoic acid, which was first treated with thionyl chloride to make the corresponding acid chloride before being converted to the ester **3.116** [69]. Fürstner *et al.* had described the addition of Grignard reagent on aromatic esters using $\text{Fe}(\text{acac})_3$ [70]. Although their focus was only on para substituted esters, it was decided to trial the same conditions on ethyl 2-iodobenzoate **3.116**.

The esterification of **3.114** worked in quantitative yield, however the Grignard addition was unsuccessful. The only compound isolated from this reaction was the starting material along with trace amounts of unknown impurities. It should be noted that the Grignard reaction was performed on the ester and not the acid directly to avoid any possible side reactions. The experiment was repeated while heating the reaction mixture to 60°C after the Grignard addition in order to force the addition of the Grignard reagent. However, it was observed that again no product was formed as only starting material could be recovered.

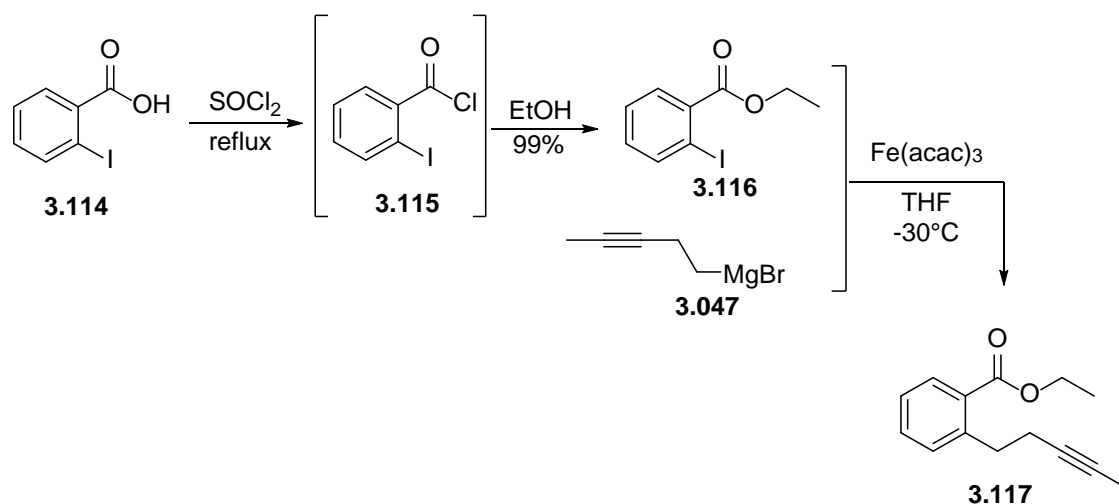


Figure 3.47: The synthetic route initially employed for the synthesis of the precursor of the aromatic acid **3.111**.

In order to ascertain if the failure of the last step was due to the alkyne Grignard reagent or the unreactivity of the ester **3.116**, it was decided to treat compound **3.116** with methyl Grignard reagent instead as shown in **Figure 3.48**. Since this reaction also failed to form the desired product **3.119**, it was realised that the ester **3.116** would not react with the Grignard reagent and thus this route could not be followed and other approaches would need to be explored.

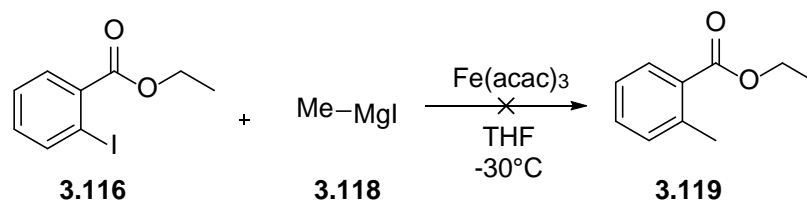


Figure 3.48: Attempted Grignard reaction using the methyl Grignard **3.118** instead of the alkyne Grignard **3.047**.

Thus it was decided to change the starting material. This approach was first trialed with 2-bromobenzonitrile using a model Grignard reagent **3.120** as shown in **Figure 3.49**. The idea being to perform the Grignard addition first in order to access **3.121** and then convert the nitrile group into the acid to achieve the desired aromatic acid. Propyl bromide was used to make the Grignard reagent **3.121** and then coupled with 2-bromobenzonitrile at -30°C using $\text{Fe}(\text{acac})_3$ as catalyst. TLC analysis after 5 h displayed formation of a new product and thus the reaction was left longer. However, even after stirring overnight, the TLC still displayed the starting material which was not

entirely consumed. The reaction mixture was quenched and purified to isolate of the desired product **3.122** in 25% yield.



Figure 3.49: Kumada coupling of model Grignard reagent on 2-bromobenzonitrile to form **3.121**.

Since the side products which can be formed in this reaction namely **3.123** and **3.124** (**Figure 3.50**) would also have the same proton NMR spectrum as the desired product and the LCMS analysis was inconclusive (since this compound failed to ionise under the LCMS conditions), carbon NMR spectrum analysis was used to verify the identity of the product. The presence of the carbon peak at 118 ppm peak (**Figure 3.51**) confirmed the presence of a CN bond, which along with the proton NMR spectrum confirmed that it was the desired product.

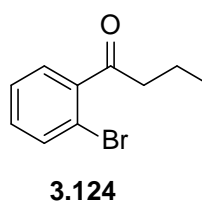
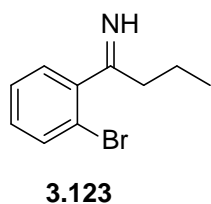


Figure 3.50: The two possible side product of the Grignard reaction illustrated in **Figure 3.49**.

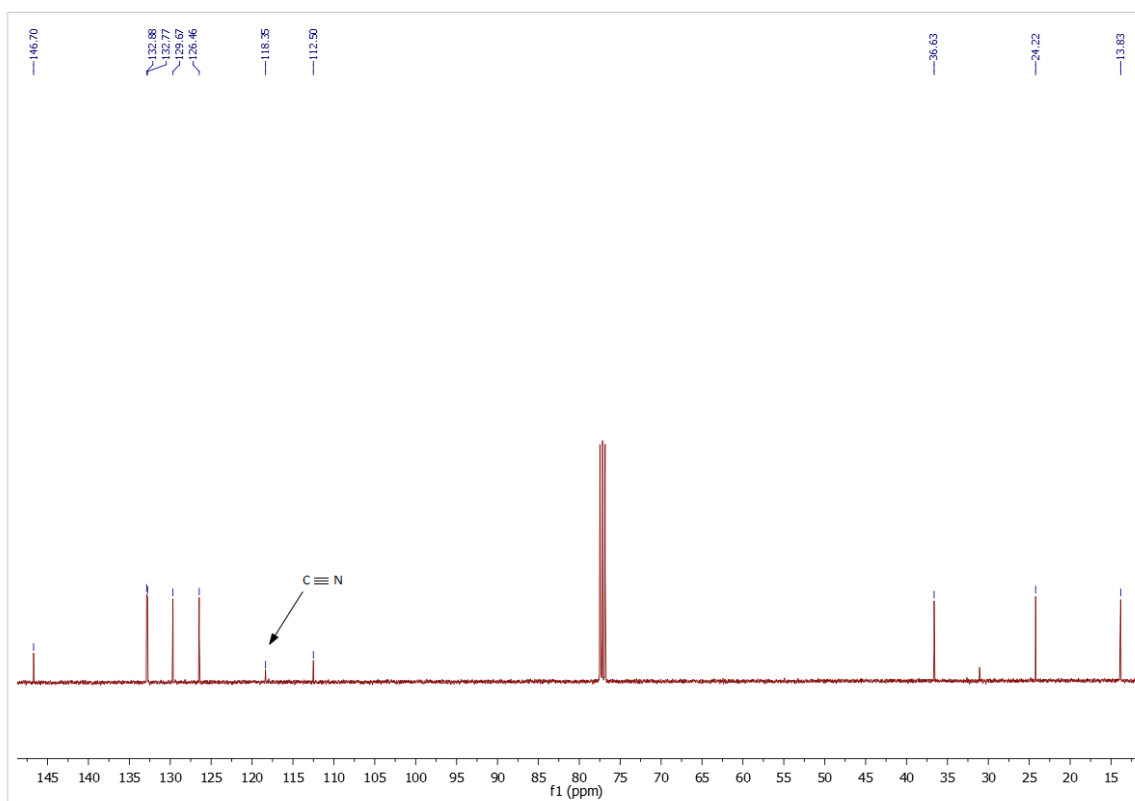


Figure 3.51: Carbon NMR spectrum of **3.122** confirming the presence of a CN bond.

The next step was to oxidise the nitrile group of **3.122** to the carboxylic acid on the model system. This was achieved by treating **3.122** with concentrated sulfuric acid, glacial acetic acid and water as shown in **Figure 3.52** [71]. The reaction proceeded smoothly leading to the formation of the desired acid in 63% yield.

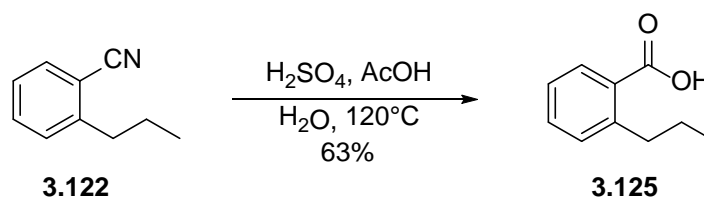


Figure 3.52: Hydrolysis of the nitrile to the corresponding carboxylic acid in the model system.

Thus it was decided to employ the same scheme with the alkyne Grignard on 2-bromobenzonitrile to obtain the aromatic acid **3.111** as illustrated in **Figure 3.53**. However, it was found that the actual alkyne Grignard failed to react with 2-bromobenzonitrile as only starting material could be recovered from this reaction even after repeated attempts (under the same condition). Thus this scheme could also not be used for the synthesis of the desired aromatic acid **3.111**.

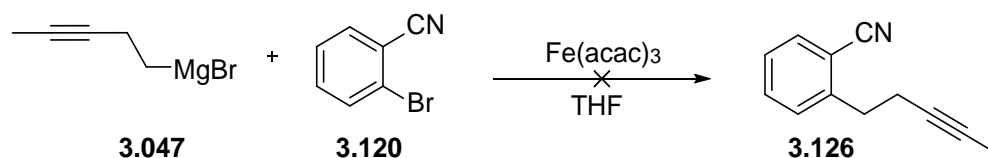


Figure 3.53: Attempted synthesis of the precursor of the aromatic acid **3.111** starting from 2-bromobenzonitrile.

Since the addition of the alkyne Grignard reagent on the halogen attached to the ring was not successful, it was decided to try and introduce the Grignard reagent one carbon away from the aromatic ring. With this in mind, we decided to use 2-bromobenzyl bromide as the starting material. Propargyl bromide was first converted to the corresponding Grignard reagent and then treated with 2-bromobenzyl bromide to be later methylated at the terminal alkyne as shown **Figure 3.54**. The Grignard reagent was prepared following the previously established protocol and then treated with 2-bromobenzyl bromide at 0°C. The reaction was then stirred for 12 h. The TLC after 12 h only indicated the presence of the starting material which was also confirmed after purification. This meant that the addition of the alkyne Grignard was not successful even at one carbon away from the aromatic ring.

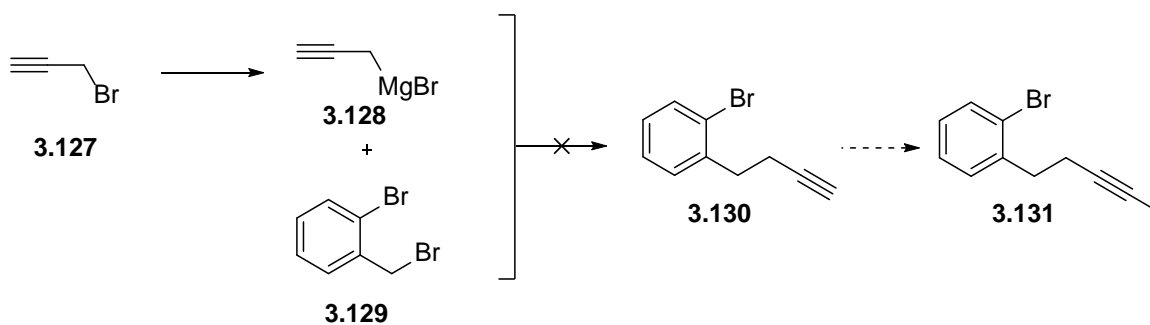


Figure 3.54: Attempted synthesis of the precursor of the aromatic acid **3.111** starting from 2-bromobenzyl bromide as the starting material.

Another approach towards the synthesis of the aromatic acid **3.111** was to start from 2-bromobenzyl bromide and convert it into the Grignard reagent **3.132** [72] as shown in **Figure 3.55**. This Grignard reagent was then used to react with 1-bromobut-2-yne **3.133** to form compound **3.131** in a 51% yield. Once the alkyne chain was introduced, the bromine atom at the *ortho* position was lithiated using *n*-BuLi and then treated with CO₂ at -78°C so as to introduce the carboxylic acid. However, it was noticed that the last step using CO₂ was irreproducible and due to time constraints was not pursued any further.

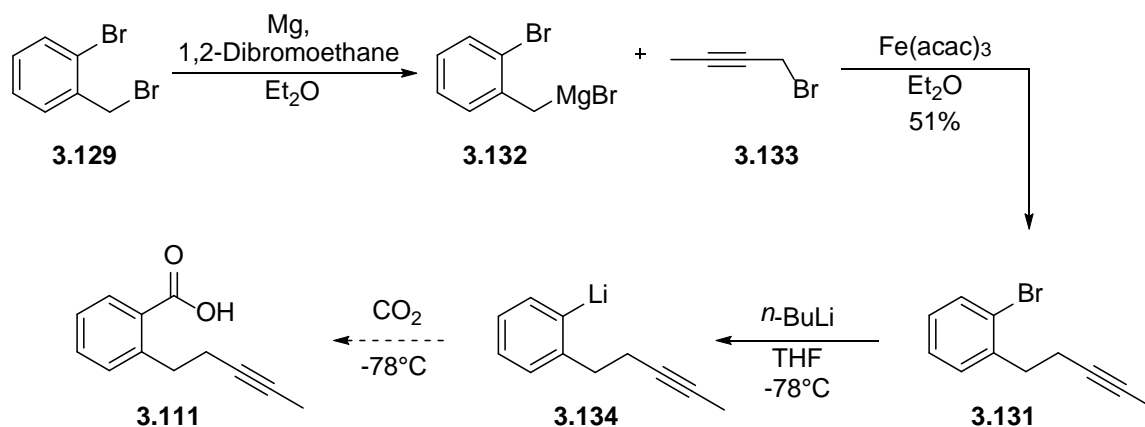


Figure 3.55: Attempted synthesis of aromatic acid **3.111** starting from 2-bromobenzyl bromide **3.129**.

The next approach was to make an aromatic Grignard reagent (instead of the aliphatic ones) and then treat it with the alkyne bromide as shown in **Figure 3.56**. This method would help accommodate any reactivity issues associated with the alkyne Grignard reagent. It was decided to

form the Grignard reagent on the *tert*-butyl 2-iodobenzoate **3.136** instead of the iodobenzoic acid to avoid any side reactions possible due to the free carboxylic acid. Thus the acid **3.114** was converted into the acid chloride using thionyl chloride and then treated with *tert*-butanol to form **3.136** in 81% yield [73]. Compound **3.136** was then treated with 1 M isopropylmagnesium chloride lithium chloride complex solution at 0°C in THF to form the corresponding Grignard reagent **3.138** [74]. Once the Grignard was formed, it was then treated with the bromo alkyne **3.050** at 0°C using Fe(acac)₃ catalyst in THF. However, the aromatic Grignard reagent **3.138** was unsuccessful in reacting with the bromo alkyne **3.050** and only the starting materials could be recovered from this reaction.

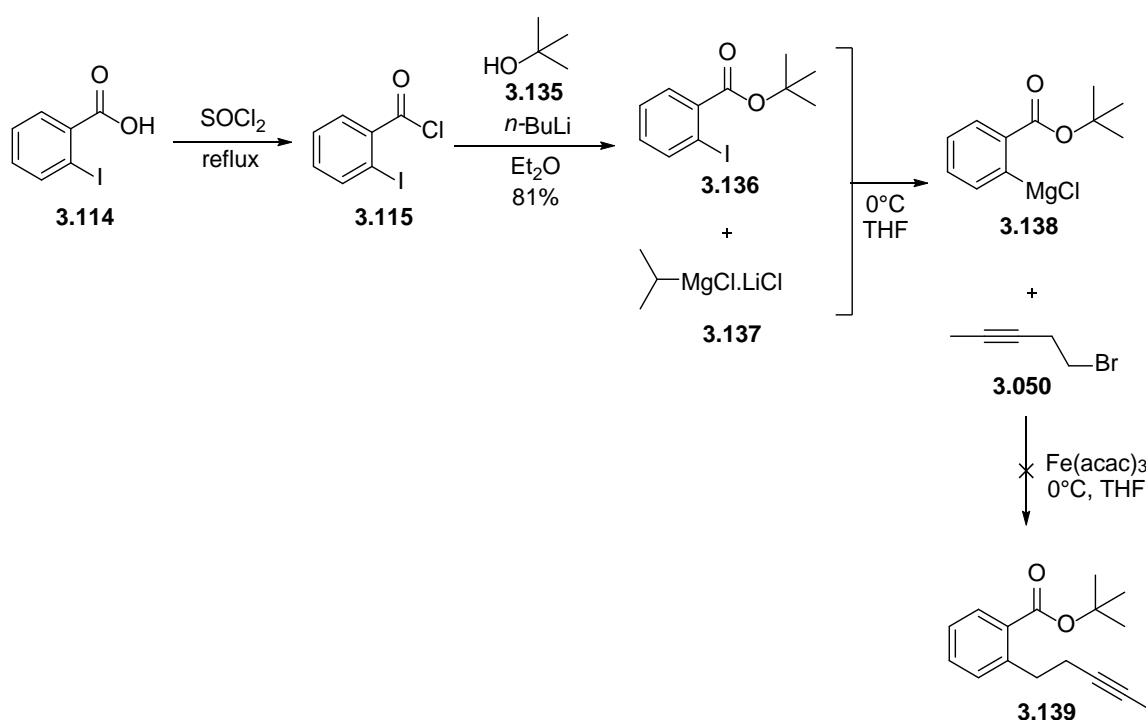


Figure 3.56: Attempted synthesis of the aromatic acid **3.111** using the aromatic Grignard method.

The above route was also repeated with 2-bromobenzonitrile as the starting material in order to rule out the reactivity of the aromatic Grignard being negatively impacted by the adjacent ester group and also to check if the coupling partner had a detrimental effect on this reaction due to the presence of the alkyne. Thus 2-bromobenzonitrile was converted into the Grignard reagent using 1 M isopropylmagnesium chloride lithium chloride complex solution and the Grignard reagent thus formed was treated with the propyl bromide **3.141** and the alkyne bromide **3.050** independently in separate flasks to see if either of them resulted in product formation (**Figure 3.57**) [75]. It was observed that the reactions with both the alkyl bromide **3.141** and the alkyne bromide **3.050** were not successful and only led to the formation of undesirable side products. Thus it was recognised

that the installation of the alkyne chain on the aromatic ring system was not feasible even with the use of the aromatic Grignard reagent.

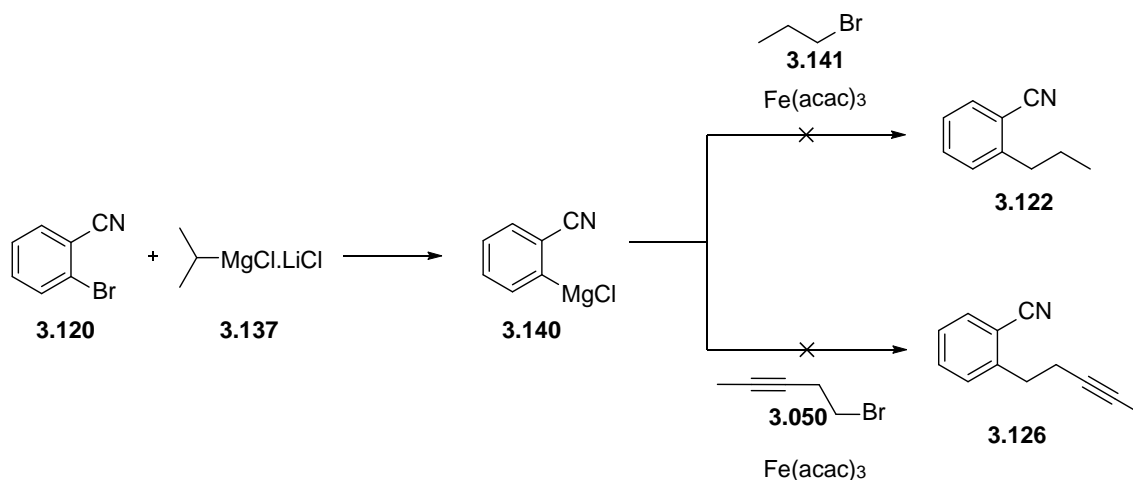


Figure 3.57: Attempted synthesis of the aromatic acid **3.111** starting from 2-bromobenzonitrile using the aromatic Grignard method.

3.2.8.1.2 Negishi Coupling

The next approach attempted was using the Negishi coupling conditions for the synthesis of the aromatic acid **3.111**. Negishi coupling involves the use of a zinc halide instead of the magnesium halide (as in Grignard reagents) [76, 77]. The zincate formation was attempted on 1-bromopropane as a model and this was used to react with the ester **3.142** as shown in **Figure 3.58** [78]. Although the TLC analysis after 12 h represented largely the starting material **3.142**, the reaction mixture was still quenched and purified since it was likely that the starting material and product might have similar polarity. It was however noticed that only a trace amount of the desired product **3.143** was formed while the major isolated compound was the unreacted starting material. The reaction was also repeated in DMSO but, the reaction only led to isolation of the starting materials.

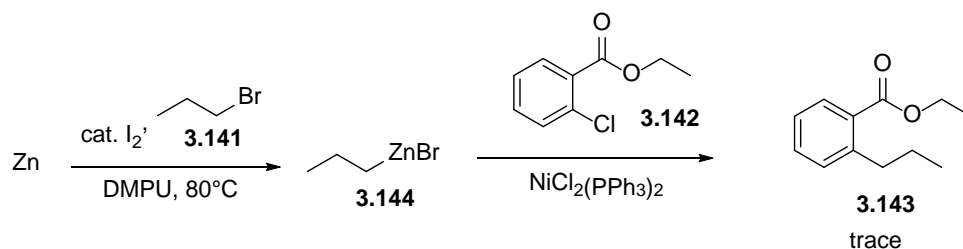


Figure 3.58: Attempted synthesis of aromatic acid **3.111** formation on a model system using Negishi coupling.

It is possible that the starting material, containing a chlorine atom, might not be reactive enough for this coupling. Thus it was decided to perform the Negishi reaction with the iodo derivative. Following the work of Knochel *et al.* in 1992, the preparation of the zincate was modified such that, zinc dust was initially activated by heating to 60-70°C followed by treatment with dibromomethane and TMSCl [79]. The coupling was performed with 2-iodobenzoate under two different catalyst systems namely a) dichlorobis(triphenylphosphine)nickel(II) ($\text{NiCl}_2(\text{PPh}_3)_2$) and b) palladium acetate with tetrabutylammonium bromide (TBAB) as shown in **Figure 3.59**. The reaction using conditions (a) did not lead to any product formation as evidenced by the recovery of starting material only. Condition (b) did lead to the formation of some new compounds by TLC analysis, however the isolated compounds were unidentifiable compounds and not the desired product.

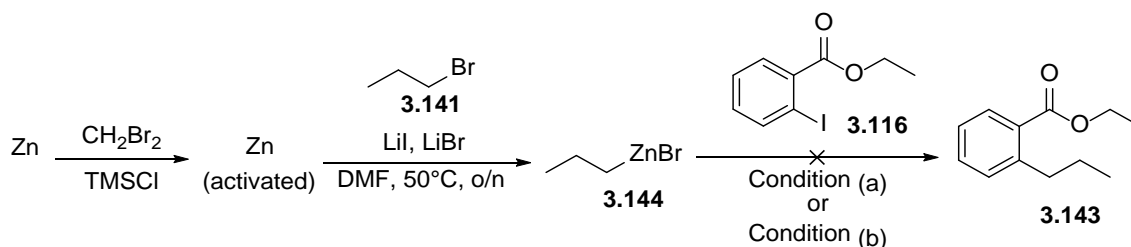


Figure 3.59: Negishi coupling using two different catalyst systems: (a) $\text{NiCl}_2(\text{PPh}_3)_2$ and (b) $\text{Pd}(\text{OAc})_2$, TBAB.

In the next approach, instead of making the zincate directly, first the Grignard reagent was made, then the magnesium of the Grignard reagent was exchanged for the zinc in a transmetallation reaction [80-82]. The zincate thus formed was then used to react with 2-bromobenzonitrile, **3.140**. **Figure 3.60** shows the scheme for this approach.

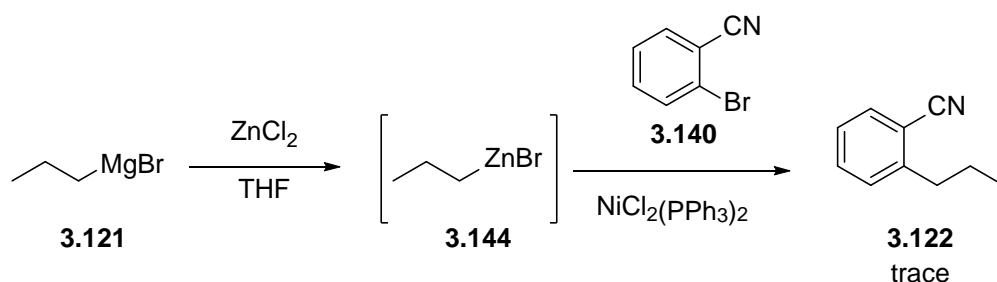


Figure 3.60: Synthesis of compound **3.122** using the zincate method.

Once the Grignard reagent was converted into the zincate **3.144** using zinc chloride in THF (zinc chloride is highly hygroscopic and was first flame dried to remove all the absorbed water and then allowed to crystallise under nitrogen), the zincate was subjected to coupling conditions with 2-bromobenzonitrile as the substrate and $\text{NiCl}_2(\text{PPh}_3)_2$ as the catalyst. The reaction was closely followed by TLC analysis and indicated the formation of a new product. However, even after prolonged reaction times, and increasing the concentration of zincate used in the reaction mixture, the reaction only yielded trace amounts of the desired product and largely unreacted starting material was recovered. Thus the reaction, although feasible, was not ideal for the synthesis and other approaches were explored.

3.2.8.1.3 Lithium-halogen exchange

The next approach was to use lithium to displace bromine from 2-bromobenzonitrile and then introduce the alkyne chain as shown in **Figure 3.61** [83, 84]. The reaction with the model substrate however only gave a trace amount of the desired product **3.122** and also trace amounts of the double addition products **3.146** or **3.147**. The presence of the double addition products suggested the importance of maintaining the temperature at -78°C to avoid side reactions. The reaction was then performed using the actual alkyne reagent ensuring the temperature was maintained at -78°C . However even with all of these factors taken into account, the reaction with the actual substrate led to a large number of side products and decomposition products as evidenced by a the number of spots present by the TLC analysis. Furthermore, none of the isolated products were the desired product. Thus it was concluded that this approach would not be ideal for the formation of the desired product in reasonable amount. This route was therefore not optimised any further.

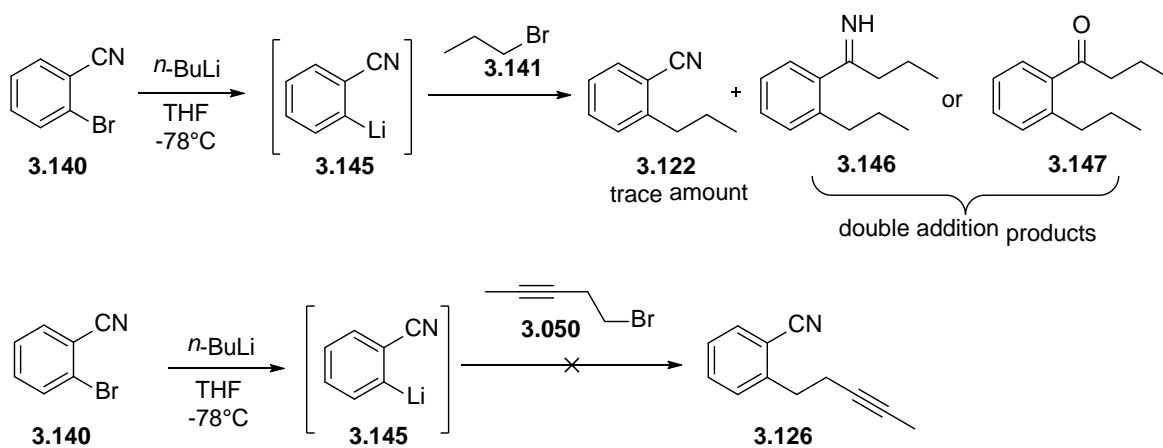


Figure 3.61: Attempted synthesis of aromatic Fragment 3 using lithium-halogen exchange.

3.2.8.1.4 Boronic acid method

The next attempted synthetic route was by making an aromatic boronic acid **3.148** [85] and using this boronic acid to form the desired aromatic acid **3.111** by Suzuki coupling [86, 87] as illustrated in **Figure 3.62**.

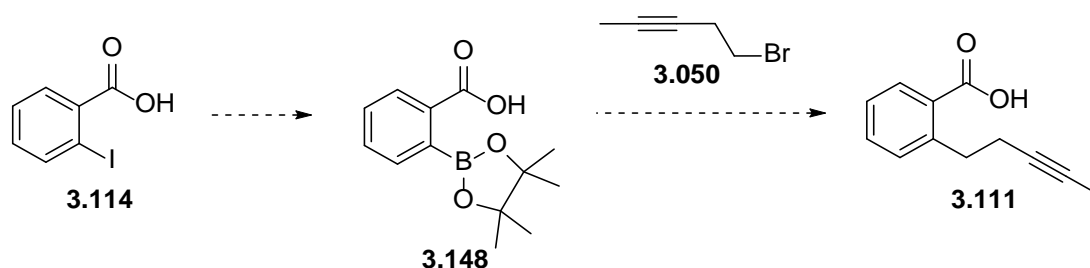


Figure 3.62: Proposed synthesis of the aromatic acid **3.111** via a boronic acid.

It was observed that the formation of the boronic acid, **3.148** was not successful when compound **3.114** was used as the starting material. As an alternative, the reaction was repeated with 2-bromobenzonitrile (**3.140**) as the substrate and it was observed that the reaction was successful yielding the desired product in 50% yield as shown in **Figure 3.63**. However, the next step of Suzuki coupling with the model alkylbromide **3.141** did not lead to the desired product, as only the starting material could be recovered after the reaction (**Figure 3.63**).

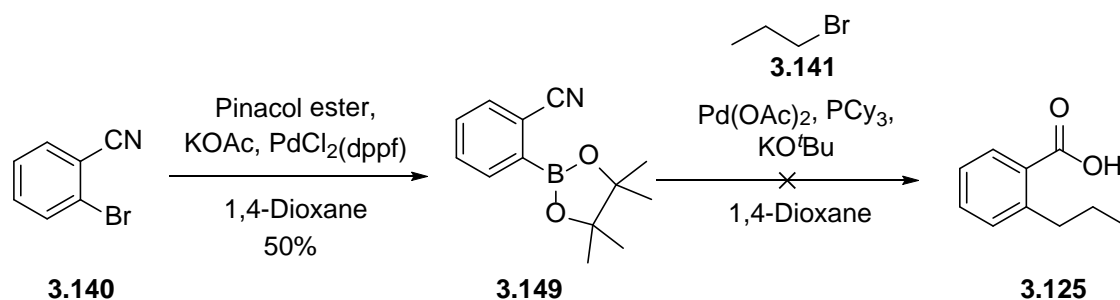


Figure 3.63: Attempted model synthesis of the aromatic Fragment 3 using the boronic acid method.

Thus all the attempts at synthesising the aromatic acid **3.111** failed to yield the desired results even after extensive studies. Due to time constraints it was not possible to optimise these conditions further and it was decided not to explore any other conditions.

3.3 Conclusion

The synthesis of the latrunculin B derivative **3.021** initially undertaken as the focus of this study, failed to proceed as described in the literature. **Figure 3.64** illustrates the three different latrunculin derivatives whose synthesis were attempted in this chapter. In order to resolve the issues associated with the synthesis of the latrunculin B derivative **3.021**, it was decided to synthesise the novel, saturated latrunculin derivative **3.095**. However the saturated acid **3.095** interferes with the ring closure and hence could not be synthesised. Another attempted strategy was to synthesise the latrunculin derivative **3.113** using the aromatic acid **3.111**, which would help in the ring closure and formation of the macrocycle. However, as discussed in the latter part of this chapter, the synthesis of the aromatic acid **3.111** was not feasible in the time frame of these studies.

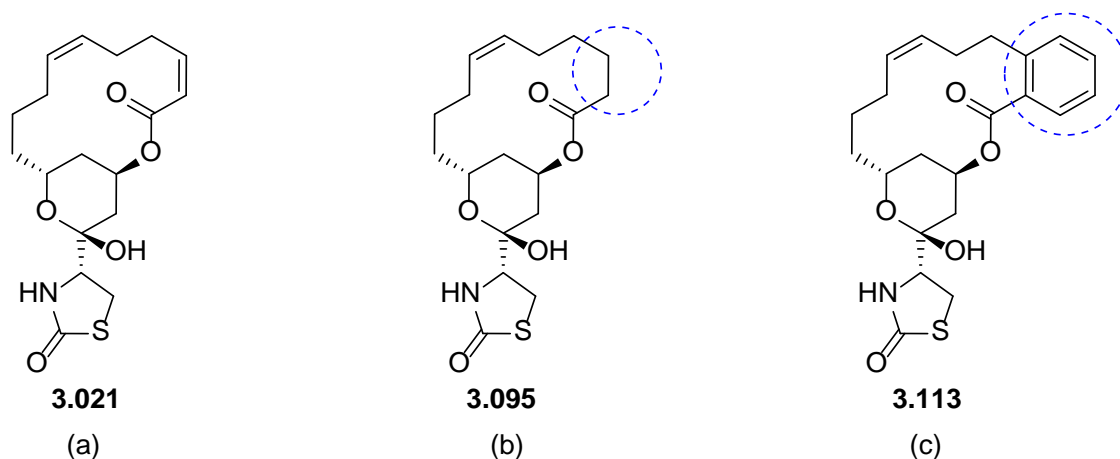


Figure 3.64: The 3 latrunculin derivatives attempted to synthesise in this chapter: (a) latrunculin B derivative **3.021**, (b) latrunculin derivative **3.095** using the saturated acid **3.095**, (c) latrunculin derivative **3.113** using the aromatic acid **3.111**.

Given the numerous difficulties encountered in the synthesis of the latrunculin derivative as initially envisaged, an entirely new approach towards the synthesis of actin inhibitors targeting malaria was identified. Examining the binding interactions of latrunculin with actin at the binding site using computational techniques allowed the determination of a different strategy towards the synthesis of actin inhibitors as discussed in the following chapters.

3.4 References

1. Fuerstner, A., et al., Total syntheses of the actin-binding macrolides latrunculin A, B, C, M, S and 16-epi-latrunculin B. *Chem-Eur J*, 2007; 13: 115-134.
2. Kashman, Y., Groweiss, A. and Shmueli, U., Latrunculin, a new 2-thiazolidinone macrolide from the marine sponge *latrunculia magnifica*. *Tetrahedron Lett*, 1980; 21: 3629-3632.
3. Nèeman, I., Fishelson, L. and Kashman, Y., Isolation of a new toxin from the sponge *Latrunculia magnifica* in the Gulf of Aquaba (Red Sea). *Mar Biol*, 1975; 30: 293-296.
4. Sayed, K.A., et al., Latrunculin A and its C-17-O-carbamates inhibit prostate tumor cell invasion and HIF-1 activation in breast tumor cells. *J Nat Prod*, 2008; 71: 396-402.
5. Morton, W.M., Ayscough, K.R. and McLaughlin, P.J., Latrunculin alters the actin-monomer subunit interface to prevent polymerization. *Nat Cell Biol*, 2000; 2: 376-378.
6. Fuerstner, A., et al., Latrunculin analogues with improved biological profiles by "diverted total synthesis": Preparation, evaluation, and computational analysis. *Chem-Eur J*, 2007; 13: 135-149.
7. Kudrimoti, S., et al., Semisynthetic latrunculin B analogs: Studies of actin docking support a proposed mechanism for latrunculin bioactivity. *Bioorg Med Chem*, 2009; 17: 7517-7522.
8. Zibuck, R., Liverton, N.J. and Smith, A.B., Total synthesis of (+)-latrunculin B. *J Am Chem Soc*, 1986; 108: 2451-2453.
9. White, J.D. and Kawasaki, M., Total synthesis of (+)-latrunculin A. *J Am Chem Soc*, 1990; 112: 4991-4993.
10. White, J.D. and Kawasaki, M., Total synthesis of (+)-latrunculin A, an ichthyotoxic metabolite of the sponge *Latrunculia magnifica* and its C-15 epimer. *J Org Chem*, 1992; 57: 5292-5300.
11. Smith, A.B., et al., Total synthesis of (+)-latrunculin A. *J Org Chem*, 1990; 55: 3977-3979.
12. Williams, B.D. and Smith, A.B., Total Synthesis of (+)-18-epi-Latrunculol A. *Org Lett*, 2013; 15: 4584-4587.
13. Han, Y., et al., Rhenium Oxo Complexes of a Chelating Diyne Ligand. Synthesis and Study of the Kinetics of Protonation. *Inorg Chem*, 2001; 40: 2942-2952.
14. Bernady, K.F., et al., Prostaglandins and congeners. 20. Synthesis of prostaglandins via conjugate addition of lithium trans-1-alkenyltrialkylalanate reagents. A novel reagent for conjugate 1,4-additions. *J Org Chem*, 1979; 44: 1438-1447.
15. Harcken, C. and Bruckner, R., Elucidation of the stereostructure of the annonaceous acetogenin (+)-montecristin through total synthesis. *Nouv J Chim*, 2001; 25: 40-54.
16. Parikh, J.R. and Doering, W.V.E., Sulfur trioxide in the oxidation of alcohols by dimethyl sulfoxide. *J Am Chem Soc*, 1967; 89: 5505-5507.
17. DeMico, A., et al., A versatile and highly selective hypervalent iodine (III)/2,2,6,6-tetramethyl-1-piperidinyloxy-mediated oxidation of alcohols to carbonyl compounds. *J Org Chem*, 1997; 62: 6974-6977.
18. Kusama, H., et al., Tungsten(0)- and Rhenium(I)-Catalyzed Tandem Cyclization of Acetylenic Dienol Silyl Ethers Based on Geminal Carbo-Functionalization of Alkynes. *Chem-Eur J*, 2011; 17: 4839-4848.
19. Heathcock, C.H., et al., Acyclic stereoselection. 36. Simple diastereoselection in the Lewis acid mediated reactions of enol silanes with aldehydes. *J Org Chem*, 1986; 51: 3027-3037.
20. Boris and Kohler, A.B., Optimized Procedure for the Cross-Aldol Condensation of Reactive Aldehydes. *Synth Commun*, 1985; 15: 39-42.
21. Keck, G.E. and Krishnamurthy, D., Pronounced Solvent and Concentration Effects in an Enantioselective Mukaiyama Aldol Condensation Using BINOL-Titanium(IV) Catalysts. *J Am Chem Soc*, 1995; 117: 2363-2364.
22. Nelson, S.G., Catalyzed enantioselective aldol additions of latent enolate equivalents. *Tetrahedron: Asymmetry*, 1998; 9: 357-389.
23. Lachance, H. and Hall, D.G., Allylboration of Carbonyl Compounds, in *Organic Reactions*, Edmonton: John Wiley & Sons, Inc; 2004.

24. Park, H., Jang, J. and Sin, K., A concise synthetic pathway for trans-metanicotine analogues. *Arch Pharm Res*, 2000; 23: 202-205.
25. Okano, T., Kiji, J. and Doi, T., Barbier-type Carbonyl-allylation with Allyl Compounds and Allyl Compounds and SnCl₂ in the Presence of PdCl₂[PPh₂(m-C₆H₄SO₃Na)]₂ under Two-phase Conditions. *Chem Lett*, 1998; 27: 5-6.
26. Shelke, A.M., et al., Asymmetric synthesis of (+)-stagonolide C and (–)-aspinolide A via organocatalysis. *Tetrahedron: Asymmetry*, 2012; 23: 1534-1541.
27. Brown, H.C. and Jadhav, P.K., Asymmetric carbon-carbon bond formation via β -allyldiisopinocampheylborane. Simple synthesis of secondary homoallylic alcohols with excellent enantiomeric purities. *J Am Chem Soc*, 1983; 105: 2092-2093.
28. Criegee, R., Mechanism of Ozonolysis. *Angew Chem Int Edit*, 1975; 14: 745-752.
29. Anderson, A., et al., α -Amino Acid Phenolic Ester Derivatives: Novel Water-Soluble General Anesthetic Agents Which Allosterically Modulate GABAA Receptors. *J Med Chem*, 2001; 44: 3582-3591.
30. Carpino, L.A. and El-Faham, A., Tetramethylfluoroformamidinium Hexafluorophosphate: A Rapid-Acting Peptide Coupling Reagent for Solution and Solid Phase Peptide Synthesis. *J Am Chem Soc*, 1995; 117: 5401-5402.
31. Sherry, B.D. and Fuerstner, A., The Promise and Challenge of Iron-Catalyzed Cross Coupling. *Accounts Chem Res*, 2008; 41: 1500-1511.
32. Amatore, M., et al., Highly Enantioselective Rhodium-Catalyzed [2+2+2] Cycloaddition of Diynes to Sulfonimines. *J Am Chem Soc*, 2013; 135: 4576-4579.
33. Trost, B.M. and Rudd, M.T., Ruthenium-Catalyzed Cycloisomerizations of Diynols. *J Am Chem Soc*, 2005; 127: 4763-4776.
34. Årstad, E., et al., ROMPgel-Supported Triphenylphosphine with Potential Application in Parallel Synthesis. *Org Lett*, 2002; 4: 1975-1977.
35. Desmaris, L., et al., Conversion of alcohols to bromides using a fluororous phosphine. *Tetrahedron Lett*, 2003; 44: 7589-7591.
36. Plagens, A. and Laue, T., *Named Organic Reactions* 2nd Edition, Wiley; 2005.
37. Albrecht, S., Defoin, A. and Tarnus, C., Simple Preparation of O-Substituted Hydroxylamines from Alcohols. *Synthesis*, 2006; 10: 1635-1638.
38. Sato, T. and Otera, J., CsF in Organic Synthesis. A Practical Method for Inversion of Secondary Mesylates. *Synlett*, 1995; 4: 336-338.
39. Matsumoto, K., et al., Simple and Convenient Synthesis of Esters from Carboxylic Acids and Alkyl Halides Using Tetrabutylammonium Fluoride. *J Oleo Sci*, 2014; 63: 539-544.
40. Kuehne, M.E. and Lambert, B.F., Reduction of aromatic acids and amides by sodium in liquid ammonia. *J. Am. Chem. Soc.*, 1959; 81: 4278-87.
41. But, T.Y.S. and Toy, P.H., The Mitsunobu Reaction: Origin, Mechanism, Improvements, and Applications. *Chem-Asian J*, 2007; 2: 1340-1355.
42. Varasi, M., Walker, K.A.M. and Maddox, M.L., A revised mechanism for the Mitsunobu reaction. *J Org Chem*, 1987; 52: 4235-4238.
43. Schenk, S., Weston, J. and Anders, E., Density Functional Investigation of the Mitsunobu Reaction. *J Am Chem Soc*, 2005; 127: 12566-12576.
44. Swamy, K.C.K., et al., Mitsunobu and Related Reactions: Advances and Applications. *Chem Rev*, 2009; 109: 2551-2651.
45. Lepore, S.D. and He, Y., Use of Sonication for the Coupling of Sterically Hindered Substrates in the Phenolic Mitsunobu Reaction. *J Org Chem*, 2003; 68: 8261-8263.
46. Volante, R.P., A new, highly efficient method for the conversion of alcohols to thioesters and thiols. *Tetrahedron Lett*, 1981; 22: 3119-3122.
47. Kim, M. and Han, K.J., Convenient Synthesis of *N*-Hydroxysuccinimide Esters from Carboxylic Acids Using Triphosgene. *Synth Commun*, 2009; 39: 4467-4472.
48. Roleira, F.M.F., et al., Activation of hydrocinnamic acids with pentafluorophenol versus pentafluorothiophenol: Reactivity towards hexylamine. *J Fluorine Chem*, 2009; 130: 169-174.
49. Voronkov, M.G., et al., Reaction of carboxylic acids with tetrachlorosilane. *Russ. J. Org. Chem.*, 2010; 46: 318-321.

50. Wu, D., et al., Preparation and properties of a novel form-stable phase change material based on a gelator. *J Mater Chem A*, 2015; 3: 2589-2600.
51. Hamper, B.C., Direct synthesis of β -ketomethylenetriphenylphosphoranes from readily available phosphonium salts. *J Org Chem*, 1988; 53: 5558-62.
52. Kim, J.G. and Jang, D.O., Mild and Efficient Cooper (II) Oxide-Catalyzed Acylation of Amines and Alcohols. *B Korean Chem Soc*, 2009; 30: 1435-1436.
53. Blough, N.V. and Simpson, D.J., Chemically mediated fluorescence yield switching in nitroxide-fluorophore adducts: optical sensors of radical/redox reactions. *J Am Chem Soc*, 1988; 110: 1915-1917.
54. Ramachandran, P.V., Nicponski, D. and Kim, B., Total Regio- and Diastereocontrol in the Aldol Reactions of Dienolborinates. *Org Lett*, 2013; 15: 1398-1401.
55. Liu, W.-Q., et al., Synthesis and structure-activity relationship of non-peptidic antagonists of neuropilin-1 receptor. *Bioorg Med Chem Lett*, 2014; 24: 4254-4259.
56. Zhang, Y.-Y., Liu, Y. and Wang, Y.-L., Design and Synthesis of Novel 3,5-Substituted Indolin-2-one Derivatives. *Asian J Chem*, 2015; 27: 491-495.
57. Song, D., Blond, G. and Fürstner, A., Study towards bioactive pyrone derivatives from the marine red alga *Phacelocarpus labillardieri*. *Tetrahedron*, 2003; 59: 6899-6904.
58. Dhaon, M.K., Olsen, R.K. and Ramasamy, K., Esterification of N-protected .alpha.-amino acids with alcohol/carbodiimide/4-(dimethylamino)pyridine. Racemization of aspartic and glutamic acid derivatives. *J Org Chem*, 1982; 47: 1962-1965.
59. Ohta, Y., et al., Synthesis of novel diketopiperazine derivative and observation of self-assembled structure. *Heterocycles*, 2009; 78: 2523-2530.
60. Fürstner, A., Alkyne Metathesis on the Rise. *Angew Chem Int Edit*, 2013; 52: 2794-2819.
61. Wu, X. and Tamm, M., Recent advances in the development of alkyne metathesis catalysts. *Beilstein J Org Chem*, 2011; 7: 82-93.
62. Heppekausen, J., et al., Practical New Silyloxy-Based Alkyne Metathesis Catalysts with Optimized Activity and Selectivity Profiles. *J Am Chem Soc*, 2010; 132: 11045-11057.
63. Bindl, M., et al., Molybdenum Nitride Complexes with Ph₃SiO Ligands Are Exceedingly Practical and Tolerant Precatalysts for Alkyne Metathesis and Efficient Nitrogen Transfer Agents. *J Am Chem Soc*, 2009; 131: 9468-9470.
64. Jyothish, K. and Zhang, W., Towards Highly Active and Robust Alkyne Metathesis Catalysts: Recent Developments in Catalyst Design. *Angew Chem Int Edit*, 2011; 50: 8478-8480.
65. Grubbs, R.H., Olefin metathesis. *Tetrahedron*, 2004; 60: 7117-7140.
66. Schuster, M. and Blechert, S., Olefin Metathesis in Organic Chemistry. *Angew Chem Int Edit*, 1997; 36: 2036-2056.
67. Choi, J. and Yoon, N.M., An excellent nickel boride catalyst for the cis-selective semihydrogenation of acetylenes. *Tetrahedron Lett.*, 1996; 37: 1057-60.
68. Zharmagambetova, A.K., et al., Hydrogenation of 2-hexyne on supported copper catalysts. *Dokl. Minist. Nauki-Akad. Nauk Resp. Kaz.*, 1996; 5: 61-64.
69. Penhoat, M., V. Levacher, and Dupas, G., Novel Extension of Meyers' Methodology: Stereoselective Construction of Axially Chiral 7,5-Fused Bicyclic Lactams. *J Org Chem*, 2003; 68: 9517-9520.
70. Fürstner, A., et al., Iron-Catalyzed Cross-Coupling Reactions. *J Am Chem Soc*, 2002; 124: 13856-13863.
71. Barchiesi, E., Bradamante, S. and Pagani, G.A., Evaluation of the polar-inductive and mesomeric effects exerted by para-substituted phenyl rings on contiguous functionalities. *J. Chem. Soc., Perkin Trans. 2*, 1987; 8: 1091-6.
72. Cassen, A., et al., B-C Bond Cleavage and Ru-C Bond Formation from a Phosphinoborane: Synthesis of a Bis- σ Borane Aryl-Ruthenium Complex. *Organometallics*, 2014; 33: 7157-7163.
73. Zhdankin, V.V., et al., Esters of 2-Iodoxybenzoic Acid: Hypervalent Iodine Oxidizing Reagents with a Pseudobenziodoxole Structure. *J Org Chem*, 2005; 70: 6484-6491.

74. Maji, M.S., Murarka, S. and Studer, A., Transition-Metal-Free Sonogashira-Type Coupling of ortho-Substituted Aryl and Alkynyl Grignard Reagents by Using 2,2,6,6-Tetramethylpiperidine-N-oxyl Radical as an Oxidant. *Org Lett*, 2010; 12: 3878-3881.
75. Steib, A.K., et al., Highly Diastereoselective Iron-Mediated C(sp²) C(sp³) Cross-Coupling Reactions between Aryl Grignard Reagents and Cyclic Iodohydrine Derivatives. *Angew Chem Int Edit*, 2011; 50: 3303-3307.
76. Liu, Z., et al., Mild Negishi Cross-Coupling Reactions Catalyzed by Acenaphthoimidazolyliene Palladium Complexes at Low Catalyst Loadings. *J Org Chem*, 2013; 78: 7436-7444.
77. Hadei, N., et al., The First Negishi Cross-Coupling Reaction of Two Alkyl Centers Utilizing a Pd-N-Heterocyclic Carbene (NHC) Catalyst. *Org Lett*, 2005; 7: 3805-3807.
78. Huo, S., Highly Efficient, General Procedure for the Preparation of Alkylzinc Reagents from Unactivated Alkyl Bromides and Chlorides. *Org Lett*, 2003; 5: 423-425.
79. Jubert, C. and Knochel, P., Preparation of new classes of aliphatic, allylic, and benzylic zinc and copper reagents by the insertion of zinc dust into organic halides, phosphates, and sulfonates. *J Org Chem*, 1992; 57: 5425-5431.
80. Corpet, M., Bai, X.-Z. and Gosmini, C., Cobalt-Catalyzed Cross-Coupling of Organozinc Halides with Bromoalkynes. *Adv. Synth. Catal.*, 2014; 356: 2937-2942.
81. Cheng, G., et al., syn Additions to 4 α -Epoxypyranosides: Synthesis of L-Idopyranosides. *Org. Lett.*, 2007; 9: 4849-4852.
82. Wang, C., et al., Highly Regio- and Stereoselective Synthesis of (Z)-Trisubstituted Alkenes via Propyne Bromoboration and Tandem Pd-Catalyzed Cross-Coupling. *Org. Lett.*, 2009; 11: 4092-4095.
83. Li, J., et al., Palladium-Catalyzed Oxidative Rearrangement of Tertiary Allylic Alcohols to Enones with Oxygen in Aqueous Solvent. *Org. Lett.*, 2014; 16: 5370-5373.
84. Schneider, Y., et al., Diazirines as Potent Electrophilic Nitrogen Sources: Application to the Synthesis of Pyrazoles. *Org. Lett.*, 2014; 16: 596-599.
85. Wang, L., et al., Cyclopalladated Ferrocenylimine as Efficient Catalyst for the Syntheses of Arylboronate Esters. *Adv. Synth. Catal.*, 2010; 352: 2002-2010.
86. Nambo, M., et al., The Concise Synthesis of Unsymmetric Triarylacetonitriles via Pd-Catalyzed Sequential Arylation: A New Synthetic Approach to Tri- and Tetraarylmethanes. *Org. Lett.*, 2015; 17: 50-53.
87. Kirchhoff, J.H., et al., Boronic Acids: New Coupling Partners in Room-Temperature Suzuki Reactions of Alkyl Bromides. Crystallographic Characterization of an Oxidative-Addition Adduct Generated under Remarkably Mild Conditions. *J Am Chem Soc*, 2002; 124: 13662-13663.

Chapter 4: Truncated latrunculin analogues

4.1 Introduction

Latrunculin A and B are large complex molecules containing 5 chiral centers, 2 Z double bonds and a 14 membered macrocyclic ring. Extraction of latrunculins from their natural source is very cumbersome and thus they are very expensive to buy commercially. The total synthesis of these natural products is also difficult (as discussed in Chapter 3). The synthetic challenges, along with the toxicity of these natural products, are some of the key reasons that limit the applicability of latrunculins as drug candidates. In order to resolve these issues, we decided to look carefully into the key pharmacophore of the molecule and design a truncated version of latrunculin whilst retaining its activity.

From the analysis of latrunculin B bound to the *Plasmodium* actin model, it can be seen that latrunculin sits in the ATP binding pocket of actin. **Figure 4.01** illustrates how the thiazolidinone ring securely resides in the deep groove of the binding site, while the macrocyclic ring laces the peripheral region of the protein.

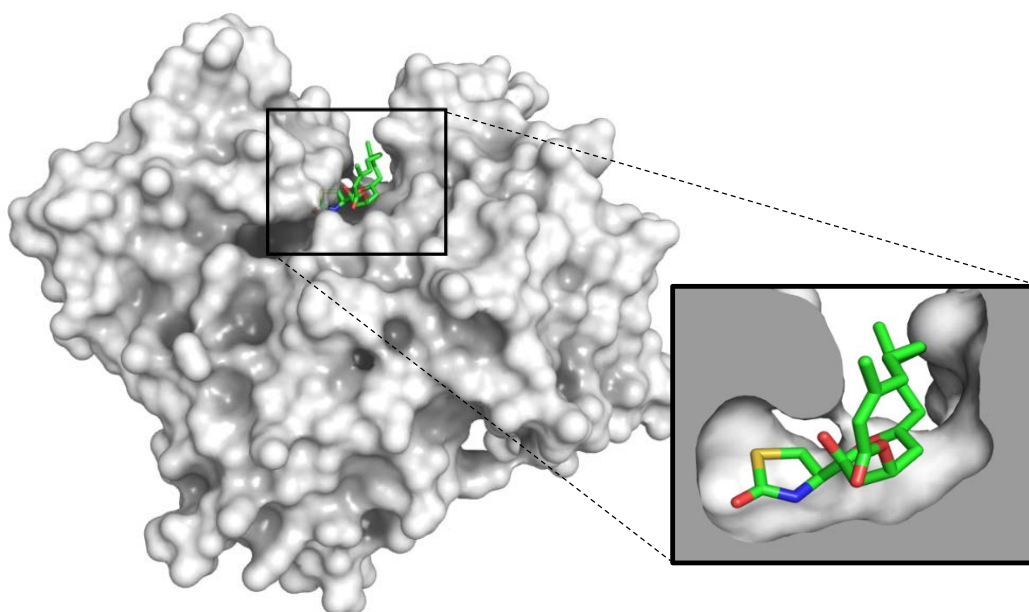


Figure 4.01: Structure of latrunculin B bound to *Plasmodium* actin model.

As discussed in Chapter 2, the heteroatoms are involved in extensive hydrogen bonding interactions with the actin protein and the macrocycle is involved in hydrophobic interactions with the protein as shown in **Figure 4.02**. A closer study of the model reveals that the thiazolidinone moiety and the THP ring together engage in 4 hydrogen bonding. This suggests that even in the absence of the macrocycle, the truncated molecule should potentially be able to interact with actin protein to some extent. There are also ample examples in literature where powerful biological activity was retained by smaller truncated fragments of the natural product [1]. Literature study also indicates that with latrunculins, the thiazolidinone and the THP ring are the key pharmacophores involved in actin binding, while the macrocyclic ring stabilises the interaction by forming hydrophobic interactions [2].

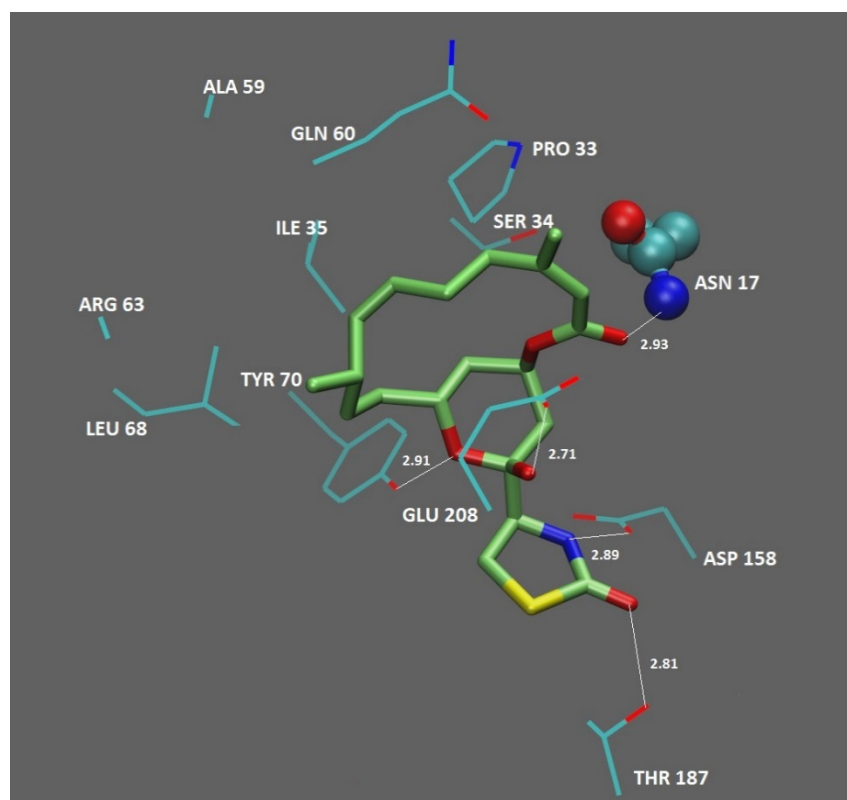


Figure 4.02: Hydrogen bond interaction between latrunculin B and *Plasmodium* actin.

With this in mind, it was proposed that a truncated latrunculin analogue, which retains the thiazolidinone and the THP ring could potentially be a starting point for the SAR studies. The hydrophobic interactions could potentially be gained by introducing hydrophobic groups at a later stage. This led to the design of a novel truncated latrunculin core, compound **4.001** (**Figure 4.03**) as the new core.

Comparison of latrunculin B with compound **4.001** shows that the latter preserves the thiazolidinone moiety of latrunculin with its correct chirality. However the THP ring resembles latrunculin B only by the presence of the oxygen and the hydroxyl group (their chirality is not conserved for synthetic ease). The entire macrocyclic ring consisting of two chiral centers and two Z double bonds were removed, thereby making this new core synthetically more accessible.

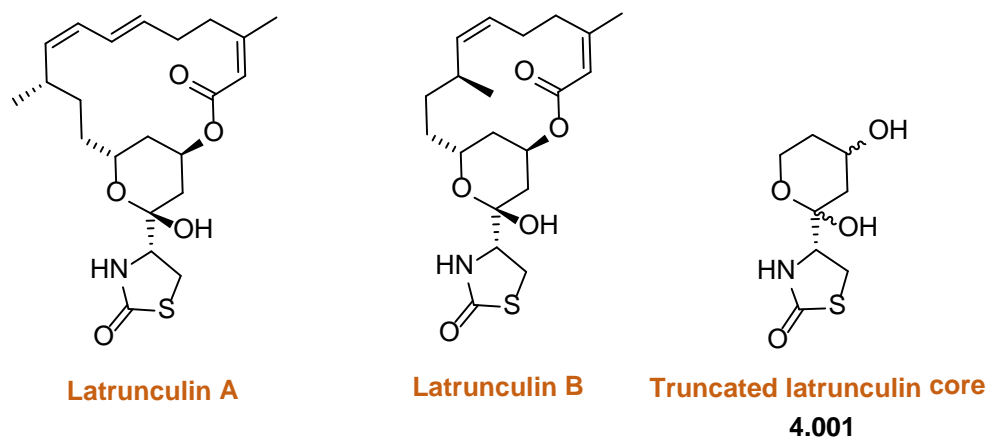


Figure 4.03: Structures of latrunculin A, B and the truncated latrunculin core, **4.001**.

The aim of this investigation would be to test the potency of this core so as to confirm the key pharmacophores and also to explore SAR around the new truncated core by creating a library of analogues. This would not only give us insights into which regions of the molecule are crucial for actin binding but will also potentially help identify key differences in binding between mammalian actin and *Plasmodium* actin so as to achieve selective binding. This could lead to the identification of a lead compound open to further in-depth SAR exploration. It should be noted that chiral purity would not be necessary at this stage, as the primary aim is to identify an initial hit. The analogues were therefore synthesised as diastereomeric mixtures and were separated.

4.2 Synthesis of the new core

The synthesis of the proposed truncated core **4.001** could be achieved by following the scheme put forth by Fürstner *et al.* (Method A) [3] or Smith *et al.* (Method B) [4].

4.2.1 Method A

The synthesis of compound **4.001** was proposed based on Fürstner's total synthesis of latrunculins [3] (described in Chapter 2). **Figure 4.04** shows the retrosynthetic approach which involves

synthesis of two fragments namely **3.007** and the TBS-protected aldehyde **4.002** coupled together by aldolisation.

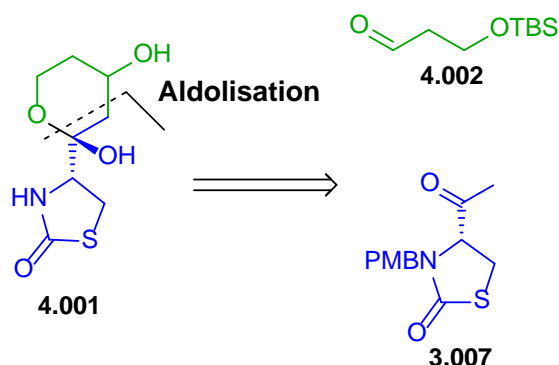


Figure 4.04: Retrosynthesis of compound **4.001** using an aldol reaction as the key step.

4.2.1.1 Synthesis of the building blocks (**3.007** and **4.002**)

Compound **3.007** was prepared as described in Chapter 3 of this thesis and compound **4.002** was prepared from 1,4-propanediol as shown in **Figure 4.05**. Mono TBS-protection of 1,4-propanediol was achieved according to the work by McDougal *et al.* using sodium hydride and TBSCl in THF [5].

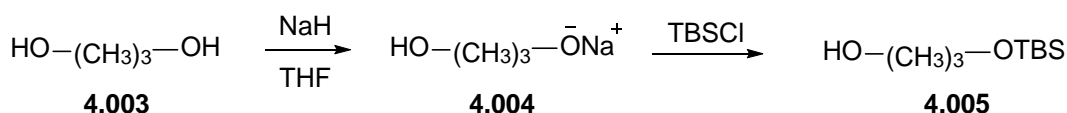


Figure 4.05: Mono TBS-protection of 1,4-propanediol [5].

The procedure involves adding the diol **4.003** to a stirred solution of NaH in THF and stirring it for 45 mins when a large amount of opaque white precipitate (**4.004**) is formed. TBSCl is then added and stirred again for 45 min as the precipitate slowly starts to go into solution. Mono silylation is possible with these conditions because as soon as the diol comes in contact with the NaH, the mono sodium salt, which is only partially soluble in THF, is formed. When TBSCl is later introduced to the reaction mixture, only the small amount of dissolved mono sodium salt undergoes silylation. The rate of silylation of the alkoxide is faster than the rate of proton transfer between the alkoxide salt and the already formed silyl alcohol, which ensures that only mono silylation occurs [5].

Both the product **4.005** and the side product (TBSOH) have the same polarity and therefore are difficult to separate by flash chromatography. The slightly impure mono TBS-protected compound **4.005** was then subjected to Swern oxidation [6-8] to yield the aldehyde **4.002** as shown in **Figure 4.06**.

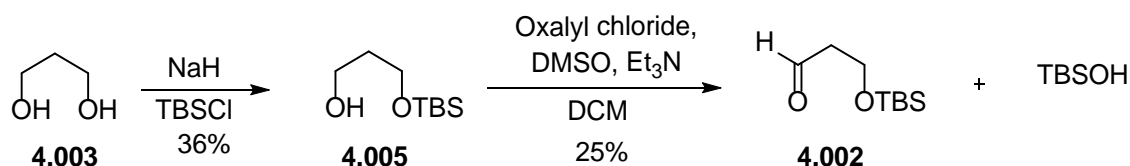


Figure 4.06: Scheme employed for the synthesis of **4.002**.

The product obtained after flash chromatography co-eluted with the TBSOH (the impurity retained from previous step) as they had similar polarity. This implies that although there was only one identifiable product by TLC, the proton NMR spectrum revealed the presence of two compounds namely the desired product compound **4.002** and TBSOH in the isolated compound. When the proton NMR spectra of compounds **4.002** and **4.005** were compared, it was observed that the ratio of TBSOH in compound **4.002** was higher than that in the starting material **4.005**. This was likely caused by the Swern oxidation conditions which produces HCl gas as a by-product which could lead to TBS-deprotection of **4.005** generating more TBSOH. This is because under classical Swern oxidation conditions, the base is introduced only after allowing sufficient time for the sulfonium cation to form [3]. **Figure 4.07** shows the mechanism of Swern oxidation and illustrates how HCl is produced during the reaction. The overall yield of the reaction was less than 25%.

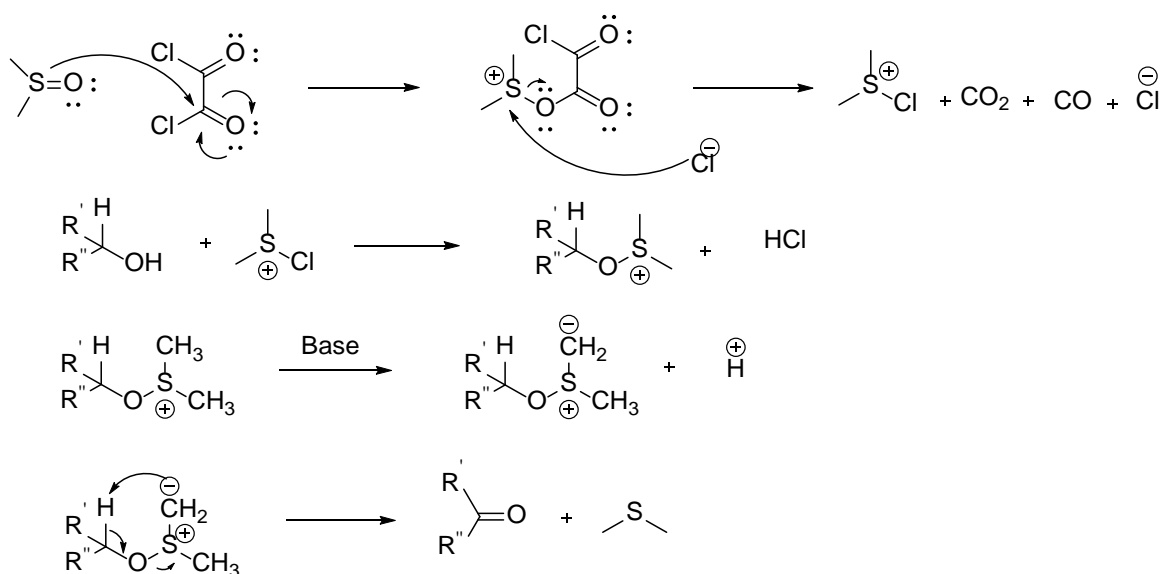


Figure 4.07: Mechanism of Swern oxidation [8].

In order to attain an efficient method of generating the aldehyde **4.002**, a number of different conditions were trialed as summarised in **Table 4.01**. The Parikh-Doering oxidation using sulphur trioxide- pyridine complex was next attempted [9, 10] (**Table 4.01**, entry 2). Since this reaction does not produce HCl gas, it was hypothesised that the reaction would eliminate the formation of TBSOH. This prediction was correct as the desired product was obtained without any TBSOH impurity; however the yield of the reaction was still low (32%). Next, an alternative Swern oxidation condition [11] using cyanuric chloride instead of oxalyl chloride was tried (**Table 4.01**, entry 3). This method is reported to be a milder and more efficient procedure for oxidation [11]. However, even after stirring the reaction mixture for 24 h, the TLC analysis did not indicate formation of any new product and thus it was not pursued further.

In 2007, Mortensen *et al.* reported Swern oxidation with a slight modification in the time of addition of Et₃N [12]. In the classical Swern reaction, DMSO is added to a stirred solution of oxalyl chloride in DCM at -78°C, stirred for 10 min followed by addition of the starting material (alcohol). This is then stirred for an hour before adding Et₃N. However in the modified Swern conditions by Mortensen *et al.*, the Et₃N is added ‘immediately’ after the addition of the starting material [12]. This would neutralise any HCl gas as soon as it is produced and therefore will not lead to TBS-deprotection. The reaction performed according to this procedure showed complete consumption of the starting material by TLC analysis, the proton NMR of the crude mixture also showed product with trace amount of TBSOH impurity (**Table 4.01**, entry 4). Since aldehydes are usually unstable on silica [12], the crude aldehyde was directly used for the next step.

Table 4.01: Optimisations for oxidation of alcohol **4.005**.

Entry	Reaction	Conditions	Yield	Comment
1	Swern oxidation	Oxalyl chloride, DMSO, DCM. Et ₃ N added after 1 h.	25%	Poor yield and undesired TBS-deprotection.
2	Parikh Doering oxidation	SO ₃ .Py, DMSO, DCM, Et ₃ N added after 1 h.	32%	Poor yield
3	Swern oxidation	Cyanuric chloride, DMSO, DCM Et ₃ N added after 1 h.	NA	No Reaction
4	Swern oxidation	Oxalyl chloride, DMSO, DCM Et ₃ N added immediately after the starting material.	>90%	

4.2.1.2 Aldolisation and ring closure

Once the building blocks **4.002** and **3.007** were synthesised, the next step was to bring them together using the aldol condensation reaction as shown in **Figure 4.08**. Fürstner's aldol condensation conditions [3] (TiCl₄, DIPEA, DCM) resulted in the formation of the desired product **4.006**, however the product and the starting material **3.007** (used in excess) had similar polarity and even with extensive efforts to separate them using flash chromatography, it was not feasible to efficiently recover the product in pure form thereby reducing the recovered yield of the product.

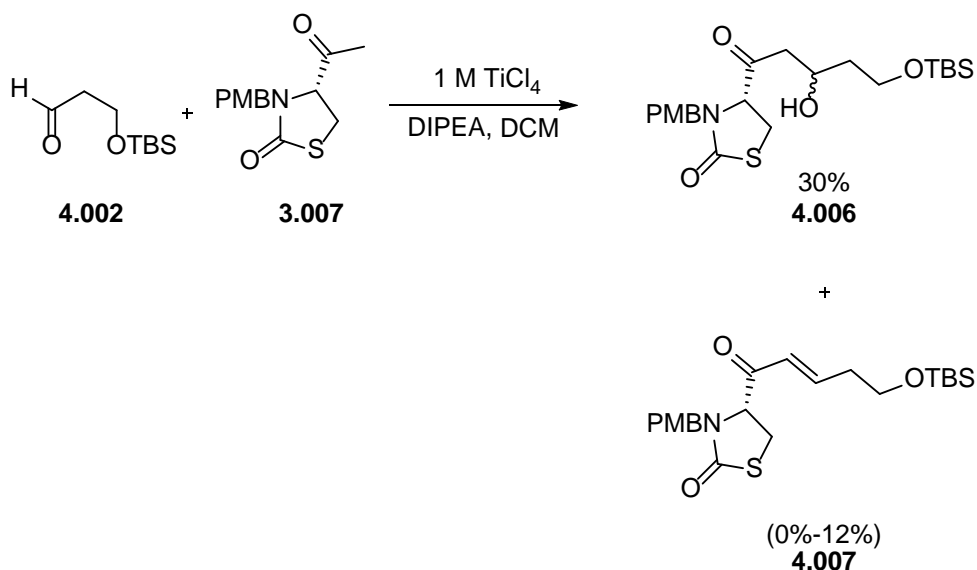


Figure 4.08: Aldol reaction leading to the formation of desired product and the eliminated product.

Another issue with this reaction was its poor reproducibility. This is because, under the aforementioned conditions, the product formed could eliminate water thereby producing compound **4.007** as the by-product. This kind of elimination during Aldol reaction was also recently observed by Sugiura *et al.* [13]. **Figure 4.09** shows the mechanism of elimination; the hydroxyl group gets protonated under acidic conditions and subsequently eliminates water to form compound **4.007**. The formation of this eliminated by-product however was not consistent and its recovered yield varied between 0% and 12%. The yield of the desired product **4.006** was also not more than 30% in any of these cases. This meant that optimisation was required to synthesise compound **4.006** more efficiently. The proton NMR spectrum also revealed that the eliminated compound **4.007** was in its *trans* form ($J = 15.69$ Hz) implying that it would not undergo ring closure upon the deprotection of the TBS group.

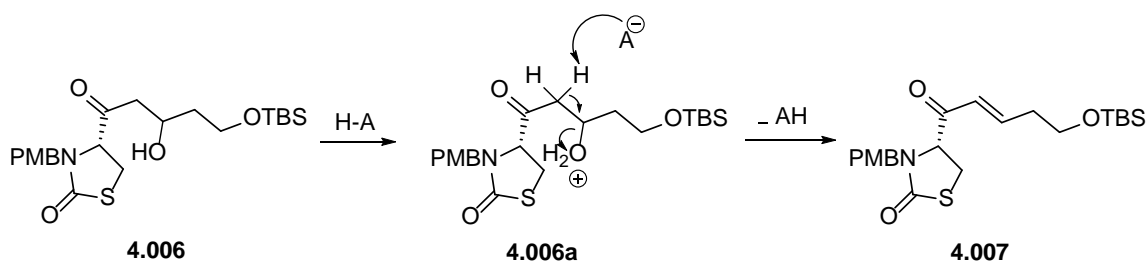


Figure 4.09: Formation of the eliminated compound **4.007**.

The role of the base is quite crucial in the aldol reaction and hence it was decided to explore other stronger bases to enolize the ketone more effectively as illustrated in **Table 4.02**. Lithium hexamethyldisilazide (LiHMDS) has been shown to be very efficient in enolizing acyclic ketones and esters with high *E/Z* selectivity [14, 15]. The use of such a strong base has the potential risk of epimerising the thiazolidinone chiral centre, nevertheless the reaction was still attempted in order to understand if the aldol reaction on these substrates was feasible in higher yields. However the attempts using LiHMDS and zinc chloride in THF [16] failed to produce any product and only led to the recovery of the starting materials (**Table 4.02**, entry 2). Next, a neutral strong base namely *tert*-butyliminotris(pyrrolidino)phosphorane (BEMP), which is known to be an efficient base in nitroaldol or Henry reactions was used (**Table 4.02**, entry 3) [17]. This reaction also did not result in any product formation. Finally, it was decided to use potassium bis(trimethylsilyl)amide (KHMDS) as the base (**Table 4.02**, entry 4) [15]. When the substrates were treated with KHMDS in THF as solvent, the TLC analysis indicated the formation of a new product within 2 h. The reaction was quenched and the product formed was identified by proton NMR spectrum to be the desired product **4.006** (**Figure 4.10**). It was found that these conditions did not lead to any eliminated product, however the reaction would not go to completion and led to inconsistent yields (7% to 58%).

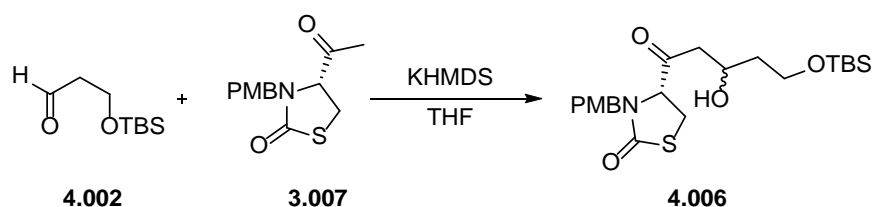


Figure 4.10: Aldol reaction using KHMDS as the base.

This observed inconsistency in the aldol adduct formation is likely due to the reversible nature of the aldol reaction [18]. **Figure 4.11** shows the mechanism of the reverse aldol reaction.

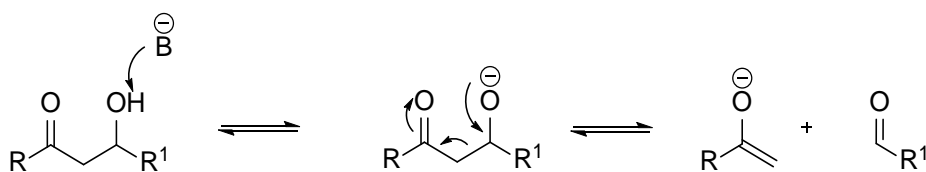
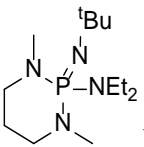


Figure 4.11: Mechanism of retro aldol reaction [18].

Table 4.02: Summary of the different conditions tried for the aldol reaction.

Entry	Condition	Yield	Comment
1	TiCl ₄ , DIPEA, DCM	30%	Inconsistent yields, formation of undesired elimination product
2	LiHMDS, ZnCl ₂ , THF	No reaction	Only starting materials recovered.
3	 BEMP, THF	No Reaction	Only starting materials recovered.
4	KHMDS, THF	7% - 46%	Inconsistent yields, undesired retro aldol reaction.

It can be seen from **Table 4.02** that none of these conditions produced an ideal procedure for the synthesis of these compounds. The issue of starting material and product having the same polarity also still remained. In order to resolve the purification issue, it was decided to use the crude product directly for the next step, which was deprotection of TBS group and spontaneous cyclisation of the resulting diol to the corresponding hemiacetal so as to obtain compound **4.008** as shown in **Figure 4.12**. Purification of the product after the oxa-cyclisation resulted in formation of the PMB protected new core **4.008** consisting of four diastereomers in 24% yields over 2 steps (approximately 50% for each individual step).

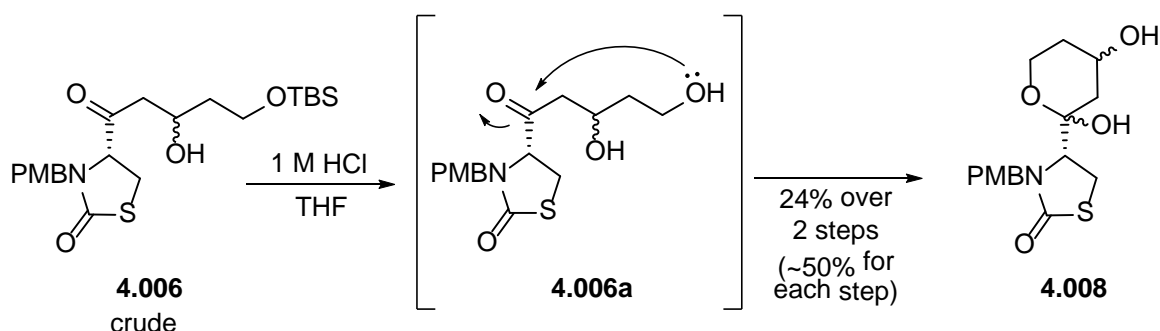


Figure 4.12: TBS-deprotection and spontaneous oxa-cyclisation leading to the formation of the hemiacetal **4.008**.

This step introduces a new chiral centre to the molecule thereby increasing the number of diastereomers to four. This escalates the complexity of the molecule and correspondingly its proton NMR spectrum. It was therefore very difficult to interpret all of the signals in the spectrum due to considerable overlap between signals from all the four diastereomers. Being a hemiacetal also increased the possibility of this compound to degradation. It was therefore necessary to convert compound **4.008** to a more stable compound. This was achieved by converting the hemiacetal to the corresponding methyl acetal using CSA in methanol to yield compound **4.009** as shown in **Figure 4.13**.

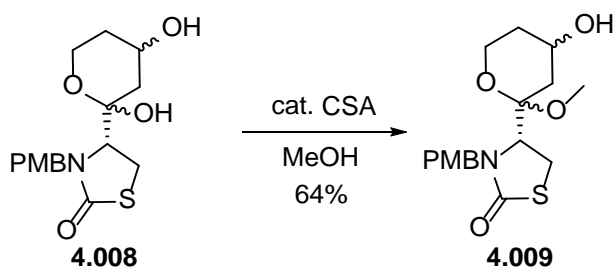


Figure 4.13: Synthesis of the acetal **4.009**.

Alternatively, we could save a step in this scheme by treating **4.006** with 1 M HCl in MeOH (instead of THF) so as to achieve TBS-deprotection, ring closure and methoxylation producing **4.009** in a single step as shown in **Figure 4.14**.

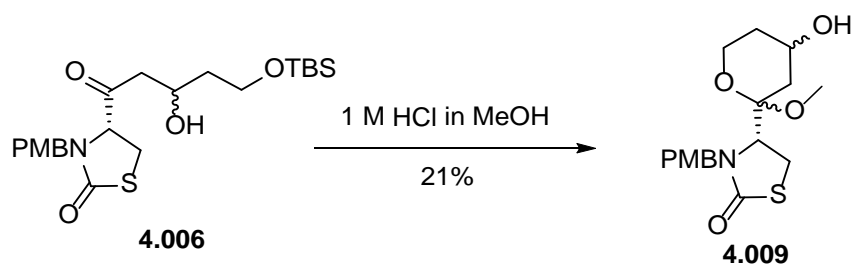


Figure 4.14: One step TBS-deprotection, ring closure and methoxylation of compound **4.006**.

When compared with the two-step process, the yield was found to be lower in the one-step process. This is because, in the one-step procedure, the methoxylation reaction does not go to completion (even after 48 h) as evidenced by the recovery of the hemiacetal **4.008** and the acetal **4.009** as products. The partial conversion of the hemiacetal to the acetal, meant that the overall yield of the reaction was reduced. It was therefore decided to embrace the two step procedure, however the crude hemiacetal was used directly (without purification) for the methoxylation step. It should be noted that compound **4.009** does not show the correct mass on LCMS. This is because, the acetal **4.009** leads to elimination of one molecule of water and one molecule of methanol under the LCMS conditions. Even when the analysis was conducted under neutral conditions, the aforementioned elimination was observed. It was concluded that this elimination was brought about by the effect of the ionisation spray and therefore could not be rectified. The compound corresponding to the mass observed (m/z : 304 positive mode) from the LCMS was eluted to be compound **4.010** as shown in **Figure 4.15**. The proton NMR spectrum (**Figure 4.16**), carbon NMR spectrum and the mass obtained from HRMS ($[M+H]^+$ 354.1355 m/z) correspond to the desired compound **4.009**.

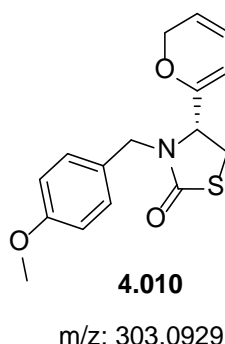


Figure 4.15: The compound corresponding to the observed mass on LCMS.

Compound **4.009** thus synthesised was found to only consist of two diastereomers (instead of four) as evidenced by the proton NMR spectrum shown in **Figure 4.16**. It can be seen from the spectrum

that all the peaks are in duplicate; this is especially clear in the signal produced by the methoxy at the chiral centre (position 24). It should be noted that the benzylic protons of the PMB protecting group are not equivalent (position 8) and results in splitting of these protons in the form of 8A₁ and 8A₂ as shown in the Figure. The two diastereomers are represented as diastereomer A and diastereomer B. For easier understanding of the proton NMR spectrum shown in **Figure 4.16**, the signals corresponding to diastereomer A are highlighted in yellow, those of diastereomer B in blue and the overlapped signals are highlighted in green.

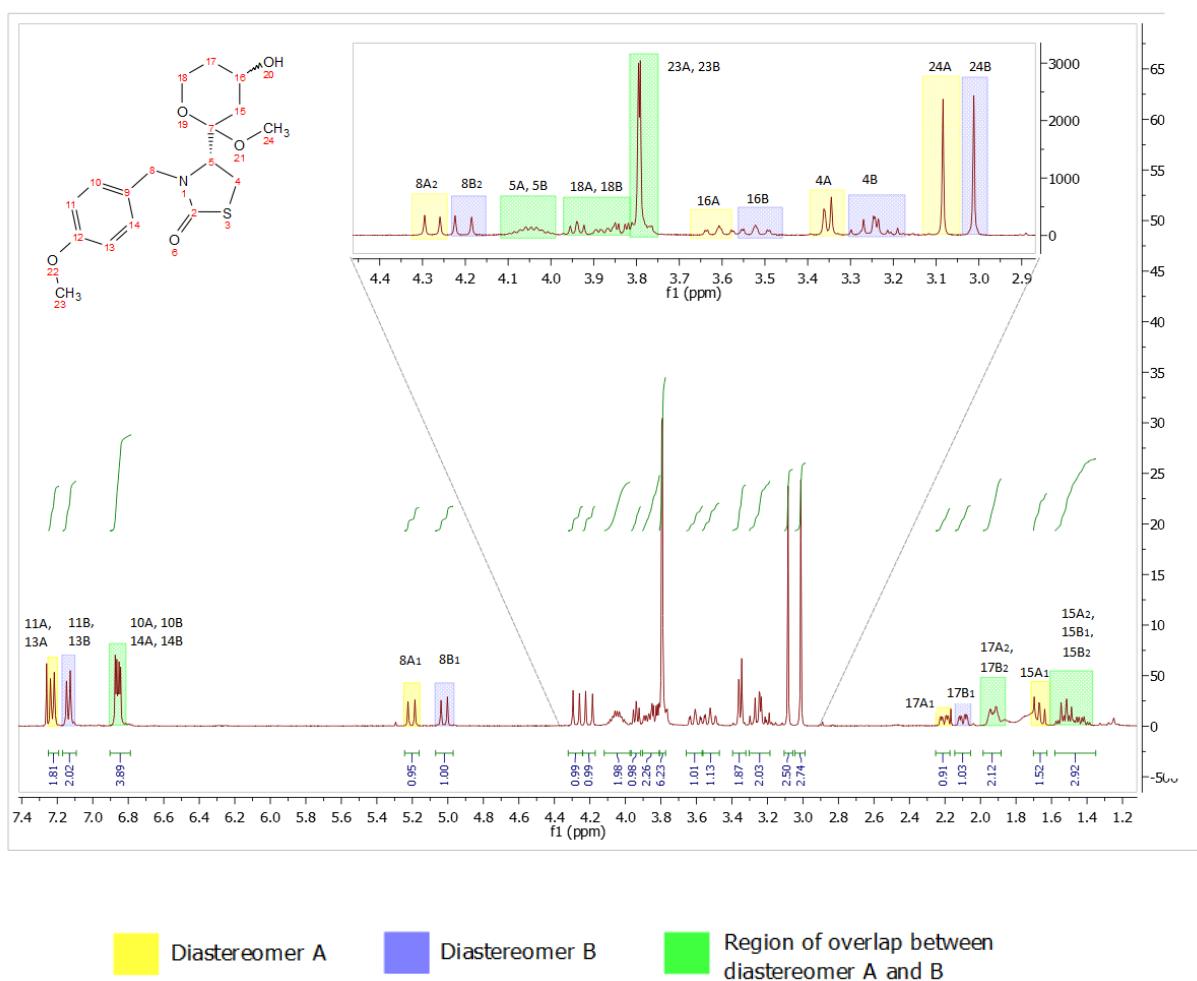


Figure 4.16: Proton NMR spectrum of the compound **4.009** showing a mixture of two diastereomers A and B in 1:1 ratio. Diastereomer A is highlighted in yellow, diastereomer B in purple and the region of overlap between diastereomer A and B in green.

The presence of only two diastereomers, implies that the stereochemistry at one of the uncontrolled centres was controlled during the acetal formation resulting in a reduction of the number of possible diastereomers. **Figure 4.17** shows the mechanism of acetal formation.

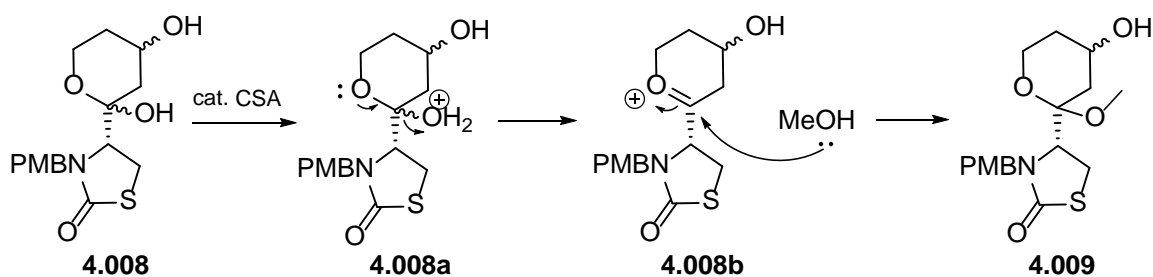


Figure 4.17: Methoxylation of hemiacetal **4.008** to acetal **4.009**.

As represented in the **Figure 4.17**, the hemiacetal **4.008** gets protonated under acidic conditions leading to elimination of water and formation of the oxonium ion, **4.008b**. Methanol then acts as a nucleophile and results in the formation of the acetal **4.009**. Thus it is likely that during the reaction, the addition of methanol is favoured from one face over the other (probably due to the steric hindrance of the hydroxyl group in order to minimise the 1,3-diaxial interaction on the six membered ring). This meant that it was the acetal centre which had gained controlled chirality (thereby leading to only one configuration at the acetal position). The proton NMR spectrum can only ascertain the ‘number’ of diastereomers formed and not the ‘configuration’ of the controlled centre. In order to determine the configuration, one has to separate the diastereomers and then determine their optical purity and relative stereochemistry.

Although theoretically, diastereomers should have different physical properties and hence be separable by flash chromatography, it was found that the diastereomers in compound **4.009** had exactly the same polarity and therefore were inseparable by column chromatography (even after repeated trials to separate them using different solvent systems). It would be possible to separate them using a High Performance Liquid Chromatography (HPLC) column, however from a medicinal chemistry perspective, and also in the interest of time, it was not relevant to undertake this procedure at this stage. The primary aim of this study was only to find an active actin binding analogue and to understand the SAR around this new core. Separation of diastereomers and determination of stereochemical configuration can be undertaken once a lead compound was identified.

The number of steps required to obtain the (PMB protected) core **4.008** starting from the acid **3.037** is three and the overall yield was 19% over these steps. Due to the inconsistency of certain reactions in this scheme, it was decided to explore an alternative scheme for this synthesis and employ the best method for scale up and SAR exploration.

4.2.2 Method B -Alternative synthesis of the core

As previously discussed, the aldol reaction had persistent issues such as poor yield using TiCl_4 and with the retroaldol using KHMDS, therefore it was rational to design an alternate synthetic scheme for the synthesis of the proposed new core without involving an aldol reaction as the key step. The alternative retrosynthetic approach attempted was based on the work by Williams and Smith in 2013 [4] and involved alkene metathesis of the TBS-protected alkene **4.011** and the α,β -unsaturated ketone **4.012** as the key step as shown in **Figure 4.18**.

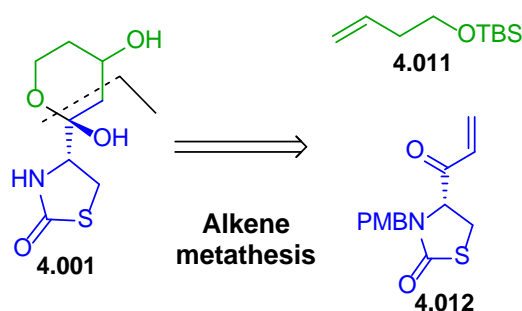


Figure 4.18: Retrosynthesis of compound **4.001** using alkene metathesis as the key step [4].

4.2.2.1 Synthesis of the building blocks (**4.011** and **4.012**)

The starting material, 3-buten-1-ol for the synthesis of **4.011** was first TBS-protected using TBSCl and imidazole in DMF [19]. Although this reaction shows complete consumption of the starting material and formation of a new product by TLC analysis, it was found that the product recovery after extraction was quite low (45%). This poor recovery of the desired product was later discovered to be due to issues with product isolation and the volatile nature of the product. Changing the solvent of the reaction from DMF to DCM eased isolation of the product and improved the recovered yield of the desired product to 99%.

The synthesis of **4.012** was started from the acid **3.037** (described in Chapter 3), which was first converted to the corresponding Weinreb amide **4.014** using *N,O*-dimethylhydroxylamine hydrochloride, the coupling agent (*O*-(Benzotriazol-1-yl)-*N,N,N',N'*-tetramethyluronium tetrafluoroborate (TBTU)) and a base (DIPEA) [4]. The Weinreb amide thus produced was treated with vinylmagnesium bromide in THF to produce the α,β -unsaturated ketone **4.012** in 93% yield as shown in **Figure 4.19**.

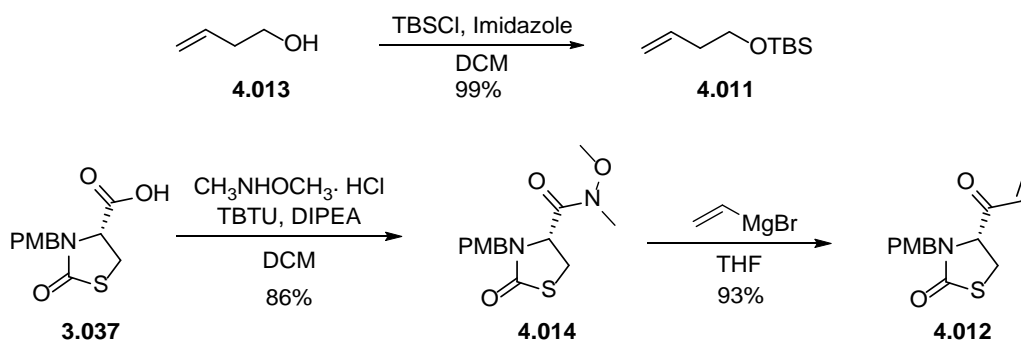


Figure 4.19: Synthesis of the building blocks for the alkene metathesis reaction.

It is necessary to convert the acid **3.037** to an acid halide or a Weinreb amide before the Grignard reaction since Grignard reagents cannot directly add to an acid moiety. This is because in addition to being nucleophilic, Grignard reagents are also basic in nature and therefore would first lead to deprotonation of the acid [20] and the resulting carboxylate is too unreactive to react further. Grignard addition via a Weinreb amide has an advantage over the acid halide method in that, the latter can lead to double addition of the Grignard reagent forming an alcohol as shown in **Figure 4.20** [21].

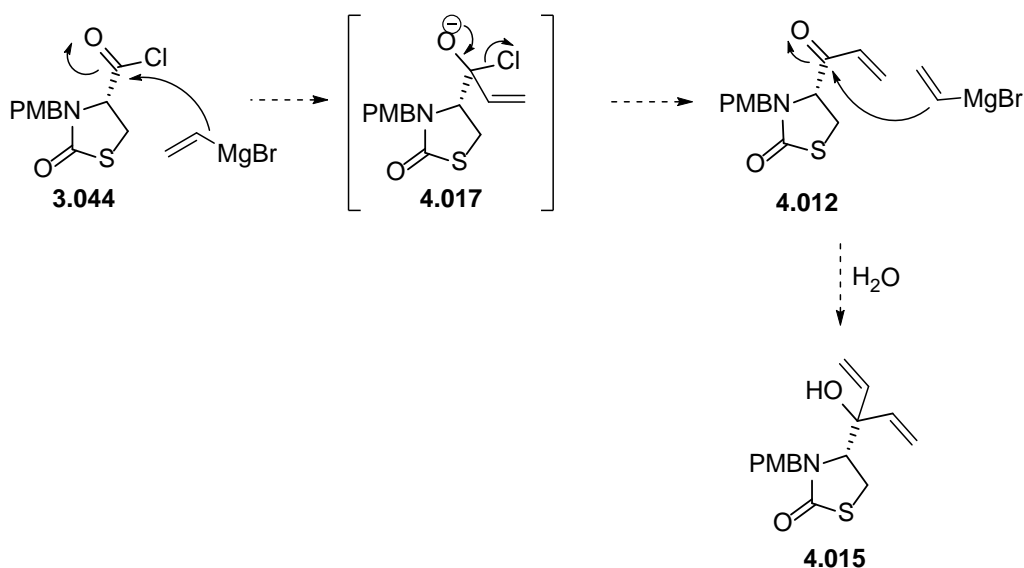


Figure 4.20: Possible double addition of the Grignard reagent to an acid halide leading to the undesired formation of an alcohol.

The mechanism of the Grignard reagent reacting with the Weinreb amide is shown in **Figure 4.21** [22]. The metal (magnesium) of the Grignard reagent forms a coordinated complex with the oxygen

atoms of the Weinreb amide. This coordinated complex collapses only when the reaction is quenched thereby preventing the double addition.

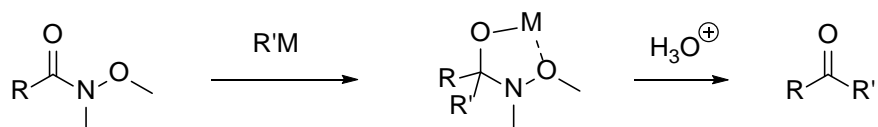


Figure 4.21: The mechanism of reaction between an organometallic compound and a Weinreb amide [22].

It was found that the reaction of the addition of the Grignard reagent although working desirably on lower scales (<1g), led to the formation of an undesired side product on larger scales. Scales larger than 3 g only led to the production of the undesired product. It was envisaged that this side product was due to the Michael addition of *N,O*-dimethylamine to the α,β -unsaturated ketone **4.012** resulting in the formation of compound **4.016a**, which tautomerises to its 'keto' form to form compound **4.016** as shown in **Figure 4.22**. NMR experiments and X-ray crystallography later confirmed that the undesired product was compound **4.016**.

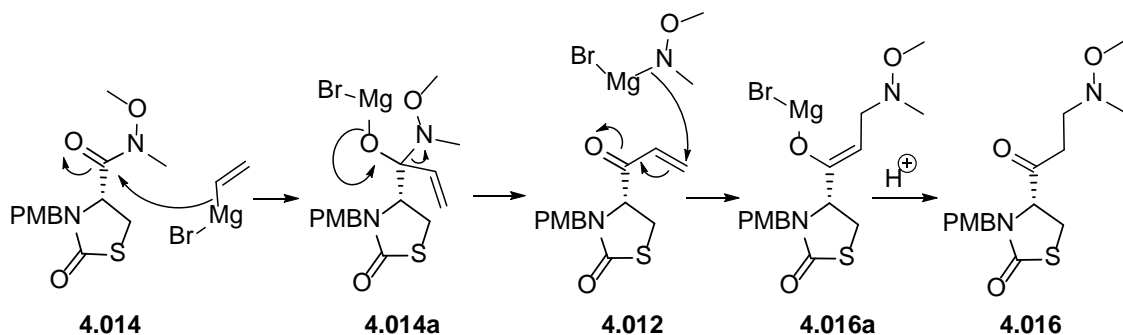


Figure 4.22: Proposed mechanism of formation of compound **4.016**.

In order to avoid the formation of this undesired compound **4.016**, the scale up reactions were diluted two times so as to lower the concentration of the reaction mixture which reduced the formation of this side product. **Figure 4.23** shows the X-ray structure of compound **4.016** confirming its structure.

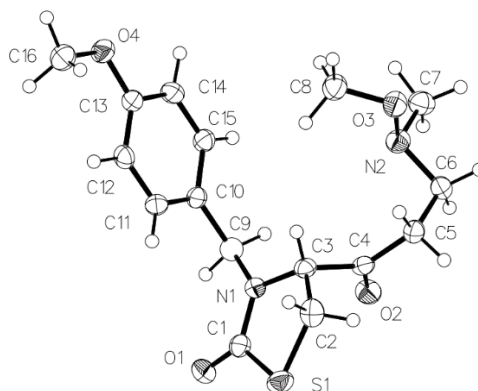


Figure 4.23: X-ray structure confirming the structure of compound **4.016**.

4.2.2.2 Alkene metathesis

Once the building blocks **4.011** and **4.012** were synthesised, they were joined together by alkene metathesis as shown in **Figure 4.24**. The conditions for this metathesis [4] involved using Hoveyda-Grubbs' Catalyst 2nd Generation (Hoveyda-Grubbs' II) with DCE as the solvent and heating the reaction mixture to 50°C for 12 h.

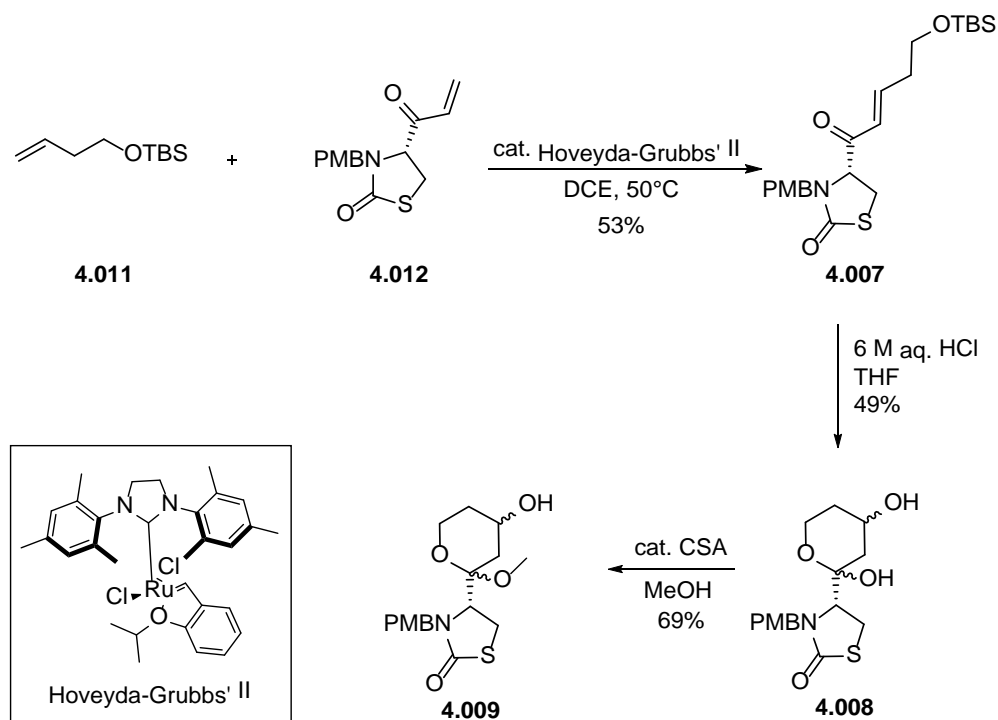


Figure 4.24: Alternative scheme for the synthesis of the PMB protected core **4.009** using alkene metathesis as the key step.

Once the TLC indicated complete consumption of the starting material, charcoal was added and the reaction mixture was allowed to stir for another hour in order to remove the ruthenium by-products [23]. The metathesis reaction was moderate yielding (53%) and the overall efficiency of this scheme was affected by the fact that this reaction utilised 3 eq. of the α,β -unsaturated ketone **4.012**. Although ideally one should be able to recover the excess starting material, in this case the α,β -unsaturated ketone **4.012** being reactive was unstable and not recoverable. It was therefore decided to switch the equivalents of the starting materials, that is, the α,β -unsaturated ketone **4.012** was taken as the limiting reagent and compound **4.011** was used in excess (2 eq.). It was found that switching the equivalents in this fashion increased the reaction time by 12 h, however the yields were not affected and hence this method was adopted for scale ups.

The coupling constant of the vinylic protons of the α,β -unsaturated ketone **4.012**, indicated that the double bond was *trans* in nature ($J = 15.7$ Hz) as shown in the proton NMR spectrum (**Figure 4.25**). As discussed previously in Chapter 3, compound **4.007** would not cyclise due to this *trans* double bond, thus the double bond needed to be saturated. Saturation of the double bond can be achieved through hydrogenation [24], however in this case we also needed to install a hydroxyl group on the THP ring in order to obtain the desired core (**4.001**).

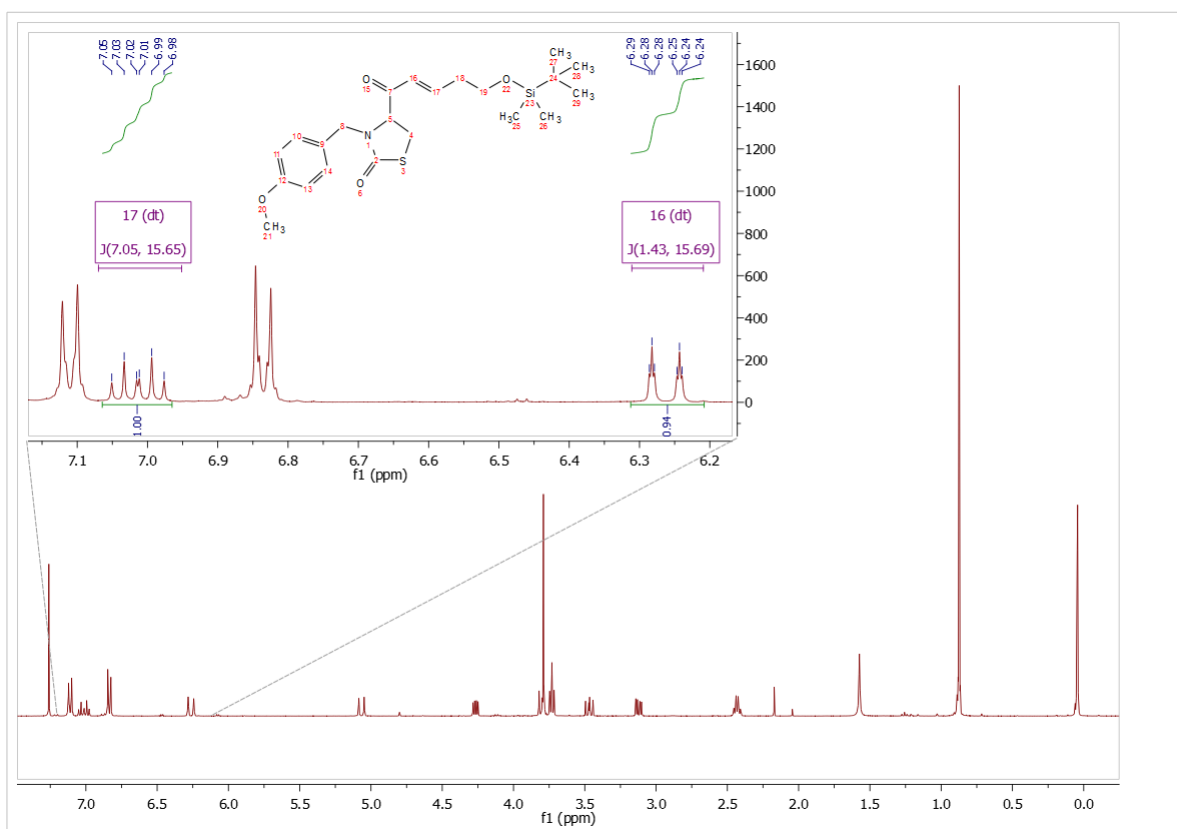


Figure 4.25: Proton NMR spectrum of compound **4.007** showing the presence of *trans* double bond ($J = 15.7\text{Hz}$).

The solution to both the issue of removing the *trans* double bond and installing a hydroxyl group on the THP ring, was achieved by employing a Michael addition reaction [4, 25]. Compound **4.007** was treated with 6 M aqueous HCl in THF, whereby addition of water takes place along with the TBS-deprotection and subsequent oxa-cyclisation resulting in the production of the PMB protected core (**4.008**) in 49% yield (which is approximately 79% for each individual step) as shown in **Figure 4.26**. As previously discussed, the hemiacetal being unstable was converted to the acetal **4.009** before further modifications.

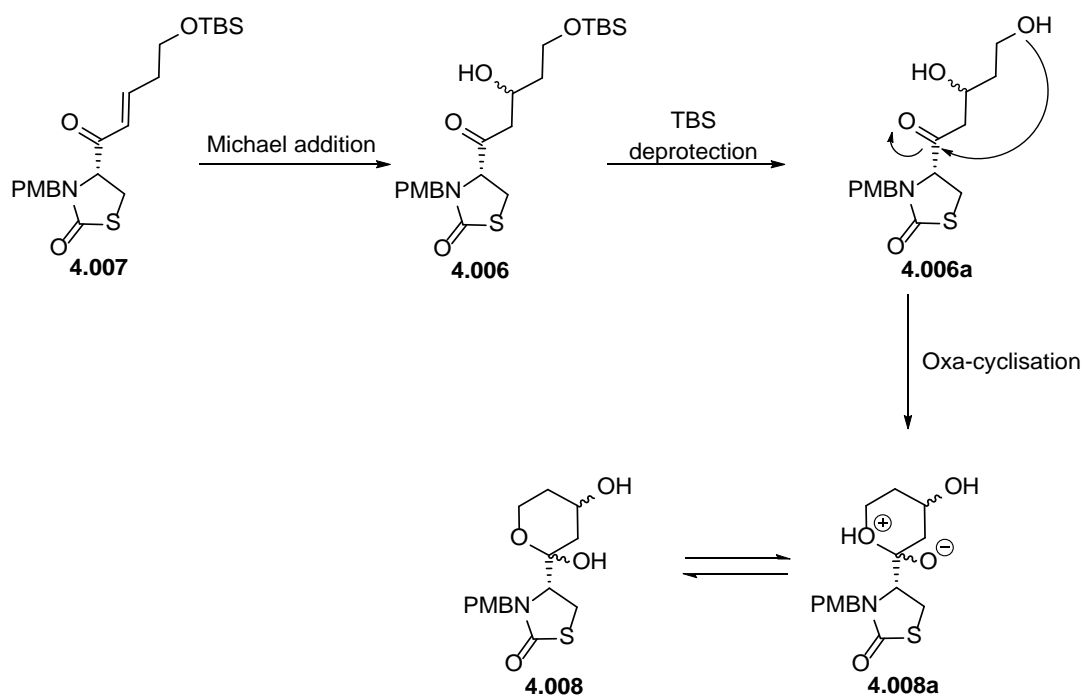


Figure 4.26: Step-wise representation of the one pot Michael addition, TBS-deprotection and oxa-cyclisation reactions leading to the formation of compound **4.008**.

This alternative approach using alkene metathesis as the key step uses 4 steps to synthesise the core **4.008** (hemiacetal) from the acid **3.037** with overall 21% yield. Although the alkene metathesis approach has one additional step when compared to the aldol method (with overall yield of 19%), the reactions were more reliable and consistent. The metathesis scheme was therefore selected as the method of choice for the scale up synthesis and the SAR studies.

4.3 Synthesis of truncated analogues of latrunculin

The newly synthesised core can be represented as shown in **Figure 4.27**, which helps visualise the various positions that can be diversified in order to obtain a library of truncated latrunculin analogues. Such a library would provide valuable SAR information about latrunculin and the effect of different substituents on the activity. Positions R^1 and R^4 were occupied by the macrocycle in latrunculin, but are now available for diversification. Position R^2 is a free alcohol in latrunculin which can be easily differentiated to study SAR at this position. Similarly, position R^3 which is a free amine can be modified with different nitrogen protecting groups to study the effect of substituents on the overall activity. This chapter will focus only on R^1 modifications and would be brought about using PMB as a protecting group installed at the R^3 position in order to avoid undesired side reactions and a methoxy installed at the R^2 position to ensure the stability of the

molecule. Compound **4.009** with the PMB protection at the nitrogen and methoxy acetal was therefore chosen as starting point for the synthesis of these analogues.

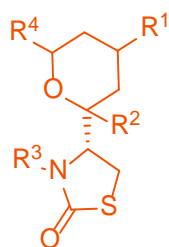


Figure 4.27: The general structure of the new core showing the different positions open for diversification.

4.3.1 R¹ Modifications

4.3.1.1 R¹ Modifications with Ester linkage

The natural product latrunculin has an ester group at the R¹ position as shown in **Figure 4.28**. Initially, analogues with an ester linkage at the R¹ position were explored as these would engage the hydrogen bonding interactions with actin that was observed in the actin-latrunculin B complex .

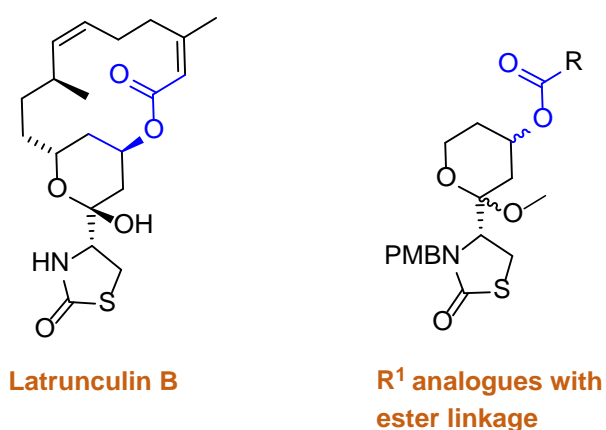


Figure 4.28: Structure of latrunculin B and the general structure of the compound with variable R¹ modification using an ester linkage.

Esterification between an acid and an alcohol can be introduced using various methods such as Fischer-Speier esterification (catalysed by Lewis or Brønstedt acid) [26], Steglich Esterification

(using dicyclohexylcarbodiimide (DCC), 4-(dimethylamino)pyridine (DMAP)) [27] and Mitsunobu reactions (esterification with inversion of the stereo centre) [28]. Esters can also be generated by converting the acid to the corresponding acid chloride first and then treating this highly activated acyl chloride with an alcohol to yield the ester [29]. In this instance, the esters were synthesised using EDCI.HCl and DMAP [30]. **Figure 4.29** represents the general procedure for this reaction.

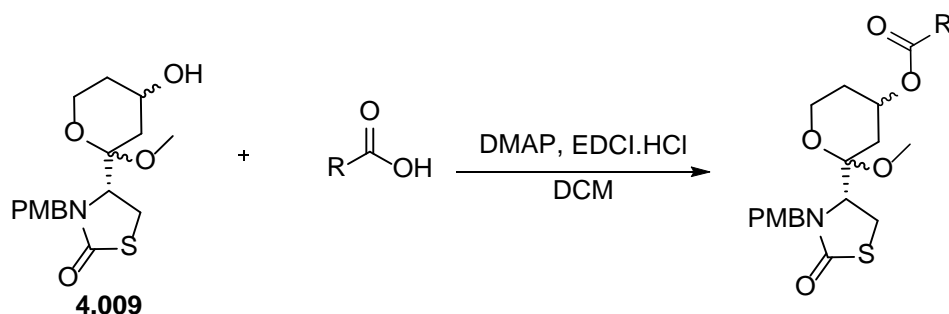


Figure 4.29: The general procedure for esterification using EDCI.HCl and DMAP.

Various esters were synthesised using this general procedure. Depending on the type of acid used, the esters were classified into three different types namely the fatty acid derivatives, the heteroaromatic acid derivatives and the benzoate derivatives as discussed below.

4.3.1.1.1 Fatty acid derivatives

The fatty acid derivatives were the ester analogues which were primarily hydrophobic in nature. This was in order to mimic the multiple hydrophobic interactions with actin exhibited by the macrocyclic moiety of latrunculin. Only two analogues were synthesised as an initial attempt to probe the effect of such substituents on actin binding. A linear and a cyclic derivative were chosen in order to diversify the analogues. This led to the synthesis of compound **4.018** (valeric acid derivative) and compound **4.019** (cyclopentanecarboxylic acid derivative) in 82% and 38% yields respectively as shown in the **Figure 4.30**.

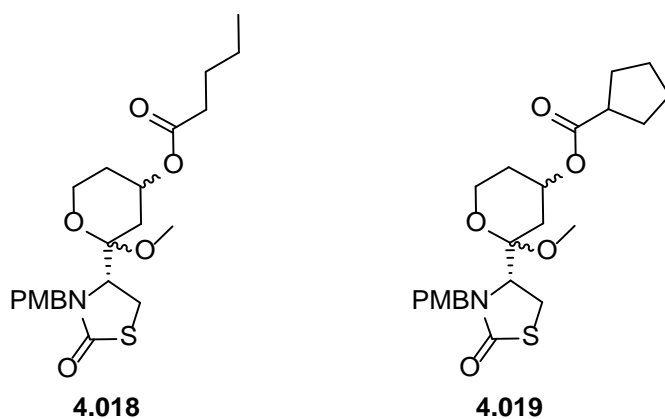


Figure 4.30: Fatty acid derivatives with esterified R¹ modifications.

4.3.1.1.2 Heteroaromatic acid derivatives

In order to study the effect of the ester linkage but with lower lipophilic character as compared to the fatty acid derivatives, it was decided to synthesise two hetero aromatic derivatives. The presence of the heteroatoms would also aid in forming any possible hydrogen bonds with actin. The two derivatives synthesised were compound **4.020** (with one hetero atom) from 2-furoic acid and compound **4.021** (with two heteroatoms) from 4-thiazolecarboxylic acid in 98% and 55% yields respectively as shown in **Figure 4.31**.

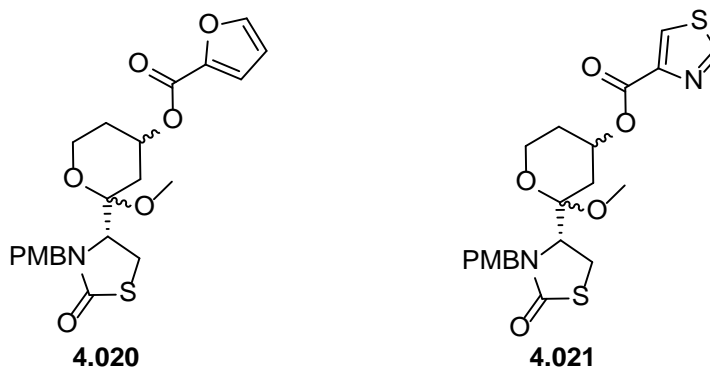


Figure 4.31: Hetero aromatic derivatives with esterified R¹ modifications.

4.3.1.1.3 Benzoate derivatives

The third group of analogues, introduced a benzoate at the R¹ position. The aim of the benzoate was to retain the ester linkage of the latrunculin and also introduce the double bond character of the alkene adjacent to the ester group as highlighted in **Figure 4.32**.

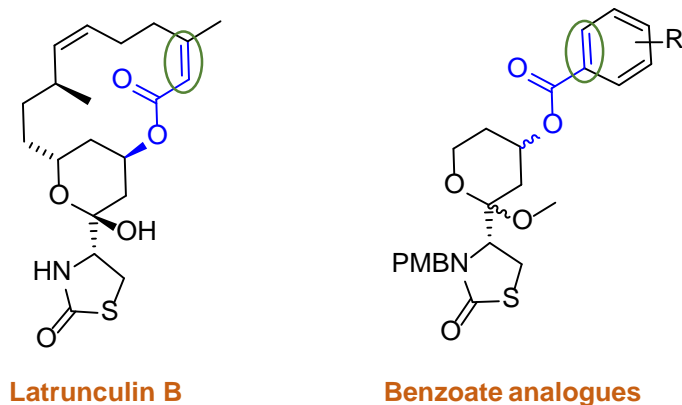
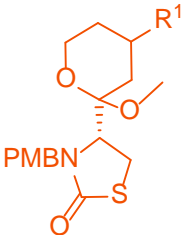
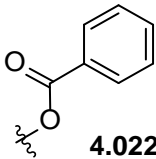
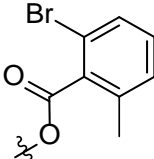
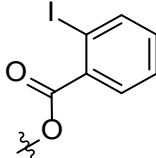
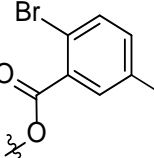
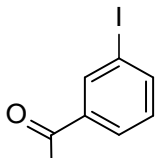
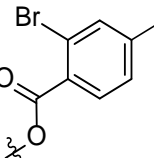
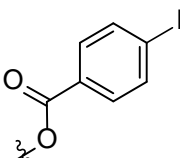


Figure 4.32: The benzoate analogues which retain the double bond character of latrunculins.

With this in mind, several analogues were synthesised beginning with the unsubstituted benzoic acid derivative. **Table 4.03** summarises all the analogues synthesised with their respective yields. All the benzoate analogues were synthesised according to the general coupling conditions described in **Figure 4.29**. It was found that the reaction with 2-bromo-6-methylbenzoic acid for the synthesis of compound **4.036**, did not go to completion even after stirring for 24 h at room temperature as the TLC analysis indicated the presence of only starting materials. In order to force the reaction to completion, it was decided to heat the reaction mixture to 40°C. However even after heating the reaction mixture and prolonging the reaction time (48 h), it was found that the reaction still remained incomplete. The poor reactivity and low yield of this reaction can be attributed to the steric hindrance posed by the presence of the methyl and the bromo group at the *ortho* positions to the acid moiety hindering it from coupling.

Table 4.03: The benzoate analogues.

	R ¹	Yield	R ¹	Yield
	 4.022	59%	 4.036	4%
	 4.023	60%	 4.037	85%
	 4.034	88%	 4.038	57%
	 4.035	96%		

Note that all these substituted phenyl derivatives contained a halogen at various positions in order to derivatise at these positions later. This further derivatisation was brought about using a Suzuki reaction. **Figure 4.33** shows the general procedure used for the Suzuki reaction using either the boronic acid or the pinacol ester [31].

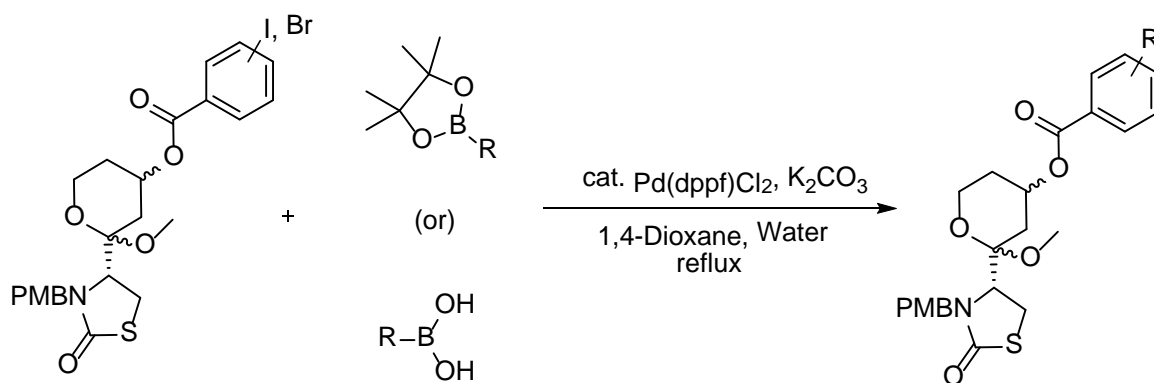


Figure 4.33: General scheme for the Suzuki reaction.

More emphasis was given to derivatise at the 2-position of the phenyl ring because in latrunculins, the top part of the macrocycle corresponds to the expanse next to the 2-position in the benzoate analogue. Therefore any substituent coming off the 2-position of the phenyl ring on these analogues should mimic the alkyl chain of the macrocycle in latrunculin. The other positions were also explored but to a lesser extent.

It was found that the Suzuki reactions with the 3-iodo and 4-iodo derivatives did not lead to product formation as expected. The proton NMR spectrum and LCMS analysis of the Suzuki reaction involving compound **4.034** with 2-thiopheneboronic acid led to the hydrolysis of the ester forming 3-(thiophen-2-yl)benzoic acid **4.039**, trace amounts of the desired product **4.040** and other decomposition products as shown in **Figure 4.34**. The production of 3-(thiophen-2-yl)benzoic acid **4.039** suggested that the ester bond was hydrolysed during the Suzuki reaction. This may be due to the presence of water, which under basic conditions and elevated temperatures led to the hydrolysis of the ester bond. Similar hydrolysis was observed in the case of the 4-iodo derivative **4.035** also.



133

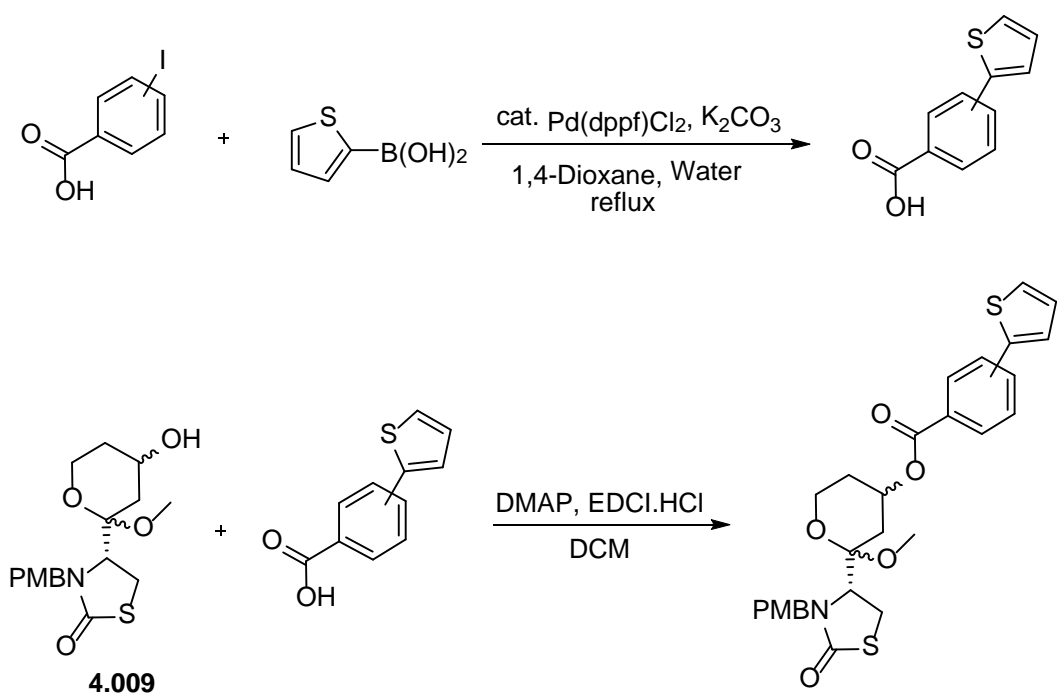
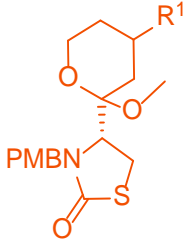
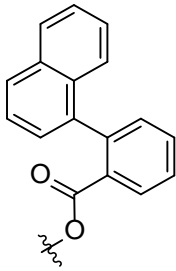
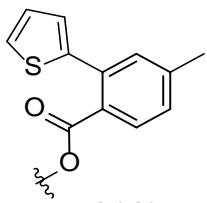
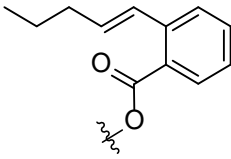
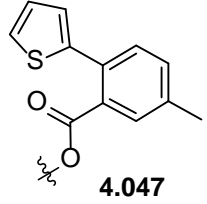
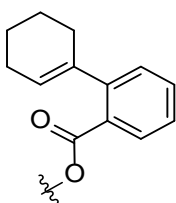
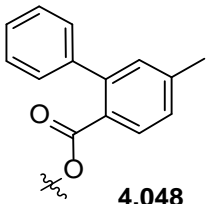
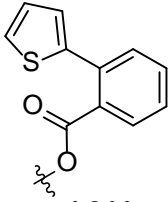
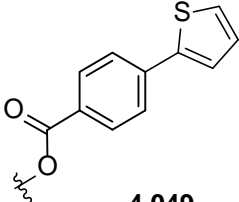
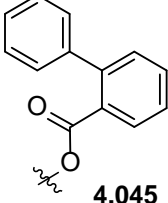
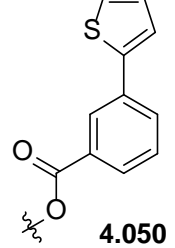


Figure 4.35: Modified scheme for the synthesis of substituted benzoic acids derivatives by first forming the thiophenebenzoic acids and then esterifying with **4.009**.

The same scheme was repeated for the 4-iodo derivatives as well to produce the analogues at the 4-position. This method led to the desired product in the same number of steps as the earlier method with yields ranging from 30% to 95% as shown in **Table 4.04**.

Table 4.04: Analogues synthesised using esterification followed by Suzuki reaction^a and direct Suzuki using substituted benzoic acid^b.

	R ¹	Yield	R ¹	Yield
	 4.041	90% ^a	 4.046	89% ^a
	 4.042	57% ^a	 4.047	88% ^a
	 4.043	85% ^a	 4.048	94% ^a
	 4.044	70% ^a	 4.049	95% ^b
	 4.045	53% ^b	 4.050	32% ^b

4.3.1.2 Ketone based R¹ modification

The next R¹ modification attempted was to oxidise the secondary alcohol of the PMB protected core **4.008** to the corresponding ketone **4.051**. This would not only remove one chiral centre from the molecule, but would also facilitate functionalising the core with other linkages such as hydrazones, amines and amides as shown in **Figure 4.36**.

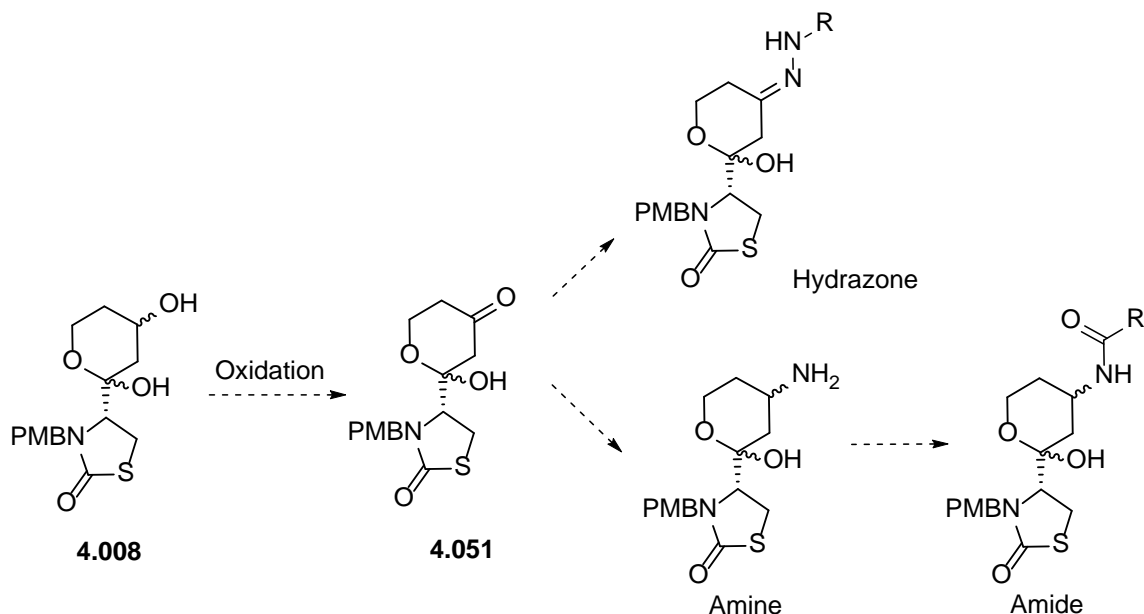


Figure 4.36: Possible functionalisations of compound **4.008** with ketone based R¹ modifications.

The first attempt for this oxidation was made using a stabilised formulation of IBX (SIBX) in *N*-methyl-2-pyrrolidone (NMP) (**Table 4.05**, entry 1) [33]. The reaction only led to the production of undesired products which were unidentifiable by proton NMR spectrum. Swern oxidation [6] was also attempted (**Table 4.05**, entry 2), however the TLC analysis after an hour displayed the presence of numerous products along with the starting material indicating that a large number of side products/ decomposition products were formed. After work up and flash chromatography, the proton NMR spectrum established that none of the isolated compounds was the desired product. Swern oxidation conditions lead to the production of a strong acid (HCl), and the acid sensitive hemiacetals may have decomposed under these conditions.

Another approach to obtain the ketone **4.051** was to start from compound **4.006** as shown in **Figure 4.37**. Oxidising the alcohol before TBS-deprotection and ring closure would mean that the hydroxyl group would be oxidised before the formation of the hemiacetal and therefore it would be more

tolerant to the oxidation conditions. Once the ketone **4.052** was formed, the TBS group can be deprotected and ring closed to obtain the desired ketone as shown in the scheme in **Figure 4.37**.

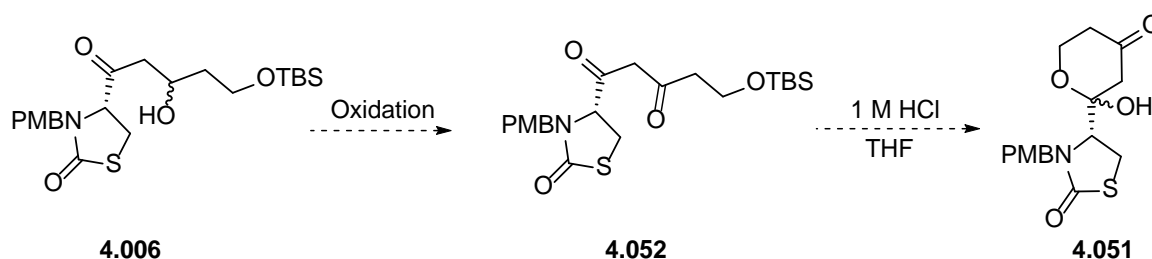


Figure 4.37: Proposed scheme for the synthesis of the ketone intermediate **4.052** starting from the uncyclised compound **4.006**.

It should be noted that the product obtained by the oxidation of the uncyclised compound **4.052**, could exist in either of its tautomeric forms namely keto (**4.052**) or enol (**4.052a**), as shown in **Figure 4.38**.

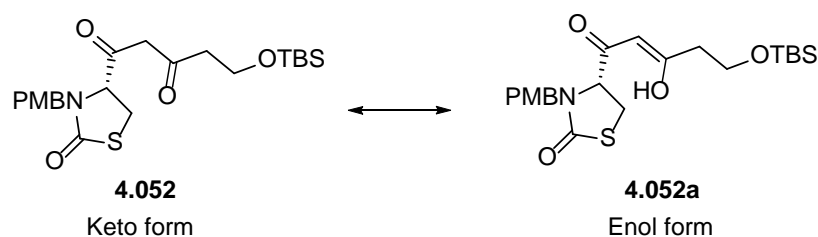


Figure 4.38: Keto-enol tautomerism.

The Swern oxidation [6] was therefore attempted on the uncyclised compound **4.06** (**Table 4.05**, entry 3). After the completion of the reaction as indicated by TLC analysis, the reaction was quenched and purified by flash chromatography. The only identifiable products by proton NMR spectrum were the *trans* alkene **4.007** (as also seen during the Aldol reaction, and the desired oxidised product as shown in the **Figure 4.39**.

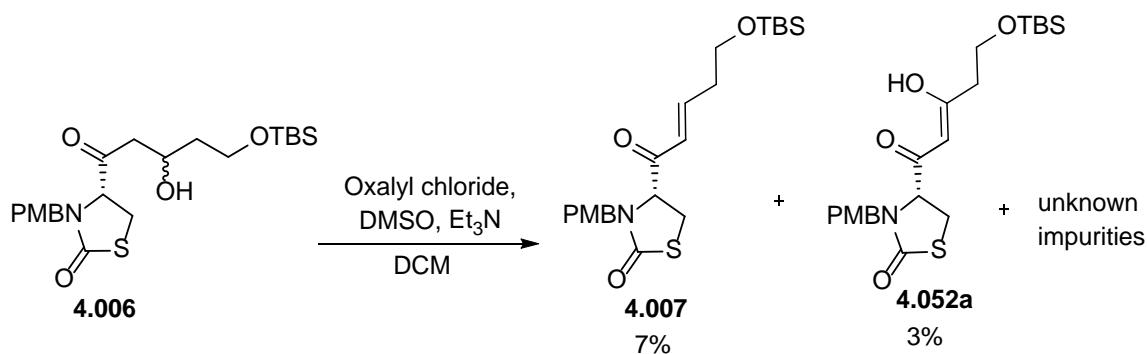


Figure 4.39: Swern oxidation of compound **4.006** leading to the formation of the eliminated alkene **4.007** and the enol **4.052a**.

Closer analysis of the proton NMR spectrum revealed that the oxidised product was in its enol form. **Figure 4.40** shows the proton NMR spectrum of compound **4.052a** highlighting the singlet at 5.65 ppm corresponding to a single proton (peak 7 in **Figure 4.40**), which confirms the enol form. The compound prefers the enol form because of the added stability attained due to the possible conjugation of the double bond with the ketone. The yield of this Swern oxidation reaction was however very low and thus other oxidation conditions needed to be trialed as illustrated in **Table 4.06**.

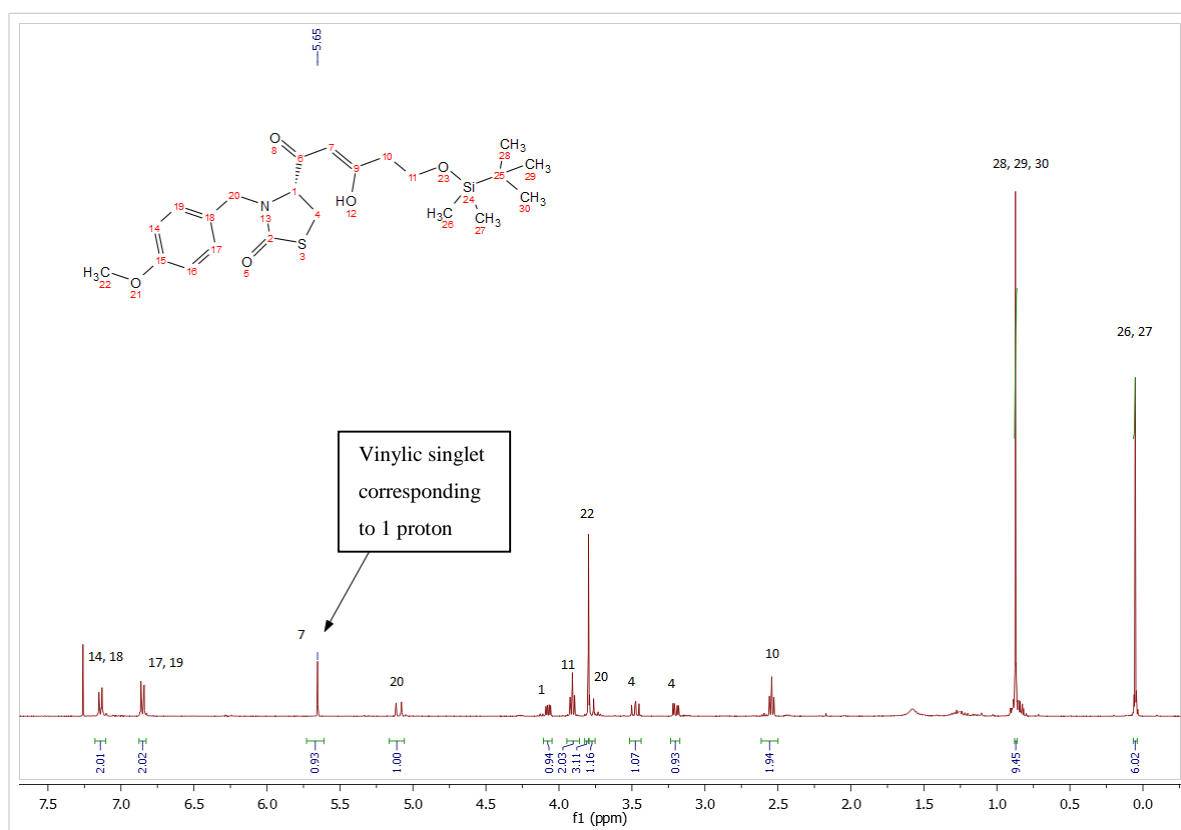


Figure 4.40: The proton NMR spectrum of compound **4.052a** confirming its enol form.

Next, Parikh Doering oxidation [9] using sulfur trioxide pyridine complex, DMSO and Et₃N was attempted on compound **4.006** (Table 4.06, entry 4). The TLC analysis indicated the formation of several new products, of which only the eliminated alkene **4.007** could be identified by the proton NMR spectrum. The yield of this eliminated alkene **4.007** was however found to be very low (<2%). TEMPO-BAIB oxidation [34] was also attempted on **4.006** (Table 4.06, entry 5), but the analysis of the reaction by TLC analysis, did not indicate the formation of any new product and thus this method was also not pursued.

The Dess-Martin periodinane (DMP) oxidation [35] was also attempted (Table 4.06, entry 6-a); and the first conditions trialed used DMP in wet DCM. However, even after stirring the reaction mixture for 12 h, TLC analysis did not indicate formation of any new product and thus was not pursued. The next conditions trialed was using *tert*-butanol instead of water [36] (Table 4.06, entry 6-b), so as to make the reaction conditions anhydrous. After 1.5 h, TLC analysis indicated the presence of starting material as well as a new product. After stirring the reaction mixture for an additional 30 min, it was found that the new product could no longer be visualised by TLC analysis and only starting material was recovered after flash chromatography. This disappearance of the new product (initially visualised by the TLC analysis), suggested that longer reaction times led to

decomposition/loss of the product. The reaction was therefore repeated with TLC analysis conducted every 10 min in order to closely monitor product formation. It was found that within 20 min, a new product was formed. The reaction was quickly quenched and purified to obtain the desired product **4.052a** (enol form) in 38% yield as represented in **Figure 4.41** (**Table 4.06**, entry 6-c).

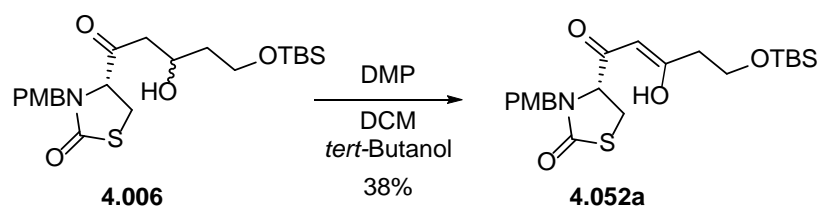


Figure 4.41: DMP oxidation of compound **4.006**.

Table 4.06: Conditions attempted for the synthesis of compound **4.052**.

Starting material	Entry	Reaction	Conditions	Comment	Yield
<p style="text-align: center;">4.008</p>	1	IBX	SIBX, NMP	Unidentifiable products	
	2	Swern	Oxalyl chloride, DMSO, DCM	Decomposition products	
<p style="text-align: center;">4.006</p>	3	Swern	Oxalyl chloride, DMSO, DCM	Desired product and eliminated compound	3%
	4	Parikh Doering	SO ₃ .Py complex, DMSO, DCM	Eliminated compound	
	5	TEMPO-BAIB	TEMPO, BAIB, DCM	No Reaction	
	6	DMP	1.DMP, DCM, H ₂ O	Decomposition product (3.007)	
	7		DMP, DCM, <i>tert</i> -Butanol (2h)	Unidentifiable product	
	8		DMP, DCM, <i>tert</i> -Butanol (20min)	Desired product	38%

Once compound **4.052a** was synthesised, the next step was to perform a cyclisation, so as to obtain the ketone **4.051** as shown in **Figure 4.42**. For this, compound **4.052a** was treated with 1 M aqueous HCl in THF until the TLC analysis indicated complete conversion of the starting material to the product. Flash chromatography and ^{13}C NMR spectrum analysis however indicated that the isolated compound was the uncyclised TBS-deprotected enol **4.051a**, meaning that the compound prefers its uncyclised form (**4.051a**) over the cyclised form (**4.051**) as shown in **Figure 4.42**.

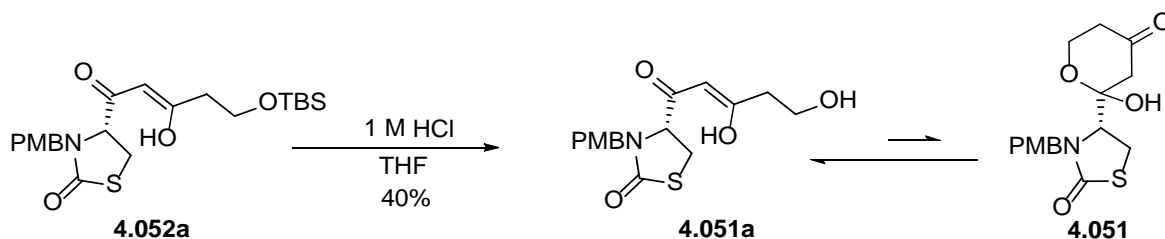


Figure 4.42: TBS-deprotection of compound **4.052a**.

Compound **4.051a** in the enol form, can adopt the *cis* or the *trans* configuration with respect to the alkene. The *trans* configuration can however form hydrogen bond between the hydroxyl group and the ketone as shown in **Figure 4.43**. This added stability in the *trans* form prevents the ring closure required in order to form compound **4.051**, as cyclisation is not possible while in its *trans* state.

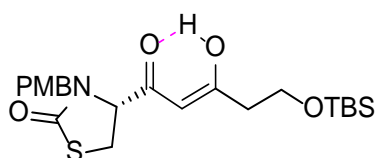


Figure 4.43: Compound **4.051a** in the enol form, with the hydrogen bonds formed (in pink) due to the *trans* nature of the double bond.

In an attempt to change the configuration of the compound **4.051a** from the enol form to its keto form, it was decided to change the solvent of the above reaction from THF to DMSO, so as to break the hydrogen bond interaction as illustrated in **Figure 4.44**. The reaction with DMSO as the solvent was however not successful, as it only led to products unidentifiable by proton NMR spectrum.

In summary, the oxidation using the hemiacetal **4.008** and the uncyclised **4.006** did not lead to the desired ketone **4.051**. It was therefore decided to discard both these schemes and try oxidising the methoxy acetal **4.009** instead, as shown in **Figure 4.44**.

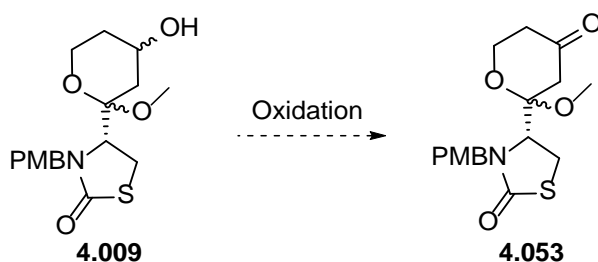


Figure 4.44: Synthesis of ketone based R¹ modification starting from the acetal **4.009**.

The first attempt at oxidising **4.009** was using DMP oxidation [35], since it had shown promising results with the uncyclised compound **4.006**. The reaction worked and the proton NMR spectrum identified the production of the desired product, however, the yields of this reaction were not consistent (varying from 44% to 68%). In order to avoid these inconsistencies and also to seek an alternative, safer route to scale up this oxidation (since DMP can be explosive under mechanical force conditions), it was decided to try the oxidation using the SIBX [33]. After the completion of the reaction with SIBX, flash chromatography led to the isolation of pure desired product **4.053** in 68% yield.

During subsequent scale up (from 20 mg to 250 mg), it was observed that the reaction undergoes side reactions. On larger scales, the elimination of methanol leading to the formation of the corresponding α,β -unsaturated ketone **4.054** was favoured over the formation of the desired product, thereby decreasing the yield of desired ketone considerably (29%) as shown in **Figure 4.45**.

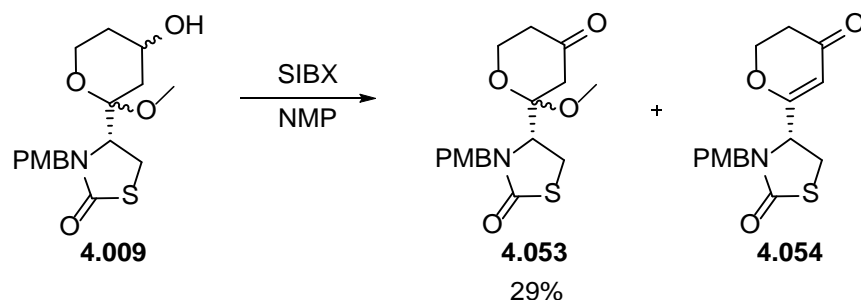


Figure 4.45: Oxidation of the acetal **4.009** leading to the formation of desired ketone **4.053** and the α,β -unsaturated ketone **4.054**.

Figure 4.46 shows the possible mechanism leading to the formation of the α,β -unsaturated ketone **4.054**. As can be seen, the base can extract a proton from the alpha carbon of compound **4.009** which then initiates a relay of electron transfers leading to the formation of compound **4.054**. In

order to avoid the formation of the α,β -unsaturated ketone **4.054** so as to improve the yield of compound **4.053**, it was decided to repeat the reaction and alter the quenching of the reaction. A milder base namely 1:1 mixture of saturated sodium thiosulfate solution and saturated sodium bicarbonate solution was used in this case. However, it was found that even with the milder base work up, the reaction still led to the formation of the α,β -unsaturated ketone **4.054**.

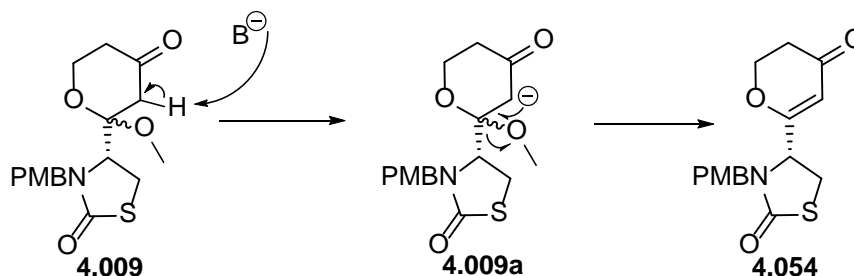


Figure 4.46: Proposed mechanism leading to the formation of the α,β -unsaturated ketone **4.054**.

Compound **4.054** was an interesting and novel molecule and its formation was inevitable on scale up reactions under the conditions investigated, it was therefore decided to utilise this compound for derivatisation along with compound **4.053**.

The isolation of these compounds however posed certain issues. With a larger scale, the amount of NMP used in the reaction increased which became an issue since it co-eluted with the products during flash chromatography. Another issue was that the α,β -unsaturated ketone **4.054** and any unreacted starting material **4.009** had the same polarity and thus were inseparable by flash chromatography. Freeze-drying was used to remove NMP from the crude product which was then subjected to flash chromatography to separate the two products **4.053** and **4.054**. Compound **4.053** was obtained in the pure form and the slightly impure compound **4.054** (with a small amount of unreacted starting material **4.009**) was directly used for subsequent reactions namely the hydrazone formation and the amine formation.

4.3.1.2.1 Hydrazone derivatives

Hydrazones are classically synthesised by treating ketones with the corresponding hydrazines in the presence of a catalytic amount of acid in ethanol [37]. In this case, the solvent of the reaction was changed from ethanol to methanol, so as to avoid possible addition of ethanol to compound **4.009c** under acidic conditions as shown in **Figure 4.47**. Using methanol as the solvent ensures that, there is no competing nucleophile (ethanol) present during the re-addition.

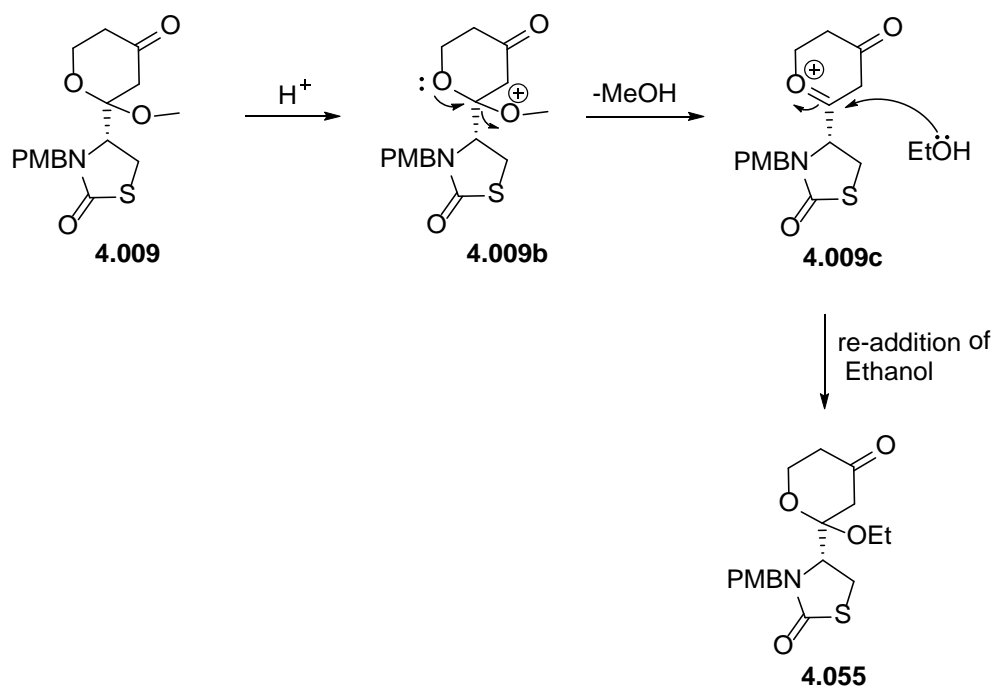
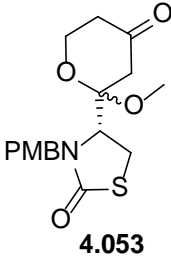
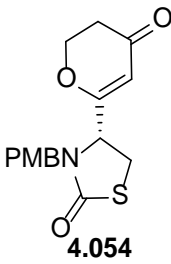


Figure 4.47: Possible elimination and re-addition of ethanol.

The first attempt at synthesizing the hydrazone utilised the ketone **4.053** with phenyl hydrazine and catalytic acetic acid in methanol [37]. Following stirring the reaction mixture for 18 h, TLC analysis indicated complete consumption of the starting material and the new product could be successfully isolated. However, it was observed that the isolated compound was an unidentifiable by-product and therefore it was decided to explore other conditions. **Table 4.07** represents all the different conditions explored for the hydrazone formation.

Table 4.07: The various conditions attempted for the synthesis of hydrazones.

Entry	Starting material	Conditions	Comment	Yield
1	 4.053	Phenylhydrazine, Acetic acid, Methanol	Undesired product	
2		Phenylhydrazine, Dowex® acidic resin, Methanol	Eliminated hydrazone 4.056 and eliminated ketone 4.054	<10% each
3		Benzylhydrazine, Dowex® acidic resin, Methanol	Eliminated hydrazine 4.056	<10%
4		<i>tert</i> -Butyl hydrazine, Dowex® acidic resin, Methanol	Eliminated ketone 4.054	<10%
5		<i>tert</i> -Butyl hydrazine (2.5 eq.), Dowex® acidic resin, Methanol	Poor recovery of the crude mixture	
6	 4.054	Benzylhydrazine, Acetic acid, Methanol	Eliminated hydrazone 4.056	<10%
7		Benzylhydrazine, Dowex® acidic resin, Methanol	No product formed	
8		Phenylhydrazine, Dowex® acidic resin, Methanol	Eliminated hydrazine 4.056	<10%

The first modification attempted for the hydrazone formation was to change the acid used (**Table 4.07**, entry 2). In 2005, Niknam *et al.* employed Dowex® acidic resins as a solid acid catalyst for the clean and less hazardous protection of carbonyl compounds [38]. Following this paper, Dowex® acidic resin was used instead of acetic acid for the synthesis of the hydrazones using compound **4.053** and phenyl hydrazine as the substrates. Although the reaction presented complete conversion by TLC analysis, the recovery of the crude product was very low. This was possibly because the

compound was trapped in the resin, and therefore the filtration was administered with repeated hot methanol washes. This only led to a minimal improvement in the amount of the crude material recovered. The crude thus recovered was purified by column chromatography to isolate two compounds which upon LCMS analysis represented the ionic mass of $[M+H]^+$ 320 m/z and $[M+H]^+$ 410 m/z; none of which corresponded to the desired hydrazone.

The proton NMR spectrum of the compound with $[M+H]^+$ 320 m/z represented the α,β -unsaturated ketone **4.054** and that of the compound with $[M+H]^+$ 410 m/z corresponded to the eliminated hydrazone **4.056** as shown in **Figure 4.48**. The yield of both these isolated products was however less than 10%.

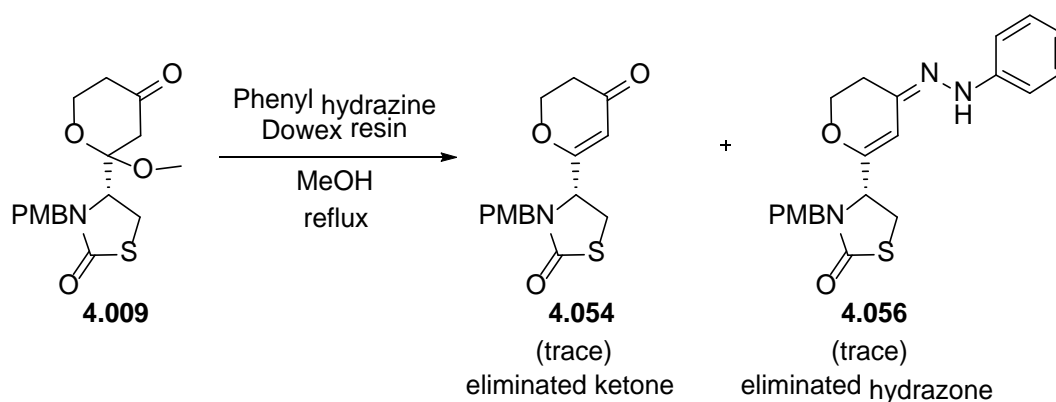


Figure 4.48: Hydrazone formation reaction leading to the formation of compounds **4.054** and **4.056**.

Unlike the base mediated elimination as shown in **Figure 4.46**, here the elimination is acid mediated due to the presence of Dowex resin. **Figure 4.49** shows the proposed acid mediated mechanism for the elimination of methanol. As can be seen from the figure, under acidic conditions the methoxy gets protonated which leads to the formation of the oxonium ion **4.009c**. The ketone of the oxonium, then adopts its enol form **4.009d**, so as to neutralise the charge on the molecule leading to the formation of the α,β -unsaturated ketone **4.054**.

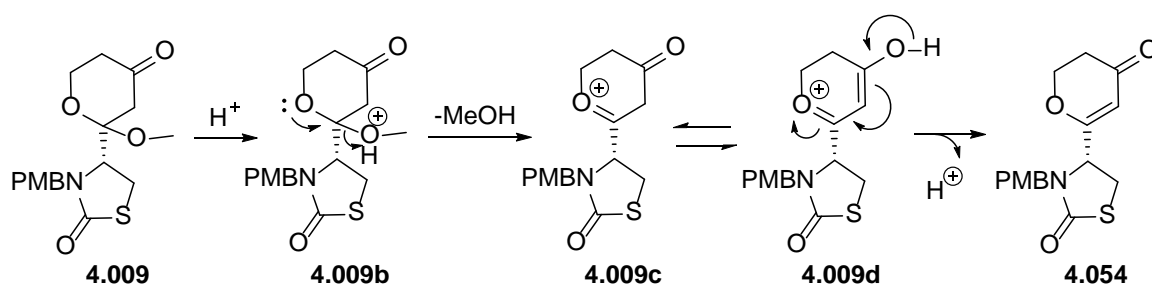


Figure 4.49: Proposed acid mediated mechanism of formation of the α,β -unsaturated ketone **4.054**.

The structure of the eliminated ketone **4.054** was ascertained by the presence of the vinylic signal integrating for one proton and the absence of the singlet corresponding to the methoxy acetal in the proton NMR spectrum. **Figure 4.50** represents the proton NMR spectrum of the eliminated ketone **4.054** highlighting the vinylic signal at 6.37 ppm.

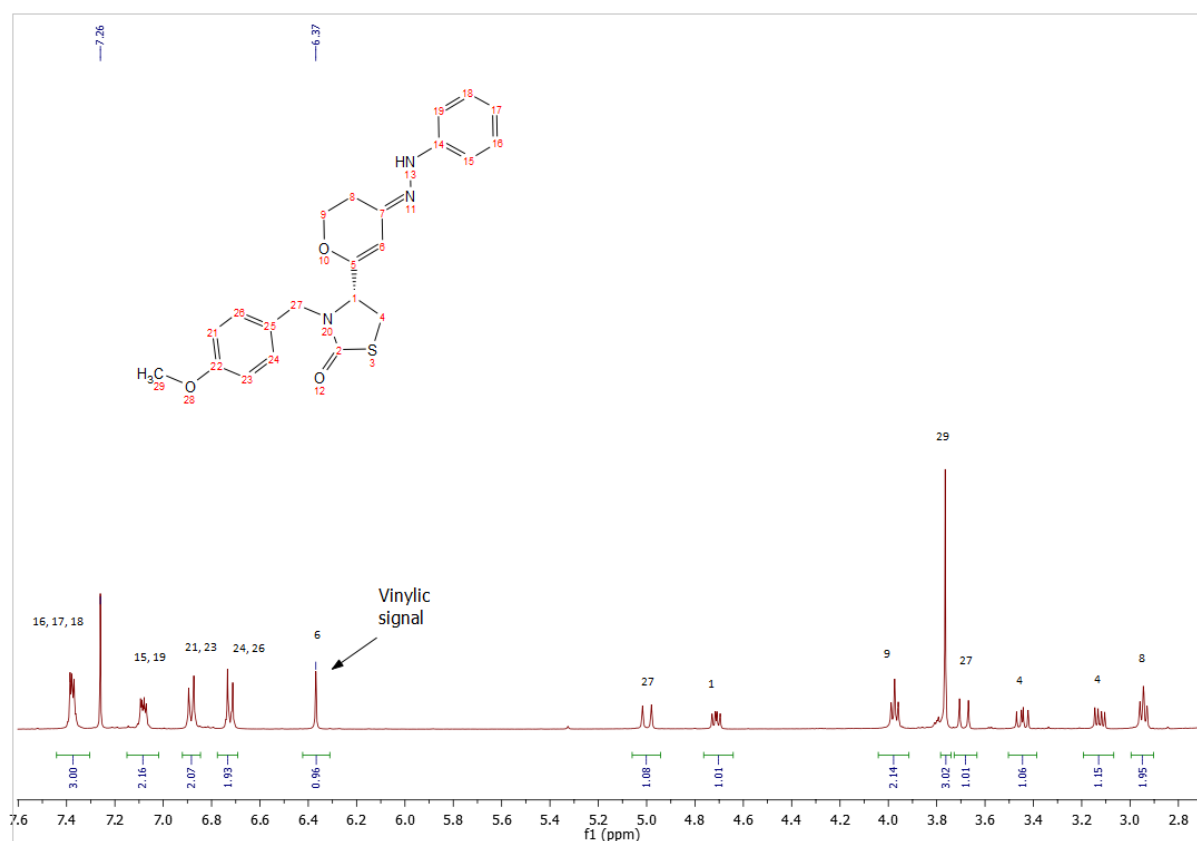


Figure 4.50: The proton NMR spectrum of the eliminated ketone **4.054**.

In order to understand any influence of the type of hydrazine (aromatic/ aliphatic) used in these reactions, the same conditions were attempted on other substrates namely, the benzylhydrazine (**Table 4.07**, entry 3) and *tert*-butylhydrazine (**Table 4.07**, entry 4). In the case of benzylhydrazine, the LCMS analysis represented the ionic mass of the eliminated hydrazine (424.2 m/z) as well as that of the eliminated ketone (318.3 m/z) in the negative mode. A similar result was also observed with the *tert*-butylhydrazine as well, thereby suggesting that irrespective of the substrate used, this reaction always led to the elimination of methanol. The yields of both the recovered products were found to be very poor in these cases (<10%).

The reaction was also trialed with higher equivalents of *tert*-butylhydrazine (2.5 eq.) in an attempt to improve the yield of the reaction (**Table 4.07**, entry 5). The reaction, however did not show any considerable increase in the yield of product formation, as the crude recovered from the reaction was still less than 10% in yield.

In light of these observations leading to the formation of the eliminated ketone **4.054**, it was decided to use **4.054** instead of compound **4.053**, as the starting material for the hydrazone formation. It was predicted that, starting from the eliminated ketone could potentially eliminate other side reactions and therefore only lead to the hydrazone formation, increasing the yield of the eliminated hydrazone.

In order to test this hypothesis, the reaction was performed using the eliminated ketone **4.054** as the starting material along with benzylhydrazine and acetic acid (Table 4.07, entry 6). Contrasting our hypothesis, the TLC analysis of this reaction displayed the formation of a large number of new products. The yield of the crude mixture was again less than 10% and therefore purification or isolation of the product was not attempted even though LCMS analysis of the crude product indicated the presence of the ionic mass of the desired hydrazone. The above reaction with ketone **4.054** and benzylhydrazine was repeated with Dowex® resin instead of acetic acid (Table 4.07, entry 7), however the LCMS analysis of the crude did not display the ionic mass corresponding to the desired product implying no product was formed and also the yield of the crude mixture was still less than 10%.

When the reaction using Dowex® resin was repeated with phenylhydrazine (Table 4.07, entry 8), the LCMS analysis indicated the desired product which was later isolated by flash chromatography as shown in Figure 4.51. The yield was however, 5%.

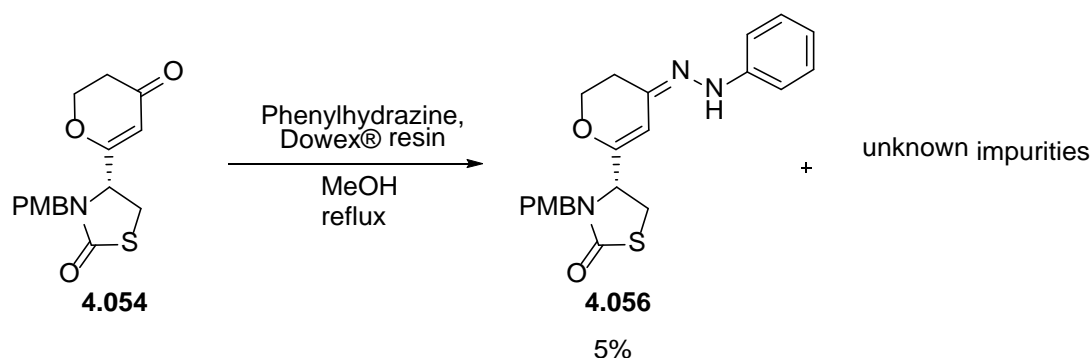


Figure 4.51: Hydrazone formation starting from the eliminated ketone **4.054**.

From the various conditions attempted it was decided that the hydrazone formation reaction always led to uncontrolled side reactions thereby decreasing the yield of the desired product. Therefore, in the interest of time, the hydrazone formation reactions were not pursued any further.

4.3.1.2.2 Amine derivatives

Ketones can be converted to amines by using a reductive amination reaction [39]. The typical procedure involves treating the ketone with a Lewis acid and the desired amine, whereby the corresponding imine is formed. The imine is then reduced to get the desired amine [40]. Figure 4.52 shows how different R substituents can lead to a variety of different analogues by simply

changing the amine used. (Note that this reaction can be attempted with both the ketone **4.053** and the α,β -unsaturated ketone **4.054** to achieve the corresponding analogues).

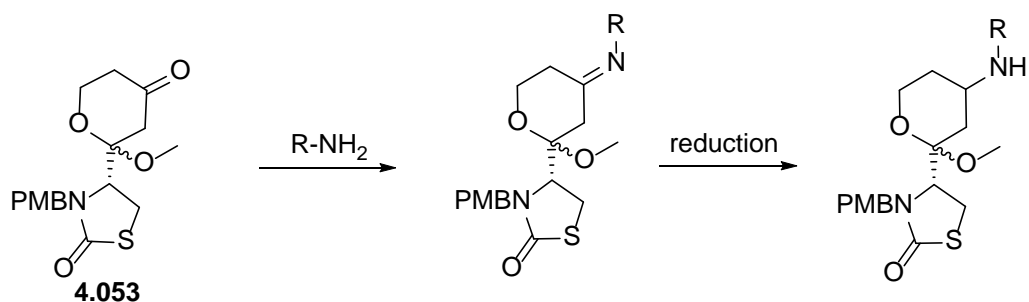


Figure 4.52: The proposed conversion of compound **4.053** to an amine using a reductive amination reaction.

The first attempted analogue utilised benzylamine with ethanol as solvent and titanium isopropoxide as the Lewis acid. The reaction was quenched when the TLC analysis indicated complete consumption of the starting material and the isolated crude was purified using flash chromatography. It was observed that the proton NMR spectrum of the isolated product did not correspond to the expected product. The aromatic peaks in the spectrum were more than expected and the methoxy acetal was also missing. The LCMS analysis indicated the ionic mass of $[M+H]^+$ 516.2 m/z and $[M-H]^-$ 514.2 m/z, both indicating the mass of the product to be 515 g/mol. It was proposed that the observed product was the result of double addition of benzylamine.

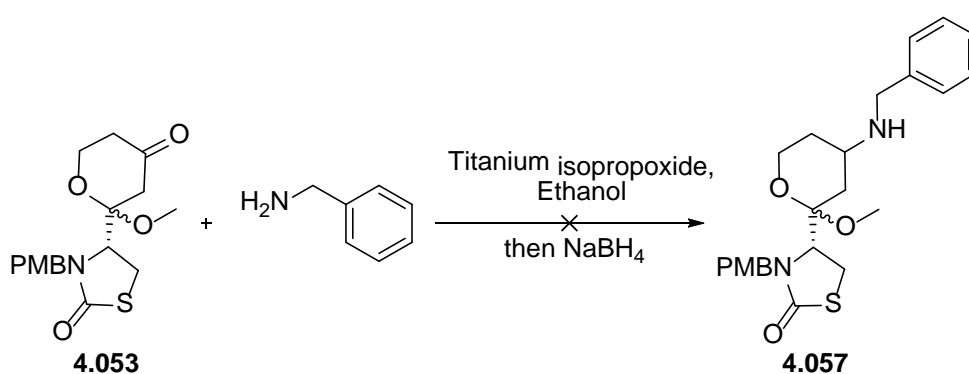


Figure 4.53: The attempted reductive amination of **4.053** with benzylamine.

The same reductive amination conditions were repeated on the α,β -unsaturated ketone **4.054** as the starting material and it was found that this reaction also did not lead to isolation of the desired

product. It was interesting to note that the proton NMR of the product isolated from this reaction was identical to the one isolated from the reductive amination of the **4.053**. Due to time constraints, the isolated product was not completely characterized to determine its structure. The synthesis of the other amine analogues were also not explored any further.

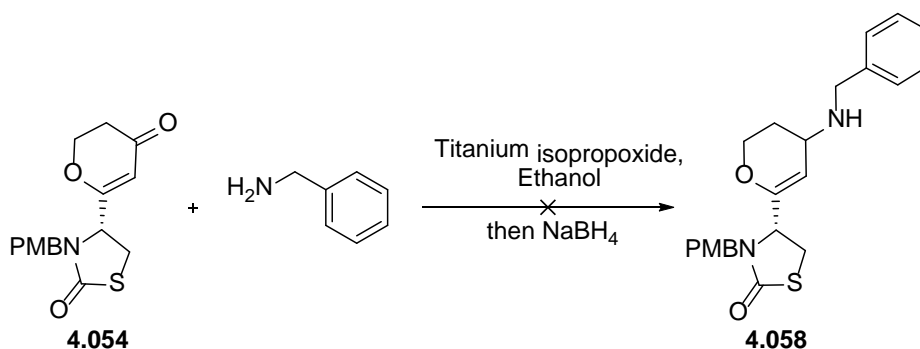


Figure 4.54: Attempted reductive amination of the α,β -unsaturated ketone **4.054** with benzylamine.

4.4 Biological studies of the R¹ modified analogues

4.4.1 *P. falciparum* growth inhibition assay

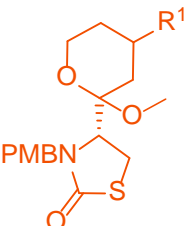
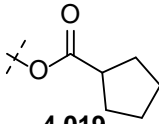
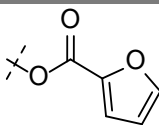
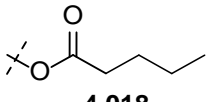
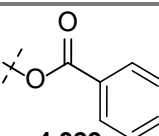
P. falciparum growth inhibition assays (GIA) were performed by researchers at the Burnet Institute, Melbourne; to determine the activity of the synthesised truncated latrunculin analogues against the *Plasmodium* parasites [41]. The parasites chosen for this assay were at their trophozoite stage which were adjusted to 0.1% parasitemia and 2% hematocrit. To 45 mL of infected red blood cells, 5 mL of stock antibody was added and mixed to generate a final culture volume of 50 mL. Parasites were allowed to develop through two cycles of erythrocyte invasion for 72 h at 37°C. Glutaraldehyde (ProSciTech) was then added to the early trophozoite stage parasites after the second round of invasion, in order to fix them for 1 hour at room temperature (final concentration of 0.25% (v/v)). After fixation, the parasites were washed in human tonicity phosphate-buffered saline (HTPBS), stained with 106 SYBR green dye (Invitrogen) and 56105 red blood cells counted per well using a BD FACSCantoII flow-cytometer. Fluorescence Activated Cell Sorting (FACS) counts were analysed using FlowJoTM(Ver 6.4.7) software (Treestar). All GIAs were run in a 96-well plate format with each antibody tested in triplicate wells.

4.4.2 SAR interpretation of the synthesised truncated latrunculin analogues

GIA was used to test the effect of the R¹ modified truncated latrunculin analogues on the *Plasmodium* parasites. The first effect studied in this regards was that of different hydrophobic groups on the benzoate derivatives of the truncated core **4.009**. **Table 4.08** illustrates the activity of these analogues and that of latrunculin B against *Plasmodium* parasites in a growth inhibition assay.

As can be seen from **Table 4.08**, the EC₅₀ of latrunculin B was 50 µM for *Plasmodium* parasites and that of the truncated core **4.009** was 100 µM. Introduction of an ester group with a butyl chain (compound **4.018**) or a furan ring (compound **4.020**) (**Table 4.08**, entry 3 and 5) did not improve activity. Although slight activity was captured using the cyclopentane derivative (compound **4.019**, EC₅₀ 87 µM), the benzoate derivative **4.022** was the first promising analogue synthesised in this series with an EC₅₀ of 37 µM. This suggested that the benzoate derivatives were promising compounds and thus it was decided to further explore around the phenyl ring so as to improve its activity.

Table 4.08: R¹ analogues of truncated latrunculin and their corresponding activity against *Plasmodium* parasites^a in a growth inhibition assay.

General structure	Entry	R ¹	EC ₅₀ (µM)	Entry	R ¹	EC ₅₀ (µM)
	1	Latrunculin B	50	4	 4.019	87
	2	-OH	100	5	 4.020	>100
	3	 4.018	100	6	 4.022	37

^a Parasite strain: 3D7, positive control: latrunculin B.

Further exploration was brought about in the form of introducing an iodo group around the phenyl ring and also introducing more substituents off the iodo groups using a Suzuki reaction. This led to

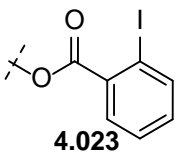
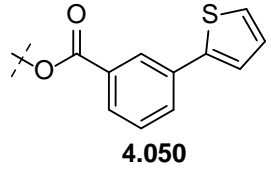
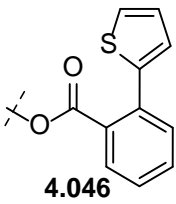
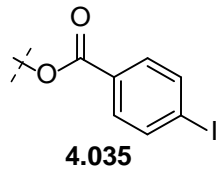
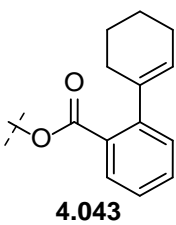
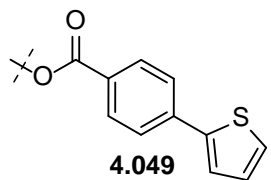
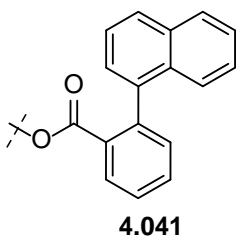
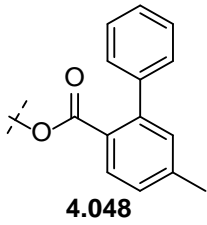
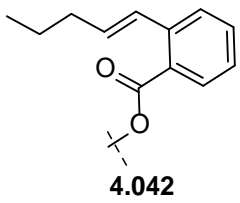
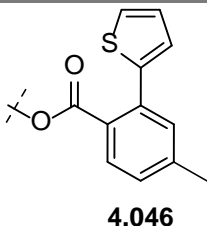
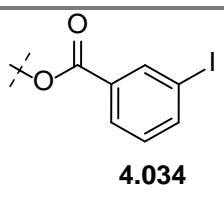
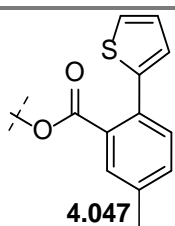
the synthesis of a library of R¹ modified benzoate analogues as shown in **Table 4.09** with their respective activity against *Plasmodium* parasites.

The SAR study reveals that the *ortho* iodo compound (**Table 4.09**, entry 1) was twice more potent than the *meta* and *para* iodo compounds (**Table 4.09**, entry 6 and 8). Further substituting the *ortho* position led to the synthesis of analogues with 5 fold increase in activity (6-8 μ M) when compared to latrunculin B. It was also observed that the presence of a linear chain off the *ortho* position (**Table 4.09**, entry 5) was less favored than any closed ring systems (**Table 4.09**, entry 2-4).

With the *meta* substituted benzoate analogues (**Table 4.09**, entry 6-7), there was a two fold increase in activity when the *meta* position had a thiophene ring rather than an iodine atom. Similar observation was also perceived at the *para* position implying that a bulkier hydrophobic group was more favored at these positions.

When methyl groups were incorporated into the *ortho* substituted benzoate analogues (**Table 4.09**, entry 10-12) it was found that the activity was not affected. This meant that although further substitution using small groups along the phenyl ring was tolerated in these compounds it does not improve the potency.

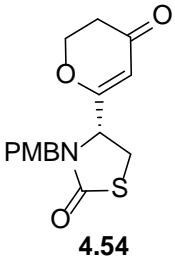
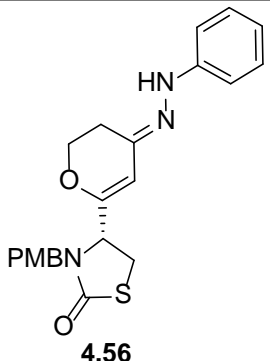
Table 4.09: R¹ modified phenyl ester analogues and their corresponding activity against *Plasmodium* parasites^a.

Entry	R ¹	EC ₅₀ (μM)	Entry	R ¹	EC ₅₀ (μM)
1	 4.023	19	7	 4.050	19
2	 4.046	8	8	 4.035	50
3	 4.043	8	9	 4.049	30
4	 4.041	6	10	 4.048	12.5
5	 4.042	41	11	 4.046	12.5
6	 4.034	50	12	 4.047	8

^a Parasite strain: 3D7, positive control: latrunculin B.

The eliminated ketone **4.054** and the hydrazone **4.056** were also tested in the growth inhibition assay but their EC₅₀ was found to be >100 μ M and 50 μ M respectively (Table 4.10). Compound **4.057** being less active than the benzoate derivative **4.034** (Table 4.09, entry 6), suggests that the ester group at R¹ position and the methoxy at R² are crucial for activity.

Table 4.10: The eliminated ketone **4.054** and the hydrazine **4.046** and their corresponding activity against *Plasmodium* parasites^a.

Entry	Compound	EC ₅₀ (μ M)
1	 <p>4.54</p>	>100
2	 <p>4.56</p>	50

^a Parasite strain: 3D7, positive control: latrunculin B.

4.4.3 Studies on *Toxoplasma gondii*

Toxoplasma gondii is a widespread parasite disease primarily affecting animals but can cause zoonotic infections in humans [42]. Humans can be infected by accidental ingestion or inhalation of oocysts, shed in the faeces of cats, or via ingestion of tissue cysts found in undercooked meat from infected animals [42].

In the absence of an assay to directly determine if the truncated latrunculin analogues were targeting actin, it was decided to test the compounds against another parasitic disease which would mimic the same binding (with respect to actin) as in *Plasmodium* parasites. With this in mind we studied the ATP binding site of *Toxoplasma* actin. It was interesting to find that the ATP binding pocket in

Toxoplasma is identical to *Plasmodium* as shown in **Figure 4.55**. Thus if the truncated latrunculin analogues show activity in the *Toxoplasma* growth inhibition assay, then it can circumstantially imply that these compounds are binding to actin. With this hypothesis, a selection of truncated latrunculin analogues were tested against *Toxoplasma* parasite by researchers at Walter Elisa Hall Institute of Medical Research (WEHI), Melbourne.

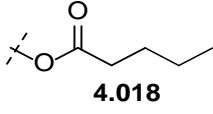
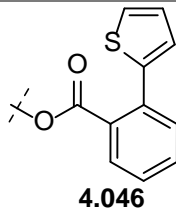
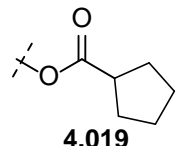
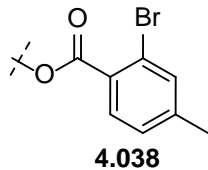
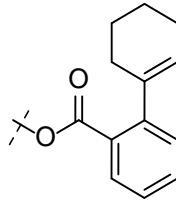
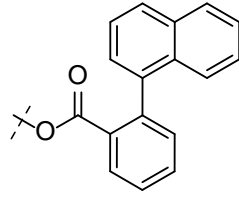
Pf	MGEEDVQALVVDNGSGNVKAGVAGDDAPRSVFPSIVGRPKNPGIMVGMEEKDAFVGDEAQ
Tg	MADEEVQALVVDNGSGNVKAGVAGDDAPRAVFPSIVGKPKNPGIMVGMEEKDCYVGDEAQ
	.::*****:*****:*****:*****:*****
Pf	TKRGILTLYPIEGIVTNWDDMEKIWHHTFYNELRAAPEEHPVLLTEAPLNPKGNRERMT
Tg	SKRGILTLYPIEGIVTNWDDMEKIWHHTFYNELRVAPEEHPVLLTEAPLNPKANRERMT
	:*****:*****:*****:*****:*****
Pf	QIMFESFNPAMYVAIQAVLSLYSSGRRTTGIVLDSGDGVSHTVPIYEGYALPHAIRMRLDL
Tg	QIMFETFNPAMYVAIQAVLSLYSSGRRTTGIVLDSGDGVSHTVPIYEGYALPHAIRMRLDL
	*****:*****:*****:*****:*****:*****
Pf	AGRDLTEYLMKILHERGYGFSTSAEKEIVRDIKEKLCYIALNFDEEMKTSEQSSDIEKSY
Tg	AGRDLTEYMMKILHERGYGFTTSAEKEIVRDIKEKLCYIALDFDEEMKAAEDSSDIEKSY
	*****:*****:*****:*****:*****:*****
Pf	ELPDGNIITVGNERFRCPEALFQPSFLGKEAAGIHTTTFNSIKKCDVDIRKDLYGNIVLS
Tg	ELPDGNIITVGNERFRCPEALFQPSFLGKEAAGVHRTTFDSIMKCDVDIRKDLYGNVLS
	*****:*****:*****:*****:*****:*****
Pf	GGTTMYEGIGERLTRDITTLAPSTMKIKVVAPPERKYSVWIGGSILSSLSTFQQMWITKE
Tg	GGTTMYEGIGERLTKELTSLAPSTMKIKVVAPPERKYSVWIGGSILSSLSTFQQMWITKE
	*****:*****:*****:*****:*****:*****
Pf	EYDESGPSIVHRKCF
Tg	EYDESGPSIVHRKCF

Figure 4.55: Comparison of the amino acid sequence of *Plasmodium* (Pf) actin and *Toxoplasmodium* (Tp) actin from a Clustal Omega alignment. An * (asterisk) indicates a position of residue conservation. A : (colon) indicates conservation between groups of strongly similar properties –(scoring > 0.5 in the Gonnet PAM 250 matrix). A . (period) indicates conservation between groups of weakly similar properties (scoring =< 0.5 in the Gonnet PAM 250 matrix). The alignment score was 93.8%.

Inhibition of the *Toxoplasma* parasite growth was determined using the 2F clone of the type I RH strain that expresses the E. coli β -galactoside enzyme (β -Gal) [42, 43]. A 10 mM stock solution was prepared by dissolving the compounds in DMSO and then diluted in medium containing 1% DMSO, which also served as a no compound control. The positive control used was the pyrazolo [3,4-d] pyrimidine inhibitor [42]. The *Toxoplasma* parasites were then mixed with the compounds and preincubated for 20 min at room temperature before being used to challenge confluent monolayers of human foreskin fibroblasts (HFF) grown in 96-well plates containing Dulbecco's Modified Eagle

Medium (DMEM) supplemented with 10% Fetal bovine serum (FBS). All samples were tested in triplicate. Following addition of 5×10^2 parasites/well containing dilutions of compounds and/or 1% DMSO, plates were centrifuged at $\sim 300g$ for 5 min and returned to culture at 37 °C, 5% CO₂. Data were analysed using Prism (GraphPad) to determine EC₅₀ values by plotting normalized, log transformed data (X axis), using nonlinear regression analysis as a sigmoidal dose–response curve with variable slope [42, 43].

Table 4.11: Selection of R¹ analogues of truncated latrunculin and their corresponding activity against *Toxoplasma* parasites^a. (R²: OMe, R³: PMB, R⁴: H)

Entry	R ¹	EC ₅₀ (μM)	Entry	R ¹	EC ₅₀ (μM)
1	 4.018	>100	4	 4.046	18
2	 4.019	>100	5	 4.038	13
3	 4.043	16	6	 4.041	14

^a *Toxoplasma gondii* strain RH, positive control: pyrazolo [3,4-**d**] pyrimidine (PP) inhibitor.

Table 4.12 shows the activity of the selected truncated derivatives against *Toxoplasma* parasites. As can be seen from **Table 4.11**, the truncated latrunculin analogues follow the same trend in activity with the *Toxoplasma* parasites as they did with the *Plasmodium* parasites. The ester analogues with alkyl chain and cyclopentane ring (**Table 4.11**, entry 1 and 2) were inactive while the benzoate ester analogues with *ortho* substitution (**Table 4.11**, entry 3–6) were active.

The fact that the activity in the *Plasmodium* parasites is mimicked by the *Toxoplasma* parasites suggests that these truncated latrunculin analogues are targeting actin as their binding site.

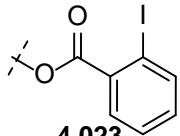
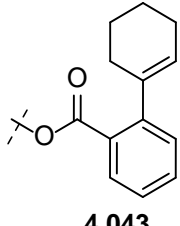
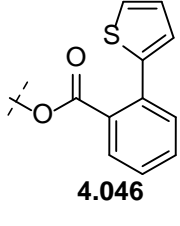
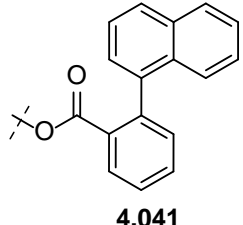
4.4.4 Pyrene Fluorescence assays

Pyrene fluorescence assay is used to study actin dynamics and is based on the enhancement of fluorescence when the pyrene G- actin (monomers) assemble to form the pyrene F-actin (filament). The increase in fluorescence can be used to follow actin polymerisation as a function of time [2, 44]. In the presence of a potent actin inhibitor, the formation of F-actin would be disrupted and therefore there would be a considerable drop in the measured fluorescence. It was anticipated that performing a pyrene fluorescence assay on mammalian actin would give an indication of the selectivity of the truncated analogues for *Plasmodium* actin over mammalian actin. It was thus decided to subject a limited selection of R¹ modified truncated analogues to pyrene fluorescence assay using rabbit actin at 10 μ M and 100 μ M concentration with latrunculin B as the positive control. These assays were performed by researchers at Imperial College, London, UK.

The pyrene-labelled actin and the unlabelled actin were mixed in general actin buffer to produce an actin stock of 5% pyrene-labelled actin. The stock was incubated at 23 °C for 2 min in 1 mM ethylene glycol tetraacetic acid (EGTA)/0.1 mM MgCl₂ in order to convert it to Mg²⁺ salt immediately prior to polymerization. Polymerization was induced by addition of 10 KMEI to a concentration of 1, with the remaining volume made up by G-Mg. The compounds were added and mixed for 1 min prior to the start of the assay. Pyrene fluorescence (excitation 365 nm, emission 407 nm) was monitored in a PC1 spectrofluorometer (Tecan Infinite M200 PRO). The time between mixing of final components and start of fluorometer data collection was measured for each assay and ranged between 12 and 15 seconds. The assays were run in triplicate.

Table 4.12 represents the results of the pyrene fluorescence assay. It was observed that none of the truncated analogues demonstrated a measurable drop in the fluorescence, indicating that these compounds did not inhibit actin filament formation in the mammalian cells. With the potent truncated analogues in the GIA being inactive in the pyrene fluorescence assay; and the fact that latrunculin B shows 100% inhibition at a 10 μ M concentration in the pyrene fluorescence assay (positive control) illustrates the selectivity of the truncated analogues for the parasites over the mammalian actin.

Table 4.12: A selection of R¹ modified analogues with their respective percentage inhibition of actin polymerization under a pyrene fluorescence assay.

Entry	R ¹	Inhibition at 10 μ M	Inhibition at 100 μ M
1	Latrunculin B	100%	100%
2	 4.023	<10%	<10%
3	 4.043	<10%	<10%
4	 4.046	<10%	<10%
5	 4.041	<10%	<10%

4.4.5 Cytotoxicity Assay

In light of the truncated latrunculin analogues showing activity against *Plasmodium* parasites in the GIA, and the fact that they fail to bind to the mammalian rabbit actin (in the pyrene fluorescence assay), it was necessary to establish if these compounds were non-cytotoxic before proceeding further with the SAR study. It was therefore decided to test the cytotoxicity of a selection of

truncated latrunculin analogues against the HEK293 and HepG2 cells lines. These assays were run by researchers at the University of Queensland, Australia.

HEK293 (human embryonic kidney) and HepG2 (Hepatocellular carcinoma) cells were seeded as 3000 and 5000 cells per well respectively, in a clear 384-well plate in a final volume of 20 μ l in DMEM medium (GIBCO-Invitrogen #11995-073), in which 10% of FBS was added. Cells were incubated for 24 hours at 37°C, 5% CO₂ to allow cells to attach to the plates. Compounds were prepared at 20 mM in 100% DMSO. The highest concentration to test the compounds was 100 μ M, in order to keep the DMSO end-concentration at 0.5%. A dilution series 1:3 fold steps in serum free medium was created, and 20 μ l of each dilution was added to the cell culture wells, resulting in 5% FBS as final concentration. 100 μ M tamoxifen served as negative control (all cells die) and in addition a serial dilution of tamoxifen, started at 100 μ M, was included as a dose response control. The cells were incubated with the compounds for 24 hours at 37°C, 5% CO₂. After the incubation, 10 μ M resazurin (dissolved in Phosphate Buffered Saline (PBS)) was added to each well. The plates were then incubated for 3 hours at 37°C, 5% CO₂. The fluorescence intensity was read using Polarstar Omega with excitation/emission 560/590. The data was analysed by Prism software. Results are presented as the average percentage of control \pm SD for each set of duplicate wells using the following equation: Percentage Viability = $(F_{\text{TEST}} - F_{\text{Negative}} / F_{\text{UNTREATED}} - F_{\text{Negative}}) * 100$.

Table 4.13: A selection of R¹ modified analogues with their respective cytotoxicity and selectivity indexes on HEK293 and HepG2 cell lines.

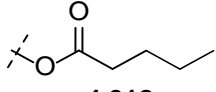
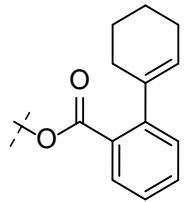
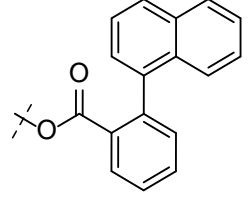
Entry	R ¹	Cytotoxicity CC ₅₀ (μM)		SI	
		HEK293	HepG2	EC ₅₀ <i>P.falciparum</i> vs HEK293	EC ₅₀ <i>P.falciparum</i> vs HepG2
1	 4.018	103	111	1	1
2	 4.043	109	123	14	15
3	 4.041	99	90	17	15

Table 4.13 shows the cytotoxicity and selectivity indexes (SI) of a limited selection of R¹ modified truncated analogues and it could be seen that the CC₅₀ of all these compounds were about 100 μM implying that none of these compounds showed any cytotoxicity with either the HEK293 or the HepG2 cell lines.

4.5 Conclusion

The simplified truncated core of latrunculin **4.009** was successfully synthesised. This truncated core was then derivatised at the R¹ position using esterification and hydrazine functionalities. It was found that unlike forming the ester analogues, the hydrazine derivatives were difficult to synthesise due to the possible side reactions. Among the various ester analogues synthesised, it was found that the benzoate esters were the most potent analogues against *Plasmodium* parasites. These analogues were also tested against *Toxoplasma* parasites and similar activity was observed suggesting that the binding target was actin. Further, pyrene fluorescence assays and cytotoxicity assays confirmed that

these compounds are selective towards the *Plasmodium* parasites over the mammalian and HEK293 and HepG2 cell lines.

4.6 References

1. Crane, E.A. and Gademann, K., Capturing Biological Activity in Natural Product Fragments by Chemical Synthesis. *Angew Chem Int Edit*, 2016, 55: 2-23.
2. Khanfar, M.A., Youssef, D.T.A. and El Sayed, K.A., Semisynthetic Latrunculin Derivatives as Inhibitors of Metastatic Breast Cancer: Biological Evaluations, Preliminary Structure–Activity Relationship and Molecular Modeling Studies. *ChemMedChem*, 2010; 5: 274-285.
3. Fuerstner, A., et al., Total syntheses of the actin-binding macrolides latrunculin A, B, C, M, S and 16-epi-latrunculin B. *Chem-Eur J*, 2007; 13: 115-134.
4. Williams, B.D. and Smith, A.B., Total Synthesis of (+)-18-epi-Latrunculinol A. *Org Lett*, 2013; 15: 4584-4587.
5. McDougal, P.G., et al., A convenient procedure for the monosilylation of symmetric 1,n-diols. *J Org Chem*, 1986; 51: 3388-3390.
6. Kusama, H., et al., Tungsten(0)- and Rhenium(I)-Catalyzed Tandem Cyclization of Acetylenic Dienol Silyl Ethers Based on Geminal Carbo-Functionalization of Alkynes. *Chem-Eur J*, 2011; 17: 4839-4848.
7. Omura, K. and Swern, D., Oxidation of alcohols by “activated” dimethyl sulfoxide. a preparative, steric and mechanistic study. *Tetrahedron*, 1978; 34: 1651-1660.
8. Mancuso, A.J., Brownfain, D.S. and Swern, D., Structure of the dimethyl sulfoxide-oxalyl chloride reaction product. Oxidation of heteroaromatic and diverse alcohols to carbonyl compounds. *J Org Chem*, 1979; 44: 4148-4150.
9. Parikh, J.R. and Doering, W.V.E., Sulfur trioxide in the oxidation of alcohols by dimethyl sulfoxide. *J Am Chem Soc*, 1967; 89: 5505-5507.
10. Evans, D.A. and Starr, J.T., A Cycloaddition Cascade Approach to the Total Synthesis of (–)-FR182877. *J Am Chem Soc*, 2003; 125: 13531-13540.
11. De Luca, L., Giacomelli, G. and Porcheddu, A., A Mild and Efficient Alternative to the Classical Swern Oxidation. *J Org Chem*, 2001; 66: 7907-7909.
12. Mortensen, M.S., Osbourn, J.M. and O'Doherty, G.A., De Novo Formal Synthesis of (–)-Virginiamycin M2 via the Asymmetric Hydration of Dienoates. *Org Lett*, 2007; 9: 3105-3108.
13. Sugiura, M., Ashikari, Y. and Nakajima, M., One-Pot Synthesis of β,β -Disubstituted α,β -Unsaturated Carbonyl Compounds. *J Org Chem*, 2015; 80: 8830-8835.
14. Godenschwager, P. and Collum, D.B., Lithium Hexamethyldisilazide-Mediated Enolizations: Influence of Triethylamine on E/Z Selectivities and Enolate Reactivities. *J Am Chem Soc*, 2008; 130: 8726-8732.
15. Lagu, B.R. and Liotta, D.C., Surprisingly high diastereoselection in the aldol reactions of sodium enolates of α -amino methyl ketones. *Tetrahedron Lett*, 1994; 35: 4485-4488.
16. Mulzer, J. and Bohlmann, R., *The Role of Natural Products in Drug Discovery*. Springer Berlin Heidelberg; 2013.
17. Angelini, T., et al., A new sustainable protocol for the synthesis of nitroaldol derivatives via Henry reaction under solvent-free conditions. *Green Chem Lett and Rev*, 2014; 7: 11-17.
18. Plagens, A. and Laue, T., *Named Organic Reactions* 2nd Edition, Wiley; 2005.
19. Christensen, B., G.; Foley, Michael, A.; Georges Evangelinos, Asimina, T.; Liu, Tao; Porter, James, R.; Ripka, Amy, S.; Zhang, Linping, Preparation of isoxazolidine derivatives for treatment of bacterial infections. WO 2006009907, 2006
20. Clayden, J., et al., *Organic Chemistry*. New York: Oxford University Press; 2001.
21. Wang, X.-J., et al., Addition of Grignard Reagents to Aryl Acid Chlorides: An Efficient Synthesis of Aryl Ketones. *Org Lett*, 2005; 7: 5593-5595.
22. Nahm, S. and Weinreb, S.M., N-methoxy-n-methylamides as effective acylating agents. *Tetrahedron Lett*, 1981; 22: 3815-3818.
23. Cho, J.H. and Kim, B.M., An Efficient Method for Removal of Ruthenium Byproducts from Olefin Metathesis Reactions. *Org Lett*, 2003; 5: 531-533.

24. Mori, A., et al., Pd/C-Catalyzed Chemoselective Hydrogenation in the Presence of Diphenylsulfide. *Org Lett*, 2006; 8: 3279-3281.
25. Resch, V., et al., On the Michael Addition of Water to α,β -Unsaturated Ketones Using Amino Acids. *European Journal of Organic Chemistry*, 2013; 34: 7697-7704.
26. Komura, K., et al., $\text{FeCl}_3 \cdot 6\text{H}_2\text{O}$ as a Versatile Catalyst for the Esterification of Steroid Alcohols with Fatty Acids. *Synthesis*, 2008; 21: 3407-3410.
27. Neises, B. and Steglich, W., Simple Method for the Esterification of Carboxylic Acids. *Angew Chem Int Edit*, 1978; 17: 522-524.
28. But, T.Y.S. and Toy, P.H., Organocatalytic Mitsunobu Reactions. *J Am Chem Soc*, 2006; 128: 9636-9637.
29. Kim, J.G. and Jang, D.O., Mild and Efficient Cooper (II) Oxide-Catalyzed Acylation of Amines and Alcohols. *B Korean Chem Soc*, 2009; 30:1435-1436.
30. Dhaon, M.K., Olsen, R.K. and Ramasamy, K., Esterification of N-protected α -amino acids with alcohol/carbodiimide/4-(dimethylamino)pyridine. Racemization of aspartic and glutamic acid derivatives. *J Org Chem*, 1982; 47: 1962-1965.
31. Wang, B., et al., Direct B-Alkyl Suzuki–Miyaura Cross-Coupling of Trialkylboranes with Aryl Bromides in the Presence of Unmasked Acidic or Basic Functions and Base-Labile Protections under Mild Non-Aqueous Conditions. *Adv Synth Catal*, 2009; 351: 415-422.
32. Wolfe, J.P., et al., Highly Active Palladium Catalysts for Suzuki Coupling Reactions. *J Am Chem Soc*, 1999; 121: 9550-9561.
33. Ozanne, A., et al., A Stabilized Formulation of IBX (SIBX) for Safe Oxidation Reactions Including a New Oxidative Demethylation of Phenolic Methyl Aryl Ethers. *Org Lett*, 2003; 5: 2903-2906.
34. DeMico, A., et al., A versatile and highly selective hypervalent iodine (III)/2,2,6,6-tetramethyl-1-piperidinyloxy-mediated oxidation of alcohols to carbonyl compounds. *J Org Chem*, 1997; 62: 6974-6977.
35. Meyer, S.D. and Schreiber, S.L., Acceleration of the Dess-Martin Oxidation by Water. *J Org Chem*, 1994; 59: 7549-7552.
36. Tsubone, K., et al., Studies toward the total synthesis of gambieric acids, potent antifungal polycyclic ethers: convergent synthesis of a fully elaborated GHJ-ring fragment. *Tetrahedron*, 2011; 67: 6600-6615.
37. Carradori, S., et al., Synthesis and cytotoxicity of novel (thiazol-2-yl)hydrazine derivatives as promising anti-Candida agents. *Eur J Med Chem*, 2013; 65: 102-111.
38. Niknam, K., Reza Kiasat, A. and Karimi, S., Dowex Polymer-Mediated Protection of Carbonyl Groups. *Synth Commun*, 2005; 35: 2231-2236.
39. Cordes, E.H. and Jencks, W.P., On the Mechanism of Schiff Base Formation and Hydrolysis. *J Am Chem Soc*, 1962; 84: 832-837.
40. Becker, O.L., et al., Preparation of piperrazinyllarylamines as 5-HT₆ modulators. WO 2006081332, 2006.
41. Drew, D.R., et al., Defining the Antigenic Diversity of *Plasmodium falciparum* Apical Membrane Antigen 1 and the Requirements for a Multi-Allele Vaccine against Malaria. *PLoS ONE*, 2012; 7: e51023.
42. Lourido, S., et al., Optimizing Small Molecule Inhibitors of Calcium-Dependent Protein Kinase 1 to Prevent Infection by *Toxoplasma gondii*. *J Med Chem*, 2013; 56: 3068-3077.
43. Nagamune, K., Moreno, S.N.J. and Sibley, L.D., Artemisinin-Resistant Mutants of *Toxoplasma gondii* Have Altered Calcium Homeostasis. *Antimicrob Agents Ch*, 2007; 51: 3816-3823.
44. Harris, E.S., et al., Mechanistic differences in actin bundling activity of two mammalian formins, FRL1 and mDia2. *J Biol Chem*, 2006; 281: 14383-92.

Chapter 5: Further exploration of the truncated latrunculin analogues.

5.1 Introduction

This chapter focuses on the work to further derivatise the truncated core represented in **Figure 5.01**. These derivatisations include imine analogues, expansion of the THP ring, modifications of the R², R³ and R⁴ positions and the introduction of aromaticity. Chapter 4 focused on the synthesis and activity of modifications at the R¹ position, and it was found that some of the analogues were potent against *Plasmodium* parasites. It was therefore decided to further explore some of the more potent R¹ analogues (such as compound **4.046**) in combination with substitutions at the other R positions which will be used in order to explore the potential for additive SAR.

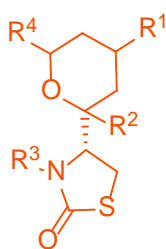


Figure 5.01: General structure of the truncated latrunculin core.

5.2 Piperidine derivatives

The first modification chosen was to change the oxygen atom of the THP ring to a nitrogen atom so as to obtain a piperidine analogue (**5.001**) as shown in **Figure 5.02**. A nitrogen at this position would provide valuable insights about the change in hydrogen bonding interaction with the putative target. A literature search revealed that such piperidine derivatives were scarcely synthesised, suggesting that the system may favour elimination, leading to the formation of cyclic imine (**5.002**) as shown in the **Figure 5.02**.

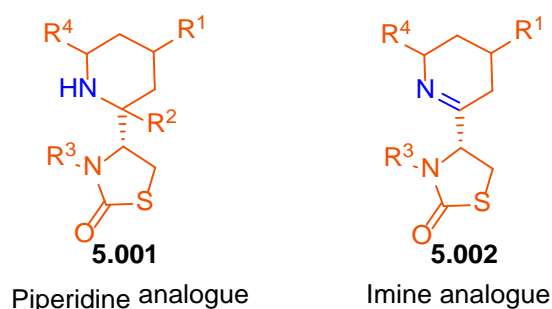


Figure 5.02: The proposed piperidine and cyclic imine analogues.

The synthesis of these analogues was performed using the alkene metathesis route described previously in Chapter 4 and is illustrated in **Figure 5.03**. The coupling partners used for this reaction were the α,β -unsaturated ketone **4.012** and the Boc protected 3-buten-1-amine. The Boc protection [1] was performed in order to decrease the nucleophilicity of the amine (since basic amines are generally incompatible with the metathesis catalysts [2]) and also to avoid any undesired side reactions. The yield of the metathesis reaction was low (38%) as the reaction failed to go to completion even with prolonged reaction time and elevated temperatures.

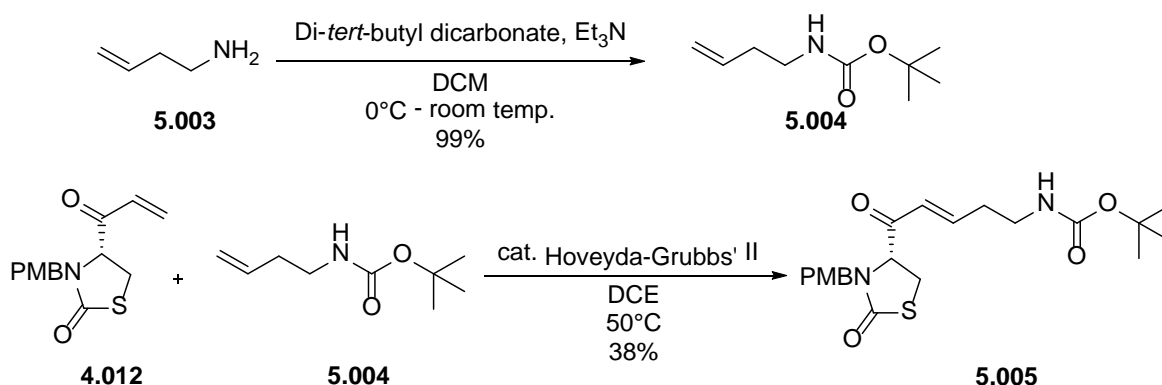


Figure 5.03: Scheme showing the formation of the precursor for the nitrogen analogue.

The next step was the Michael addition of water with simultaneous TBS-deprotection and oxacyclisation. This was brought about using 6 M HCl in THF. TLC analysis indicated formation of new products and complete consumption of starting material, however, the products obtained after flash chromatography were difficult to identify since each isolated product (clean by TLC analysis) represented multiple products by proton NMR. This meant that the isolated products had the same polarity and were therefore inseparable by flash chromatography. It was clear from the proton NMR spectrum that the Boc had undergone deprotection, but the presence of vinylic proton signals observed, could possibly mean any of the five compounds as shown in **Figure 5.04** had formed.

Since the compounds could not be separated by flash chromatography, it was not feasible to identify the products formed. It was also not possible to determine how the reaction had proceeded, because the presence of compound **5.006** would mean that the Michael addition of water was unsuccessful, while formation of compounds **5.007**, **5.008**, **5.009** and **5.010** would imply the elimination of water from the imine or the piperidine after its formation.

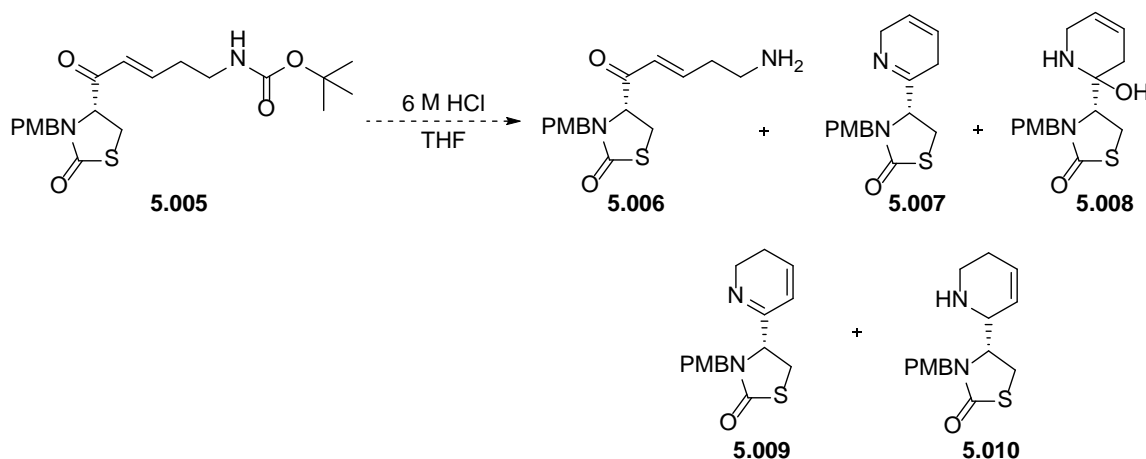


Figure 5.04: The possible products of Boc deprotection.

In order to simplify the scenario, the metathesis reaction was performed with a tertiary nitrogen source. Tertiary nitrogen would ensure that the imine is not formed during the ring closure step, thereby narrowing the number of possible products of this reaction. It was proposed that this could lead to the isolation of clean products thereby enabling their identification. Thus, compound **5.004** was methylated using sodium hydride and iodomethane to obtain compound **5.011** in 92% yield, which was then subjected to alkene metathesis with the α,β -unsaturated ketone **4.012** to form compound **5.012** in 51% yield as shown in **Figure 5.05**.

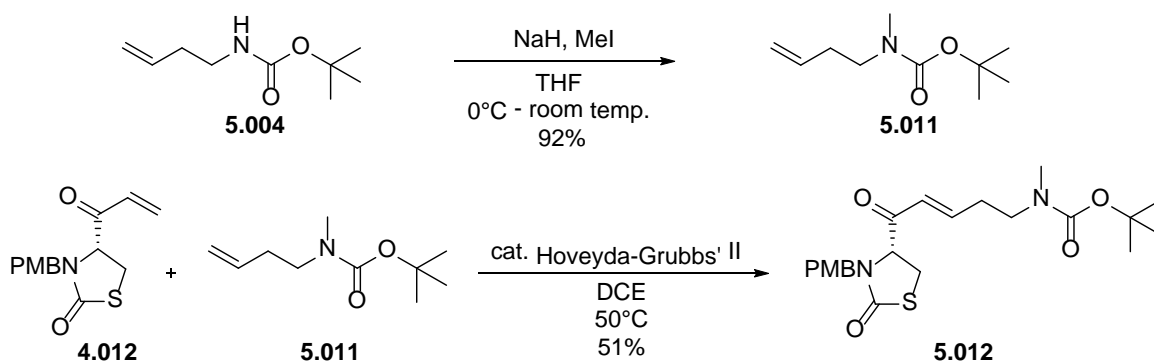


Figure 5.05: Formation of the methylated nitrogen analogue precursor.

Compound **5.012** was then treated with a 6 M aq. HCl solution in order to effect the Michael addition of water, Boc deprotection and spontaneous ring closure, however the reaction led to the formation of multiple products with identical polarity, meaning the identification of the isolated products was not possible.

In order to understand the reaction better, it was decided that instead of a one step process, the Michael addition should be brought about first, and later the Michael adduct would be subjected to Boc deprotection and ring closure as shown in **Figure 5.06**. This would also help ensure the completeness of the Michael addition.

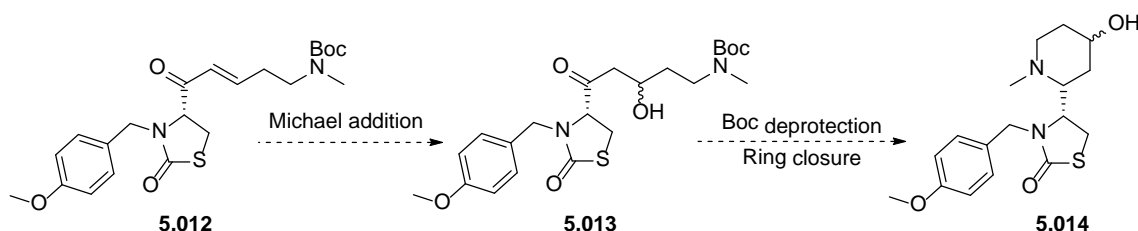


Figure 5.06: Proposed two step procedure to obtain the compound **5.014**.

Of the few Michael addition reactions reported in literature on similar systems, the one by De Run Li *et al.* [3], using boronic acid to bring about Michael addition of hydroxyl group to an α,β -unsaturated ketone was employed in this instance. As a test reaction, the oxygen containing compound **5.015** was used, since the PMB protected compound **4.007** has been proven to undergo Michael addition (Chapter 4). The starting material **5.015** was first treated with phenylboronic acid and *N,N*-diisopropylamine to form the boron complex which was then treated with hydrogen peroxide and sodium carbonate to produce compound **5.017** as shown in **Figure 5.07**. The proton NMR spectrum and LCMS analysis ($[M+H]^+$ 310.1 m/z) confirmed the formation of the desired product.

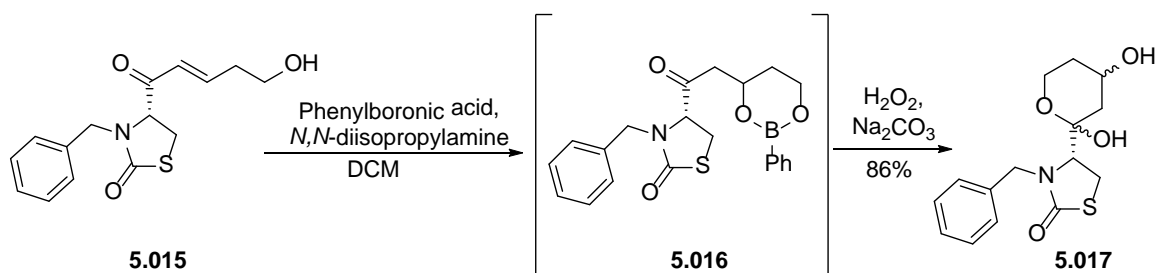


Figure 5.07: Michael addition using phenyl boronic acid on the α,β -unsaturated ketone **5.015**.

However when the same procedure was applied to the nitrogen containing compound **5.005**, the reaction did not lead to any product formation as shown in **Figure 5.08**. The proton NMR of the crude mixture indicated the presence of starting material only. The fact that this procedure works on the oxygen containing compound **5.015** and not on the nitrogen containing compound **5.005**, suggests that the reaction is substrate dependent. It is possible that the presence of Boc in compound **5.005**, decreases the nucleophilicity of the nitrogen, thereby hindering the bond formation with boron. An unprotected nitrogen would be potentially nucleophilic enough for this reaction to take place, however, as nucleophilic amines are known to be incompatible with the metathesis catalysts, this approach was not attempted [2].

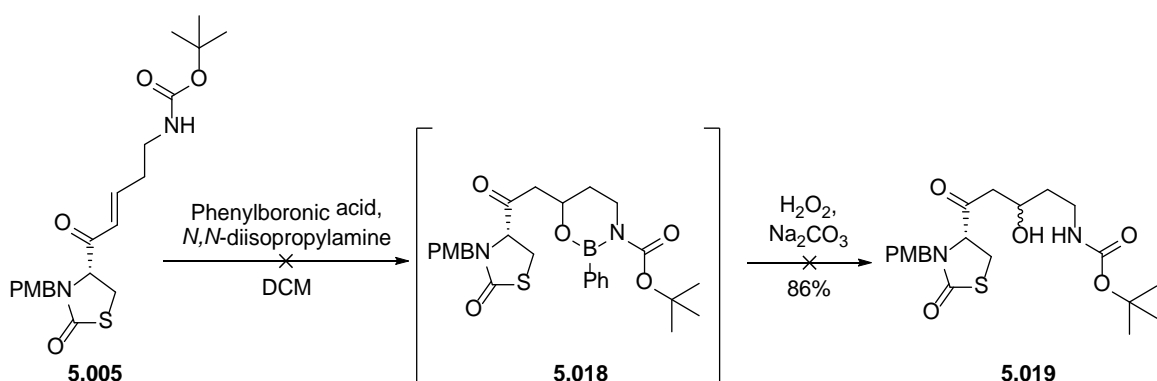


Figure 5.08: Michael addition using phenyl boronic acid on the α,β -unsaturated ketone **5.005**.

Due to the unreactive nature of the nitrogen analogue **5.005** and the non-specific nature of these substrates towards Boc deprotection and ring closure, the piperidine/imine analogues were not pursued further.

5.3 Expansion of the THP ring

The next modification was to change the 6-membered THP ring to a 7-membered oxepane ring as shown in **Figure 5.09**. Such an expansion of the THP ring would help us understand the changes in the actin binding pattern with a bigger ring size. The method chosen for this ring expansion was using the Aldol condensation route previously described in Chapter 4.

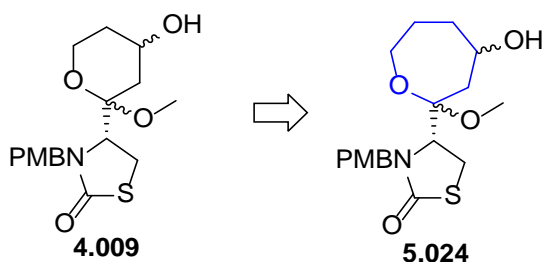


Figure 5.09: Proposed expansion of the THP ring to the 7-membered oxepane ring.

The first step was to synthesise the aldehyde **5.022**. For this 1,4-butanediol was treated with NaH and TBSCl to selectively protect one of the alcohols [4], and then subjected to Swern oxidation to convert the free alcohol into the corresponding aldehyde so as to obtain the desired compound **5.022** in 24% yield as shown in **Figure 5.10**.

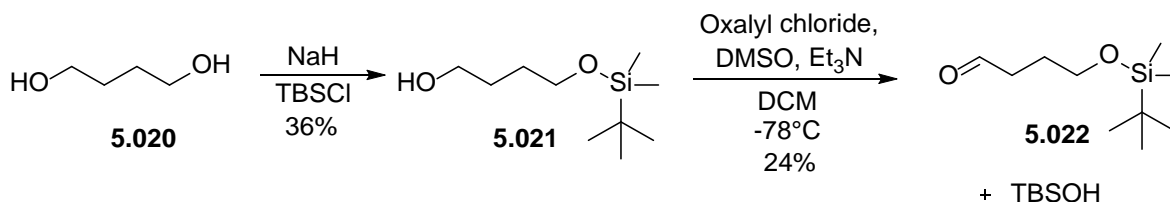


Figure 5.10: Synthesis of the aldehyde **5.022**.

Next, the aldehyde **5.022** thus formed was treated with compound **3.007** utilising aldol reaction conditions [5] so as to obtain compound **5.023** as shown in **Figure 5.11**. Compound **5.023** was then treated with 1 M HCl in THF to effect TBS-deprotection and spontaneous ring closure [5] to obtain the desired product **5.024**. However, it was found that the last step did not lead to the desired product formation as shown in **Figure 5.11**. On closer examination it was revealed that the compound had undergone decomposition as one of the isolated products was compound **3.007** (confirmed by proton NMR). Since, the 7-membered ring fails to form, the ring expansion of the THP ring was not pursued further.

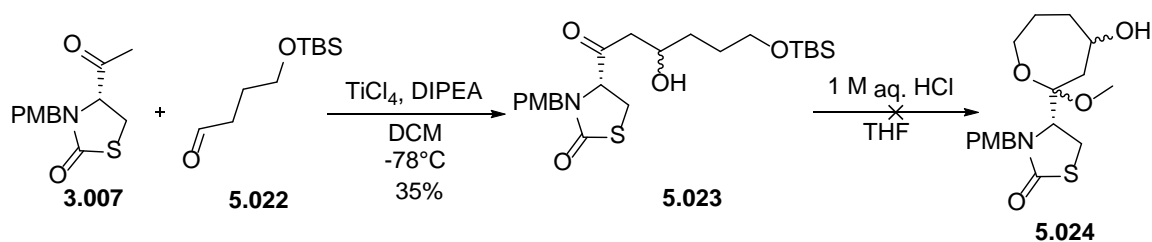


Figure 5.11: Failure of the 7-membered ring formation.

5.4 R² Modification

The next position explored was the R² position. In Chapter 4, it was discussed why the methoxy acetal at the R² position was necessary in order to enhance the stability of the molecule. Here, some more substituents would be explored at the R² position such that the SAR around this region could be understood. Six analogues were chosen for derivatisation at the R² position as illustrated in **Figure 5.12**.

The first three analogues using ethanol (**Figure 5.12**, entry 1), *n*-butanol (**Figure 5.12**, entry 2) and 2-phenylethanol (**Figure 5.12**, entry 3) were chosen to explore how well larger hydrophobic groups were tolerated at this position. Next, the 2-methoxyethanol derivative (**Figure 5.12**, entry 4) would be synthesised in order to have a long alkyl chain but with lower hydrophobicity. And finally, two analogues were proposed with a nitrogen atom replacing the oxygen atom from the hemiacetal, one with small alkyl group (dimethyl amine) attached to the nitrogen atom (**Figure 5.12**, entry 5) and the other with a benzyl group attached to the nitrogen atom (**Figure 5.12**, entry 6). The nitrogen analogues would help explore the effect of the differential size with respect to the oxygen atom and also hydrogen bonding interactions with actin.

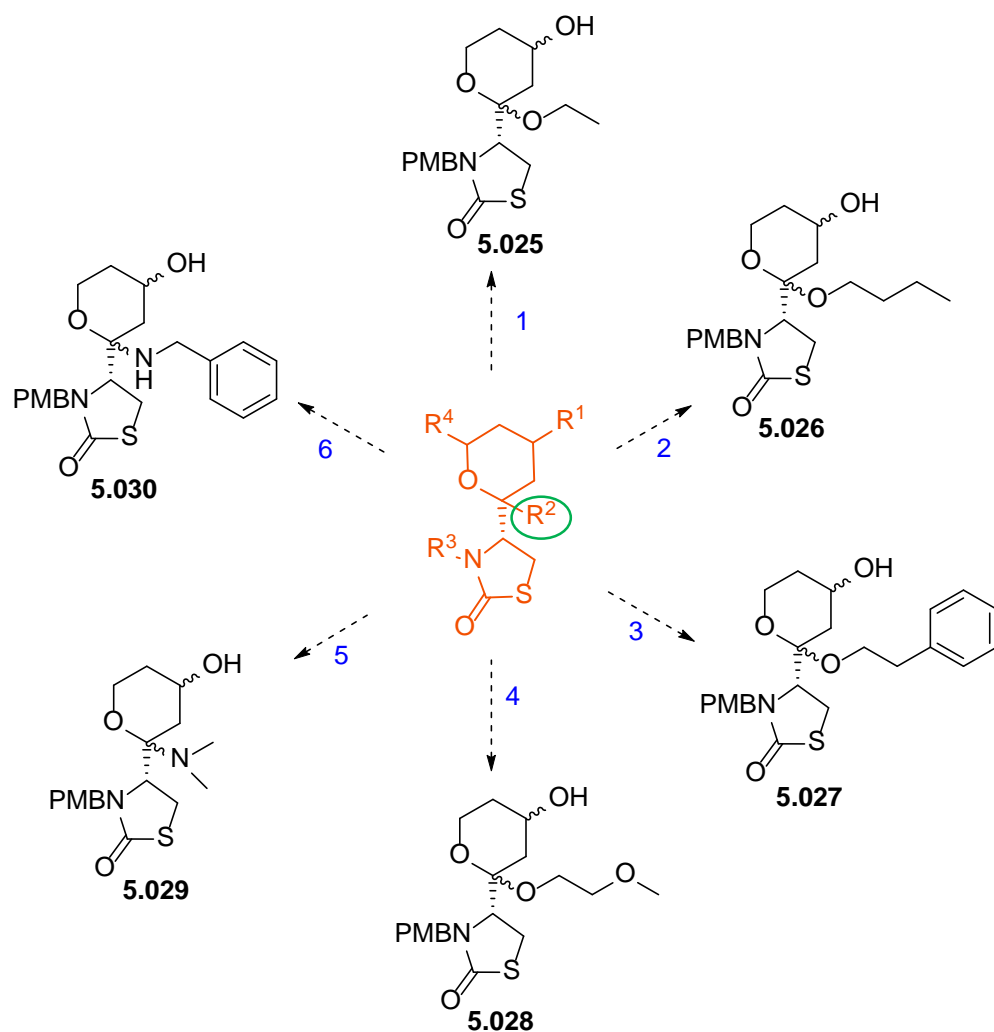
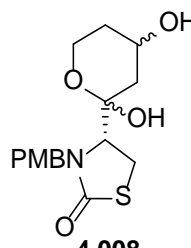
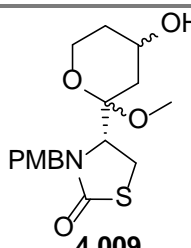


Figure 5.12: Proposed R^2 modified compounds.

Table 5.01 shows the various R^2 modifications explored with their respective conditions and yields. The starting material used for entry one to five was the PMB protected hemiacetal core **4.008** and that for entry six was the methoxy acetal derivative **4.009**. The initial conditions attempted for these transformations were using catalytic CSA and the corresponding alcohol as described in Chapter 4 [6, 7]. The reaction using ethanol (**Table 5.01**, entry 1) and *n*-butanol (**Table 5.01**, entry 2) proceeded as expected and led to the production of the desired products, **5.025** and **5.026** as shown in **Figure 5.13**. The yield of these reactions were moderate due to the incomplete conversion of the starting material to the product even after prolonged reaction times. The starting material was recovered and this improved the overall efficiency of these reactions.

Table 5.01: Summary of the attempted R² modifications.

#	Starting material	Substrate	Condition	Yield/ comment
1	 4.008	Ethanol	CSA	42%
2		<i>n</i> -Butanol	CSA	44%
3		Phenylethanol	CSA	Only starting material recovered
			Et ₂ O BF ₃	Only Starting material recovered
4		2-Methoxyethanol	CSA	32%
5		Dimethylamine.HCl	Methanol	Only Starting material recovered
			Methanol, reflux	Undesired product formation
	2 M Dimethylamine in THF	Et ₂ O.BF ₃	Undesired product formation	
6	 4.009	Benzylamine	Titanium isopropoxide	Undesired product formation

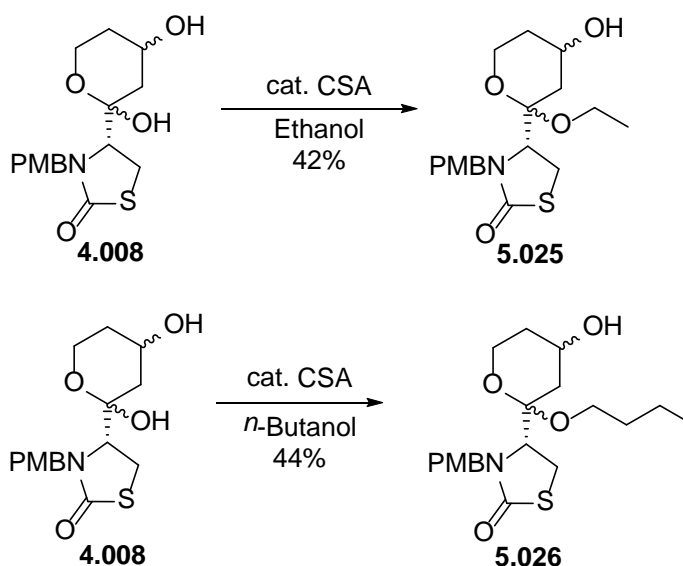


Figure 5.13: Synthesis of compounds **5.025** and **5.026** using CSA and the corresponding alcohol.

The synthesis of the 2-phenylethanol derivative **5.027** posed certain difficulties (**Table 5.01**, entry 3). TLC analysis of this reaction did not indicate the formation of any new product. The reaction only led to the isolation of the starting materials. The reaction was also attempted using a Lewis acid (boron trifluoride diethyl etherate) instead of CSA (**Table 5.01**, entry 3) [8]. But again the TLC analysis did not show any new product formation and only starting material could be isolated after the reaction. Since both the attempts at forming the 2-phenylethanol derivative only led to unreacted starting material, it was assumed that the bulkiness of the substrate was the issue with this analogue and thus synthesis of compound **5.027** was not pursued any further. The synthesis of the 2-methoxyethanol **5.028** derivative was relatively straightforward and was synthesised using CSA as catalyst in 32% yield (**Table 5.01**, entry 4) as shown in **Figure 5.14**. The reaction however did not go to completion even after 2 days and accounts for the low yield of the reaction; the unreacted starting material was recovered.

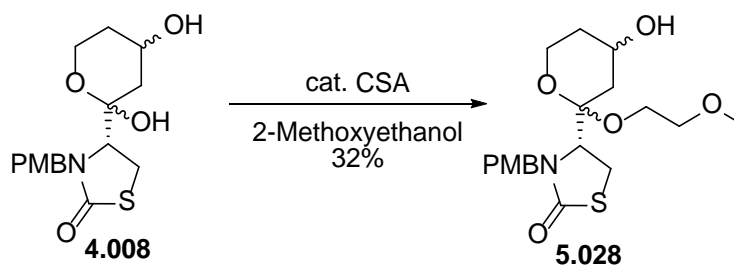


Figure 5.14: Synthesis of the 2-methoxyethanol analogue.

Next, the nitrogen analogues (**5.029** and **5.030**) were attempted, the first trial was using dimethylamine.HCl in methanol (**Table 5.01**, entry 5). TLC analysis after 12 h did not indicate the presence of any new product. Nevertheless, the reaction was quenched and a proton NMR of the crude mixture obtained. The proton NMR spectrum did not contain the two singlets (integrating for three protons each) which should have been characteristic of the two methyl groups on the nitrogen atom in the desired product, indicating that the desired product **5.029** was not formed. In order to force the reaction to product formation, it was decided to repeat the experiment under reflux conditions (**Table 5.01**, entry 5). The TLC analysis indicated the formation of a new product, however, isolation of this new product by flash chromatography and identification using proton NMR, indicated that the isolated compound was the methoxy compound **4.009** as shown in **Figure 5.15** and not the desired product **5.029**. This meant that unexpectedly, the solvent (methanol) had undergone nucleophilic addition preferably over the dimethylamine. Steric hindrance could potentially be the reason for the addition of methanol over the dimethylamine.

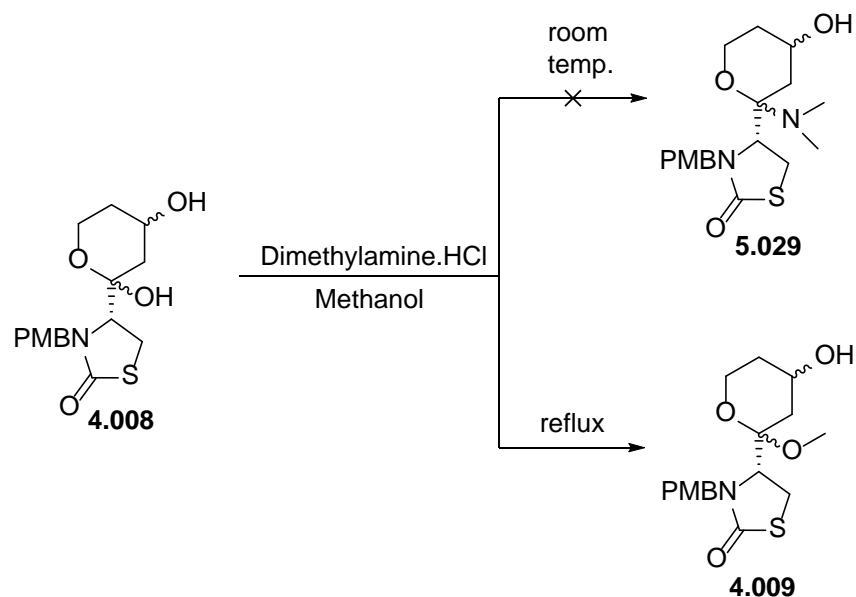


Figure 5.15: Attempts at synthesising the dimethylamine derivative **5.029**.

The reaction was also attempted with 2 M dimethylamine in THF (to avoid methanol addition) and the Lewis acid, boron trifluoride diethyl etherate (**Table 5.01**, entry 5); the isolated compounds after flash chromatography were not the desired product.

The last analogue attempted with a R^2 modification was using benzylamine (**Table 5.01**, entry 6) in the presence of the Lewis acid (titanium isopropoxide), hoping that the Lewis acid would lead to the formation of the oxonium intermediate which could potentially favour nucleophilic addition by benzylamine. This reaction resulted in the formation of a number of new products as indicated by TLC analysis; however none of the isolated compounds from flash chromatography corresponded to the desired product **5.030**. In the interest of time, R^2 modifications were not explored any further.

Once the aforementioned R^2 analogues were synthesised, these compounds were then subjected to limited R^1 modification, in order to understand the combined effect of both the R^1 and R^2 modifications that have been previously discussed. The R^1 modification chosen for the study was using the 2-thiophenylbenzoic acid and led to the synthesis of compounds **5.034**, **5.035** and **5.036** with yields as shown in **Figure 5.16**. The low yield of compound **5.036** (18%) was due to the fact that the desired product and the side products of the reaction had very similar polarity which made the recovery of the desired product in pure form difficult. These compounds would also enable us to compare the activity with the methoxy acetal **4.046**.

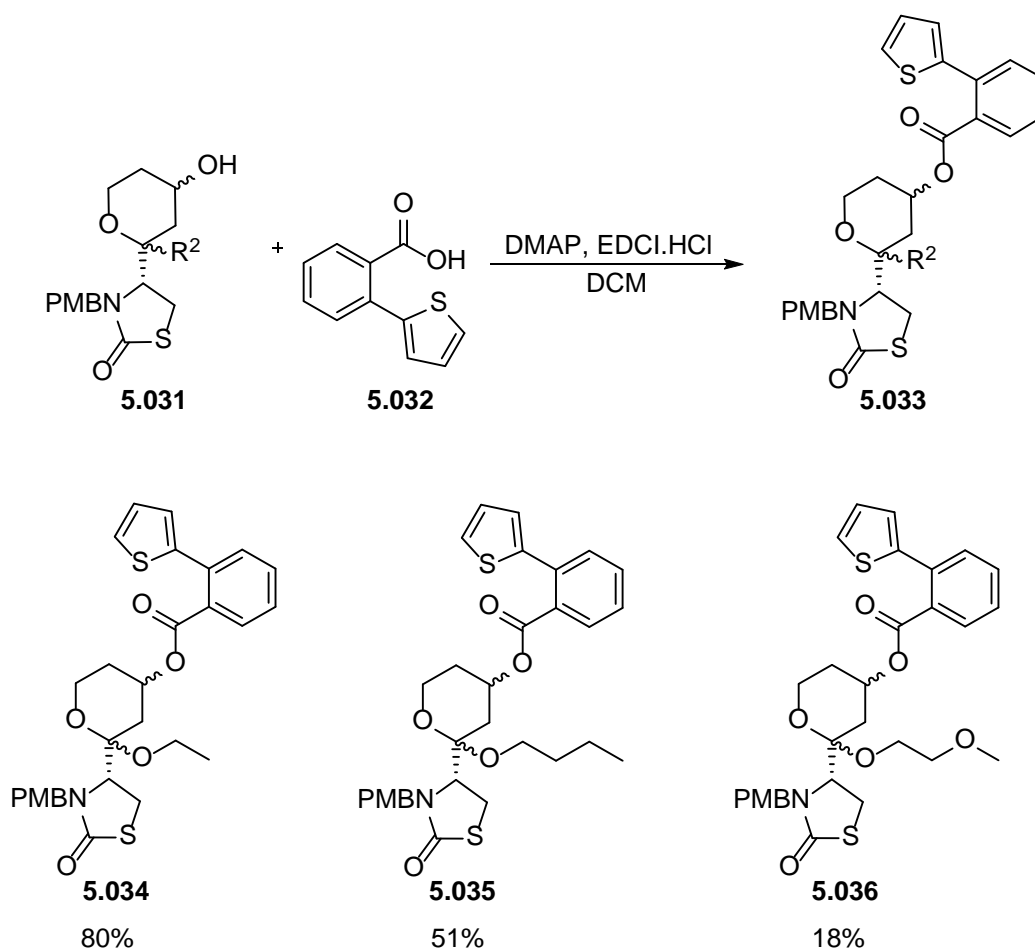


Figure 5.16: R^2 modified analogues of the methyl 2-(thiophen-2-yl)benzoate derivatives.

5.5 R^3 modifications

It was discussed in Chapter 4 that the nitrogen was protected with a PMB group in order to avoid any unwanted reaction at this position. Also, Sayed *et al.* in 2010 had shown that latrunculin analogues with benzyl protection at the nitrogen were more potent than the deprotected form found in the natural product [8]. Thus it was decided to synthesise all the truncated analogues with the PMB protection in place. Since most of the truncated analogues with the PMB protecting group were found to be active against the malarial parasites, it was decided to explore other substituents at R^3 position and also to deprotect the nitrogen and study the effect of the unsubstituted and substituted nitrogen at the R^3 position. The analogues chosen in this context were designed to specifically explore the effect of the methoxy in the benzyl protection, and hence it was decided to synthesise and test the activity of compounds with no methoxy group (benzyl protection) and also a dimethoxy derivative (3,4-dimethoxy benzyl). **Figure 5.17** shows the three R^3 modifications explored in this thesis of which the synthesis and effect of the PMB protection was previously discussed in Chapter 4.

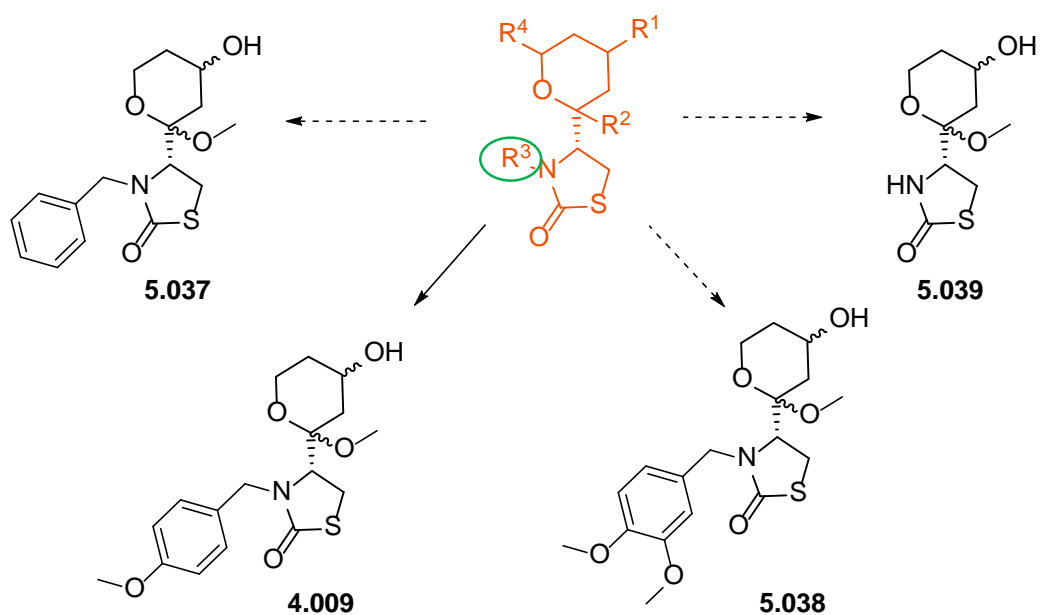


Figure 5.17: The proposed R^3 modifications.

Figure 5.18 outlines the various steps involved in the synthesis of the two R^3 substituents namely, the benzyl and 3,4-dimethoxybenzyl (DMB) derivatives. Each of the individual steps is represented by letters (A-H) and **Table 5.02** shows the respective yields for both the R^3 substituents for each of the steps. The procedure employed for both of these analogues was according to method B for the PMB derivatives described in Chapter 4. The only difference between the two R^3 substituted analogues was in step B where the respective nitrogen protecting groups were installed. For the benzyl protection, the reagent used was benzyl bromide and that for the 3,4-dimethoxybenzyl, the reagent used was 3,4-dimethoxybenzyl chloride.

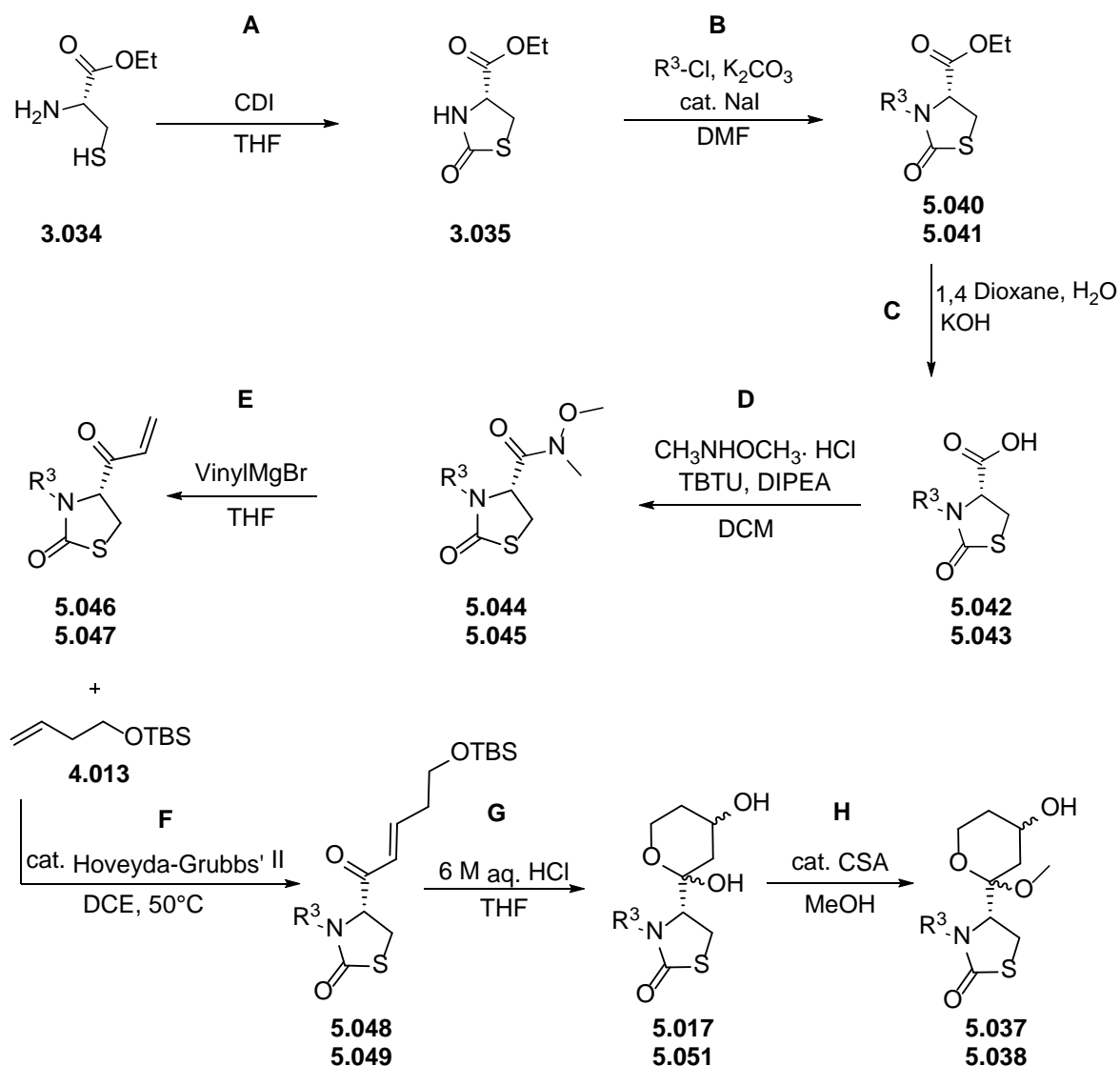
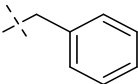
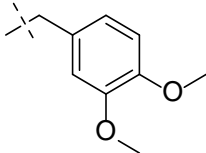


Figure 5.18: The general scheme for the synthesis of the R^3 substituted analogues. R^3 = benzyl for compounds **5.040**, **5.042**, **5.044**, **5.046**, **5.048**, **5.017**, **5.037** and R^3 = DMB for compounds **5.041**, **5.043**, **5.045**, **5.047**, **5.049**, **5.051** and **5.038**.

The thiazolidinone ester **3.035** was synthesised from L-cysteine ethyl ester hydrochloride as described in Chapter 3, which was then treated with the respective protecting group (**Figure 5.18**). The nitrogen protected esters (**5.040** and **5.041**) were then hydrolysed and subsequently converted into the corresponding Weinreb amides (**5.044** and **5.045**), before treatment with the vinyl magnesium bromide to form the α,β -unsaturated ketone.

Table 5.02: The respective yields of the two R³ modified analogues.

Step	A	B	C	D	E	F	G	H
	3.035 56%	5.040 62%	5.042 85%	5.044 93%	5.046 95%	5.048 67%	5.017 88%	5.037 57%
		5.041 75%	5.043 90%	5.045 70%	5.047 48%	5.049 49%	5.038 43% over 2 steps.	

The α,β -unsaturated ketone was then subjected to alkene metathesis with **4.013** using Hoveyda-Grubbs' II catalyst resulting in the formation of compound **5.048** and **5.049**, which were subsequently treated with 6 M aq. HCl in THF in order to effect the Michael addition of water followed by simultaneous TBS-deprotection and ring closure to yield the hemi acetal **5.017** and **5.051**.

In the case of the benzyl protected analogues, it was found that the Michael addition step was sometimes incomplete, leading to the formation of the TBS-deprotected uncyclised α,β -unsaturated ketone **5.015** along with the desired hemiacetal **5.017** as shown in **Figure 5.19**. Both the hemiacetal **5.017** and the TBS-deprotected uncyclised α,β -unsaturated ketone **5.015** had exactly the same polarity and were therefore impossible to separate by flash chromatography (combined yield of 88% for both of the products). The mixture of both these compounds was used to form the methyl acetal **5.037** and the TBS-deprotected uncyclised α,β -unsaturated ketone **5.015** was removed from the methyl acetal by flash chromatography at this point.

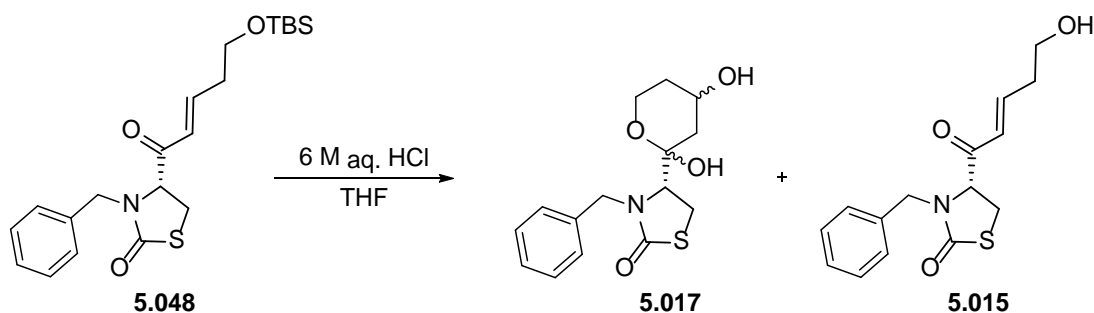
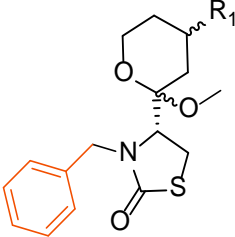
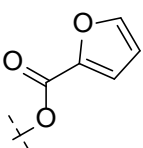
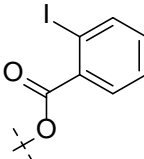
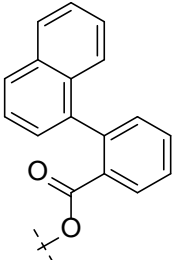
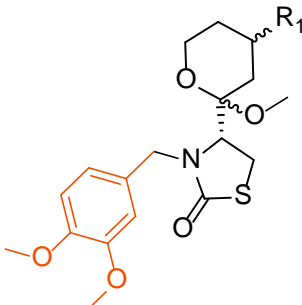
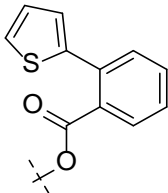


Figure 5.19: The formation of the TBS-deprotected uncyclised α,β -unsaturated ketone **5.015**.

With the 3,4-dimethoxy derivative, step G worked successfully leading to the formation of the corresponding hemiacetal **5.051**, which was directly converted to the methoxy acetal **5.038** without purification. The overall yield for both these steps was 43% as shown in **Table 5.02**.

The two R^3 modified methyl acetal **5.037** and **5.038** thus produced, were subjected to limited R^1 derivatisations in order to compare the additive effect of the both the R^1 and R^3 modification on these analogues. These R^1 modifications were brought about using an esterification reaction followed by Suzuki coupling as described in Chapter 4. **Table 5.03** shows the different analogues synthesised with the combined R^1 and R^3 modifications. Three R^1 analogues were generated with the benzyl R^3 modification namely the heterocyclic furan derivative **5.052**, the iodobenzene derivative **5.053** and the polycyclic derivative **5.054**. With the dimethoxybenzyl R^3 modification, only the bicyclic thiophene derivative **5.055** was synthesised.

Table 5.03: Analogues with combined R¹ and R³ modifications with their respective yields.

Entry	R ¹
	<div> 5.052 99%</div> <div> 5.053 89%</div> <div> 5.054a (27%) 5.054b (21%)</div>
	<div> 5.055 3%</div>

In the case of the polycyclic analogue **5.054**, it was found that the two diastereomers were separable by flash chromatography. Upon separation, however it was found that the proton NMR spectrum of both the diastereomers (**5.054a** and **5.054b**) represented two peaks for each proton. The carbon NMR spectrum also demonstrated two peaks for each carbon. Since it was unlikely that the Suzuki coupling reaction had led to epimerization, it is proposed that this observation was due to the axial chirality [9] by virtue of restricted rotation about the bond joining the naphthalene ring and the phenyl ring with the ester substituent as shown in **Figure 5.20**.

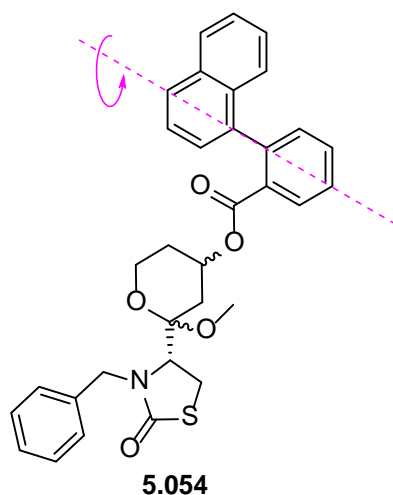
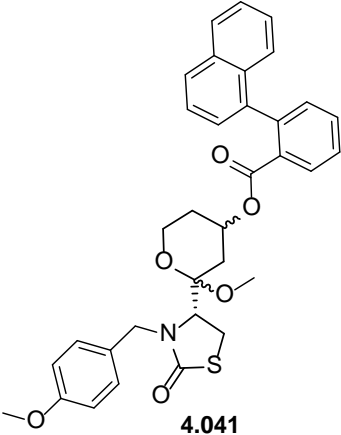
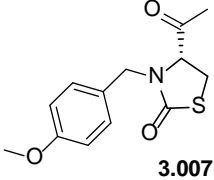
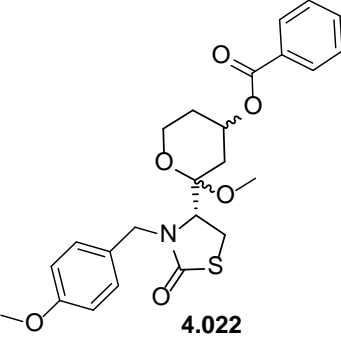
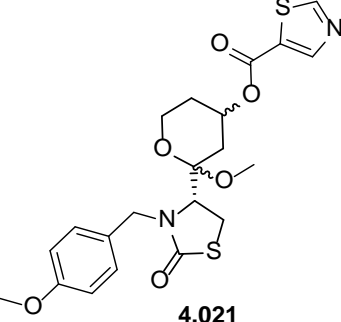


Figure 5.20: Structure of **5.054** showing the axis with restricted rotation which results in axial chirality.

5.5.1 Deprotection of PMB group

As discussed earlier, it would be interesting to synthesise latrunculin analogues without any protecting group at the nitrogen atom in order to understand the effect of having a free hydrogen bond donor at this position. Thus it was decided to remove the PMB group as shown in **Table 5.04**. The first condition trialed for the removal of the PMB group was using cerium ammonium nitrate (CAN) (**Table 5.04**, entry 1) as was also employed by Fürstner for the total synthesis of latrunculins [6, 10]. The substrate chosen for this deprotection was the naphthalene derivative, compound **4.041**. It was found that the reaction led to the formation of a large number of products as indicated by TLC analysis. However, none of the products isolated after flash chromatography corresponded to the desired product. In order to test the feasibility of this reaction, the reaction was also performed on **3.007** as the substrate (**Table 5.04**, entry 2). It was found that the deprotection of PMB was successful in this case, although the yield was quite low (23%).

Table 5.04: Summary of attempts made at deprotecting the PMB group.

Entry	Conditions	Substrate	Comment
1	CAN, MeCN, H ₂ O	 4.041	Unidentified products
2		 3.007	Product (23%)
3	TFA	 4.022	Unidentified product
4	DDQ, DCM, H ₂ O	 4.021	Starting material

The next condition trialed was using trifluoroacetic acid (TFA) using compound **4.022** as the substrate (**Table 5.04**, entry 3) [11]. The TLC analysis demonstrated complete consumption of starting material and formation of a new product, however upon isolation it was found that the

product obtained was an unidentifiable side product with the PMB group still installed on it as evidenced by the distinctive singlet of the PMB methoxy at 3.7 ppm. This meant that the reaction had led to formation of undesirable side product without undergoing PMB deprotection. The third trial was performed using 2,3-dichloro-5,6-dicyano-1,4-benzoquinone (DDQ) with compound **4.021** as the substrate (**Table 5.04**, entry 4) [12]. The reaction was monitored by TLC analysis and did not indicate the formation of any new product even after 24 h. The reaction was quenched to recover only the starting material.

The fact that the CAN deprotection works on compound **3.007** and not on compound **4.041**, suggests that the deprotection is substrate dependent. Although attempts could be made at deprotecting the benzyl or the 3,4-dimethoxybenzyl latrunculin analogues to achieve the same result, in the interest of time, the synthesis of the analogues with the free nitrogen was not pursued further.

5.6 R⁴ Modification

In order to understand the binding interaction of actin with the substituents off the R⁴ position, it was proposed to make three analogues as illustrated in **Figure 5.21**. The analogues were chosen so as to differ in their size and structure; the first analogue had a phenyl ring attached to the THP ring (**5.056**), the second analogue had the phenyl ring at one carbon distance from the THP ring (**5.057**) and the final analogue had a 5 carbon alkyl chain (**5.058**). Note that all the projected analogues were hydrophobic in nature in order to mimic the hydrophobic macrocycle of latrunculin at this position.

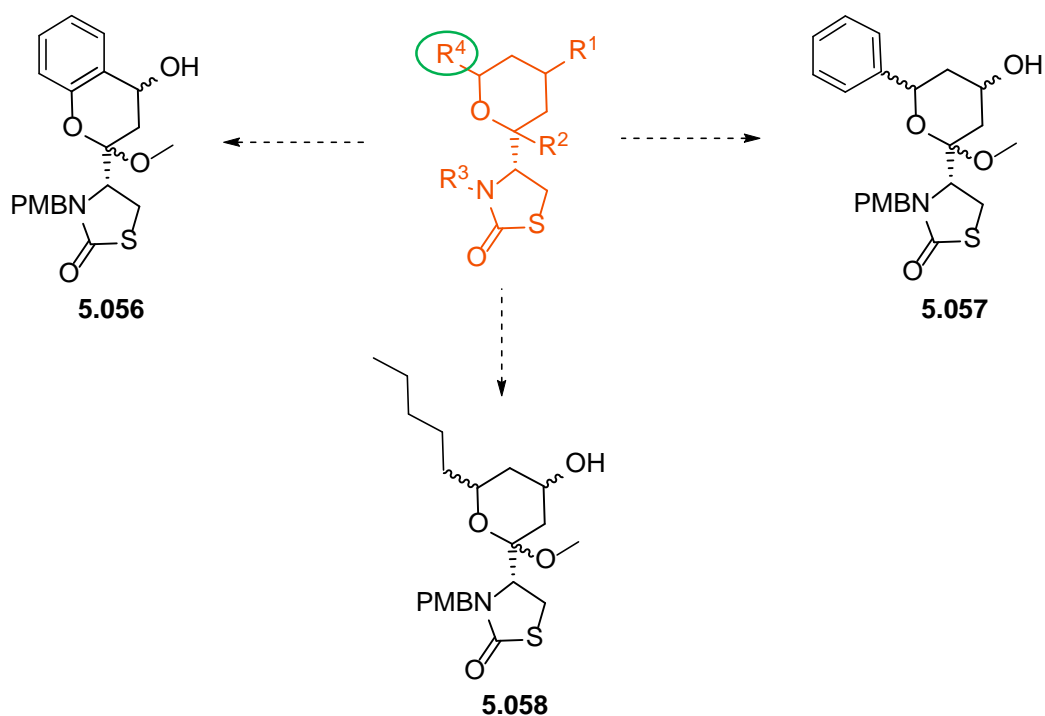


Figure 5.21: The proposed analogues at the R⁴ position.

The synthesis of the first analogue was attempted using the aldol condensation method described in Chapter 4 starting with compound **3.007** and 2-((*tert*-butyldimethylsilyl)oxy)benzaldehyde **5.060**. **Figure 5.22** outlines the scheme used for the synthesis of this analogue.

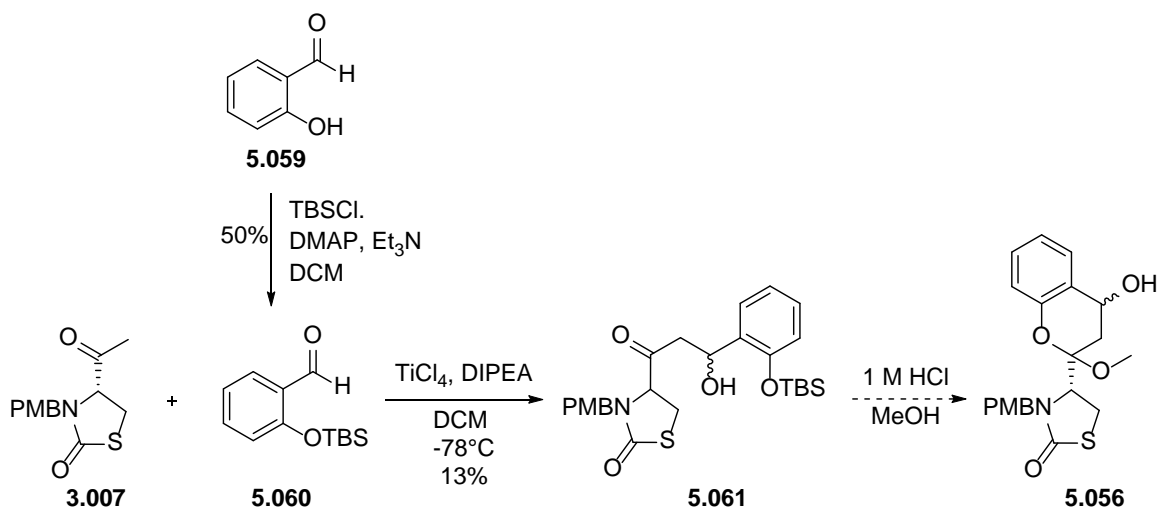


Figure 5.22: Scheme followed for the synthesis of compound **5.056**.

Compound **5.060** was prepared by TBS-protecting salicylaldehyde using TBSCl. The TBS-protected salicylaldehyde **5.060** thus formed was treated with **3.007** under aldol conditions to yield **5.061** in

13% yield. This low yield was because these aldol reactions led to the formation of a large number of side products including the eliminated compound **5.062** as shown in **Figure 5.23**.

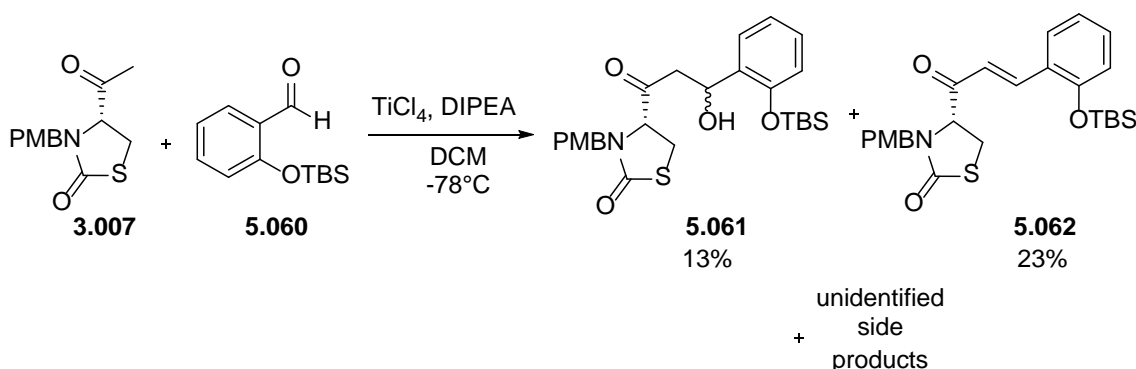


Figure 5.23: Aldol reaction leading to the formation of desired product and the eliminated product.

The aldol adduct **5.061** thus formed was used for the next step of TBS-deprotection and spontaneous ring closure. However instead of forming the hemiacetal first and then converting into the more stable methoxy acetal, the reaction was performed in 1 M HCl in methanol so that the methoxy acetal could be achieved in one step as shown in **Figure 5.22**. The product isolated from this reaction however was very unstable (decomposed in less than a day), thus it could not be characterised completely to ascertain if it was the desired product. Such an unstable compound would also not be suitable for biological assays and therefore was not pursued any further.

The second analogue attempted was compound **5.057** (**Figure 5.24**). This synthesis of this analogue was attempted using the alkene metathesis route highlighted in Chapter 4. Since this is a primary screen to understand the SAR and to identify an initial hit, it was not necessary to have chirally pure substituents at R^4 . With this in mind, the phenyl and the hexyl derivatives discussed below were not attempted with chirally pure starting materials at this stage.

For the synthesis of compound **5.057**, benzaldehyde was initially treated with allyl magnesium bromide to obtain compound **5.065**, which was subsequently TBS-protected to obtain compound **5.066** in 76% yield. Compound **5.066** was then subjected to alkene metathesis [13] conditions with the α,β -unsaturated ketone **4.012** to obtain compound **5.067**, which was treated with 6 M aq. HCl in THF in order to undergo simultaneous TBS-deprotection and ring closure to obtain compound **5.068**. Crude compound **5.068** was lastly methoxylated using catalytic CSA in methanol in order to convert the hemiacetal into the corresponding methyl acetal **5.057**. However, it was found that the methoxylation reaction was unsuccessful in this case, as the isolated compound lacked the methyl

group in the proton NMR spectrum implying that the recovered compound was actually the hemiacetal **5.068** (26% yield).

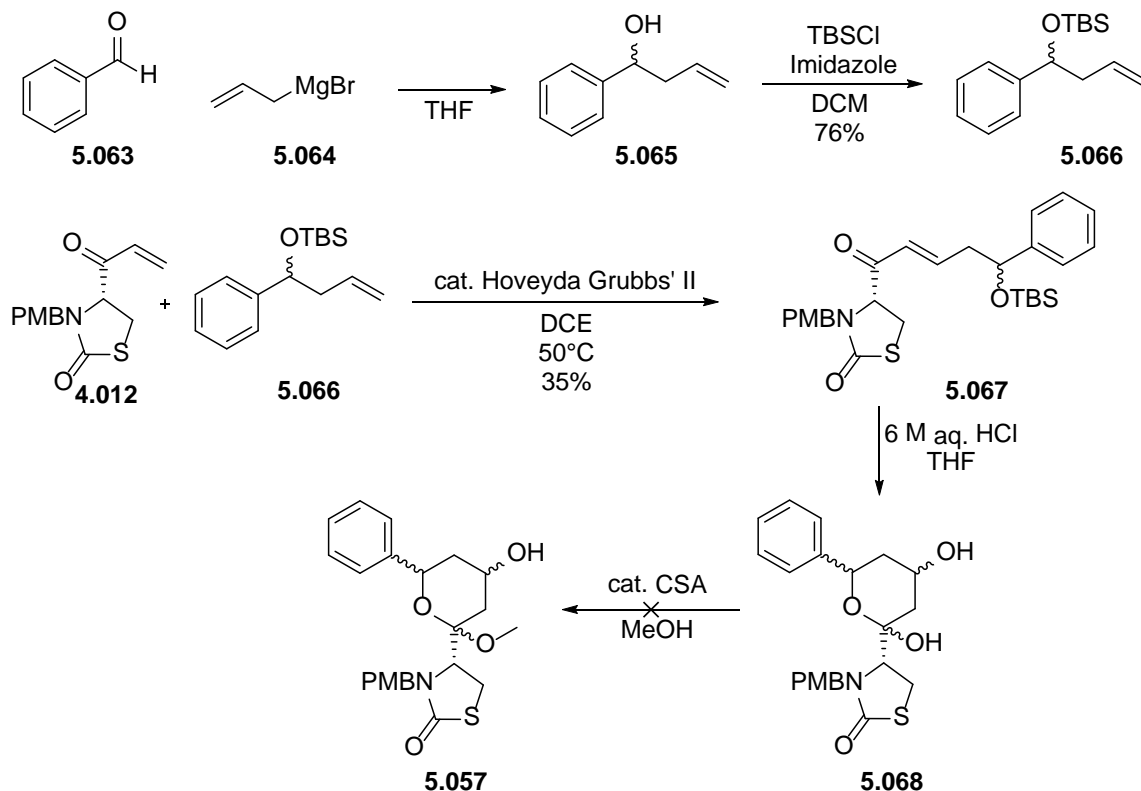


Figure 5.24: Schematic representation of synthesis of compound **5.057**.

The third R⁴ modification was the *n*-hexyl analogue. The scheme for the synthesis of this analogue was similar to the phenyl derivative and is illustrated in **Figure 5.25**. As can be seen from the scheme, the first step was to treat *n*-hexanal with the allyl magnesium Grignard followed by TBS-protection to yield compound **5.071** in 44% yield. This relatively low yield of the TBS-protected compound was due to the fact that the impurities from this reaction had similar polarities making the isolation of the pure product difficult. Compound **5.071** thus obtained, was then treated with the α,β -unsaturated ketone **4.012** in order to obtain compound **5.072**. This compound was then treated with 6 M aq. HCl in THF to undergo simultaneous TBS-deprotection and ring closure to obtain compound **5.073**. Compound **5.073** was directly used for the last step of methoxylation in order to obtain the desired analogue **5.058** in moderate yield (~53% per step).

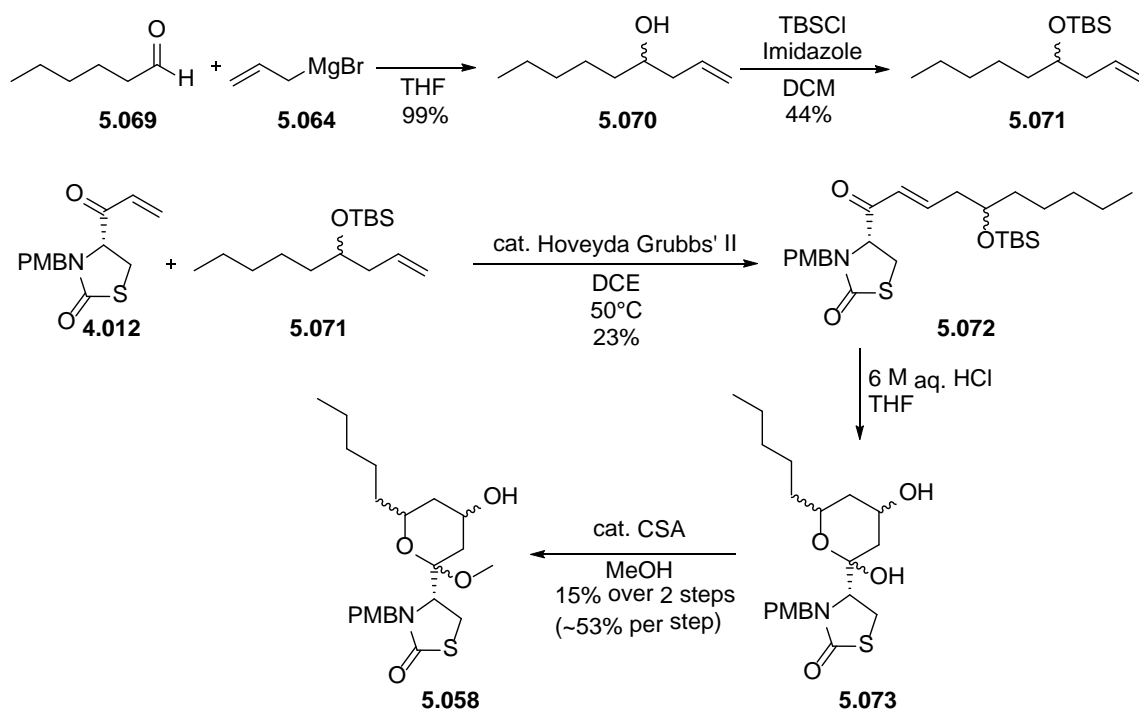


Figure 5.25: Synthesis of compound **5.058**.

The R⁴ modified analogues namely the phenyl **5.068** and the hexyl **5.058** were then subjected to esterification reactions with 2-(thiophen-2-yl)benzoic acid as shown **Figure 5.26**. These esterified analogues were synthesised to compare the effect of the R⁴ modification on the activity of the R⁴ unmodified thiophene benzoic derivative **4.044**. It was observed that the yield of the phenyl derivative **5.074** was very poor (5%) during the esterification reaction. This was expected as the hemiacetal would be very unstable leading to ring opening and therefore many side reactions. This evidently reduces the formation of the desired product. The hexyl derivative on the other hand, led to the formation of two diastereomers namely **5.075a** and **5.075b** in 1:1.4 ratio respectively (combined yield of 50%). These diastereomers were separable by flash chromatography and resulted in the isolation of optically pure compounds.

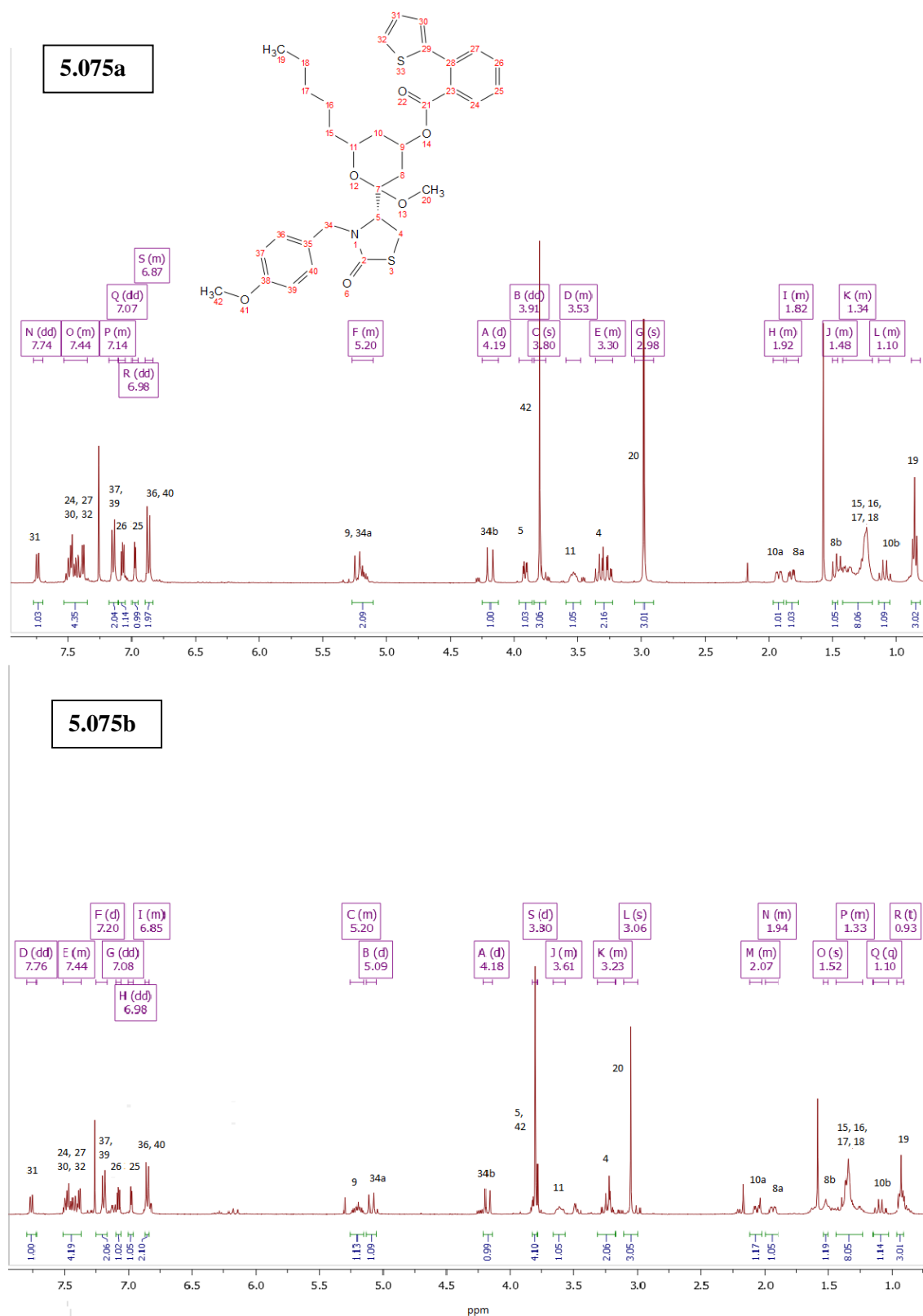


Figure 5.27: The NMR spectra of the diastereomers **5.075a** and **5.075b** respectively.

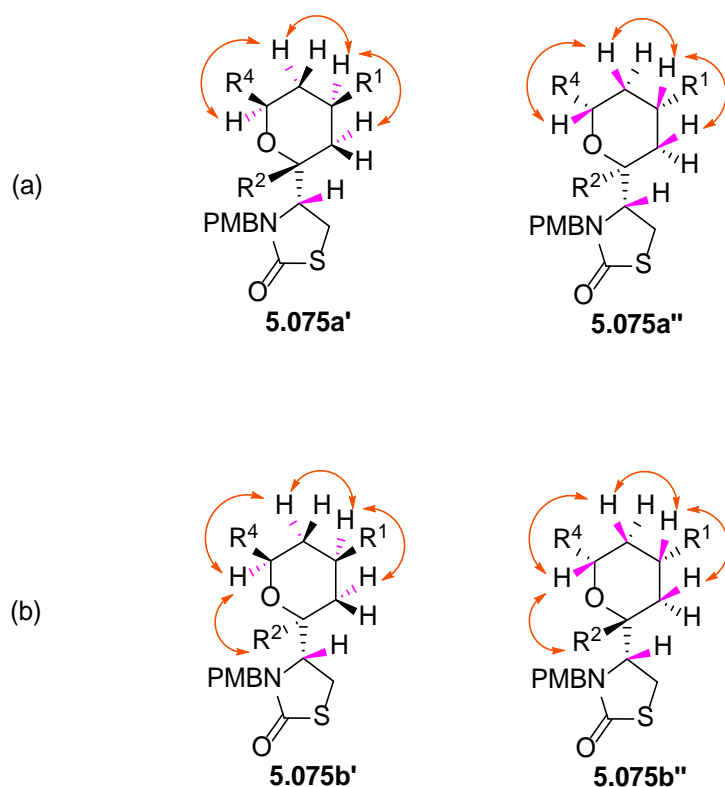


Figure 5.28: (a) The two possible structures of **5.075a** namely **5.75a'** and **5.75a''** highlighting the observed proton interactions (in orange) as inferred from the 2D NMR spectroscopic studies. (b) The two possible structures of **5.075b** namely **5.75b'** and **5.75b''** highlighting the observed proton interactions (in orange) as inferred from the 2D NMR spectroscopic studies.

5.7 Aromatic analogues

The next modification attempted was to convert the THP ring of the truncated core to a phenyl ring. This aromatisation of the THP ring, not only helps us understand the differential activity when the three dimensional THP ring is swapped for a planar six membered ring, these compounds would also be much simpler to synthesise and derivatise. Thus any activity observed in such aromatic analogues would be of great interest. Compound **5.076** shown in **Figure 5.29** was used as the building block for the synthesis of aromatic latrunculin-like truncated analogues.

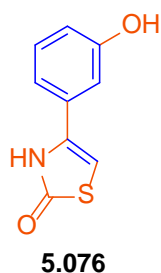


Figure 5.29: The aromatic building block for the synthesis of aromatic analogues.

As can be seen from **Figure 5.29**, the proposed compound **5.076** had no chiral centre in the molecule. The presence of unsaturation in the thiazolidinone ring imparts a partial aromatic nature to the thiazolidinone part of the molecule as well, due to the resonance from the lone pair of electrons from the nitrogen. The synthesis of this aromatic compound **5.076** was brought about starting from 1-(3-hydroxyphenyl)ethan-1-one **5.077** as shown in **Figure 5.30** [14].

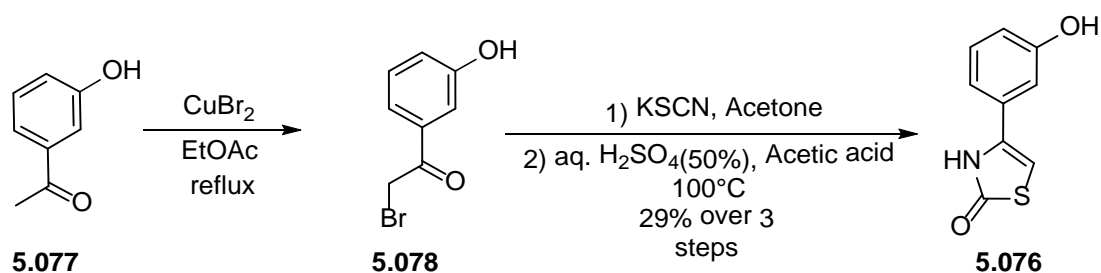


Figure 5.30: Synthesis of the aromatic building block **5.076** [14].

Compound **5.077** was first brominated using copper (II) bromide in ethyl acetate to yield compound **5.078**. Compound **5.078** in its crude form was then treated with potassium thiocyanate in acetone followed by aq. sulfuric acid (50%) and acetic acid in order to obtain compound **5.076** in 29% yield over 3 steps. Once this building block was synthesised, it was subjected to R¹ based modifications using an esterification reaction to form the three analogues shown in **Figure 5.31**.

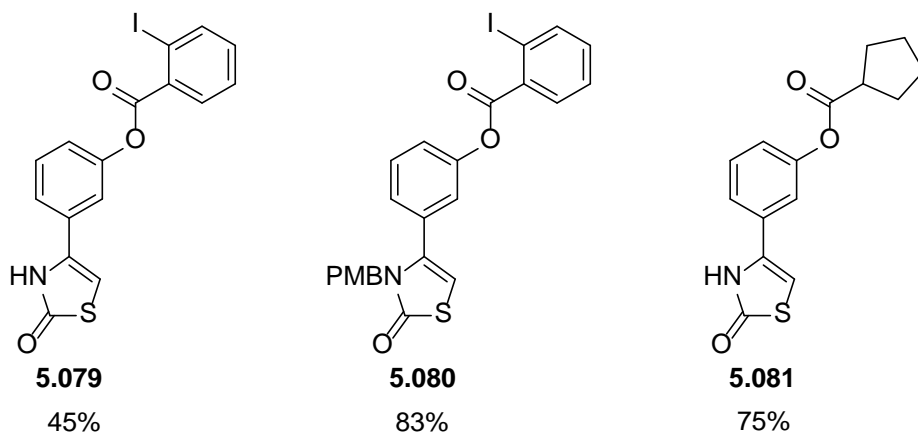


Figure 5.31: The aromatic analogues with their respective yields.

As can be seen from **Figure 5.31**, the analogues synthesised were chosen to understand a variety of different aspects in the molecule. Comparison of the activity of compounds **5.079** and **5.080** would help understand the effect of the PMB protection and compound **5.081** was synthesised in order to study the effect of a non-aromatic derivative at the R^1 position. Next, it was decided to introduce a thiophene group using Suzuki coupling at the halide position. It was however, observed that the Suzuki coupling led to the hydrolysis of the ester bond forming compound **5.076** as shown in **Figure 5.32**.

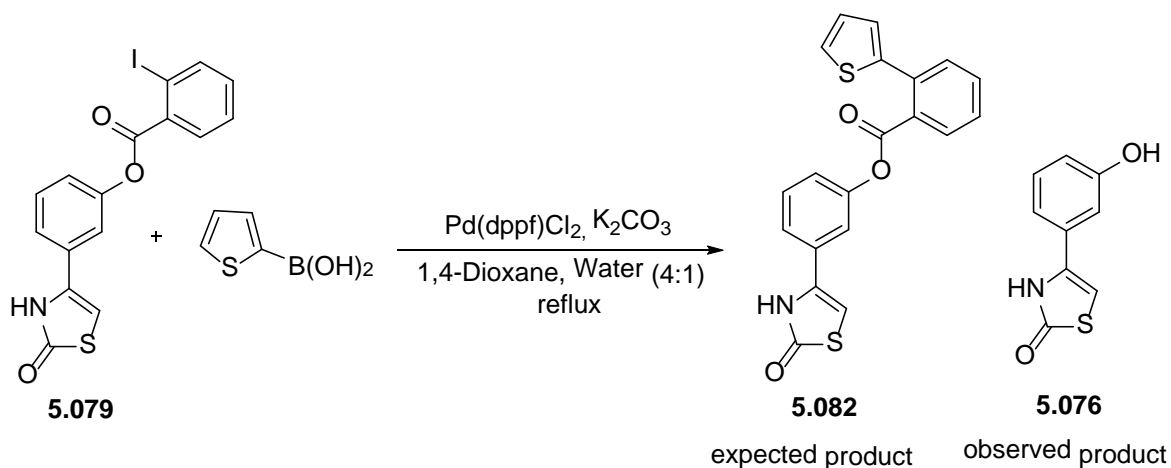


Figure 5.32: Suzuki reaction leading to hydrolysis.

Thus it was decided to synthesise the thiophene derivatives by first coupling the boronic acid with the corresponding iodobenzoic acid using a Suzuki coupling and then perform the esterification reaction in order to obtain the desired product. This led to the synthesis of the aromatic analogues shown in **Figure 5.33**. Compounds **5.083** and **5.084** were synthesised to study the effect of the

thiophene substituent at the 2- and 3- position of the phenyl ring respectively. Compounds **5.084** and **5.085** would help understand the effect of PMB protection on these analogues.

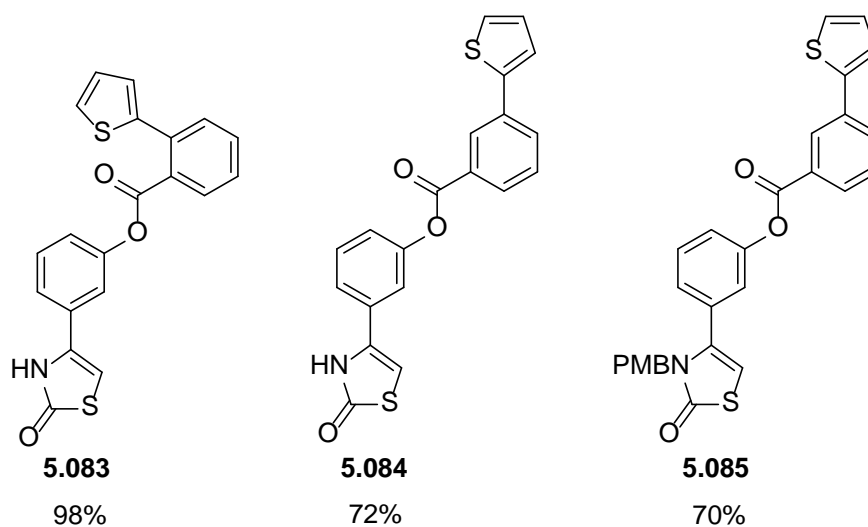


Figure 5.33: The aromatic analogues synthesised from the building block **5.076** with their respective yields.

5.8 SAR interpretation of the synthesised truncated latrunculin analogues

The SAR of the truncated latrunculins analogues were studied to understand the effect of the various substitutions on the activity of these compounds.

5.8.1 SAR for R² modified analogues and analysis of the results observed

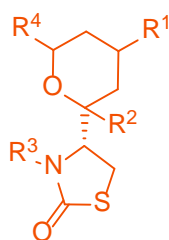
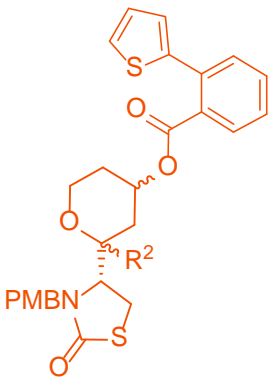
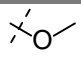
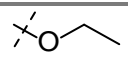
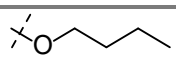
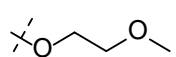


Figure 5.34: General structure of the truncated latrunculin core showing the various positions that were modified as denoted by R¹-R⁴.

The SAR study with respect to the R² modified analogues involved studying the effect of longer chain substituents at the R² position of the truncated latrunculin analogue (**Figure 5.34**). The other positions were maintained as: R¹ position was the thiophene benzoate, R³ was a PMB group and R⁴

was a hydrogen. These substituents were chosen for R¹, R³ and R⁴ since reasonable activity was observed with these substituents with R² being methoxy substituted (compound **4.044**). **Table 5.05** shows the observed activity against *Plasmodium* parasites in a growth inhibition assay.

Table 5.05: R² analogues of truncated latrunculin and their corresponding activity against *Plasmodium* parasites^a.

General structure	Entry	R ²	EC ₅₀ (μM)
	1	 4.044	8
	2	 5.025	8
	3	 5.026	>100
	4	 5.028	>100

^a Parasite strain: 3D7, positive control: latrunculin B.

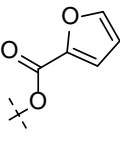
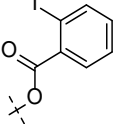
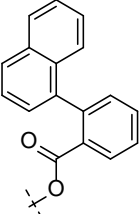
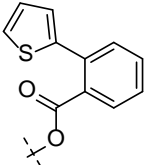
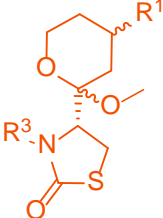
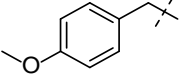
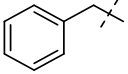
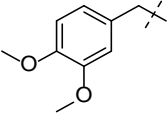
As discussed in Chapter 4, one of the most active R¹ modified compounds was the thiophene benzoate derivative with a methoxy substituent at the R² position (**Table 5.05**, entry 1) (compound **4.044** with EC₅₀ of 8 μM). Here we observe a similar EC₅₀ of 8 μM with the ethoxy derivative **5.025** (**Table 5.05**, entry 2). This similarity in the activity of the methoxy and ethoxy compounds suggested that small hydrophobic groups were tolerated at this position. This effect of hydrophobicity was further explored by the introduction of a more hydrophobic group in the form of the butane derivative **5.026** (**Table 5.05**, entry 3). However, this led to complete loss of activity in this assay. Even decreasing the hydrophobicity slightly with the 2-methoxyethane derivative **5.028** (**Table 5.05**, entry 4) was not tolerated. This suggested that steric hindrance is playing a role in the activity of substituents at this position and that the binding pocket at the R² position can only tolerate small alkyl chains.

5.8.2 SAR for R³ modified analogues and analysis of the results observed

The protecting group used on the nitrogen of the thiazolidinone was a PMB group and, as discussed in Chapter 4, the PMB protection is tolerated at this position. With this in mind, the benzyl and the

3,4-dimethoxybenzyl derivatives were tested against *Plasmodium* parasites. As can be seen from **Table 5.06**, both the benzyl and the DMB had a similar effect on the activity of these analogues.

Table 5.06: R³ analogues of truncated latrunculin and their corresponding activity against *Plasmodium* parasites^a as EC₅₀ values.

General structure	R^1				
	R^3				
		>100 μ M (4.020)	19 μ M (4.023)	6 μ M (4.014)	8 μ M (4.044)
		>100 μ M (5.052)	50 μ M (5.053)	19 μ M (5.054a) and (5.054b)	
					10 μ M (5.055)

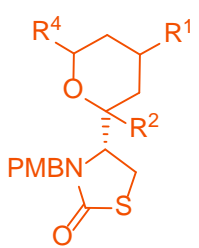
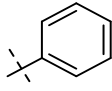
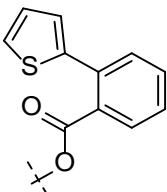
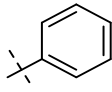
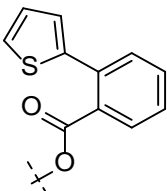
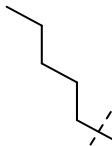
^a Parasite strain: 3D7, positive control: latrunculin B.

The analogues with benzyl protection at the nitrogen atom, followed the same trend as the PMB protected analogues with the thiophene benzoate and naphthalene benzoate derivatives (compound **4.044** and **4.041**) exhibiting low micromolar activity against *Plasmodium* parasites while the 2-iodobenzene analogue **5.053**, had moderate potency and the furan derivative **5.052** was inactive. Comparison of the benzyl and PMB protected analogues also revealed that the presence of the methoxy group at the 4-position was enhancing the activity of these analogues. To confirm this, we also synthesised a thiophene benzoate analogue with DMB group at the R³ position. It was observed that the presence of the additional methoxy group in the 3,4-dimethoxy derivative (with respect to the PMB derivative) did not lead to any further increase in the activity of the thiophene benzoate analogues since both of these analogues had similar activity as shown in **Table 5.06**.

5.8.3 SAR for R⁴ modified analogues and analysis of the results observed

The R⁴ modification was brought about to essentially introduce hydrophobic groups at this position to mimic the effect of the macrocycle in the naturally occurring latrunculins. The R⁴ modified compounds were then subjected to the most potent R¹ modification namely the thiophene benzoate analogue leading to the synthesis of compounds with phenyl ring (compound **5.074**) and the 5-membered alkyl chain (compound **5.075a** and **5.075b**) as shown in **Table 5.07**. The phenyl ring being cyclic and planar would introduce hydrophobic interactions in a rigid manner whereas the flexible alkyl chain could possibly assume any favorable position so as to form the best interaction within the binding site.

Table 5.07: R⁴ analogues of truncated latrunculin and their corresponding activity against *Plasmodium* parasites^a.

General structure	Entry	R ¹	R ²	R ⁴	EC ₅₀ (μM)
	1	OH	OH		37 (5.068)
	2		OH		25 (5.074)
	3		OMe		12 (5.075a) 15 (5.075b)

^a Parasite strain: 3D7, positive control: latrunculin B.

As can be seen from **Table 5.07**, the hemiacetal compound **5.068** with the unsubstituted R¹ position (**Table 5.07**, entry 1) showed only moderate activity of 37 μM against *Plasmodium* parasites. When the thiophene benzoate group was introduced at the R¹ position (**5.074**) (**Table 5.07**, entry 2), there was a boost in the activity suggesting the importance of the R¹ substitution in these compounds.

The methoxy acetal compounds **5.075a** and **5.075b**, with the 5-membered alkyl chain at the R⁴ position and the thiophene benzoate at the R¹ position (Table 5.07, entry 3) were the most potent compound in this series with an EC₅₀ of 12 and 15 μ M against *Plasmodium* parasites. This suggests that the removal of the H-bond acceptor is important for activity although this effect would need to be further explored in order to confirm.

Figure 5.35 shows the structure and activity of compound **4.044** and **5.075a**. It can be seen that both of these compounds have comparable activity, suggesting that there is no increase in the activity due to the introduction of a R⁴ substituent, in other words R⁴ substitution is reasonably well tolerated but is not crucial for activity.

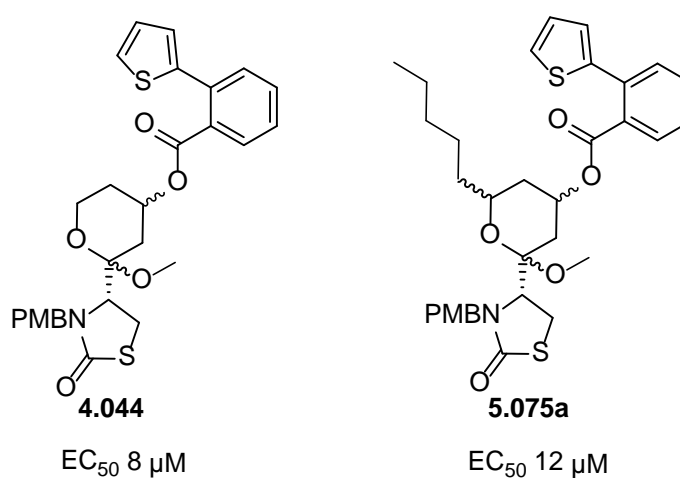
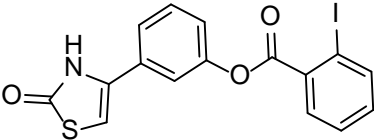
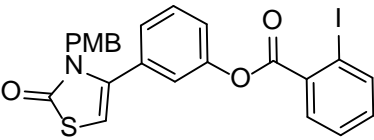
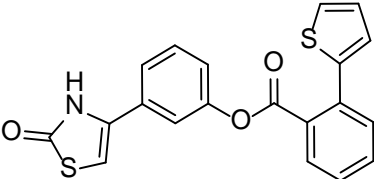
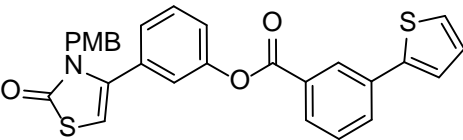


Figure 5.35: Structure and activity of compounds **4.044** and **5.075a**.

5.9 SAR for the aromatic analogues and analysis of the results observed

The aromatic analogues when tested against *Plasmodium* parasites were found to be mostly inactive. The only weakly active compound identified in this series was compound **5.079** (Table 5.08, entry 1). This inactivity of these analogues emphasizes the influence of the 6-membered ring with sp³ character over the flat sp² hybridised aromatic ring. It also suggests that the hydrogen bond acceptor (oxygen) in the THP ring is important for activity.

Table 5.08: Aromatic analogues of truncated latrunculin and their corresponding activity against *Plasmodium* parasites^a.

Entry	Compound	EC ₅₀ (μM)
1	 5.079	50
2	 5.080	>100
3	 5.083	>100
4	 5.085	>100

^a Parasite strain: 3D7, positive control: latrunculin B.

5.10 Computational studies to understand the SAR

The synthesis of all the different R modified analogues, and the corresponding biological studies led to the understanding that the R¹ modification is most crucial for activity. It was therefore decided to study one of these R¹ modified analogues using computational techniques to further understand the binding interactions and SAR.

For this, the thiophene benzoate analogue **4.044** was chosen. The thiophene derivative **4.044** which was one of the most potent analogues of truncated latrunculins (EC₅₀ 8 μM) was constructed in YASARA[®] with the *Plasmodium* actin model and was then subjected to energy minimisation experiment. The energy minimised model was then subjected to cell neutralisation and pKa

prediction experiments followed by a very short molecular dynamic simulation for 100,000 time steps. The simulated model thus obtained by subjected to a final energy minimisation to obtain the model of truncated latrunculin derivative **4.044** bound to the *Plasmodium* actin. The model thus obtained was then read into VMD and the various interactions were carefully studied. **Figure 5.36** illustrates and compares the various interactions possible with latrunculin B and the truncated latrunculin derivative **4.044**.

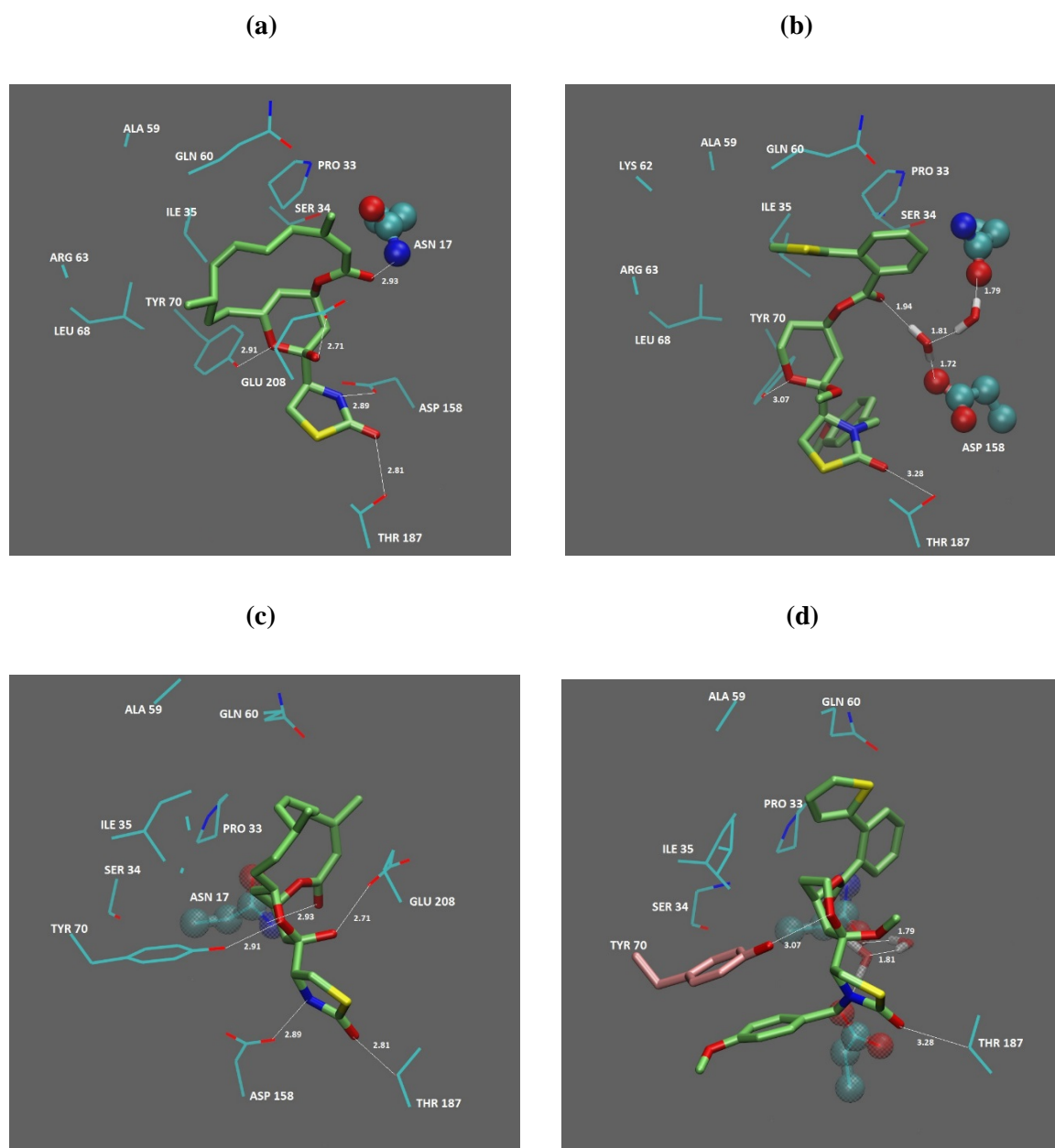


Figure 5.36: Comparison of the binding interactions possible with latrunculin B and truncated latrunculin derivative **4.044**. **(a)** Latrunculin B bound to *Plasmodium* model actin. (Latrunculin B represented in tubes (green), the interacting actin residues in lines, residue Asp 17 in ball and stick). **(b)** Truncated latrunculin derivative **4.044** bound to *Plasmodium* actin model. (**4.044** represented in tubes (green), the interacting actin residues in lines, residues Asp 17 and Thr 187 in ball and stick, interacting water molecule in tubes). **(c)** Latrunculin B bound to *Plasmodium* actin model. (Latrunculin B represented in tubes (green), the interacting actin residues in lines, residue Asp 17 in transparent ball and stick). **(d)** Truncated latrunculin derivative **4.044** bound to *Plasmodium* actin model. (**4.044** represented in tubes (green), the interacting actin residues in lines, residues Asp 17 and Thr 187 in ball and stick, Tyr 70 in tubes (pink)).

*hydrogen bonding with water molecules are shown with respect to distance between the hydrogen and the oxygen, all other hydrogen bonding distances are shown with respect to the hydrogen bond donor and acceptor.

As can be seen in **Figure 5.36 (a)** and **(b)**, the truncated latrunculin derivative, **4.044** can successfully make interactions with Tyr 70 and Thr 187, however interactions with Glu 208 and Asp 158 are lost due to the methoxylation of the chiral alcohol, and the PMB protection of the nitrogen atom respectively. Interestingly, although direct hydrogen bonding between the ester carbonyl with Asn 17 is lost with **4.044**, a water mediated hydrogen bond involving Asp 158 is predicted to form, illustrated in **Figure 5.36 (b)**, likely improving binding affinity. Also, in addition to all the hydrophobic interactions possible as with latrunculin B, **4.044** achieves added stability due to the π stacking possible with Tyr 70 and the PMB group as shown in **Figure 5.36 (d)**. This potentially explains the increased activity of **4.044** over latrunculin B in *Plasmodium* parasites.

Figure 5.37 shows the surface of the *Plasmodium* actin model with **4.044** bound to it. As can be seen, the R^I region readily accommodates the thiophene benzoate group, helping make all the possible hydrophobic interactions which stabilise the compound. It can be inferred from **Figure 5.37**, that the naphthalene derivative **4.041** would also be well accommodated accounting for the increased activity of both **4.044** and **4.041**.

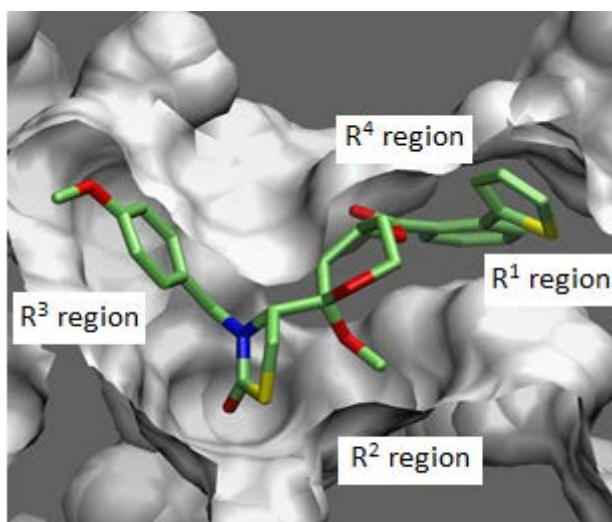


Figure 5.37: Truncated latrunculin derivative **4.044** bound to the *Plasmodium* actin model, showing the tight spacial binding between the protein and the ligand.

It can also be seen from the **Figure 5.37**, that there is not much space for further expansion at the R^2 region. This explains the loss of activity for all the derivatives which were more than 3 carbon length at this position. With respect to the R^3 modification, it can be seen that the PMB group sits neatly in the binding pocket. This explains why the benzyl, PMB and the DMB groups were well tolerated at this position. There is also room for expansion around the R^4 region, which accounts for why the R^4 modifications were well tolerated. It should be noted that the observed activity is influenced by the presence of diastereomers and ideally enantiopure compounds would be required to validate the model.

5.11 Conclusion

Several modifications based at R^2 , R^3 and R^4 positions were successfully synthesised. Selected analogues were also subjected to R^1 modification so as to compare the activity of these analogues in an additive SAR fashion. It was found that small alkyl chains were tolerated at R^2 position; benzyl, PMB and DMB substituents at R^3 positions were favored and in general hydrophobic substituents at R^1 and R^4 positions improved the activity of these analogues. The aromatic analogues generated were found to be inactive suggesting the importance of the two hydrogen bond acceptors and the sp^3 character of the THP ring.

5.12 References

1. Combettes, L.E., et al., Synthesis of 3-Fluoropyrrolidines and 4-Fluoropyrrolidin-2-ones from Allylic Fluorides. *Chem-Eur J*, 2012; 18: 13126-13132.
2. Compain, P., Olefin Metathesis of Amine-Containing Systems: Beyond the Current Consensus. *Adv Synth Catal*, 2007; 349: 1829-1846.
3. Li, D.R., Murugan, A. and Falck, J.R., Enantioselective, Organocatalytic Oxy-Michael Addition to γ/δ -Hydroxy- α,β -enones: Boronate-Amine Complexes as Chiral Hydroxide Synthons. *J Am Chem Soc*, 2008; 130: 46-48.
4. McDougal, P.G., et al., A convenient procedure for the monosilylation of symmetric 1,n-diols. *J Org Chem*, 1986; 51: 3388-3390.
5. Furstner, A. and Turet, L., Concise and practical synthesis of latrunculin A by ring-closing enyne-yne metathesis. *Angew Chem Int Edit*, 2005; 44: 3462-3466.
6. Fuerstner, A., et al., Total syntheses of the actin-binding macrolides latrunculin A, B, C, M, S and 16-epi-latrunculin B. *Chem-Eur J*, 2007; 13: 115-134.
7. Fuerstner, A., et al., Total synthesis and evaluation of the actin-binding properties of microcarpalide and a focused library of analogues. *Chem-Eur J*, 2007; 13: 1452-1462.
8. Khanfar, M.A., Youssef, D.T.A. and El Sayed, K.A., Semisynthetic Latrunculin Derivatives as Inhibitors of Metastatic Breast Cancer: Biological Evaluations, Preliminary Structure–Activity Relationship and Molecular Modeling Studies. *ChemMedChem*, 2010; 5: 274-285.
9. Clayden, J., et al., *Organic Chemistry*. New York: Oxford University Press; 2001
10. Fuerstner, A., et al., Latrunculin analogues with improved biological profiles by "diverted total synthesis": Preparation, evaluation, and computational analysis. *Chem-Eur J*, 2007; 13: 135-149.
11. Tully, D.C., et al., Arylaminoethyl carbamates as a novel series of potent and selective cathepsin S inhibitors. *Bioorg Med Chem Lett*, 2006; 16: 5107-5111.
12. Fernandes, R.A. and Yamamoto, Y., Catalytic Asymmetric Carbalkoxyallylation of Imines with the Chiral Bis- π -allylpalladium Complex. *J Org Chem*, 2004; 69: 3562-3564.
13. Smith, A.B., et al., Total Synthesis Of The Latrunculins. *J Am Chem Soc*, 1992; 114: 2995-3007.
14. Zhao, L., et al., Fragment-Based Drug Discovery of 2-Thiazolidinones as Inhibitors of the Histone Reader BRD4 Bromodomain. *J Med Chem*, 2013; 56: 3833-3851.

Chapter 6. Conclusion and Future directions

6.1 Conclusion

Latrunculins being natural actin inhibitors are a great starting point for the synthesis of actin inhibitory compounds with improved activity and selectivity for the *Plasmodium* parasites. The challenge however remains in the total synthesis of such compounds which appears to be very complex and challenging.

The homology modelling of human actin and *Plasmodium* actin generated from the homology modelling of the known rabbit actin bound with latrunculin crystal structure, suggested that the sequence similarity is high enough to enable the known mammalian actin inhibitors would inhibit *Plasmodium* actin as well. At the same time, the key differences identified between the human and the *Plasmodium* actin also points towards the possibility of achieving selectivity with SAR studies.

It was observed that the total synthesis of latrunculin derivatives was challenging with respect to maintaining the right chiral center and the *Z* double bonds in place. The various attempts to synthesise latrunculin analogues without the epimerisation and isomerization problem also posed other difficulties such as challenges in forming the macrocycle and also in the synthesis of the aromatic precursors as discussed in Chapter 3. In light of all these difficulties, it was decided to look at actin binding in a different perspective, so as to simplify the synthesis and also obtain a more drug like actin inhibitor. This led to the proposal of truncated latrunculin derivatives.

Compound **4.001** was proposed as the new truncated core from which all the analogues were generated. This led to the generation of a library of truncated latrunculin analogues which looked at preliminary SAR studies. The main focus was on the development of various R modifications, the results of which are summarized in **Figure 6.01**. It was found that R¹ modification with *ortho* substituted benzoate esters were the most active analogues with a methoxy at the R² position and a PMB group at the R³ position. The R⁴ position was found to tolerate hydrophobic groups, although it did not lead to any considerable boost in potency. The initial SAR study undertaken in this regards led to the identification of novel truncated latrunculin analogues with 6-8 μM potency against *Plasmodium* parasites. These compounds were also found to be potent against *Toxoplasma gondii*, were non-cytotoxic and did not demonstrate any binding to the mammalian actin. Computational analysis of one of the most active analogue namely compound **4.044** (EC₅₀ 8 μM), revealed all the hydrogen bonding, hydrophobic and π stacking interactions possible in these compounds. This

understanding can help further explore the SAR of truncated latrunculin analogues so as to improve their potency and selectivity.

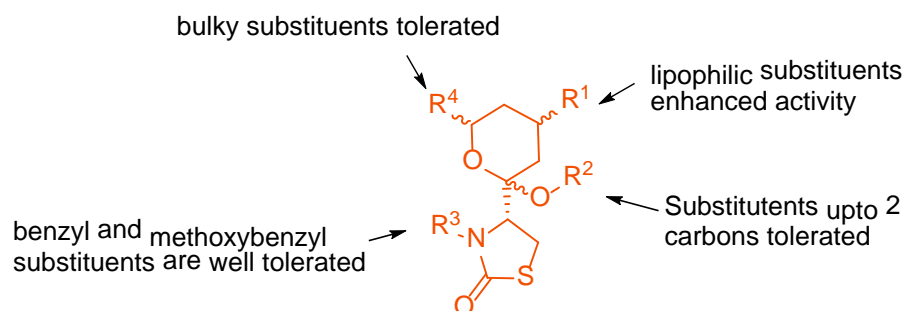


Figure 6.01: Summary of the SAR observed with the truncated latrunculin analogues.

6.2 Future work

In light of the results obtained from the preliminary SAR studies and the computational studies on the *Plasmodium* actin model, it would be interesting to further explore the truncated core. It was observed that the benzoate esters at the R¹ position were the most potent compounds. It is therefore necessary to understand the importance of the ester linkage for this activity. This could involve synthesis of the truncated latrunculin analogues with ester bioisosteres, ether linkage, oxime linkage and ketone linkages as shown in **Figure 6.02**.

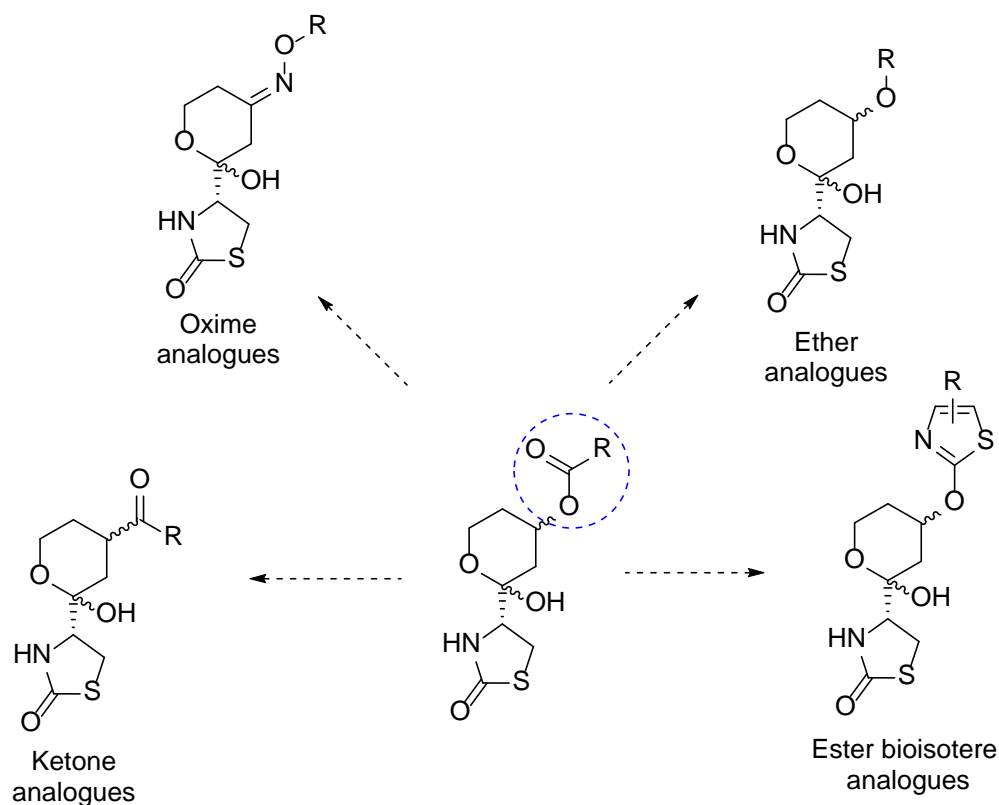


Figure 6.02: Proposed replacements of the ester linkage at R^1 position.

The THP ring has thus far only been explored at three positions, namely the R^1 , R^2 and the R^4 position. It would be interesting to further explore the THP ring at the R^5 and R^6 positions as shown in **Figure 6.03**.

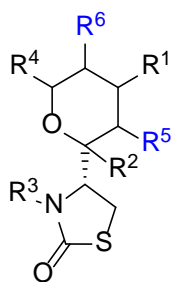


Figure 6.03: Proposed positions R^5 and R^6 for further exploration on the THP ring.

The R^3 position substituted with the benzyl, PMB and the DMB group were all found to be comparably potent. The computational studies on the thiophene benzoate analogue **4.044** reveals the π stacking interaction which adds to the stability of these compounds thereby increasing their potency. Thus it would be interesting to study effect of other substituents at R^3 positions, especially with substituents such as nitro group on the aromatic ring, which would make the ring electron deficient as shown in **Figure 6.04**.

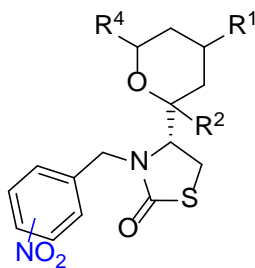


Figure 6.04: Proposed modification at the R³ position to study the effect of electron deficient groups on the aromatic ring.

Furthermore, pharmacokinetic studies need to be undertaken to determine and improve the drugability of these compounds. It would also be ideal to test these compounds on isolated *Plasmodium* actin to further establish the target.

Chapter 7. Experimental

7.1 General experimental

Solvents were of analytical grade: ethyl acetate (EtOAc); dichloromethane (DCM); dimethyl formamide (DMF); methanol (MeOH); tetrahydrofuran (THF). Analytical TLC was performed on silica gel 60/F₂₅₄ pre-coated aluminium sheets (0.25 mm, Merck). Flash column chromatography was carried out with silica gel 60, 0.63–0.20 mm (70–230 mesh, Merck).

¹H, and ¹³C NMR spectra were recorded at 400.13, and 100.62 MHz, respectively, on a Bruker Avance III Nanobay spectrometer with BACS 60 sample changer, using solvents from Cambridge Isotope Laboratories. Chemical shifts (δ , ppm) are reported relative to the solvent peak (CDCl₃: 7.26 [¹H] or 77.16 [¹³C], DMSO-*d*₆: 2.50 [¹H] or 39.52 [¹³C]). Proton resonances are annotated as: chemical shift (ppm), multiplicity (s, singlet; d, doublet; t, triplet; q, quartet; m, multiplet), coupling constant (*J*, Hz), and number of protons.

Analytical HPLC was acquired on an Agilent 1260 Infinity analytical HPLC coupled with a G1322A degasser, G1312B binary pump, G1367E high performance autosampler, G4212B diode array detector. Conditions: Zorbax Eclipse Plus C18 Rapid resolution column (4.6 x 100 mm) with UV detection at 254 nm and 214 nm, 30 °C; sample was eluted using a gradient of 5 – 100% of solvent B in solvent A where solvent A: 0.1% aq. TFA, and solvent B: 0.1% TFA in CH₃CN (5 to 100% B [9 min], 100% B [1 min]; 0.5 ml/min).

Low resolution mass spectrometry was performed on an Agilent 6100 Series Single Quad LCMS coupled with an Agilent 1200 Series HPLC, G1311A quaternary pump, G1329A thermostatted autosampler, and G1314B variable wavelength detector (214 and 254 nm). LC conditions: Phenomenex Luna C8(2) column (100 Å, 5 μ m, 50 x 4.6 mm), 30 °C; sample (5 μ L) was eluted using a binary gradient (solvent A: 0.1% aq. HCO₂H; solvent B: 0.1% HCO₂H in CH₃CN; 5 to 100% B [10 min], 100% B [10 min]; 0.5 ml/min). MS conditions: quadrupole ion source with multimode-ESI; drying gas temperature, 300 °C; vaporizer temperature, 200 °C; capillary voltage, 2000 V (positive mode) or 4000 V (negative mode); scan range, 100–1000 *m/z*; step size, 0.1 s over 10 min.

High resolution MS was performed on an Agilent 6224 TOF LCMS coupled to an Agilent 1290 Infinity LC. All data were acquired and reference mass corrected via a dual-spray electrospray ionisation (ESI) source. Each scan or data point on the total ion chromatogram (TIC) is an average

of 13,700 transients, producing a spectrum every second. Mass spectra were created by averaging the scans across each peak and subtracting the background from first 10 s of the TIC. Acquisition was performed using the Agilent Mass Hunter Data Acquisition software ver. B.05.00 Build 5.0.5042.2 and analysis was performed using Mass Hunter Qualitative Analysis ver. B.05.00 Build 5.0.519.13. Acquisition parameters: mode, ESI; drying gas flow, 11 L/min; nebuliser pressure, 45 psi; drying gas temperature, 325 °C; voltages: capillary, 4000 V; fragmentor, 160 V; skimmer, 65 V; octapole RF, 750 V; scan range, 100–1500 m/z ; positive ion mode internal reference ions, m/z 121.050873 and 922.009798. LC conditions: Agilent Zorbax SB-C18 Rapid Resolution HT (2.1 × 50 mm, 1.8 μ m column), 30 °C; sample (5 μ L) was eluted using a binary gradient (solvent A: 0.1% aq. HCO₂H; solvent B: 0.1% HCO₂H in CH₃CN; 5 to 100% B [3.5 min], 0.5 ml/min).

Optical rotations were recorded in a 10 cm microcell on a JASCO P-2000 polarimeter for a 1 mL solution.

All described compounds were characterised by proton NMR only. The novel compounds were characterised by HPLC, LRMS, HRMS, proton NMR and carbon NMR spectrum. It should be noted that some of the compounds failed to ionise under LRMS and HRMS conditions. The proton NMR spectrum of the mixture of diastereomers have been described separately for both the diastereomers where ever they had distinct signals. In cases where the peaks of both the diastereomers overlapped, they have been described as one NMR spectrum. Optical rotations were obtained for compounds where applicable.

7.2 General procedures

General procedure A: Swern oxidation

To a -78°C cooled solution oxalyl chloride (1.1 eq.) in DCM (1.8 M), was added dry DMSO (2.5 eq.) dropwise. After stirring for 1 h at -78°C, the alcohol (1 eq.) dissolved in DCM (44 M) was added and the reaction stirred for 1 h at -78°C. Triethylamine (2.6 eq.) was then added at -78°C and the reaction was stirred for 12 h while the temperature was allowed to warm up to room temperature. The reaction as then quenched with brine, and the organic layer was extracted 3 times with diethyl ether. The combined organic layers were then dried with magnesium sulphate and evaporated to dryness.

General procedure B: TBS-protection of alcohol

To the alcohol (1 eq.) dissolved in DMF (0.6 M), *tert*-butyldimethylsilyl chloride (TBSCl) (1.2 eq.) and imidazole (2 eq.) were added and stirred for 12 h. The reaction mixture was then diluted with hexane and washed successively with 5% aq. HCl, saturated sodium bicarbonate, water and brine. Sodium sulphate was used to dry the organic layer and then evaporated to dryness. Purification was performed by flash chromatography, eluting with 10% DCM/petroleum spirits to yield the product.

General procedure C: Ester hydrolysis

To potassium hydroxide (3 eq.) dissolved in water (0.4 M), was successively added 1,4-dioxane (0.26 M) and the ester (1 eq.). The reaction was allowed to stir for 1 h before being diluted with 3 M aq. HCl. The aqueous layer was then extracted several times with diethyl ether. The combined organic layer was washed with brine, dried with magnesium sulphate and evaporated to dryness to yield the desired product.

General Procedure D: Aldol reaction

To the ketone (0.8 eq.) dissolved in DCM (0.2 M), 1 M solution of titanium tetrachloride in DCM (1.3 eq.) was added and stirred for 20 minutes. Next, 1 M solution of DIPEA in DCM (1.6 eq.) was added and stirred for 2 h before increasing the temperature to 0°C and stirring for 3 h. The aldehyde (1.1 eq.) dissolved in DCM (0.55 M) was then added at -78°C and stirred for 3 h. When the TLC analysis indicated completion of reaction, ammonium chloride solution was added to quench the reaction mixture and the temperature was increased to room temperature. Water was then added to dissolve the salts formed and the aqueous layer washed with DCM. The combined organic layer was washed with sodium bicarbonate solution and brine, dried with sodium sulphate and evaporated to dryness. Flash chromatography eluting with 25% ethyl acetate/petroleum spirits yielded the desired product.

General Procedure E: TBS-deprotection and spontaneous ring closure

The TBS-protected alcohol (1 eq.) was dissolved in THF (0.05 M) and 1 M aq. HCl (0.35 M) and stirred for 12 h. The reaction was then quenched with sodium bicarbonate solution and the aqueous layer washed with DCM. The combined organic layer was washed with brine, dried with sodium sulphate and evaporated *in vacuo*. Flash chromatography eluting with 100% diethyl ether yielded the desired product.

General Procedure F: O-alkylation

The hemiacetal (1 eq.) was dissolved in the corresponding alcohol (0.05 M) and catalytic CSA (0.1 eq.) was added. The reaction was stirred for 12 h before being quenched with sodium bicarbonate solution and extracted repeatedly with DCM. The combined organic layer was washed with brine and dried with sodium sulphate before evaporating to dryness to yield the product.

General Procedure G: EDCI coupling

To the alcohol (1 eq.) dissolved in DCM (0.02 M), was added the carboxylic acid (2.8 eq.), DMAP (3 eq.) and EDCI.HCl (3 eq.). The solution was then stirred at room temperature till the completion of the reaction, as indicated by the TLC analysis. Saturated ammonium chloride solution was then added and the aqueous layer extracted with DCM (x 3). The combined organic layer was then dried with sodium sulphate and evaporated to dryness. Flash chromatography, eluting with 15% EtOAc/petroleum spirits yielded the product.

General procedure H: Weinreb amide

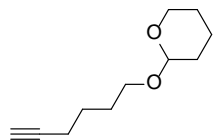
To the carboxylic acid (1 eq.) dissolved in DCM (0.3 M), was added DIPEA (3 eq.), *N,O*-dimethylhydroxylamine hydrochloride (3 eq.) and TBTU (1.5 eq.), and the reaction stirred for 12 h. After the completion of reaction as indicated by TLC analysis, 1 M aq. HCl solution was added and the aqueous layer extracted with DCM (x 3 times). The organic layer was then washed with 0.5 M aq. NaOH solution, dried with sodium sulphate and then evaporated to dryness. Flash chromatography, eluting with 50% EtOAc/petroleum spirits yielded the product.

General procedure I: Suzuki coupling

To the corresponding halide (1 eq.) dissolved in 4:1 ratio of 1,4-dioxane and water (0.05 M), was added potassium carbonate (3 eq.). The solution was degassed to remove all the dissolved oxygen from the solution, before catalytic amount of Pd(dppf)Cl₂ (0.05 eq.) was added and the reaction mixture refluxed for 12 h. The reaction was allowed to cool to room temperature and then filtered through celite to remove most of the catalyst. The filtrate was then diluted with EtOAc and washed with brine. The organic layer was dried with sodium sulphate and evaporated to dryness. Flash chromatography, eluting with 15% EtOAc/petroleum spirits yielded the desired product.

7.3 Chapter 3 compounds

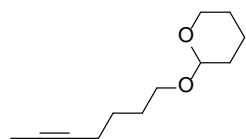
2-(hex-5-yn-1-yloxy)tetrahydro-2H-pyran (3.029) [1]



To a well stirred solution of 5 hexyn-1-ol (2 g, 20.3 mmol) and dihydropyran (9.19 mL, 100.69 mmol) in DCM (80.7 mL), *p*-toluene sulphonic acid monohydrate (38.9 mg, 0.20 mmol) was added and the reaction was stirred for 1.5 h at room temperature. Diethyl ether was then added and the organic layer was washed with saturated sodium bicarbonate solution, water and brine. The product was extracted with diethyl ether, dried with magnesium sulphate and then evaporated to dryness. Purification was performed by flash chromatography, eluting with 12% diethyl ether/petroleum spirits, to obtain the product as a clear colourless oil (3.09 g, 83%).

^1H NMR (400 MHz, CDCl_3) δ 4.61 – 4.54 (m, 1H), 3.91 – 3.70 (m, 2H), 3.54 – 3.35 (m, 2H), 2.23 (td, $J = 7.0, 2.6$ Hz, 2H), 1.94 (t, $J = 2.6$ Hz, 1H), 1.83 – 1.39 (m, 10H).

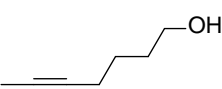
2-(hept-5-yn-1-yloxy)tetrahydro-2H-pyran (3.030) [2]



2-(hex-5-yn-1-yloxy)tetrahydro-2H-pyran (1 g, 5.5 mmol) was added to THF (50 mL) and cooled to -78°C . To this, 2.5 M butyl lithium solution (3.4 mL, 8.25 mmol) was added dropwise and stirred for 20 min. The temperature was then increased to 0°C and stirred for 1 h. The reaction was again cooled to -78°C and iodomethane (0.53 mL, 8.25 mmol) was added. After 30 minutes, the temperature was increased to 0°C and stirred for 12 h as the reaction slowly warmed up to room temperature. Saturated ammonium chloride solution was then added to quench the reaction. The aqueous layer was extracted with diethyl ether, dried with sodium sulphate and evaporated to dryness. The crude product was directly used for the next step.

^1H NMR (400 MHz, CDCl_3) δ 4.57 (dd, $J = 4.2, 2.8$ Hz, 1H), 3.86 (m, 1H), 3.75 (m, 1H), 3.54 – 3.45 (m, 1H), 3.39 (ddd, $J = 6.5, 6.0, 3.9$ Hz, 1H), 2.23 – 2.09 (m, 2H), 1.77 (t, $J = 2.6$ Hz, 3H), 1.71 – 1.47 (m, 10H).

hept-5-yn-1-ol (3.025) [3]

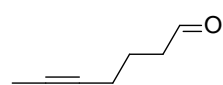


To a well stirred solution of 2-(hept-5-yn-1-yloxy)tetrahydro-2H-pyran (1.2 g, 6.11 mmol) in methanol (40 mL), *p*-toluene sulphonic acid monohydrate (0.465 g, 2.45 mmol) was added and the reaction stirred for 2 h. The reaction

was then diluted with diethyl ether and washed with brine. The organic layer was extracted with diethyl ether (x 3), dried with magnesium sulphate and evaporated to dryness. Purification by flash chromatography, eluting with 12% diethyl ether/petroleum spirits gave the product as a pale yellow oil (0.57 g, 83%).

^1H NMR (400 MHz, CDCl_3) δ 3.66 (t, J = 6.4 Hz, 2H), 2.16 (tt, J = 6.9, 2.5 Hz, 2H), 1.77 (t, J = 2.6 Hz, 3H), 1.71 – 1.62 (m, 2H), 1.59 – 1.50 (m, 2H).

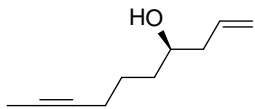
hept-5-ynal (3.026) [4]



Title compound was synthesised according to General Procedure A using 5-heptyn-1-ol (100 mg, 0.89 mmol). Since the product is volatile and unstable, *in vacuo* evaporation was carried out at 0°C. The NMR of the crude mixture was found to be clean and thus no further purification was carried out (99%).

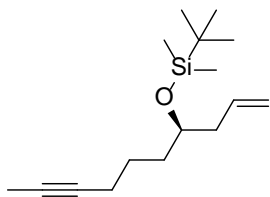
^1H NMR (400 MHz, CDCl_3) δ 9.80 (t, J = 1.5 Hz, 1H), 2.57 (td, J = 7.2, 1.5 Hz, 2H), 2.20 (tt, J = 6.9, 2.5 Hz, 2H), 1.85 – 1.75 (m, 5H).

(*R*)-dec-1-en-8-yn-4-ol (3.027) [4]



Hept-5-ynal (0.92 g, 8.35 mmol) dissolved in diethyl ether (13 mL) was cooled to -100°C, and a 1 M in pentane solution of (-)-Ipc₂B(allyl) (8.3 mL, 8.35 mmol) at -100°C was added and stirred for 2 h at the same temperature. The reaction was then quenched with methanol (1.1 mL) and evaporated at 0°C to remove the solvent. Methanol (17.3 mL) and 8-hydroxyquinoline (1.5 g, 10.3 mmol) were then added and the reaction stirred overnight. The yellow precipitate formed was filtered off and the filtrate evaporated to dryness. Purification by flash chromatography, eluting with 5% ethyl acetate/petroleum spirits yielded a slightly impure alcohol which was directly used for the next step.

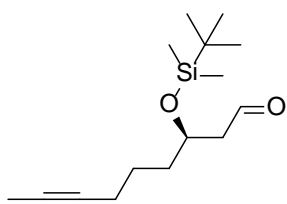
(*R*)-*tert*-butyl(dec-1-en-8-yn-4-yloxy)dimethylsilane (3.028) [4]



Title compound was prepared from (*R*)-dec-1-en-8-yn-4-ol (2.75 g, 18.1 mmol) using General procedure B as a clear oil (240 mg, 52% over 2 steps).

^1H NMR (400 MHz, CDCl_3) δ 5.81 (ddt, J = 19.5, 10.4, 7.2 Hz, 1H), 5.09 – 4.97 (m, 2H), 3.80 – 3.59 (m, 1H), 2.25 – 2.18 (m, 2H), 2.16 – 2.08 (m, 2H), 1.78 (m, 3H), 1.58 – 1.47 (m, 4H), 0.89 (s, 9H), 0.05 (s, 6H).

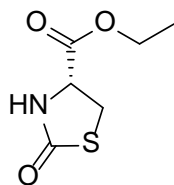
(R)-3-((tert-butyl dimethylsilyl)oxy)non-7-ynal (3.022) [4]



(*R*)-tert-butyl(dec-1-en-8-yn-4-yloxy)dimethylsilane (700 mg, 2.63 mmol) was dissolved in methanol (35 mL) and sudan red was added to impart a red colour to the solution. After cooling the reaction mixture to -78°C , ozone gas was bubbled through the reaction mixture till the colour of the sudan red disappeared. Nitrogen gas was then bubbled through the mixture for 15 minutes, followed by addition of triphenylphosphine (1 g, 3.8 mmol) was then added and the reaction mixture stirred overnight. The solvent was then evaporated and the product purified by flash chromatography, eluting with 5% ethyl acetate/petroleum spirits to give the aldehyde as a colourless oil (506 mg, 72%).

^1H NMR (400 MHz, CDCl_3) δ 9.81 (t, $J = 2.5$ Hz, 1H), 4.28 – 4.16 (m, 1H), 2.58 – 2.48 (m, 2H), 2.14 (tt, $J = 6.9, 2.5$ Hz, 2H), 1.77 (t, $J = 2.5$ Hz, 3H), 1.69 – 1.46 (m, 4H), 0.87 (s, 9H), 0.07 (d, $J = 9.2$ Hz, 6H).

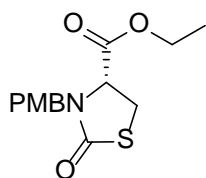
(R)-ethyl 2-oxothiazolidine-4-carboxylate (3.035) [5]



To a slurry of L-cysteine ethyl ester hydrochloride (11.45 g, 61.7 mmol) in THF (180 mL), carbonyldiimidazole (10 g, 61.7 mmol) was added in small portions and stirred for 20 h. The reaction mixture was then filtered through a pad of silica, evaporated *in vacuo* and subjected to flash chromatography, eluting with 50% EtOH/petroleum spirits to yield the product as a colourless oil (6.53 g, 56%).

^1H NMR (400 MHz, CDCl_3) δ 5.99 (s, 1H), 4.42 (ddd, $J = 8.1, 5.4, 0.8$ Hz, 1H), 4.28 (q, $J = 7.1$ Hz, 2H), 3.70 (dd, $J = 11.3, 8.1$ Hz, 1H), 3.63 (dd, $J = 11.3, 5.4$ Hz, 1H), 1.32 (t, $J = 7.1$ Hz, 3H).

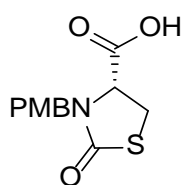
(R)-ethyl 3-(4-methoxybenzyl)-2-oxothiazolidine-4-carboxylate (3.036) [5]



To a stirred suspension of (*R*)-ethyl 2-oxothiazolidine-4-carboxylate (6.53 g, 34.30 mmol) in DMF (127 mL), potassium carbonate (7.1 g, 51.49 mmol), catalytic amount of sodium iodide (450 mg, 3 mmol) and 4-methoxybenzyl chloride (7.88 mL, 59.52 mmol) were added and the reaction stirred for 12 h. After the completion of the reaction as indicated by TLC analysis, diethyl ether was added and the suspension washed with brine (x 3). The organic layer was dried with magnesium sulphate, filtered and evaporated to dryness. The residue was purified by flash chromatography eluting with 30% EtOH/petroleum spirits to yield the product (5.68 g, 56%).

^1H NMR (400 MHz, CDCl_3) δ 7.16 (d, J = 8.5 Hz, 2H), 6.86 (d, J = 8.7 Hz, 2H), 5.08 (d, J = 14.8 Hz, 1H), 4.25 (q, J = 7.1 Hz, 2H), 4.12 (dd, J = 8.5, 3.1 Hz, 1H), 3.99 (d, J = 14.8 Hz, 1H), 3.80 (s, 3H), 3.48 (dd, J = 11.4, 8.5 Hz, 1H), 3.33 (dd, J = 11.4, 3.1 Hz, 1H), 1.30 (t, J = 7.1 Hz, 3H).

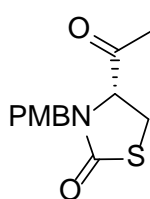
(*R*)-3-(4-methoxybenzyl)-2-oxothiazolidine-4-carboxylic acid (3.037s) [5]



Title compound was prepared from (*R*)-ethyl 2-oxothiazolidine-4-carboxylate (5.5g, 18.52 mmol) using General Procedure C as a pale yellow coloured semisolid (5.5 g, 84%).

^1H NMR (400 MHz, CDCl_3) δ 7.19 (d, J = 8.5 Hz, 2H), 6.88 (d, J = 8.7 Hz, 2H), 5.14 (d, J = 14.8 Hz, 1H), 4.20 (dd, J = 8.6, 2.5 Hz, 1H), 4.01 (d, J = 14.8 Hz, 1H), 3.80 (s, 3H), 3.54 (dd, J = 11.5, 8.6 Hz, 1H), 3.41 (dd, J = 11.5, 2.5 Hz, 1H).

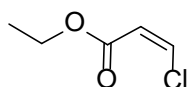
(*R*)-4-acetyl-3-(4-methoxybenzyl)thiazolidin-2-one (3.007) [5]



To a -78°C cooled solution of (*R*)-3-(4-methoxybenzyl)-2-oxothiazolidine-4-carboxylic acid (208 mg, 0.78 mmol) in THF (5 mL), 1-chloro-2,*N,N*-trimethylprop-1-en-1-ylamine (0.5 mL, 3.9 mmol) was added and the solution kept at -18°C for 40 h. The acid chloride thus formed was then again cooled to -78°C and then catalytic amount of $\text{Fe}(\text{acac})_3$ (14 mg, 0.04 mmol) and 1.9 M methylmagnesium bromide solution (870 μL) were added. After stirring the solution for 30 min at 0°C , the reaction was quenched with saturated ammonium chloride solution. The aqueous layer was then extracted with diethyl ether, dried with magnesium sulphate and evaporated *in vacuo* to yield the product. Flash chromatography, eluting with 35% ethyl acetate/petroleum spirits afforded the product (150 mg, 93%).

^1H NMR (400 MHz, CDCl_3) δ 7.13 (d, J = 8.6 Hz, 2H), 6.86 (d, J = 8.7 Hz, 2H), 5.02 (d, J = 14.7 Hz, 1H), 4.09 (dd, J = 9.3, 4.0 Hz, 1H), 3.92 (d, J = 14.7 Hz, 1H), 3.80 (s, 3H), 3.50 (dd, J = 11.5, 9.3 Hz, 1H), 3.11 (dd, J = 11.5, 4.0 Hz, 1H), 2.14 (s, 3H).

(*Z*)-ethyl 3-chloroacrylate (3.046) [4]

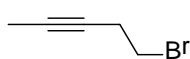


Ethyl propiolate (3.4 mL, 34 mmol) dissolved in acetonitrile (50 mL) was mixed with lithium chloride (3.2 g mg, 74.7 mmol) and glacial acetic acid (2.2 mL) in a sealed tube and heated at 170°C for 3 days. After cooling to room temperature, water followed by aq. potassium carbonate solution were added till the effervescence ceased (or

was not acidic). The organic phase was then extracted with diethyl ether, dried with sodium sulphate and evaporated to dryness. Purification was performed by flash chromatography eluting with 5% ethyl acetate/petroleum spirits to yield the product as a clear colourless oil (3.6 g, 79%).

^1H NMR (400 MHz, CDCl_3) δ 6.70 (d, $J = 8.2$ Hz, 1H), 6.19 (d, $J = 8.2$ Hz, 1H), 4.24 (q, $J = 7.1$ Hz, 2H), 1.31 (t, $J = 7.1$ Hz, 3H).

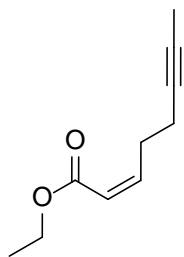
5-bromopent-2-yne (3.050) [6]



Triphenylphosphine (1.1 g, 3.6 mmol) and *N*-bromosuccinimide (0.7 g, 4 mmol) were added to 3-pentyn-1-ol (0.33 mL, 3.6 mmol) in THF (7 mL) at -20°C . The temperature was then increased to 0°C and stirred for 12 h. Saturated ammonium chloride solution was added to quench the reaction and the organic layer was extracted with diethyl ether, dried with sodium sulphate and evaporated *in vacuo* at 0°C . Purification was attained by kugelrohr distillation (55%).

^1H NMR (400 MHz, CDCl_3) δ 3.41 (t, $J = 7.3$ Hz, 2H), 2.69 (ddd, $J = 9.8, 4.9, 2.5$ Hz, 2H), 1.79 (t, $J = 2.5$ Hz, 3H).

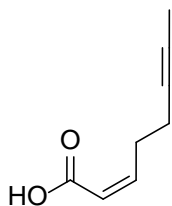
(*Z*)-ethyl oct-2-en-6-ynoate (3.048) [4]



In a flame dried glassware, magnesium turnings (437 mg, 18 mmol) were stirred with catalytic amount of iodine and dry THF (3 mL) for 1 h. Further, THF (7 mL) was added and the reaction heated to gentle reflux. 5-bromopent-2-yne (2.4 g, 16.35 mmol) in THF (9 mL) was then added drop wise so as to maintain gentle reflux. After completion of addition of 5-bromopent-2-yne, the reaction mixture was stirred for 2.5 h to obtain the Grignard reagent. The Grignard reagent thus obtained was immediately added to a mixture of (*Z*)-ethyl-3-chloroacrylate (930 mg, 6.9 mmol) and $\text{Fe}(\text{acac})_3$ (579 mg, 1.64 mmol) in THF (15 mL) at -30°C . After stirring for 15 minutes, the reaction was quenched with saturated ammonium chloride solution. The organic layer was extracted using diethyl ether, dried with sodium sulphate and evaporated to dryness. Flash chromatography, eluting with 2% ethyl acetate/ petroleum spirits yielded the product (670 mg, 58%).

^1H NMR (400 MHz, CDCl_3) δ 6.32 (dt, $J = 11.5, 7.2$ Hz, 1H), 5.82 (dt, $J = 11.5, 1.8$ Hz, 1H), 4.17 (q, $J = 7.1$ Hz, 2H), 2.82 (qd, $J = 7.1, 1.8$ Hz, 2H), 2.32 – 2.22 (m, 2H), 1.77 (t, $J = 2.6$ Hz, 3H), 1.29 (t, $J = 7.1$ Hz, 3H).

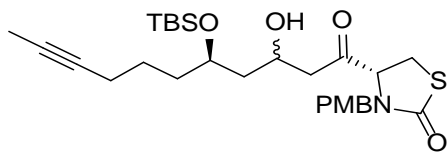
(Z)-oct-2-en-6-ynoic acid (3.023) [4]



(Z)-ethyl oct-2-en-6-ynoate (580 mg, 3.5 mmol) was dissolved in 1 M aq. NaOH solution (9.3 mL) and methanol (7.5 mL) and stirred for 12 h. The solvent was then removed *in vacuo* and the aqueous layer was washed with diethyl ether and then acidified with 2 M aq. HCl solution, till the pH drops to 1. The aqueous layer was then extracted with DCM, dried with sodium sulphate and evaporated to dryness. Purification by flash chromatography eluting with 5% ethyl acetate/petroleum spirits yielded the product as a colourless oil (60 mg, 41%).

^1H NMR (400 MHz, CDCl_3) δ 6.46 (dt, $J = 11.5, 7.2$ Hz, 1H), 5.86 (dt, $J = 11.5, 1.8$ Hz, 1H), 2.84 (qd, $J = 7.1, 1.8$ Hz, 2H), 2.29 (ddd, $J = 9.6, 4.6, 2.6$ Hz, 2H), 1.78 (t, $J = 2.5$ Hz, 3H).

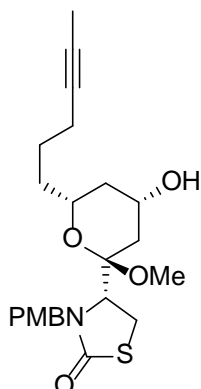
4-(5-((*tert*-butyldimethylsilyl)oxy)-3-hydroxyundec-9-ynoyl)-3-(4-methoxybenzyl)thiazolidin-2-one (3.059+3.060) [7]



Title compound was prepared from (*R*)-4-acetyl-3-(4-methoxybenzyl)thiazolidin-2-one (350 mg, 1.32 mmol) and (*R*)-3-((*tert*-butyldimethylsilyl)oxy)non-7-ynal (296 mg, 1.1 mmol) according to General Procedure D as a mixture of two diastereomers in 1: 0.9 ratios as a clear oil (495 mg, 86%).

^1H NMR (400 MHz, CDCl_3) δ 7.21 – 7.08 (m, 3.8H), 6.89 – 6.77 (m, 3.8H), 5.09 (d, $J = 14.8$ Hz, 1H), 5.00 (d, $J = 14.7$ Hz, 0.9H), 4.51 – 4.36 (m, 1H), 4.28 – 4.20 (m, 1.9H), 4.18 (dd, $J = 9.3, 3.7$ Hz, 0.9H), 4.06 – 3.92 (m, 1.9H), 3.89 – 3.81 (m, 1.9H), 3.79 (d, $J = 1.8$ Hz, 5.7H), 3.46 (ddd, $J = 12.0, 9.4, 2.8$ Hz, 1.9H), 3.21 (ddd, $J = 22.8, 11.5, 3.7$ Hz, 1.9H), 2.69 – 2.53 (m, 1.9H), 2.47 (dd, $J = 16.1, 4.2$ Hz, 0.9H), 2.28 (dd, $J = 15.4, 3.6$ Hz, 1H), 2.20 – 2.10 (m, 3.8H), 1.78 (dd, $J = 5.6, 2.6$ Hz, 5.7H), 1.74 – 1.38 (m, 11.4H), 0.89 (d, $J = 2.8$ Hz, 17.1H), 0.16 – 0.05 (m, $J = 3.3$ Hz, 11.4H).

(R)-4-((2R,4S,6R)-6-(hex-4-yn-1-yl)-4-hydroxy-2-methoxytetrahydro-2H-pyran-2-yl)-3-(4-methoxybenzyl)thiazolidin-2-one (3.063) [7]



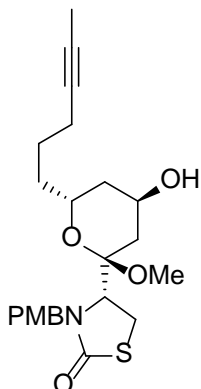
Title compound was prepared in two steps. Firstly, 4-(5-((*tert*-butyldimethylsilyl)oxy)-3-hydroxyundec-9-ynoyl)-3-(4-methoxybenzyl)thiazolidin-2-one (474 mg, 0.91 mmol) was used to synthesise (*R*)-4-((2*R*,4*S*,6*R*)-6-(hex-4-yn-1-yl)-2,4-dihydroxytetrahydro-2H-pyran-2-yl)-3-(4-methoxybenzyl)thiazolidin-2-one according to General Procedure E (Flash chromatography eluting with 100% diethyl ether separated the diastereomers).

(*R*)-4-((2*R*,4*S*,6*R*)-6-(hex-4-yn-1-yl)-2,4-dihydroxytetrahydro-2H-pyran-2-yl)-3-(4-methoxybenzyl)thiazolidin-2-one was then used to synthesis title compound according to the General Procedure

F as a clear oil (170 mg, 71%).

¹H NMR (400 MHz, CDCl₃) δ 7.25 – 7.19 (m, 2H), 6.91 – 6.84 (m, 2H), 5.12 (d, *J* = 14.4 Hz, 1H), 4.24 (d, *J* = 14.4 Hz, 1H), 4.06 (m, 1H), 3.84 (dd, *J* = 8.8, 3.1 Hz, 1H), 3.81 (s, 3H), 3.64 – 3.55 (m, 1H), 3.32 – 3.19 (m, 2H), 3.05 (s, 3H), 2.27 – 2.17 (m, 3H), 2.04 – 1.96 (m, 1H), 1.84 – 1.72 (m, 5H), 1.68 – 1.47 (m, 4H).

(R)-4-((2R,4R,6R)-6-(hex-4-yn-1-yl)-4-hydroxy-2-methoxytetrahydro-2H-pyran-2-yl)-3-(4-methoxybenzyl)thiazolidin-2-one (3.064) [7]

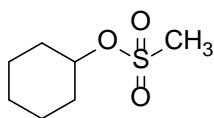


Title compound was prepared in two steps. Firstly, 4-(5-((*tert*-butyldimethylsilyl)oxy)-3-hydroxyundec-9-ynoyl)-3-(4-methoxybenzyl)thiazolidin-2-one (474 mg, 0.91 mmol) was used to synthesise (*R*)-4-((2*R*,4*R*,6*R*)-6-(hex-4-yn-1-yl)-2,4-dihydroxytetrahydro-2H-pyran-2-yl)-3-(4-methoxybenzyl)thiazolidin-2-one according to General Procedure E (Flash chromatography eluting with 100% diethyl ether separated the diastereomers). (*R*)-4-((2*R*,4*R*,6*R*)-6-(hex-4-yn-1-yl)-2,4-dihydroxytetrahydro-2H-pyran-2-yl)-3-(4-methoxybenzyl)thiazolidin-2-one was then used to

synthesis title compound according to the General Procedure F as a clear oil (28 mg, 16%).

¹H NMR (400 MHz, CDCl₃) δ 7.22 (m, 2H), 6.91 – 6.83 (m, 2H), 5.10 (d, *J* = 14.4 Hz, 1H), 4.22 (d, *J* = 14.4 Hz, 1H), 3.99 – 3.88 (m, 1H), 3.81 (s, 3H), 3.80 – 3.74 (m, 1H), 3.68 (m, 1H), 3.37 – 3.22 (m, 2H), 3.15 (s, 3H), 2.23 (m, 2H), 2.12 – 2.05 (m, 1H), 1.92 – 1.78 (m, 3H), 1.77 (t, *J* = 2.5 Hz, 3H), 1.70 – 1.52 (m, 3H), 1.52 – 1.42 (m, 1H).

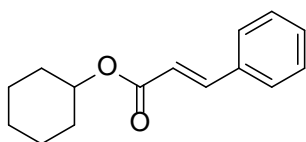
cyclohexyl methanesulfonate (3.077) [8]



Cyclohexanol (150 mg, 1.5 mmol) and triethylamine (0.3 mL, 1.6 mmol) were dissolved in DCM (3 mL). The solution was then cooled to 0°C and methanesulfonyl chloride (172 mg, 1.5 mmol) was introduced dropwise. After stirring for 12 h, the reaction was quenched with saturated sodium bicarbonate solution and washed with EtOAc, the organic layer was dried using sodium sulphate and evaporated to dryness. Flash chromatography eluting with 15% EtOAc/petroleum spirits yielded the product as a clear oil (148 mg, 83%).

¹H NMR (400 MHz, CDCl₃) δ 4.77 – 4.61 (m, 1H), 3.00 (s, 3H), 2.04 – 1.91 (m, 2H), 1.78 (ddd, *J* = 10.5, 8.7, 4.4 Hz, 2H), 1.72 – 1.47 (m, 4H), 1.47 – 1.24 (m, 2H).

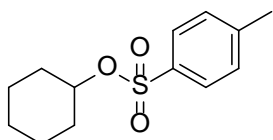
cyclohexyl cinnamate (3.074) [9]



Cyclohexyl methanesulfonate (74 mg, 0.4 mmol), cinnamic acid (296 mg, 2 mmol) and cesiumfluoride (304 mg, 2 mmol) were dissolved in DMF (4 mL) and heated at 90°C for 8 h. After cooling to room temperature, EtOAc and ice cold water were added and the organic layer washed with saturated sodium bicarbonate solution and brine before drying with sodium sulphate and evaporating to dryness. Flash chromatography, eluting with 10% EtOAc/petroleum spirits yielded the product in (7.3 mg, 8%).

¹H NMR (400 MHz, CDCl₃) δ 7.67 (d, *J* = 16.0 Hz, 1H), 7.56 – 7.47 (m, 2H), 7.43 – 7.34 (m, 3H), 6.43 (d, *J* = 16.0 Hz, 1H), 5.01 – 4.79 (m, 1H), 1.98 – 1.87 (m, 2H), 1.77 (m, 2H), 1.59 – 1.23 (m, 6H).

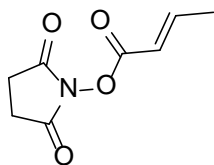
cyclohexyl 4-methylbenzenesulfonate (3.078) [10]



Cyclohexanol (0.1 mL, 1 mmol) and DMAP (6.24 mg, 0.05 mmol) were dissolved in pyridine (1 mL) and cooled to 0°C. *p*-toluene sulfonyl chloride (248 mg, 1.3 mmol) was then added portion-wise over 30 min and stirred for 6 h. The reaction was quenched with saturated sodium bicarbonate solution and extracted with EtOAc (x 3). Sodium sulphate was used to dry the solution and was then evaporated *in vacuo* to yield the product as a clear oil (209 mg, 82%).

¹H NMR (400 MHz, CDCl₃) δ 7.83 – 7.76 (m, 2H), 7.32 (d, *J* = 8.0 Hz, 2H), 4.55 – 4.45 (m, 1H), 2.44 (s, 3H), 1.95 – 1.12 (m, 10H).

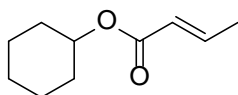
2,5-dioxopyrrolidin-1-yl (*E*)-but-2-enoate (3.089) [11]



Crotonic acid (100 mg, 1.16 mmol) was dissolved in DCM (5.8 mL) and cooled to 0°C. To this cooled solution, triphosgene (172 mg, 0.58 mmol) and triethylamine (0.81 mL, 5.8 mmol) were added, followed by *N*-hydroxysuccinamide (133.5 mg, 1.16 mmol). The reaction was stirred for 30 min at room temperature. The solution was then filtered and evaporated to dryness. Flash chromatography, eluting with 25% EtOAc/petroleum spirits yielded the product as yellow solid (170 mg, 40%).

¹H NMR (400 MHz, CDCl₃) δ 7.36 – 7.23 (m, 1H), 6.05 (dq, *J* = 15.6, 1.7 Hz, 1H), 2.85 (s, 4H), 2.00 (dd, *J* = 7.0, 1.7 Hz, 3H).

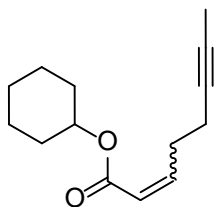
cyclohexyl (*E*)-but-2-enoate (3.090) [12]



Crotonyl chloride (0.06 mL, 0.62 mmol) and CuO (5 mg, 0.06 mmol) were dissolved in acetonitrile (0.6 mL). Cyclohexanol (62.2 mg, 0.62 mmol) was then added dropwise and stirred for 3 h. When the TLC analysis indicated completion of the reaction, DCM was added to dilute the reaction mixture. The organic layer was washed with water, dried with sodium sulphate and evaporated to dryness. Flash chromatography, eluting with 5% EtOAc/ petroleum spirits afforded the product (44.4 mg, 44%).

¹H NMR (400 MHz, CDCl₃) δ 6.88 (dq, *J* = 15.5, 6.9 Hz, 1H), 5.76 (dq, *J* = 15.5, 1.7 Hz, 1H), 4.80 – 4.68 (m, 1H), 1.80 (dd, *J* = 6.9, 1.7 Hz, 3H), 1.78 – 1.06 (m, 10H).

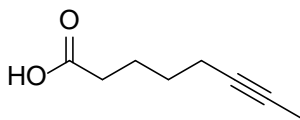
cyclohexyl (*Z*)-oct-2-en-6-ynoate (3.093 + 3.094)



To (*Z*)-oct-2-en-6-ynoic acid (24.2 mg, 0.175 mmol), thionyl chloride (0.63 mL) was added and refluxed for 2 h. After 2 h, the thionyl chloride was evaporated off by *in vacuo* evaporation at 0°C. The residue was dissolved in acetonitrile (2 mL) and then CuO (1.2 mg, 0.015 mmol) and cyclohexanol (14.6 mg, 0.146 mmol) were added dropwise and stirred for 12 h. Flash chromatography, eluting with 1% EtOAc/petroleum spirits yielded the product as a mixture of *cis* and *trans* isomer in 1: 0.33 ratio (18.7 mg, 58%).

¹H NMR (400 MHz, CDCl₃) δ 6.96 (dt, *J* = 15.6, 6.6 Hz, 1H), 6.30 (dt, *J* = 11.5, 7.2 Hz, 0.33H), 5.83 (m, 1.33H), 4.92 – 4.76 (m, 1.33H), 3.08 – 1.06 (m, 22.61H).

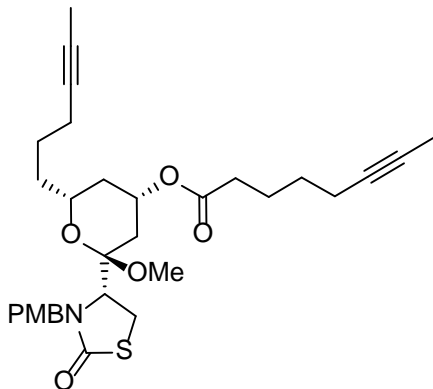
oct-6-ynoic acid (3.095) [13]



To diisopropylamine (0.5 mL, 3.3 mmol) in THF (32 mL) at -78°C, was added *n*-BuLi (3.3 mL, 3.3 mmol) dropwise and stirred for 10 min at -78°C. Then, 6-heptanoic acid (0.2 mL, 1.58 mmol) was added dropwise and stirring continued for 3 h at -78°C. This was followed by addition of *N,N*-dimethyl propylene urea (0.4 mL, 3.2 mmol) and iodomethane (0.15 mL, 2.4 mmol). The reaction mixture was then allowed to slowly warm to 0°C and then to room temperature and stirring was continued for 12 h. The reaction was acidified with 6 M aq. HCl solution and the aqueous layer washed with diethyl ether (x 3). The combined organic layer was dried with sodium sulphate and evaporated to dryness. Flash chromatography, eluting 12% EtOAc/petroleum spirits gave the product (21.1 mg, 10%).

¹H NMR (400 MHz, CDCl₃) δ 2.38 (t, *J* = 7.5 Hz, 2H), 2.16 (ddd, *J* = 9.5, 4.6, 2.6 Hz, 2H), 1.77 (t, *J* = 2.6 Hz, 3H), 1.76 – 1.70 (m, 2H), 1.60 – 1.48 (m, 2H).

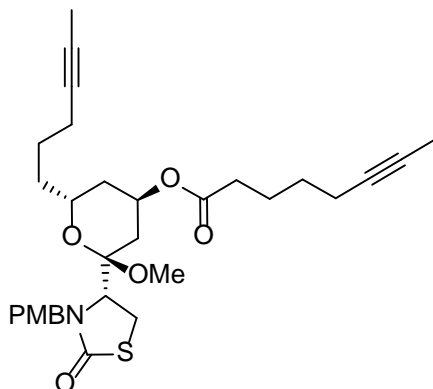
(2*R*,4*S*,6*R*)-6-(hex-4-yn-1-yl)-2-methoxy-2-((*R*)-3-(4-methoxybenzyl)-2-oxothiazolidin-4-yl)tetrahydro-2H-pyran-4-yl oct-6-ynoate (3.100)



Title compound was prepared from (*R*)-4-((2*R*,4*S*,6*R*)-6-(hex-4-yn-1-yl)-4-hydroxy-2-methoxytetrahydro-2H-pyran-2-yl)-3-(4-methoxybenzyl)thiazolidin-2-one (13.7 mg, 0.032 mmol) and the oct-6-ynoic acid (21 mg, 0.09 mmol) according to the General Procedure G as a pale yellow oil (11 mg, 63%).

¹H NMR (400 MHz, CDCl₃) δ 7.22 (m, 2H), 6.91 – 6.83 (m, 2H), 5.21 – 5.10 (m, 2H), 4.24 (d, *J* = 14.4 Hz, 1H), 3.84 (dd, *J* = 8.8, 3.0 Hz, 1H), 3.81 (s, 3H), 3.66 (m, 1H), 3.32 – 3.19 (m, 2H), 3.07 (s, 3H), 2.30 (t, *J* = 7.5 Hz, 2H), 2.26 – 2.11 (m, 5H), 2.09 – 1.99 (m, 1H), 1.77 (dt, *J* = 5.1, 2.5 Hz, 7H), 1.74 – 1.45 (m, 9H); ¹³C NMR (101 MHz, CDCl₃) δ 173.1, 173.1, 159.3, 129.9, 128.8, 114.2, 103.2, 78.8, 78.6, 76.4, 76.0, 69.8, 67.4, 59.0, 55.4, 47.7, 47.4, 37.0, 35.4, 34.2, 33.4, 28.6, 25.4, 25.4, 24.3, 18.9, 18.6, 3.6.

(2*R*,4*R*,6*R*)-6-(hex-4-yn-1-yl)-2-methoxy-2-((*R*)-3-(4-methoxybenzyl)-2-oxothiazolidin-4-yl)tetrahydro-2H-pyran-4-yl oct-6-ynoate (3.101)



Title compound was prepared from (*R*)-4-((2*R*,4*R*,6*R*)-6-(hex-4-yn-1-yl)-4-hydroxy-2-methoxytetrahydro-2H-pyran-2-yl)-3-(4-methoxybenzyl)thiazolidin-2-one (24.7 mg, 0.05 mmol) and the oct-6-ynoic acid (38 mg, 0.17 mmol) according to the General Procedure G as a pale yellow oil (13.1 mg, 47%).

HPLC – rt 9.15 min > 99% purity at 254 nm; LRMS [M+Na]⁺ 578.3 m/z; HRMS [M+H]⁺ 578.2547 m/z, found 578.254 m/z; ¹H NMR (400 MHz, CDCl₃) δ 7.20 (m, 2H), 6.85 (m, 2H), 5.17 – 5.00 (m, 2H), 4.24 (d, *J* = 14.4 Hz, 1H), 3.89 (m, 1H), 3.83 – 3.70 (m, 4H), 3.27 – 3.16 (m, 2H), 3.07 (s, 3H), 2.33 – 1.44 (m, 24H); ¹³C NMR (101 MHz, CDCl₃) δ 173.3, 173.1, 159.3, 129.9, 128.9, 114.2, 101.8, 78.8, 78.6, 76.3, 75.9, 66.4, 66.0, 59.3, 55.4, 47.6, 47.5, 35.4, 34.7, 34.4, 30.0, 28.5, 25.5, 25.3, 24.2, 19.0, 18.6, 3.6, 3.6.

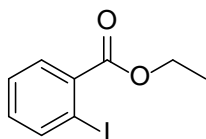
propylmagnesium bromide (3.121)

MgBr To diethyl ether (10 mL), magnesium (267 mg, 11 mmol) and catalytic iodine were added. The reaction mixture was warmed gently before adding 1-bromopropane (0.91 mL, 10 mmol) dropwise. The reaction turned exothermic and was cooled in an ice bath. After the addition of 1-bromopropane was complete, the reaction was stirred for 1 h to obtain the Grignard reagent.

prop-2-yn-1-ylmagnesium bromide (3.128)

MgBr Magnesium (218 mg, 8.9 mmol) and zinc bromide (40.5 mg, 0.18 mmol) were heated under vacuum and then diethyl ether (5 mL) was added. This was followed by dropwise addition of propargyl bromide (0.5 mL, 4.5 mmol) in diethyl ether (4 mL). The reaction turned exothermic and was cooled in an ice bath. After the addition was complete, the reaction was stirred for a further 1 h to obtain the Grignard reagent.

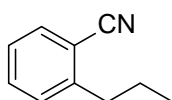
ethyl 2-iodobenzoate (3.116) [14]



2-Iodobenzoic acid (1 g, 4.03 mmol) was treated with thionyl chloride (10 mL) and heated to reflux for 3 h. The reaction mixture was then allowed to cool to room temperature and the solvent evaporated off. The residue was then dissolved in ethanol at 0°C and stirred for 12 h. At the end of the reaction as indicated by TLC analysis, the solvent was evaporated off, washed with 5% aq. potassium carbonate solution, extracted with DCM, dried with magnesium sulphate and evaporated to dryness to obtain the desired product (1 g, 99%).

^1H NMR (400 MHz, CDCl_3) δ 7.98 (dd, $J = 7.9, 0.9$ Hz, 1H), 7.85 – 7.72 (m, 1H), 7.40 (td, $J = 7.6, 1.2$ Hz, 1H), 7.14 (ddd, $J = 7.9, 7.4, 1.7$ Hz, 1H), 4.40 (q, $J = 7.1$ Hz, 2H), 1.41 (t, $J = 7.1$ Hz, 3H).

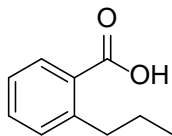
2-propylbenzonitrile (3.122) [15]



2-bromobenzonitrile (50 mg, 0.275 mmol) was dissolved in THF (0.6 mL). Catalytic $\text{Fe}(\text{acac})_3$ (10 mg, 0.028 mmol) was added and the solution cooled to -30°C before propylmagnesium bromide solution (1 M in THF) was added dropwise. The solution was then allowed to stir for 12 h at room temperature before being quenched with saturated ammonium chloride solution. The aqueous layer was washed with diethyl ether (x 3), the combined organic layer dried with sodium sulphate and evaporated to dryness to obtain the product (9.6 mg, 25%).

^1H NMR (400 MHz, CDCl_3) δ 7.60 (dd, $J = 7.7, 1.1$ Hz, 1H), 7.50 (td, $J = 7.7, 1.4$ Hz, 1H), 7.33 – 7.26 (m, 2H), 2.85 – 2.77 (m, 2H), 1.78 – 1.65 (m, 2H), 0.98 (t, $J = 7.3$ Hz, 3H).

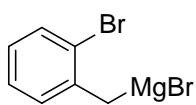
2-propylbenzoic acid (3.125) [16]



To 2-propylbenzonitrile (9.6 mg, 0.07 mmol), water (0.07 mL), concentrated H_2SO_4 (0.18 mL) and glacial acetic acid (0.18 mL) were added and the solution heated to 120°C for 8 h. When the TLC indicated completion of the reaction, the heating was stopped and the solution allowed to cool to room temperature before it was filtered. The solid obtained was washed with 50% aq. NaOH solution and then with 4 M aq. HCl. The solid was then dried to obtain the product (6.9 mg, 63%).

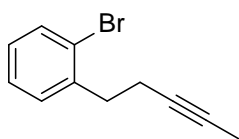
^1H NMR (400 MHz, CDCl_3) δ 7.45 (d, $J = 5.9$ Hz, 1H), 7.42 – 7.34 (m, 1H), 7.24 (m, 2H), 3.08 – 2.68 (m, 2H), 1.64 (m, 2H), 1.03 – 0.78 (m, 3H).

2-bromobenzyl)magnesium bromide (3.132)



1,2 dibromoethane (5 μ L, 0.06 mmol) and magnesium (32.1 mg, 1.32 mmol) were added to diethyl ether (2.4 mL) and stirred for 15 min. This was followed by dropwise addition of 2-bromobenzyl bromide (300 mg, 1.2 mmol) in diethyl ether (1 mL). The reaction mixture was gently heated to initiate the reaction, once initiated the reaction was exothermic and did not require any further heating. The reaction was allowed to stir for 1 h after completion of addition of 2-bromobenzyl bromide to obtain the Grignard reagent.

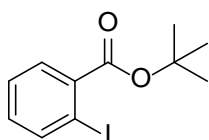
1-bromo-2-(pent-3-yn-1-yl)benzene (3.131)



To 1-bromo-2-butyne (0.052 mL, 0.6 mmol) in diethyl ether (0.6 mL), was added catalytic $\text{Fe}(\text{acac})_3$ (10 mg) and the solution was cooled to -30°C . Freshly prepared 2-bromobenzyl)magnesium bromide solution (0.3 M) was then added dropwise. After addition of the Grignard reagent, the reaction mixture was stirred at room temperature till the completion of the reaction as indicated by the TLC analysis. The reaction was then quenched with saturated ammonium chloride solution and washed with diethyl ether (x 3). The combined organic layer was then dried with sodium sulphate and evaporated to dryness to yield the product as a yellow oil (69 mg, 51%).

LRMS $[\text{M}-\text{H}]^-$ 221.3 m/z; HRMS $[\text{2M}+\text{H}]^+$ 447.0142 m/z, found 447.0142 m/z; ^1H NMR (400 MHz, CDCl_3) δ 7.53 (dd, $J = 7.9, 1.0$ Hz, 1H), 7.30 – 7.21 (m, 2H), 7.08 (ddd, $J = 8.0, 6.9, 2.3$ Hz, 1H), 2.93 (t, $J = 7.6$ Hz, 2H), 2.44 (ddq, $J = 10.0, 5.1, 2.5$ Hz, 2H), 1.78 (t, $J = 2.5$ Hz, 3H); ^{13}C NMR (101 MHz, CDCl_3) δ 140.2, 132.9, 130.8, 128.1, 127.5, 124.5, 78.3, 76.6, 35.9, 19.4, 3.6.

tert-butyl 2-iodobenzoate (3.136) [14]

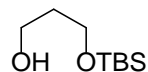


2-iodobenzoic acid (1.5 g, 6 mmol) was treated with thionyl chloride (15 mL) and heated to reflux for 3 h. The reaction mixture was then allowed to cool to room temperature and the solvent evaporated *in vacuo*. The residue was then dissolved in *tert*-butanol (0.6 mL, 6.3 mL) at 0°C and stirred for 12 h. At the end of the reaction as indicated by TLC analysis, the solvent was evaporated off washed with 5% aq. potassium carbonate solution, extracted with DCM, dried with magnesium sulphate and evaporated to dryness to obtain the desired product (1.46 g, 81%).

^1H NMR (400 MHz, CDCl_3) δ 7.94 (dd, $J = 7.9, 0.9$ Hz, 1H), 7.68 (dd, $J = 7.7, 1.6$ Hz, 1H), 7.37 (td, $J = 7.6, 1.2$ Hz, 1H), 7.10 (ddd, $J = 7.9, 7.4, 1.7$ Hz, 1H), 1.62 (s, 9H).

7.4 Chapter 4 compounds

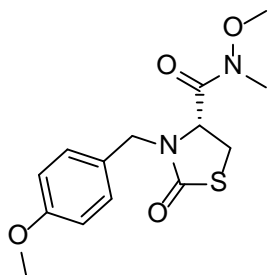
3-((*tert*-butyldimethylsilyl)oxy)propan-1-ol (4.005) [17]



Sodium hydride (524 mg, 21.8 mmol) was suspended in THF (26 mL), to which 1,4-propanediol (1g, 13.1 mmol) was added and stirred for 45 min when a large amount of white precipitate was formed. This was followed by the addition of TBSCl (2g, 13.1 mmol) portion wise. The reaction was allowed to stir for 4 h and then diluted with diethyl ether. The reaction mixture was washed with 10% aq. potassium carbonate solution and brine before being dried with sodium sulphate and evaporated to dryness. Flash chromatography, eluting with 20% EtOAc/petroleum spirits yielded the product as clear oil (910 mg, 36%).

^1H NMR (400 MHz, CDCl_3) δ 3.92 – 3.72 (m, 4H), 1.78 (dt, J = 11.1, 5.6 Hz, 2H), 0.90 (s, 9H), 0.08 (s, 6H).

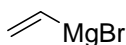
N-methoxy-3-(4-methoxybenzyl)-*N*-methyl-2-oxothiazolidine-4-carboxamide (4.014) [18]



Title compound was prepared from (*R*)-3-(4-methoxybenzyl)-2-oxothiazolidine-4-carboxylic acid (676 mg, 2.53 mmol) according to the General Procedure H as a white sticky oil (676.5 mg, 86%).

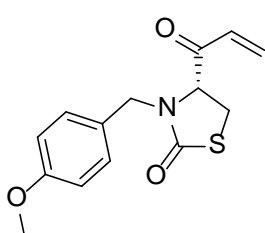
^1H NMR (400 MHz, CDCl_3) δ 7.20 – 7.09 (m, 2H), 6.89 – 6.81 (m, 2H), 5.12 (d, J = 14.7 Hz, 1H), 4.39 (dd, J = 8.8, 5.0 Hz, 1H), 3.83 (d, J = 14.7 Hz, 1H), 3.78 (s, 3H), 3.45 (dd, J = 11.3, 8.8 Hz, 1H), 3.37 (s, 3H), 3.20 (s, 3H), 3.14 (dd, J = 11.3, 5.0 Hz, 1H).

Vinylmagnesium bromide



Magnesium (401 mg, 16.5 mmol) and catalytic iodine were added to THF (10 mL). The reaction mixture was warmed gently before adding vinylbromide (15 mL, 15 mmol) dropwise. The reaction turned exothermic and was cooled in an ice bath. After the addition was complete, the reaction was stirred for 1 h to obtain the Grignard reagent.

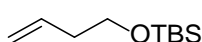
4-acryloyl-3-(4-methoxybenzyl)thiazolidin-2-one (4.012) [18]



To *N*-methoxy-3-(4-methoxybenzyl)-*N*-methyl-2-oxothiazolidine-4-carboxamide (641 mg, 2.06 mmol) in THF (7ml) at 0°C, 1.5 M vinylmagnesium bromide (7.5 mL, 10.3 mmol) was added drop wise and stirred overnight. After completion of the reaction, 2 M aq. HCl was added and then the aqueous layer extracted with DCM (x 3). The combined organic layer was washed with saturated sodium bicarbonate solution, dried with sodium sulphate and evaporated to dryness. Flash chromatography, eluting with a gradient from 10% to 50% EtOAc/petroleum spirits led to the isolation of the product (436 mg, 93%).

¹H NMR (400 MHz, CDCl₃) δ 7.17 – 7.03 (m, 2H), 6.89 – 6.77 (m, 2H), 6.48 (dd, *J* = 17.4, 10.4 Hz, 1H), 6.35 (dd, *J* = 17.4, 1.3 Hz, 1H), 5.90 (dd, *J* = 10.4, 1.3 Hz, 1H), 5.06 (d, *J* = 14.7 Hz, 1H), 4.33 (dd, *J* = 9.4, 4.5 Hz, 1H), 3.82 (d, *J* = 14.8 Hz, 1H), 3.79 (s, 3H), 3.50 (dd, *J* = 11.5, 9.4 Hz, 1H), 3.13 (dd, *J* = 11.5, 4.5 Hz, 1H).

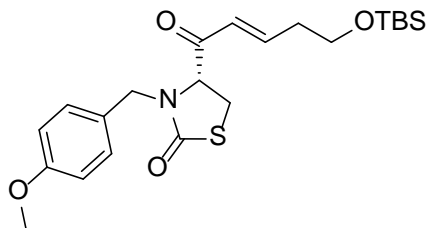
(but-3-en-1-yloxy)(*tert*-butyl)dimethylsilane (4.013) [19]



To 3-buten-1-ol (3ml, 34.9 mmol) in DCM (90 ml), imidazole (4.8 mg, 70 mmol) and TBSCl (5.8 g, 38.3 mmol) was added and stirred for 20 h. On completion of the reaction, water was added to quench the reaction followed by extraction with DCM (x 3). The combined organic layer was washed with ice cold 1 M aq. HCl and then with water (x 3). The organic layer was then dried with sodium sulphate, filtered and evaporated to dryness to yield the product (6.48 g, 99% yield).

¹H NMR (400 MHz, CDCl₃) δ 5.82 (ddt, *J* = 17.1, 10.2, 6.9 Hz, 1H), 5.16 – 4.95 (m, 2H), 3.66 (t, *J* = 6.8 Hz, 2H), 2.27 (qt, *J* = 6.8, 1.3 Hz, 2H), 0.89 (s, 9H), 0.05 (s, 6H).

(*E*)-4-(5-((*tert*-butyldimethylsilyl)oxy)pent-2-enoyl)-3-(4-methoxybenzyl)thiazolidin-2-one (4.007)

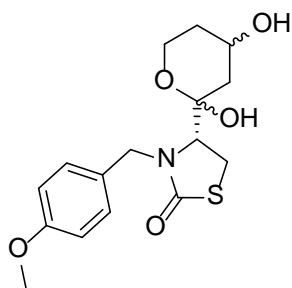


To 4-acryloyl-3-(4-methoxybenzyl)thiazolidin-2-one (661 mg, 2.9 mmol) dissolved in DCE (16 mL) was added (but-3-en-1-yloxy)(*tert*-butyl)dimethylsilane (1.1 g, 5.8 mmol) and catalytic Hoveyda-Grubbs' II catalyst (91 mg, 0.145 mmol). The reaction was then heated to 50°C for 12 h. Upon completion of the reaction, as indicated by TLC analysis, the reaction mixture was filtered through

celite to remove the catalyst and then subjected to flash chromatography, eluting with 10% EtOAc/petroleum spirits to obtain the product (693 mg, 53%).

HPLC – rt 4.03 min > 99% purity at 254 nm; LRMS $[M+H]^+$ no mass ion was detected; HRMS $[M+H]^+$ 436.1972 m/z, found 436.1980 m/z; 1H NMR (400 MHz, $CDCl_3$) δ 7.10 (d, J = 8.6 Hz, 2H), 7.00 (dt, J = 15.7, 7.0 Hz, 1H), 6.83 (d, J = 8.7 Hz, 2H), 6.25 (dt, J = 15.7, 1.4 Hz, 1H), 5.05 (d, J = 14.8 Hz, 1H), 4.27 (dd, J = 9.3, 4.6 Hz, 1H), 3.81 (d, 1H), 3.78 (s, 3H), 3.72 (t, J = 6.1 Hz, 2H), 3.46 (dd, J = 11.4, 9.4 Hz, 1H), 3.11 (dd, J = 11.4, 4.6 Hz, 1H), 2.48 – 2.34 (m, J = 6.3, 1.4 Hz, 2H), 0.87 (s, 9H), 0.04 (s, 6H); ^{13}C NMR (101 MHz, $CDCl_3$) δ 194.8, 172.1, 159.5, 148.7, 130.1, 127.5, 126.3, 114.3, 63.9, 61.2, 55.4, 47.3, 36.3, 28.0, 25.9, 18.3, -5.3.

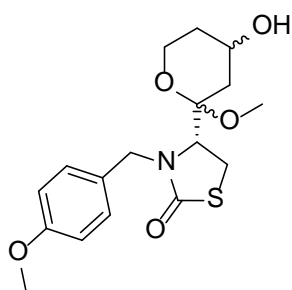
4-(2,4-dihydroxytetrahydro-2H-pyran-2-yl)-3-(4-methoxybenzyl)thiazolidin-2-one (4.008)



Title compound was prepared from

(*E*)-4-(5-((*tert*-butyldimethylsilyl)oxy)pent-2-enoyl)-3-(4-methoxybenzyl)thiazolidin-2-one (1.72 mg, 3.95 mmol) according to the General Procedure E as clear oil (1.14 g, 85%). Due to the unstable nature of this compound it was immediately used for the next step.

4-(4-hydroxy-2-methoxytetrahydro-2H-pyran-2-yl)-3-(4-methoxybenzyl)thiazolidin-2-one (4.009)

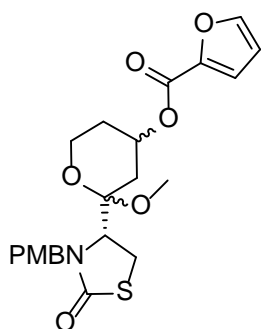


Title compound was prepared from 4-(2,4-dihydroxytetrahydro-2H-pyran-2-yl)-3-(4-methoxybenzyl)thiazolidin-2-one (1.14 g, 3.36 mmol) according to the General Procedure F as clear oil as a mixture of two diastereomers; A and B in 1:1 ratio respectively (826 mg, 69%).

HPLC – rt 5.96 min > 98% purity at 254 nm; LRMS (only mass ion for the fragment obtained after elimination of water and methanol was observed) $[M-(H_2O + MeOH)]^+$ 304.1 m/z; HRMS $[M+H]^+$ 354.137 m/z, found 354.1355 m/z; 1H NMR (**diastereomer A**) (400 MHz, $CDCl_3$) δ 7.23 (m, 2H), 6.91 – 6.82 (m, 2H), 5.20 (d, J = 15.4 Hz, 1H), δ 4.28 (d, J = 14.4 Hz, 1H), 4.11 – 3.99 (m, 1H), 3.97 – 3.91 (m, 1H), 3.86 – 3.81 (m, 1H), 3.79 (d, J = 1.7 Hz, 3H), 3.66 – 3.57 (m, 1H), 3.39 – 3.30 (m, 1H), 3.29 – 3.18 (m, 1H), 3.08 (s, 3H), 2.20 (ddd, J = 12.6, 4.6, 1.8 Hz, 1H), 1.98 – 1.88 (m, 1H), 1.67 (m, 1H), 1.54 – 1.38 (m, 1H); 1H NMR (**diastereomer B**) (400 MHz, $CDCl_3$) 7.14 (m, J = 8.5 Hz, 2H), 6.91 – 6.82 (m, 2H), 5.02 (d, J = 14.3 Hz, 1H), 4.20 (d, J = 15.5 Hz, 1H), 4.11 – 3.99 (m, 1H), 3.88 (m, 1H), 3.86 – 3.81

(m, 1H), 3.79 (d, $J = 1.7$ Hz, 3H), 3.57 – 3.48 (m, 1H), 3.39 – 3.30 (m, 1H), 3.29 – 3.18 (m, 1H), 3.01 (s, 3H), 2.10 (ddd, $J = 12.8, 4.7, 1.8$ Hz, 1H), 1.98 – 1.88 (m, 1H), 1.55 – 1.48 (m, 1H), 1.54 – 1.38 (m, 1H); ^{13}C NMR (101 MHz, CDCl_3) δ 159.2, 130.2, 129.0, 128.6, 114.3, 114.1, 103.3, 64.5, 60.5, 60.3, 59.3, 56.9, 55.4, 47.8, 47.6, 47.5, 46.8, 38.0, 37.35, 34.8, 34.5, 26.2, 25.4.

2-methoxy-2-((*R*)-3-(4-methoxybenzyl)-2-oxothiazolidin-4-yl)tetrahydro-2H-pyran-4-yl furan-2-carboxylate (4.020)

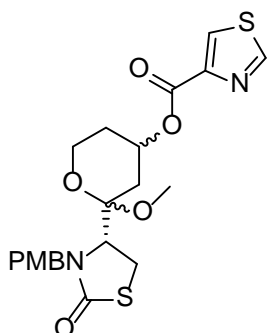


Title compound was prepared from

4-(4-hydroxy-2-methoxytetrahydro-2H-pyran-2-yl)-3-(4-methoxybenzyl)thiazolidin-2-one (40 mg, 0.113 mmol) and 2-furoic acid (38 mg, 0.34 mmol) according to the General Procedure G as a white semisolid and a mixture of two diastereomers; A and B in 1:0.65 ratio respectively (50.2 mg, 98%).

HPLC – rt 7.80 min > 94% purity at 254 nm; LRMS no mass ion was detected; HRMS $[\text{M}+\text{H}]^+$ 448.1424 m/z , found 448.1424 m/z ; ^1H NMR (**diastereomer A**) (400 MHz, CDCl_3) δ 7.58 (m, 1H), 7.23 (m, 2H), 7.20 – 7.16 (m, 1H), 6.90 – 6.82 (m, 2H), 6.51 (m, 1H), 5.37 (m, 1H), 5.07 (d, $J = 14.4$ Hz, 1H), 4.29 (d, $J = 14.4$ Hz, 1H), 4.01 – 3.89 (m, 1H), 3.89 – 3.81 (m, 1H), 3.79 (s, 3H), 3.77 – 3.69 (m, 1H), 3.42 – 3.35 (m, 1H), 3.32 – 3.18 (m, 1H), 3.12 (s, 3H), 2.30 (ddd, $J = 12.5, 4.8, 1.9$ Hz, 1H), 2.10 (m, 1H), 1.80 (dd, $J = 12.4, 11.5$ Hz, 1H), 1.76 – 1.60 (m, 1H); ^1H NMR (**diastereomer B**) (400 MHz, CDCl_3) δ 7.58 (m, 1H), 7.20 – 7.16 (m, 1H), 7.17 – 7.11 (m, 2H), 6.90 – 6.82 (m, 2H), 6.51 (m, 1H), 5.37 (m, 1H), 5.21 (d, $J = 15.5$ Hz, 1H), 4.20 (d, $J = 15.5$ Hz, 1H), 4.01 – 3.89 (m, 1H), 3.89 – 3.81 (m, 1H), 3.80 (s, 3H), 3.69 – 3.58 (m, 1H), 3.32 – 3.18 (m, 2H), 3.04 (s, 3H), 2.20 (ddd, $J = 12.7, 4.9, 1.9$ Hz, 1H), 2.10 (m, 1H), 1.94 (dd, $J = 12.7, 11.3$ Hz, 1H), 1.76 – 1.60 (m, 1H); ^{13}C NMR (101 MHz, CDCl_3) δ 173.3, 159.3, 158.2, 146.6, 144.7, 130.2, 128.9, 128.6, 118.4, 118.3, 114.3, 114.1, 112.0, 103.3, 102.5, 68.1, 68.0, 60.1, 59.9, 59.2, 56.8, 55.4, 47.8, 47.7, 47.5, 46.8, 34.3, 33.7, 31.3, 26.2, 25.3.

2-methoxy-2-(3-(4-methoxybenzyl)-2-oxothiazolidin-4-yl)tetrahydro-2H-pyran-4-yl thiazole-4-carboxylate (4.021)

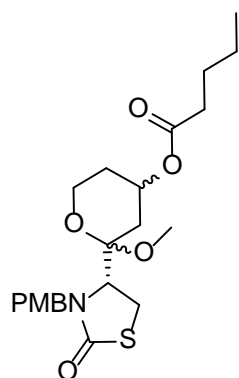


Title compound was prepared from

4-(4-hydroxy-2-methoxytetrahydro-2H-pyran-2-yl)-3-(4-methoxybenzyl)thiazolidin-2-one (50 mg, 0.14 mmol) and 4-thiazolecarboxylic acid (54 mg, 0.42 mmol) according to the General Procedure G as a white solid and a mixture of two diastereomers; A and B in 1:0.5 ratio respectively (36 mg, 55%).

HPLC – rt 7.10 min > 99% purity at 254 nm; LRMS $[M+H]^+$ 465.1 m/z; HRMS $[M+H]^+$ 465.1149 m/z, found 465.1158 m/z; 1H NMR (**diastereomer A**) (400 MHz, $CDCl_3$) δ 8.84 (m, 1H), 8.25 (m, 1H), 7.22 (m, 2H), 6.89 – 6.80 (m, 2H), 5.44 (m, 1H), 5.06 (d, $J = 14.4$ Hz, 1H), 4.27 (d, $J = 14.4$ Hz, 1H), 4.01 – 3.90 (m, 1H), 3.85 (m, 1H), 3.78 (s, 3H), 3.76 – 3.70 (m, 1H), 3.41 – 3.33 (m, 1H), 3.31 – 3.19 (m, 1H), 3.12 (s, 3H), 2.34 (ddd, $J = 12.4, 4.8, 1.8$ Hz, 1H), 2.19 – 2.06 (m, 1H), 1.91 – 1.82 (m, 1H), 1.73 (m, 1H); 1H NMR (**diastereomer B**) (400 MHz, $CDCl_3$) δ 8.84 (m, 1H), 8.25 (m, 1H), 7.13 (m, 2H), 6.89 – 6.80 (m, 2H), 5.44 (m, 1H), 5.20 (d, $J = 15.5$ Hz, 1H), 4.20 (d, $J = 15.5$ Hz, 1H), 4.01 – 3.90 (m, 1H), 3.85 (m, 1H), 3.78 (s, 3H), 3.70 – 3.59 (m, 1H), 3.31 – 3.19 (m, 2H), 3.04 (s, 3H), 2.24 (ddd, $J = 12.7, 4.8, 1.7$ Hz, 1H), 2.19 – 2.06 (m, 1H), 1.99 (dd, $J = 12.6, 11.4$ Hz, 1H), 1.73 (m, 1H); ^{13}C NMR (101 MHz, $CDCl_3$) δ 173.2, 172.8, 160.6, 160.5, 159.2, 159.1, 153.6, 147.9, 130.2, 128.8, 128.5, 127.8, 127.7, 114.2, 114.1, 103.3, 102.3, 68.5, 60.0, 59.8, 59.1, 56.7, 55.4, 55.3, 47.7, 47.6, 47.4, 46.7, 34.2, 33.6, 31.1, 31.1, 26.1, 25.2.

2-methoxy-2-((R)-3-(4-methoxybenzyl)-2-oxothiazolidin-4-yl)tetrahydro-2H-pyran-4-yl pentanoate (4.018)

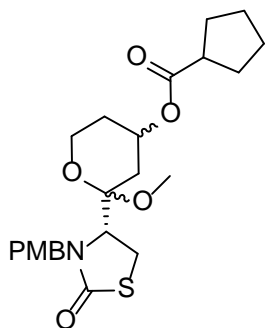


Title compound was prepared from 4-(4-hydroxy-2-methoxytetrahydro-2H-pyran-2-yl)-3-(4-methoxybenzyl)thiazolidin-2-one (40 mg, 0.113 mmol) and valeric acid (37 μ L, 0.34 mmol) according to the General Procedure G as a clear oil and a mixture of two diastereomers; A and B in 1:0.6 ratio respectively (40.4 mg, 82%).

HPLC – rt 8.62 min > 99% purity at 254 nm; LRMS $[M+Na]^+$ 460.2 m/z; HRMS $[M+H]^+$ 438.1945 m/z, found 438.1950 m/z; 1H NMR (**diastereomers A**) (400 MHz, $CDCl_3$) δ 7.25 – 7.19 (m, 2H), 6.90 – 6.82 (m, 2H), 5.14 (m, 1H), 5.05 (d, $J = 14.4$ Hz, 1H), 4.28 (d, $J = 14.4$ Hz, 1H), 3.99 – 3.86 (m, 1H), 3.84 (m, 1H), 3.80 (s, 3H), 3.68 (m, 1H), 3.37 (m, 1H), 3.25 (m, 1H), 3.10 (s, 3H), 2.34 – 2.25 (m, 2H), 2.19 (ddd, $J =$

12.5, 4.8, 1.9 Hz, 1H), 1.98 (m, 1H), 1.69 – 1.46 (m, 4H), 1.35 (m, 2H), 0.96 – 0.88 (m, 3H); ¹H NMR (**diastereomers B**) (400 MHz, CDCl₃) δ 7.14 (m, 2H), 6.90 – 6.82 (m, 2H), 5.21 (d, *J* = 15.4 Hz, 1H), 5.14 (m, 1H), 4.20 (d, *J* = 15.5 Hz, 1H), 3.99 – 3.86 (m, 1H), 3.84 (m, 1H), 3.80 (s, 3H), 3.64 – 3.55 (m, 1H), 3.25 (m, 2H), 3.02 (s, 3H), 2.34 – 2.25 (m, 2H), 2.09 (ddd, *J* = 12.8, 4.9, 1.9 Hz, 1H), 1.98 (m, 1H), 1.80 (dd, *J* = 12.7, 11.3 Hz, 1H), 1.69 – 1.46 (m, 3H), 1.35 (m, 2H), 0.96 – 0.88 (m, 3H); ¹³C NMR (101 MHz, CDCl₃) δ 173.4, 173.0, 159.2, 159.2, 130.2, 128.9, 128.6, 128.6, 114.3, 114.1, 103.2, 102.4, 67.0, 67.0, 60.1, 59.9, 59.2, 56.7, 55.4, 55.4, 47.7, 47.6, 47.5, 46.8, 34.4, 34.4, 34.3, 33.7, 31.2, 27.2, 26.2, 25.3, 22.4, 22.4, 13.9.

2-methoxy-2-((*R*)-3-(4-methoxybenzyl)-2-oxothiazolidin-4-yl)tetrahydro-2H-pyran-4-yl cyclopentanecarboxylate (4.019)

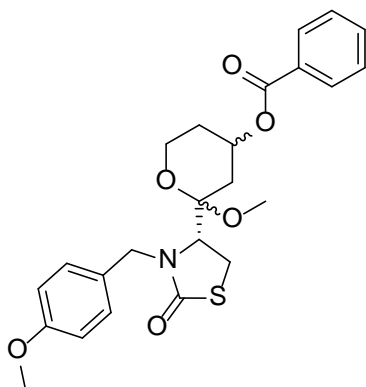


Title compound was prepared from

4-(4-hydroxy-2-methoxytetrahydro-2H-pyran-2-yl)-3-(4-methoxybenzyl)thiazolidin-2-one (41 mg, 0.116 mmol) and cyclopentane carboxylic acid (38 μL, 0.35 mmol) according to the General Procedure G as a clear oil and a mixture of two diastereomers; A and B in 1:0.74 ratio respectively (20 mg, 38%).

HPLC – rt (diastereomer A) 9.268 min (55%), (diastereomer B) 9.297 min (45%), collectively > 99% purity at 254 nm; LRMS no mass ion was detected; HRMS [M+H]⁺ 450.1945 m/z, found 450.1950 m/z; ¹H NMR (**diastereomers A**) (400 MHz, CDCl₃) δ 7.25 – 7.19 (m, 2H), 6.89 – 6.82 (m, 2H), 5.17 – 5.07 (m, 1H), 5.04 (d, *J* = 14.4 Hz, 1H), 4.28 (d, *J* = 14.4 Hz, 1H), 3.91 – 3.81 (m, 2H), 3.80 (s, 3H), 3.68 (m, 1H), 3.36 – 3.24 (m, 2H), 3.10 (s, 3H), 2.76 – 2.61 (m, 1H), 2.21 – 2.13 (m, 1H), 1.97 (m, 1H), 1.92 – 1.44 (m, 10H); ¹H NMR (**diastereomers B**) (400 MHz, CDCl₃) δ 7.13 (m, 2H), 6.89 – 6.82 (m, 2H), 5.21 (d, *J* = 15.5 Hz, 1H), 5.17 – 5.07 (m, 1H), 4.20 (d, *J* = 15.5 Hz, 1H), 3.95 (m, 1H), 3.91 – 3.81 (m, 1H), 3.79 (s, 3H), 3.63 – 3.54 (m, 1H), 3.36 – 3.24 (m, 2H), 3.02 (s, 3H), 2.76 – 2.61 (m, 1H), 2.07 (ddd, *J* = 12.8, 4.8, 1.8 Hz, 1H), 1.97 (m, 1H), 1.92 – 1.44 (m, 10H); ¹³C NMR (101 MHz, CDCl₃) δ 176.3, 176.2, 173.4, 173.1, 159.2, 159.2, 130.2, 129.0, 128.6, 128.6, 114.3, 114.1, 103.3, 102.5, 66.9, 66.9, 60.1, 60.0, 59.3, 56.8, 55.4, 47.7, 47.6, 47.5, 46.8, 44.0, 34.2, 33.6, 31.2, 30.2, 30.1, 30.1, 26.2, 26.0, 25.3.

2-methoxy-2-(3-(4-methoxybenzyl)-2-oxothiazolidin-4-yl)tetrahydro-2H-pyran-4-yl benzoate (4.022)

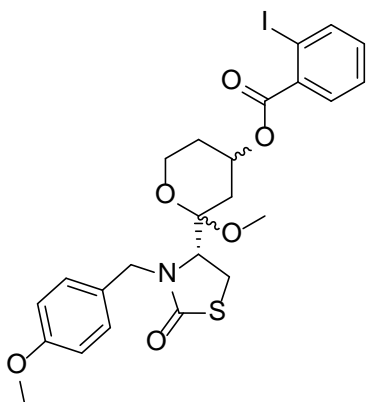


Title compound was prepared from

4-(4-hydroxy-2-methoxytetrahydro-2H-pyran-2-yl)-3-(4-methoxybenzyl)thiazolidin-2-one (52.7 mg, 0.15 mmol) and benzoic acid (55 mg, 0.45 mmol) according to the General Procedure G as a white semisolid as a mixture of two diastereomers; A and B in 1: 0.8 ratio respectively (41 mg, 59%).

HPLC – rt 8.3 min > 99% purity at 254 nm; LRMS no mass ion was detected; HRMS $[M+H]^+$ 458.1632 m/z, found 458.1646 m/z; 1H NMR (**diastereomer A**) (400 MHz, $CDCl_3$) δ 8.04 (m, 2H), 7.57 (t, $J = 7.4$ Hz, 1H), 7.45 (t, $J = 7.7$ Hz, 2H), 7.25 (m, 2H), 6.91 – 6.83 (m, 2H), 5.47 – 5.32 (m, 1H), 5.08 (d, $J = 14.4$ Hz, 1H), 4.32 (d, $J = 14.4$ Hz, 1H), 3.90 – 3.82 (m, 2H), 3.81 (s, 3H), 3.79 – 3.72 (m, 1H), 3.43 – 3.38 (m, 1H), 3.32 – 3.24 (m, 1H), 3.14 (s, 3H), 2.33 (ddd, $J = 12.4, 4.7, 1.8$ Hz, 1H), 2.17 – 2.08 (m, 1H), 1.87 – 1.77 (m, 1H), 1.69 – 1.61 (m, 1H); 1H NMR (**diastereomer B**) (400 MHz, $CDCl_3$) δ 8.04 (m, 2H), 7.57 (t, $J = 7.4$ Hz, 1H), 7.45 (t, $J = 7.7$ Hz, 2H), 7.15 (m, 2H), 6.94 – 6.80 (m, 2H), 5.49 – 5.32 (m, 1H), 5.23 (d, $J = 15.5$ Hz, 1H), 4.22 (d, $J = 15.5$ Hz, 1H), 3.97 (m, 2H), 3.80 (s, 3H), 3.72 – 3.62 (m, 1H), 3.33 – 3.21 (m, 2H), 3.06 (s, 3H), 2.24 (ddd, $J = 12.7, 4.8, 1.7$ Hz, 1H), 2.16 – 2.07 (m, 1H), 1.96 (dd, $J = 12.6, 11.3$ Hz, 1H), 1.74 (m, 1H); ^{13}C NMR (101 MHz, $CDCl_3$) δ 173.3, 173.1, 166.0, 166.0, 159.3, 159.2, 133.2, 130.2, 129.8, 129.8, 128.9, 128.6, 128.6, 128.5, 114.3, 114.1, 103.3, 102.5, 68.0, 67.8, 60.1, 59.9, 59.3, 56.8, 55.4, 47.8, 47.7, 47.6, 46.8, 34.3, 33.7, 31.3, 27.0, 26.2, 25.3.

2-methoxy-2-(3-(4-methoxybenzyl)-2-oxothiazolidin-4-yl)tetrahydro-2H-pyran-4-yl 2-iodobenzoate (4.023)



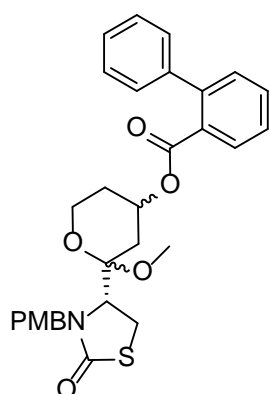
Title compound was prepared from

4-(4-hydroxy-2-methoxytetrahydro-2H-pyran-2-yl)-3-(4-methoxybenzyl)thiazolidin-2-one (151 mg, 0.43 mmol) and 2-iodobenzoic acid (318 mg, 1.28 mmol) according to the General Procedure G as a white semisolid and a mixture of two diastereomers; A and B in 1:0.9 ratio respectively (151 mg, 60%).

HPLC – rt 9.43 min > 91% purity at 254 nm; LRMS no mass ion was detected; HRMS $[M+H]^+$ 584.0598 m/z, found 584.0594 m/z; 1H NMR (**diastereomer A**) (400 MHz, $CDCl_3$) δ 7.99 (d, $J = 8.0$ Hz, 1H), 7.79 (ddd, $J = 7.8, 3.7, 1.7$ Hz, 1H), 7.42 (td, $J = 7.5, 0.9$

Hz, 1H), 7.24 (m, 1H), 7.19 – 7.12 (m, 2H), 6.87 (dd, $J = 8.8, 2.8$ Hz, 2H), 5.49 – 5.38 (m, 1H), 5.05 (d, $J = 14.3$ Hz, 1H), 4.32 (d, $J = 14.4$ Hz, 1H), 4.00–3.92 (m, 1H), 3.91 – 3.82 (m, 1H), 3.81 (s, 3H), 3.79 – 3.71 (m, 1H), 3.44 – 3.37 (m, 1H), 3.28 (m, 1H), 3.14 (s, 3H), 2.38 (ddd, $J = 12.4, 4.8, 1.9$ Hz, 1H), 2.23 – 2.11 (m, 1H), 1.87 – 1.79 (dd, $J = 12.3, 11.5$ Hz, 1H), 1.71 – 1.64 (m, 1H). ^1H NMR (**diastereomer B**) (400 MHz, CDCl_3) δ 7.99 (d, $J = 8.0$ Hz, 1H), 7.79 (ddd, $J = 7.8, 3.7, 1.7$ Hz, 1H), 7.42 (td, $J = 7.5, 0.9$ Hz, 1H), 7.26 – 7.21 (m, 1H), 7.19 – 7.11 (m, 2H), 6.87 (m, $J = 8.8, 2.8$ Hz, 2H), 5.52 – 5.34 (m, 1H), 5.23 (d, $J = 15.5$ Hz, 1H), 4.23 (d, $J = 15.5$ Hz, 1H), 4.03 – 3.90 (m, 1H), 3.91 – 3.82 (m, 1H), 3.80 (s, 3H), 3.71 – 3.62 (m, 1H), 3.28 (m, 2H), 3.06 (s, 3H), 2.27 (ddd, $J = 12.8, 5.1, 1.9$ Hz, 1H), 2.17 (m, 1H), 1.99 (dd, $J = 12.7, 11.3$ Hz, 1H), 1.79 – 1.71 (m, 1H); ^{13}C NMR (101 MHz, CDCl_3) δ 173.2, 172.9, 165.9, 165.8, 159.1, 159.1, 141.3, 141.3, 135.1, 134.9, 132.7, 132.7, 131.0, 130.9, 130.1, 130.1, 128.8, 128.5, 128.5, 128.0, 114.2, 114.0, 103.1, 102.4, 94.1, 94.0, 69.0, 68.9, 59.9, 59.8, 59.3, 56.7, 55.3, 55.3, 47.7, 47.6, 47.6, 46.7, 34.1, 33.6, 31.1, 31.0, 26.1, 25.3.

2-methoxy-2-((R)-3-(4-methoxybenzyl)-2-oxothiazolidin-4-yl)tetrahydro-2H-pyran-4-yl [1,1'-biphenyl]-2-carboxylate (4.045)

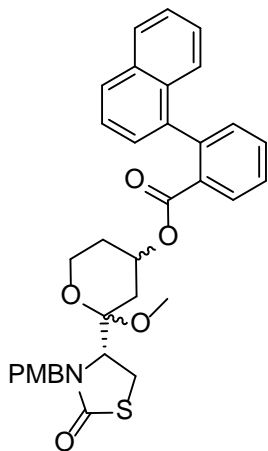


Title compound was prepared from

4-(4-hydroxy-2-methoxytetrahydro-2H-pyran-2-yl)-3-(4-methoxybenzyl)thiazolidin-2-one (30 mg, 0.085 mmol) and [1,1'-biphenyl]-2-carboxylic acid (50.5 mg, 0.25 mmol) according to the General Procedure G as a white solid and a mixture of two diastereomers; A and B in 1: 0.5 ratio respectively (24 mg, 53%).

HPLC – rt 9.09 min > 88% purity at 254 nm; LRMS $[\text{M}+\text{Na}]^+$ 556.2 m/z; HRMS $[\text{M}+\text{H}]^+$ 534.1945 m/z, found 534.1959 m/z; ^1H NMR (400 MHz, CDCl_3) δ 7.86 – 7.81 (m, 1.5H), 7.57 – 7.49 (m, 1.5H), 7.46 – 7.34 (m, 10.5H), 7.29 (m, 2H), 7.20 (m, 1H), 7.13 (m, 3H), 6.90 – 6.81 (d, $J = 15.5, 0.5$ Hz, 0.5H), 5.22 (m, 1.5H), 5.16 – 5.04 (d, $J = 14.4$, 1H), 5.00 – 4.15 (m, 1.5H), 4.16 (dd, $J = 9.6, 3.5, 0.5$ Hz, 0.5H), 3.89 – 3.66 (m, 7H), 3.63 – 3.55 (m, 1H), 3.54 – 3.45 (m, 0.5H), 3.34 – 3.11 (m, 3H), 3.06 (s, 3H), 2.96 (s, 1.5H), 1.92 (ddd, $J = 12.6, 4.7, 1.7$ Hz, 1H), 1.73 (m, 2H), 1.38 – 1.12 (m, 3H); ^{13}C NMR (101 MHz, CDCl_3) δ 173.2, 172.8, 168.3, 168.2, 159.2, 159.1, 143.2, 142.8, 142.7, 141.7, 141.2, 131.9, 131.4, 131.2, 131.1, 130.7, 130.6, 130.2, 130.1, 130.0, 129.9, 128.9, 128.6, 128.6, 128.5, 128.5, 128.2, 128.2, 127.6, 127.5, 127.4, 127.3, 127.3, 114.3, 114.0, 103.0, 102.3, 67.9, 59.9, 59.8, 59.2, 56.6, 55.4, 55.4, 47.6, 47.6, 47.4, 46.7, 33.3, 32.9, 30.6, 30.6, 26.1, 25.1.

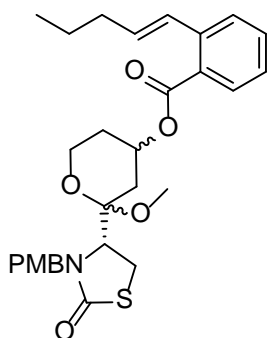
2-methoxy-2-((R)-3-(4-methoxybenzyl)-2-oxothiazolidin-4-yl)tetrahydro-2H-pyran-4-yl 2-(naphthalen-1-yl)benzoate (4.041)



Title compound was prepared from 2-methoxy-2-(3-(4-methoxybenzyl)-2-oxothiazolidin-4-yl)tetrahydro-2H-pyran-4-yl 2-iodobenzoate (53.4 mg, 0.09 mmol) and 1-naphthaleinboronic acid (19 mg, 0.11 mmol) according to General Procedure I as a mixture of three diastereomers; A, B and C in 1: 0.7 : 0.5 ratios respectively (53.1 mg, 90%).

HPLC– rt 3.98 min, 4.12 min, and 4.17 min for the 3 diastereomers > 98% combined purity at 254 nm; LRMS $[M+Na]^+$ 606.2 m/z; HRMS $[M+Na]^+$ 606.1921 m/z, found 606.1935 m/z; 1H NMR (400 MHz, $CDCl_3$) δ 8.15 – 6.80 (m, 33H), 5.14 (dd, J = 15.4, 5.4 Hz, 1H), 5.04 (d, J = 14.4 Hz, 0.7H), 4.98 (d, J = 14.4 Hz, 0.5H), 4.91 – 4.69 (m, 2.2H), 4.08 – 2.77 (m, 26.4H), 1.65 – 0.54 (m, 8.8H); ^{13}C NMR (101 MHz, $CDCl_3$) δ 173.4, 172.9, 172.7, 167.2, 167.1, 167.0, 159.2, 159.13, 141.6, 141.4, 141.3, 141.3, 140.2, 133.3, 133.3, 132.6, 132.5, 132.1, 132.0, 131.9, 131.8, 130.9, 130.8, 130.6, 130.5, 130.4, 130.2, 130.2, 130.1, 130.0, 129.3, 128.9, 128.9, 128.6, 128.5, 128.4, 128.3, 127.9, 127.8, 126.3, 126.1, 126.0, 125.9, 125.8, 125.7, 125.6, 125.3, 125.1, 114.7, 114.5, 114.4, 114.3, 114.2, 114.1, 114.0, 102.8, 102.7, 102.2, 102.1, 67.4, 67.4, 67.3, 59.7, 59.6, 59.2, 59.0, 56.7, 55.4, 47.6, 47.5, 47.3, 47.2, 46.7, 32.9, 32.5, 32.3, 30.4, 29.9, 29.7, 27.1, 26.1, 24.9, 24.9.

2-methoxy-2-((R)-3-(4-methoxybenzyl)-2-oxothiazolidin-4-yl)tetrahydro-2H-pyran-4-yl 2-(E-pent-1-en-1-yl)benzoate (4.042)

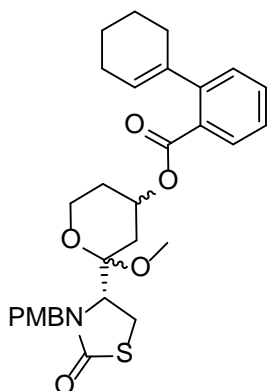


Title compound was prepared from 2-methoxy-2-(3-(4-methoxybenzyl)-2-oxothiazolidin-4-yl)tetrahydro-2H-pyran-4-yl 2-iodobenzoate (15.1 mg, 0.026 mmol) and (*E*)-1-pentenylboronic acid pinacol ester (7 μ L, 0.031 mmol) according to General Procedure I as a mixture of three diastereomers; A and B in 1: 0.7 ratios respectively (7.8 mg, 57%).

LRMS $[M+H]^+$ 526.2 m/z; HRMS $[M+H]^+$ 526.2258 m/z, found 526.2264 m/z; 1H NMR (400 MHz, $CDCl_3$) δ 7.83 (m, 1.7H), 7.53 (m, 1.7H), 7.44 (m, 1.7H), 7.29 – 7.21 (m, 4.1H), 7.13 (m, 2.7H), 6.91 – 6.80 (m, 3.4H), 6.13 (m, 1.7H), 5.46 – 5.32 (m, 1.7H), 5.23 (d, J = 15.5 Hz, 0.7H), 5.07 (d, J = 14.3 Hz, 1H), 4.31 (d, J = 14.4 Hz, 1H), 4.23 (d, J = 15.5 Hz, 0.7H), 4.02 – 3.91 (m, 1.7H), 3.90 – 3.82 (m, 1.7H), 3.80 (m, 5.1H), 3.80 – 3.71 (m, 1H), 3.71 – 3.62 (m, 0.7H), 3.43 – 3.21 (m, 3.4H), 3.14 (s, 3H), 3.06 (s, 2.1H), 2.35 (ddd, J = 12.5, 4.7, 1.9 Hz, 1H), 2.28 – 2.19 (m, 4.1H), 2.19 – 2.07 (m, 1.7H), 1.95 (dd, J = 12.6, 11.3 Hz, 0.7H), 1.80 (dd, J = 12.3, 11.5 Hz, 1H), 1.76 – 1.63 (m, 1.7H), 1.53 (m, 3.4H), 0.97 (m, 5.1H); ^{13}C NMR (101 MHz, $CDCl_3$) δ

167.3, 162.5, 153.5, 140.0, 134.0, 132.2, 131.9, 130.2, 128.7, 128.6, 127.4, 126.7, 121.0, 114.3, 114.1, 89.6, 67.9, 60.0, 59.3, 55.4, 47.8, 47.7, 47.6, 35.4, 31.4, 31.1, 26.2, 25.4, 22.6, 14.0.

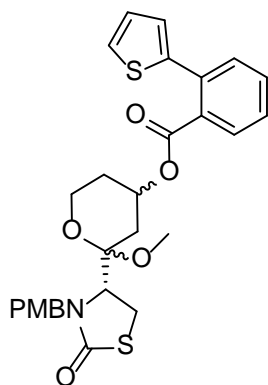
2-methoxy-2-((*R*)-3-(4-methoxybenzyl)-2-oxothiazolidin-4-yl)tetrahydro-2H-pyran-4-yl 2',3',4',5'-tetrahydro-[1,1'-biphenyl]-2-carboxylate (4.043)



Title compound was prepared from 2-methoxy-2-(3-(4-methoxybenzyl)-2-oxothiazolidin-4-yl)tetrahydro-2H-pyran-4-yl 2-iodobenzoate (43.8 mg, 0.075 mmol) and cyclohexene-1-boronic acid pinacol ester (19.6 μ L, 0.09 mmol) according to General Procedure I as a mixture of two diastereomers; A and B in 1:1 ratio respectively (34.6 mg, 85%).

HPLC – rt (diastereomer A) 9.73 min (61%), (diastereomer B) 9.69 min (39%), collectively > 99% purity at 254 nm; LRMS $[M+Na]^+$ 560.3 m/z; HRMS $[M+H]^+$ 538.2258 m/z, found 538.2265 m/z; 1H NMR (400 MHz, $CDCl_3$) δ 7.75 – 7.67 (m, 2H), 7.41 (m, 2H), 7.31 – 7.22 (m, 4H), 7.17 (m, 4H), 6.91 – 6.81 (m, 4H), 5.53 (m, 2H), 5.34 (m, 2H), 5.22 (d, J = 15.5 Hz, 1H), 5.06 (d, J = 14.3 Hz, 1H), 4.30 (d, J = 14.4 Hz, 1H), 4.22 (d, J = 15.5 Hz, 1H), 3.95 (m, 2H), 3.89 – 3.82 (m, 2H), 3.80 (s, 6H), 3.78 – 3.70 (m, 1H), 3.70 – 3.60 (m, 1H), 3.38 (m, 2H), 3.27 (m, 2H), 3.13 (s, 3H), 3.05 (s, 3H), 2.35 – 2.20 (m, 6H), 2.20 – 2.06 (m, 6H), 1.97 – 1.85 (m, 1H), 1.77 (m, 5H), 1.73 – 1.58 (m, 6H); ^{13}C NMR (101 MHz, $CDCl_3$) δ 173.1, 172.8, 168.2, 168.1, 159.2, 159.2, 145.6, 145.5, 139.1, 139.1, 131.4, 130.2, 130.2, 129.8, 129.5, 129.5, 128.9, 128.6, 128.6, 126.5, 126.5, 125.4, 125.4, 114.3, 114.1, 103.3, 102.5, 77.5, 67.9, 67.8, 66.0, 60.1, 60.0, 59.8, 59.2, 56.7, 55.4, 55.4, 47.8, 47.7, 47.5, 46.8, 34.3, 33.7, 31.2, 30.2, 30.2, 26.2, 25.6, 25.3, 23.2, 22.1.

2-methoxy-2-((*R*)-3-(4-methoxybenzyl)-2-oxothiazolidin-4-yl)tetrahydro-2H-pyran-4-yl 2-(thiophen-2-yl)benzoate (4.044)

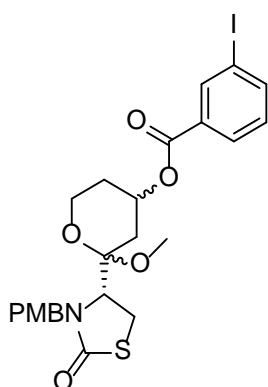


Title compound was prepared from 2-methoxy-2-(3-(4-methoxybenzyl)-2-oxothiazolidin-4-yl)tetrahydro-2H-pyran-4-yl 2-iodobenzoate (43.8 mg, 0.075 mmol) and thiophene-2-boronic acid (11.5 mg, 0.09 mmol) according to General Procedure I as a mixture of two diastereomers; A and B in 1:1 ratio respectively (28.4 mg, 70%).

HPLC – rt (diastereomer A) 9.00 min (52%), (diastereomer B) 9.06 min (48%), collectively > 99% purity at 254 nm; LRMS $[M+Na]^+$ 562.2 m/z; HRMS $[M+Na]^+$ 562.1329 m/z, found 562.1338 m/z; 1H NMR

(diastereomer A) (400 MHz, CDCl₃) δ 7.76 (m, 1H), 7.56 – 7.31 (m, 4H), 7.22 (m, 2H), 7.10 – 7.02 (m, 1H), 6.98 (m, 1H), 6.87 (m, 2H), 5.26 – 5.11 (m, 2H), 4.22 (d, J = 14.4 Hz, 1H), 3.91-3.71 (m, 2H), 3.87 – 3.78 (s, 3H), 3.68 – 3.59 (m, 1H), 3.37 – 3.15 (m, 2H), 3.08 (s, 3H), 2.07 (ddd, J = 12.5, 4.7, 1.7 Hz, 1H), 1.95 – 1.79 (m, 1H), 1.51 (dd, J = 12.7, 11.3 Hz, 1H), 1.47 – 1.28 (m, 1H); ¹H NMR **(diastereomer B)** (400 MHz, CDCl₃) δ 7.76 (m, 1H), 7.56 – 7.31 (m, 4H), 7.14 (m, 2H), 7.10 – 7.02 (m, 1H), 6.98 (m, 1H), 6.87 (m, 2H), 5.26 – 5.11 (m, 1H), 5.00 (d, J = 14.4 Hz, 1H), 4.18 (d, J = 15.5 Hz, 1H), 3.91-3.71 (m, 2H), 3.87 – 3.78 (s, 3H), 3.59 – 3.50 (m, 1H), 3.37 – 3.15 (m, 2H), 3.00 (s, 3H), 1.95 – 1.79 (m, 2H), 1.47 – 1.28 (m, 2H); ¹³C NMR (101 MHz, CDCl₃) δ 173.2, 172.8, 168.2, 168.1, 159.2, 159.2, 142.2, 134.6, 134.5, 132.4, 132.2, 131.5, 131.4, 131.2, 131.2, 131.0, 130.2, 130.2, 129.8, 129.8, 129.6, 129.0, 128.6, 128.6, 128.0, 128.0, 127.9, 127.4, 127.3, 126.6, 126.6, 126.2, 126.0, 125.9, 114.3, 114.1, 103.1, 102.4, 68.2, 60.0, 59.9, 59.3, 56.6, 55.4, 55.4, 47.7, 47.6, 47.5, 46.7, 33.5, 33.1, 30.8, 30.7, 26.1, 25.2.

2-methoxy-2-(3-(4-methoxybenzyl)-2-oxothiazolidin-4-yl)tetrahydro-2H-pyran-4-yl 3-iodobenzoate (4.034)

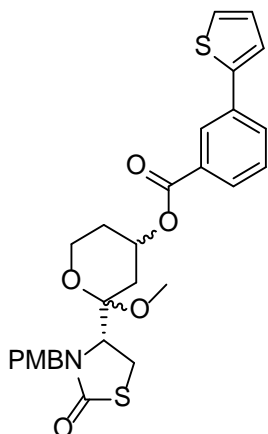


Title compound was prepared from

4-(4-hydroxy-2-methoxytetrahydro-2H-pyran-2-yl)-3-(4-methoxybenzyl)thiazolidin-2-one (93 mg, 0.26 mmol) and 3-iodobenzoic acid (196 mg, 0.79 mmol) according to the General Procedure G as a yellow oil and a mixture of two diastereomers; A and B in 1: 0.6 ratio respectively (136 mg, 88%).

HPLC – rt 9.36min > 99% purity at 254 nm; LRMS no mass ion was detected; HRMS [M+H]⁺ 584.0598 m/z, found 584.0607 m/z; ¹H NMR (400 MHz, CDCl₃) δ 8.35 (m, 1.6H), 8.04 – 7.95 (m, 1.6H), 7.92 – 7.85 (m, 1.6H), 7.25 – 7.11 (m, 4.8H), 6.92 – 6.80 (m, 3.2H), 5.39 (m, 1.6H), 5.23 (d, J = 15.5 Hz, 0.6H), 5.08 (d, J = 14.4 Hz, 1H), 4.32 (d, J = 14.4 Hz, 1H), 4.21 (d, J = 15.5 Hz, 0.6H), 4.03 – 3.83 (m, 3.2H), 3.81 (m, 4.8H), 3.78 – 3.71 (m, 1H), 3.70 – 3.63 (m, 0.6H), 3.43 – 3.21 (m, 3.2H), 3.14 (s, 3H), 3.06 (s, 1.8H), 2.32 (ddd, J = 12.5, 4.8, 1.9 Hz, 1H), 2.26 – 2.20 (m, 0.6H), 2.16 – 1.58 (m, 4.8H); ¹³C NMR (101 MHz, CDCl₃) δ 173.1, 164.5, 159.3, 142.1, 138.6, 138.6, 132.2, 130.2, 130.2, 129.0, 128.9, 128.6, 114.3, 114.1, 103.4, 102.5, 93.9, 68.6, 68.4, 60.1, 59.9, 59.3, 56.8, 55.4, 47.8, 47.7, 47.6, 46.8, 34.3, 33.7, 31.2, 26.2, 25.4.

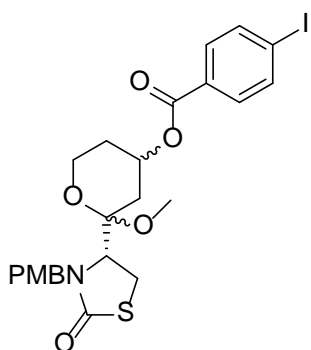
2-methoxy-2-(3-(4-methoxybenzyl)-2-oxothiazolidin-4-yl)tetrahydro-2H-pyran-4-yl 3-(thiophen-2-yl)benzoate (4.050)



Title compound was prepared from 4-(4-hydroxy-2-methoxytetrahydro-2H-pyran-2-yl)-3-(4-methoxybenzyl)thiazolidin-2-one (40 mg, 0.11 mmol) and 3-(thiophen-2-yl)benzoic acid (70 mg, 0.34 mmol) according to General Procedure G as a mixture of two diastereomers; A and B in 1:0.3 ratio respectively (20 mg, 32%).

HPLC – rt 9.41 min > 99% purity at 254 nm; LRMS no mass ion was detected; HRMS $[M+H]^+$ 540.1509 m/z, found 540.1513 m/z; 1H NMR (**diastereomer A**) (400 MHz, $CDCl_3$) δ 8.26 (m, 1H), 7.97 – 7.91 (m, 1H), 7.79 (m, 1H), 7.46 (m, 1H), 7.41 (m, 1H), 7.33 (m, 1H), 7.29 – 7.23 (m, 2H), 7.11 (m, 1H), 6.91 – 6.85 (m, 2H), 5.48 – 5.37 (m, 1H), 5.09 (d, J = 14.4 Hz, 1H), 4.34 (d, J = 14.4 Hz, 1H), 4.03 – 3.92 (m, 1H), 3.89 (m, 1H), 3.81 (s, 3H), 3.78–3.74 (m, 1H), 3.34 – 3.21 (m, 2H), 3.15 (s, 3H), 2.35 (ddd, J = 12.4, 4.7, 1.8 Hz, 1H), 2.13 (m, 1H), 1.89 – 1.81 (m, 1H), 1.68 (m, 1H); 1H NMR (**diastereomer B**) (400 MHz, $CDCl_3$) δ 8.26 (m, 1H), 7.97 – 7.91 (m, 1H), 7.79 (m, 1H), 7.46 (m, 1H), 7.41 (m, 1H), 7.33 (m, 1H), 7.16 (m, 2H), 7.11 (m, 1H), 6.91 – 6.85 (m, 2H), 5.48 – 5.37 (m, 1H), 5.24 (d, J = 15.5 Hz, 1H), 4.23 (d, J = 15.5 Hz, 1H), 4.03 – 3.92 (m, 1H), 3.89 (m, 1H), 3.81 (s, 3H), 3.73 – 3.65 (m, 1H), 3.44 – 3.39 (m, 1H), 3.34 – 3.21 (m, 1H), 3.07 (s, 3H), 2.26 (m, 1H), 2.13 (m, 1H), 1.98 (m, 1H), 1.68 (m, 1H); ^{13}C NMR (101 MHz, $CDCl_3$) δ 165.8, 159.3, 134.9, 131.0, 130.6, 130.2, 129.1, 129.0, 128.7, 128.6, 128.3, 127.1, 125.6, 124.1, 114.3, 114.1, 103.4, 68.2, 60.0, 59.3, 55.4, 47.8, 47.7, 47.6, 46.9, 33.7, 31.3, 25.4.

2-methoxy-2-(3-(4-methoxybenzyl)-2-oxothiazolidin-4-yl)tetrahydro-2H-pyran-4-yl 4-iodobenzoate (4.035)

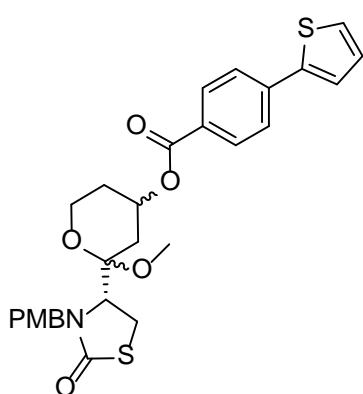


Title compound was prepared from 4-(4-hydroxy-2-methoxytetrahydro-2H-pyran-2-yl)-3-(4-methoxybenzyl)thiazolidin-2-one (93 mg, 0.26 mmol) and 4-iodobenzoic acid (195 mg, 0.79 mmol) according to the General Procedure G as a white solid and a mixture of two diastereomers; A and B in 1:0.6 ratio respectively (149 mg, 96%).

HPLC – rt 9.36 min > 84% purity at 254 nm; LRMS no mass ion was detected; HRMS $[M+H]^+$ 584.0598 m/z, found 584.0621 m/z; 1H NMR (**diastereomer A**) (400 MHz, $CDCl_3$) δ 7.84 – 7.71 (m, 4H), 7.25 (m, 2H), 6.87 (m, 2H), 5.44 – 5.31 (m, 1H), 5.08 (d, J =

14.4 Hz, 1H), 4.31 (d, $J = 14.4$ Hz, 1H), 4.01 – 3.90 (m, 1H), 3.91 – 3.82 (m, 1H), 3.81 (s, 3H), 3.79 – 3.71 (m, 1H), 3.45 – 3.35 (m, 1H), 3.27 (m, 1H), 3.13 (s, 3H), 2.32 (ddd, $J = 12.5, 4.8, 1.8$ Hz, 1H), 2.12 (m, 1H), 1.81 (dd, $J = 12.3, 11.6$ Hz, 1H), 1.76 – 1.48 (m, 1H); ^1H NMR (**diastereomer B**) (400 MHz, CDCl_3) δ 7.84 – 7.71 (m, 4H), 7.15 (m, 2H), 6.87 (m, 2H), 5.44 – 5.31 (m, 1H), 5.23 (d, $J = 15.5$ Hz, 1H), 4.21 (d, $J = 15.5$ Hz, 1H), 4.01 – 3.90 (m, 1H), 3.91 – 3.82 (m, 1H), 3.80 (s, 3H), 3.70 – 3.60 (m, 1H), 3.27 (m, 2H), 3.06 (s, 3H), 2.23 (ddd, $J = 12.6, 4.8, 1.7$ Hz, 1H), 2.12 (m, 1H), 1.95 (dd, $J = 12.6, 11.3$ Hz, 1H), 1.76 – 1.48 (m, 1H); ^{13}C NMR (101 MHz, CDCl_3) δ 173.3, 173.1, 165.5, 159.3, 159.2, 138.0, 137.8, 131.3, 131.2, 130.2, 129.8, 128.9, 128.6, 114.3, 114.1, 103.4, 102.5, 101.1, 68.4, 68.3, 60.1, 59.9, 59.3, 56.8, 55.4, 47.8, 47.7, 47.6, 46.8, 34.3, 33.7, 31.3, 26.2, 25.4.

2-methoxy-2-((*R*)-3-(4-methoxybenzyl)-2-oxothiazolidin-4-yl)tetrahydro-2H-pyran-4-yl 4-(thiophen-2-yl)benzoate (4.049)

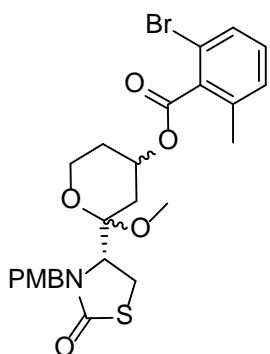


Title compound was prepared from 4-(4-hydroxy-2-methoxytetrahydro-2H-pyran-2-yl)-3-(4-methoxybenzyl)thiazolidin-2-one (50 mg, 0.14 mmol) and 4-(thiophen-2-yl)benzoic acid (86 mg, 0.42 mmol) according to General Procedure G as a mixture of two diastereomers; A and B in 1:0.4 ratio respectively (73.9 mg, 95%).

HPLC – rt 9.41 min > 99% purity at 254 nm; LRMS $[\text{M}+\text{Na}]^+$ 562.0 m/z; HRMS $[\text{M}+\text{H}]^+$ 540.1509 m/z, found 540.1513 m/z;

^1H NMR (**diastereomer A**) (400 MHz, CDCl_3) δ 8.08 – 7.99 (m, 2H), 7.72 – 7.65 (m, 2H), 7.47 – 7.41 (m, 1H), 7.40 – 7.33 (m, 1H), 7.29 – 7.22 (m, 2H), 7.14 – 7.09 (m, 1H), 6.92 – 6.84 (m, 2H), 5.47 – 5.35 (m, 1H), 5.09 (d, $J = 14.4$ Hz, 1H), 4.33 (d, $J = 14.4$ Hz, 1H), 4.04 – 3.91 (m, 1H), 3.91 – 3.83 (m, 1H), 3.81 (s, 3H), 3.80 – 3.73 (m, 1H), 3.34 – 3.23 (m, 2H), 3.14 (s, 3H), 2.34 (ddd, $J = 12.5, 4.8, 1.8$ Hz, 1H), 2.21 – 2.08 (m, 1H), 1.83 (dd, $J = 12.3, 11.5$ Hz, 1H), 1.79 – 1.60 (m, 1H); ^1H NMR (**diastereomer B**) (400 MHz, CDCl_3) δ 8.08 – 7.99 (m, 2H), 7.72 – 7.65 (m, 2H), 7.47 – 7.41 (m, 1H), 7.40 – 7.33 (m, 1H), 7.19 – 7.14 (m, 1H), 7.14 – 7.09 (m, 2H), 6.92 – 6.84 (m, 2H), 5.47 – 5.35 (m, 1H), 5.24 (d, $J = 15.5$ Hz, 1H), 4.23 (d, $J = 15.5$ Hz, 1H), 4.04 – 3.91 (m, 1H), 3.91 – 3.83 (m, 1H), 3.80 (s, 3H), 3.72 – 3.64 (m, 1H), 3.46 – 3.37 (m, 2H), 3.07 (s, 3H), 2.26 (ddd, $J = 12.8, 4.9, 1.8$ Hz, 1H), 2.21 – 2.08 (m, 1H), 1.97 (dd, $J = 12.6, 11.3$ Hz, 1H), 1.79 – 1.60 (m, 1H); ^{13}C NMR (101 MHz, CDCl_3) δ 173.3, 173.1, 165.7, 159.3, 159.2, 143.2, 138.9, 130.5, 130.5, 130.2, 129.0, 128.9, 128.7, 128.6, 128.5, 126.5, 125.6, 124.7, 114.3, 114.1, 103.4, 102.6, 68.1, 67.9, 60.2, 60.0, 59.3, 56.8, 55.4, 47.8, 47.7, 47.6, 46.8, 34.4, 33.8, 31.4, 26.2, 25.4.

2-methoxy-2-((*R*)-3-(4-methoxybenzyl)-2-oxothiazolidin-4-yl)tetrahydro-2H-pyran-4-yl 2-bromo-6-methylbenzoate (4.036)

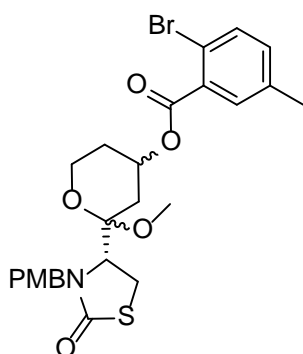


Title compound was prepared from 4-(4-hydroxy-2-methoxytetrahydro-2H-pyran-2-yl)-3-(4-methoxybenzyl)thiazolidin-2-one (80 mg, 0.23 mmol) and 2-bromo-6-methylbenzoic acid (146 mg, 0.68 mmol) according to the General Procedure G as a clear oil and a mixture of two diastereomers; A and B in 1:0.6 ratio respectively (4.8 mg, 4%).

HPLC – rt 9.50 min > 78% purity at 254 nm; LRMS $[M+H]^+$ 550.0 m/z; HRMS $[M+H]^+$ 550.0893 m/z, found 550.0901 m/z; 1H NMR

(diastereomer A) (400 MHz, $CDCl_3$) δ 7.44 – 7.36 (m, 2H), 7.19 – 7.11 (m, 3H), 6.92 – 6.83 (m, 2H), 5.47 (m, 1H), 5.22 (d, J = 15.5 Hz, 1H), 4.24 (d, J = 15.5 Hz, 1H), 4.00 – 3.91 (m, 1H), 3.91 – 3.82 (m, 1H), 3.80 (s, 3H), 3.72 – 3.63 (m, 1H), 3.45 – 3.35 (m, 1H), 3.32 – 3.24 (m, 1H), 3.08 (s, 3H), 2.33 (d, J = 3.8 Hz, 4H), 2.23 (m, 1H), 2.03 – 1.89 (m, 1H), 1.85 – 1.73 (m, 1H); 1H NMR **(diastereomer B)** (400 MHz, $CDCl_3$) δ 7.26 – 7.21 (m, 2H), 7.19 – 7.11 (m, 3H), 6.92 – 6.83 (m, 2H), 5.37 (m, 1H), 5.01 (d, J = 14.4 Hz, 1H), 4.30 (d, J = 14.4 Hz, 1H), 4.00 – 3.91 (m, 1H), 3.91 – 3.82 (m, 1H), 3.81 (s, 3H), 3.79 – 3.71 (m, 1H), 3.45 – 3.35 (m, 2H), 3.15 (s, 3H), 2.57 (d, J = 4.3 Hz, 3H), 2.33 (d, J = 3.8 Hz, 1H), 2.23 (m, 1H), 2.03 – 1.89 (m, 1H), 1.73 – 1.60 (m, 1H); ^{13}C NMR (101 MHz, $CDCl_3$) δ 173.3, 167.4, 167.4, 159.2, 136.9, 135.7, 130.6, 130.2, 130.1, 129.1, 129.1, 128.6, 128.5, 119.1, 114.3, 114.1, 103.3, 102.6, 77.2, 69.0, 69.0, 60.0, 59.9, 59.3, 56.9, 55.4, 47.9, 47.7, 47.7, 47.0, 34.1, 33.7, 31.1, 31.0, 26.3, 25.5, 19.8.

2-methoxy-2-((*R*)-3-(4-methoxybenzyl)-2-oxothiazolidin-4-yl)tetrahydro-2H-pyran-4-yl 2-bromo-5-methylbenzoate (4.037)



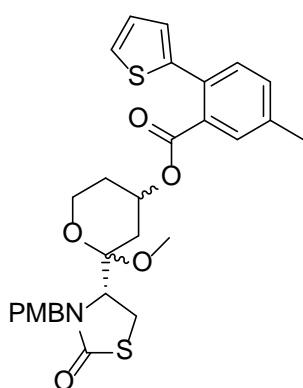
Title compound was prepared from

4-(4-hydroxy-2-methoxytetrahydro-2H-pyran-2-yl)-3-(4-methoxybenzyl)thiazolidin-2-one (80 mg, 0.226 mmol) and 2-bromo-5-methylbenzoic acid (146 mg, 0.68 mmol) according to the General Procedure G as a clear oil and a mixture of two diastereomers; A and B in 1:0.6 ratio respectively (106.5 mg, 85%).

HPLC – rt 9.04 min > 99% purity at 254 nm; LRMS $[M+H]^+$ 550.10 m/z; HRMS $[M+H]^+$ 550.0893 m/z, found 550.0906 m/z; 1H NMR **(diastereomer A)** (400 MHz, $CDCl_3$) δ 7.57 (m, 1H), 7.51 (m, 1H), 7.24 (d, J = 8.6 Hz, 2H), 7.17 – 7.09 (m, 1H), 6.90 – 6.83 (m, 2H), 5.47 – 5.34 (m, 1H), 5.04 (d, J = 14.4 Hz, 1H), 4.32 (d, J = 14.4 Hz, 1H), 4.01 – 3.90 (m, 1H),

3.86 (m, 1H), 3.80 (s, 3H), 3.78 – 3.70 (m, 1H), 3.41 – 3.37 (m, 1H), 3.33 – 3.22 (m, 1H), 3.13 (s, 3H), 2.39 – 2.30 (m, 4H), 2.21 – 2.09 (m, 1H), 1.85 – 1.77 (m, 1H), 1.77 – 1.59 (m, 1H); ¹H NMR (**diastereomer B**) (400 MHz, CDCl₃) δ 7.57 (m, 1H), 7.51 (m, 1H), 7.17 – 7.09 (m, 3H), 6.90 – 6.83 (m, 2H), 5.47 – 5.34 (m, 1H), 5.22 (d, *J* = 15.5 Hz, 1H), 4.23 (d, *J* = 15.5 Hz, 1H), 4.01 – 3.90 (m, 1H), 3.86 (m, 1H), 3.79 (s, 3H), 3.70 – 3.61 (m, 1H), 3.33 – 3.22 (m, 2H), 3.05 (s, 3H), 2.39 – 2.30 (m, 3H), 2.25 (ddd, *J* = 12.7, 4.8, 1.7 Hz, 1H), 2.21 – 2.09 (m, 1H), 1.96 (dd, *J* = 12.6, 11.4 Hz, 1H), 1.77 – 1.59 (m, 1H); ¹³C NMR (101 MHz, CDCl₃) δ 173.3, 173.0, 165.7, 165.6, 159.2, 159.1, 137.4, 137.4, 134.1, 134.0, 133.6, 133.5, 131.7, 131.7, 130.1, 128.9, 128.5, 128.5, 118.3, 118.1, 114.2, 114.0, 103.2, 102.4, 68.8, 68.7, 60.0, 59.8, 59.3, 56.7, 55.3, 55.3, 47.7, 47.6, 47.6, 46.7, 34.1, 33.5, 31.0, 26.1, 25.3, 20.8.

2-methoxy-2-(3-(4-methoxybenzyl)-2-oxothiazolidin-4-yl)tetrahydro-2H-pyran-4-yl 5-methyl-2-(thiophen-2-yl)benzoate (4.047)

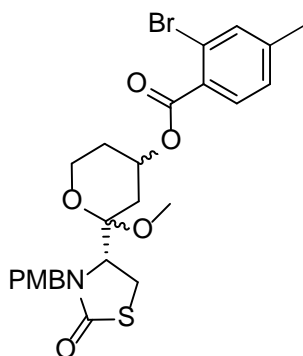


Title compound was prepared from 2-methoxy-2-((R)-3-(4-methoxybenzyl)-2-oxothiazolidin-4-yl)tetrahydro-2H-pyran-4-yl 2-bromo-5-methylbenzoate (15.6 mg, 0.028 mmol) and thiophene-2-boronic acid (11 mg, 0.085 mmol) according to General Procedure I as a yellow oil and a mixture of two diastereomers; A and B in 1:0.6 ratio respectively (13.7 mg, 88%).

HPLC – rt (diastereomer A) 9.31 min (50.4%), (diastereomer B) 9.37 min (46.9%) collectively > 97% purity at 254 nm; LRMS [M+Na]⁺

576.2 m/z; HRMS [M+Na]⁺ 576.1485 m/z, found 576.1498 m/z; ¹H NMR (**diastereomer A**) (400 MHz, CDCl₃) δ 7.56 (m, 1H), 7.37 – 7.32 (m, 2H), 7.33 – 7.27 (m, 1H), 7.21 (m, 2H), 7.06 (m, 1H), 6.95 (m, 1H), 6.91 – 6.81 (m, 2H), 5.22 – 5.12 (m, 1H), 5.01 (d, *J* = 14.4 Hz, 1H), 4.23 (d, *J* = 14.4 Hz, 1H), 3.87 (m, 1H), 3.80 (s, 3H), 3.78 – 3.71 (m, 1H), 3.69 – 3.59 (m, 1H), 3.36 – 3.16 (m, 2H), 3.08 (s, 3H), 2.42 (s, 3H), 2.11 – 2.02 (m, 1H), 1.92 – 1.81 (m, 1H), 1.43 – 1.35 (m, 1H), 1.47 – 1.23 (m, 1H); ¹H NMR (**diastereomer B**) (400 MHz, CDCl₃) δ 7.56 (m, 1H), 7.37 – 7.32 (m, 2H), 7.33 – 7.27 (m, 1H), 7.14 (m, 2H), 7.06 (m, 1H), 6.95 (m, 1H), 6.91 – 6.81 (m, 2H), 5.22 (d, *J* = 15.6 Hz, 1H), 5.22 – 5.12 (m, 1H), 4.18 (d, *J* = 15.6 Hz, 1H), 3.87 (m, 1H), 3.80 (s, 3H), 3.78 – 3.71 (m, 1H), 3.59 – 3.50 (m, 1H), 3.36 – 3.16 (m, 2H), 3.00 (s, 3H), 2.42 (s, 3H), 1.92 – 1.81 (m, 2H), 1.52 (dd, *J* = 12.7, 11.3 Hz, 1H), 1.47 – 1.23 (m, 1H); ¹³C NMR (101 MHz, CDCl₃) δ 173.2, 172.8, 168.3, 168.1, 159.2, 159.2, 142.3, 138.2, 138.1, 132.2, 132.0, 131.9, 131.9, 131.7, 131.6, 131.5, 131.4, 130.3, 130.2, 130.1, 129.0, 128.7, 128.6, 127.3, 126.4, 126.4, 125.9, 125.7, 114.3, 114.1, 103.1, 102.4, 68.1, 60.0, 59.9, 59.3, 56.6, 55.4, 55.4, 47.7, 47.6, 47.5, 46.7, 33.6, 33.1, 30.8, 30.7, 26.1, 25.2, 21.1.

2-methoxy-2-((*R*)-3-(4-methoxybenzyl)-2-oxothiazolidin-4-yl)tetrahydro-2H-pyran-4-yl 2-bromo-4-methylbenzoate (4.038)

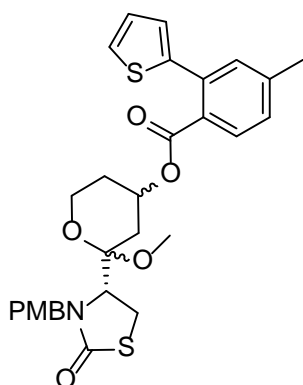


Title compound was prepared from

4-(4-hydroxy-2-methoxytetrahydro-2H-pyran-2-yl)-3-(4-methoxybenzyl)thiazolidin-2-one (80 mg, 0.226 mmol) and 2-bromo-4-methylbenzoic acid (146 mg, 0.68 mmol) according to the General Procedure G as a white solid and a mixture of two diastereomers; A and B in 1:0.7 ratio respectively (71.6 mg, 57%).

HPLC – rt 9.06 min > 99% purity at 254 nm; LRMS no mass ion was detected; HRMS $[M+H]^+$ 550.0893 m/z, found 550.0907 m/z; 1H NMR (400 MHz, $CDCl_3$) δ 7.71 (dd, J = 7.9, 2.8 Hz, 1.7H), 7.49 (m, 1.7H), 7.24 (m, 2H), 7.16 (m, 3.1H), 6.93 – 6.81 (m, 3.4H), 5.47 – 5.32 (m, 1.7H), 5.22 (d, J = 15.5 Hz, 0.7H), 5.04 (d, J = 14.4 Hz, 1H), 4.32 (d, J = 14.4 Hz, 1H), 4.23 (d, J = 15.5 Hz, 0.7H), 3.98 (dd, J = 7.3, 5.5 Hz, 0.7H), 3.96 – 3.90 (m, 1H), 3.90 – 3.82 (m, 1.7H), 3.82 – 3.78 (m, 5.1H), 3.78 – 3.70 (m, 1H), 3.70 – 3.61 (m, 0.7H), 3.49 – 3.25 (m, 3.4H), 3.13 (s, 3H), 3.05 (s, 2.1H), 2.37 (s, 5.1H), 2.33 (m, 1H), 2.24 (ddd, J = 12.7, 4.8, 1.8 Hz, 0.7H), 2.21 – 2.08 (m, 1.7H), 1.95 (dd, J = 12.6, 11.3 Hz, 0.7H), 1.79 – 1.61 (m, 2.7H); ^{13}C NMR (101 MHz, $CDCl_3$) δ 173.1, 165.5, 165.4, 159.3, 143.9, 135.1, 135.1, 131.6, 131.6, 130.2, 129.9, 129.0, 128.8, 128.7, 128.6, 128.1, 122.0, 114.3, 114.1, 103.3, 102.5, 68.7, 68.6, 60.1, 60.0, 59.4, 56.8, 55.4, 47.8, 47.7, 47.7, 46.9, 34.3, 33.7, 31.2, 26.2, 25.4, 21.2.

2-methoxy-2-((*R*)-3-(4-methoxybenzyl)-2-oxothiazolidin-4-yl)tetrahydro-2H-pyran-4-yl 4-methyl-2-(thiophen-2-yl)benzoate (4.046)

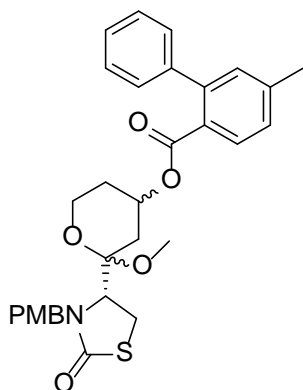


Title compound was prepared from 2-methoxy-2-((*R*)-3-(4-methoxybenzyl)-2-oxothiazolidin-4-yl)tetrahydro-2H-pyran-4-yl 2-bromo-4-methylbenzoate (46 mg, 0.083 mmol) and thiophene-2-boronic acid (32 mg, 0.25 mmol) according to General Procedure I as a yellow oil as a mixture of two diastereomers; A and B in 1:0.7 ratio respectively (40.7 mg, 89%).

HPLC - rt (diastereomer A) 9.33 min (56%), (diastereomer B) 9.34 min (43%) collectively > 99% purity at 254 nm; LRMS $[M+Na]^+$ 576.2 m/z; HRMS $[M+Na]^+$ 576.1485 m/z, found 576.1499 m/z; 1H NMR (**diastereomer A**) (400 MHz, $CDCl_3$) δ 7.69 (m, 1H), 7.37 (m, 1H), 7.29 – 7.18 (m, 4H), 7.07 (m, 1H), 6.98 – 6.93 (m, 1H), 6.86 (m, 2H), 5.16 (m, 1H), 5.01 (d, J = 14.4 Hz, 1H), 4.22 (d, J = 14.4 Hz, 1H), 3.94 – 3.73 (m, 2H), 3.80 (s, 3H), 3.68 – 3.59 (m, 1H), 3.37 – 3.17 (m, 2H), 3.08 (s, 3H), 2.41 (s, 3H), 2.05 (dd, J = 11.8, 3.9 Hz, 1H), 1.85 (m, 1H), 1.46

– 1.24 (m, 2H); ^1H NMR (**diastereomer B**) (400 MHz, CDCl_3) δ 7.69 (m, 1H), 7.37 (m, 1H), 7.29 – 7.18 (m, 2H), 7.14 (m, 2H), 7.07 (m, 1H), 6.98 – 6.93 (m, 1H), 6.86 (m, 2H), 5.22 (d, $J = 15.4$ Hz, 1H), 5.16 (m, 1H), 4.18 (d, $J = 15.5$ Hz, 1H), 3.94 – 3.73 (m, 2H), 3.80 (s, 3H), 3.53 (m, 1H), 3.37 – 3.17 (m, 2H), 2.99 (s, 3H), 2.41 (s, 3H), 1.85 (m, 2H), 1.50 (dd, $J = 12.8, 11.4$ Hz, 1H), 1.46 – 1.24 (m, 1H); ^{13}C NMR (101 MHz, CDCl_3) δ 173.2, 172.8, 168.0, 167.8, 159.2, 159.1, 142.5, 141.8, 141.7, 134.8, 134.7, 132.3, 132.2, 130.2, 130.1, 130.0, 129.4, 129.2, 128.9, 128.7, 128.6, 128.5, 127.2, 126.4, 126.4, 125.9, 125.8, 114.3, 114.0, 103.1, 102.4, 67.9, 67.9, 60.0, 59.8, 59.2, 56.6, 55.4, 55.4, 47.7, 47.6, 47.4, 46.7, 33.5, 33.1, 30.8, 30.7, 26.1, 25.2, 21.5.

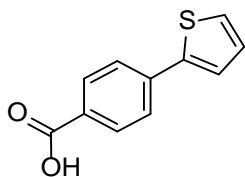
2-methoxy-2-(3-(4-methoxybenzyl)-2-oxothiazolidin-4-yl)tetrahydro-2H-pyran-4-yl 5-methyl-[1,1'-biphenyl]-2-carboxylate (4.048)



Title compound was prepared from 2-methoxy-2-((*R*)-3-(4-methoxybenzyl)-2-oxothiazolidin-4-yl)tetrahydro-2H-pyran-4-yl 2-bromo-4-methylbenzoate (41 mg, 0.074 mmol) and phenyl boronic acid (27.5 mg, 0.223 mmol) according to General Procedure I as a clear oil and a mixture of two diastereomers; A and B in 1:0.6 ratio respectively (38.4 mg, 94%).

HPLC – rt (diastereomer A) 9.42 min (53%), (diastereomer B) 9.47 min (44%), collectively > 97% purity at 254 nm; LRMS $[\text{M}+\text{Na}]^+$ 570.3 m/z; HRMS $[\text{M}+\text{Na}]^+$ 570.1921 m/z, found 570.1934 m/z; ^1H NMR (**diastereomer A**) (400 MHz, CDCl_3) δ 7.77 (m, 1H), 7.44 – 7.09 (m, 9H), 6.85 (m, 2H), 5.08 (m, 1H), 5.00 (d, $J = 14.4$ Hz, 1H), 4.19 (d, $J = 12.0$ Hz, 1H), 3.88 (m, 1H), 3.79 (s, 3H), 3.77 – 3.65 (m, 1H), 3.63 – 3.54 (m, 1H), 3.34 – 3.09 (m, 2H), 3.05 (s, 3H), 2.42 (s, 3H), 1.92 (ddd, $J = 12.6, 4.7, 1.8$ Hz, 1H), 1.84 – 1.67 (m, 1H), 1.35 – 1.12 (m, 2H); ^1H NMR (**diastereomer B**) (400 MHz, CDCl_3) δ 7.77 (m, 1H), 7.44 – 7.09 (m, 9H), 6.85 (m, 2H), 5.21 (d, $J = 15.5$ Hz, 1H), 5.08 (m, 1H), 4.15 (d, $J = 13.2$ Hz, 1H), 3.88 (m, 1H), 3.79 (s, 3H), 3.77 – 3.65 (m, 1H), 3.54 – 3.44 (m, 1H), 3.34 – 3.09 (m, 2H), 2.96 (s, 3H), 2.42 (s, 3H), 1.84 – 1.67 (m, 2H), 1.35 – 1.12 (m, 2H); ^{13}C NMR (101 MHz, CDCl_3) δ 173.1, 172.8, 168.1, 167.9, 159.2, 159.1, 143.1, 142.9, 142.0, 141.9, 141.9, 131.8, 131.6, 131.5, 130.4, 130.3, 130.2, 130.2, 130.1, 128.9, 128.6, 128.6, 128.5, 128.2, 128.1, 128.1, 128.1, 128.0, 128.0, 127.5, 127.4, 127.2, 114.3, 114.0, 103.0, 102.3, 67.7, 67.7, 59.9, 59.8, 59.2, 56.6, 55.4, 55.4, 47.6, 47.5, 47.4, 46.7, 33.4, 32.9, 30.7, 30.6, 26.1, 25.1, 21.6.

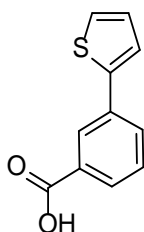
4-(thiophen-2-yl)benzoic acid



Title compound was prepared from 4-iodobenzoic acid (100 mg, 0.4 mmol) and thiophene-2-boronic acid (153.6 mg, 1.2 mmol) according to General Procedure I as a brown solid (81 mg, 99%).

HPLC – rt 6.37 min > 99% purity at 254 nm; LRMS $[M+H]^+$ 205.1 m/z; HRMS $[M+H]^+$ 205.0318 205.0323 m/z, found m/z; 1H NMR (400 MHz, $CDCl_3$) δ 8.17 – 8.05 (m, 2H), 7.76 – 7.67 (m, 2H), 7.45 (dd, J = 3.6, 1.1 Hz, 1H), 7.38 (dd, J = 5.1, 1.0 Hz, 1H), 7.13 (dd, J = 5.1, 3.7 Hz, 1H); ^{13}C NMR (101 MHz, $CDCl_3$) δ 184.4, 134.8, 131.4, 131.1, 128.5, 128.3, 127.8, 126.7, 126.7, 125.8, 124.9.

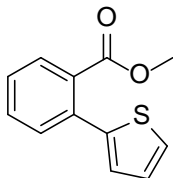
3-(thiophen-2-yl)benzoic acid



Title compound was prepared from 3-iodobenzoic acid (200 mg, 0.8 mmol) and thiophene-2-boronic acid (307 mg, 2.4 mmol) according to General Procedure I as a brown solid (162 mg, 99%).

HPLC – rt 6.37 min > 99% purity at 254 nm; LRMS $[M+H]^+$ 205.1 m/z; HRMS $[M+H]^+$ 205.0318 m/z, found 205.0316 m/z; 1H NMR (400 MHz, $CDCl_3$) δ 8.37 (t, J = 1.6 Hz, 1H), 8.08 – 7.97 (m, 1H), 7.85 (ddd, J = 7.8, 1.9, 1.1 Hz, 1H), 7.50 (t, J = 7.8 Hz, 1H), 7.41 (dd, J = 3.6, 1.1 Hz, 1H), 7.34 (dd, J = 5.1, 1.1 Hz, 1H), 7.12 (dd, J = 5.1, 3.6 Hz, 1H); ^{13}C NMR (101 MHz, $CDCl_3$) δ 168.2, 135.1, 131.2, 130.0, 129.3, 129.1, 128.4, 127.6, 125.8, 125.0, 124.1.

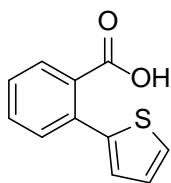
methyl 2-(thiophen-2-yl)benzoate [20]



Title compound was prepared from methyl-2-iodobenzoate (200 mg, 0.76 mmol) and thiophene-2-boronic acid (293 mg, 2.3 mmol) according to General Procedure I (165 mg, 99%).

1H NMR (400 MHz, $CDCl_3$) δ 7.72 (d, J = 7.7 Hz, 1H), 7.53 – 7.46 (m, 2H), 7.44 – 7.36 (m, 1H), 7.35 (dd, J = 5.0, 1.2 Hz, 1H), 7.05 (m, 2H), 3.74 (s, 3H).

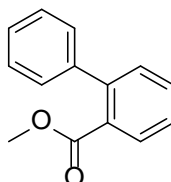
2-(thiophen-2-yl)benzoic acid [20]



To methyl 2-(thiophen-2-yl)benzoate (198 mg, 0.76 mmol) in EtOH (1 mL) was added KOH (128 mg, 2.28 mmol) and stirred for 8 h. The reaction mixture was then diluted with diethyl ether and washed with saturated sodium bicarbonate solution (x 3). The aqueous layer was then acidified with 6 M aq. HCl solution and extracted repeatedly with EtOAc. The combined organic layer was dried with magnesium sulphate and evaporated to dryness to yield the product as a white solid (152 mg, 98%).

^1H NMR (400 MHz, CDCl_3) δ 7.90 (ddd, $J = 7.8, 1.3, 0.4$ Hz, 1H), 7.57 – 7.47 (m, 2H), 7.42 (ddd, $J = 7.7, 7.2, 1.6$ Hz, 1H), 7.36 (dd, $J = 5.0, 1.3$ Hz, 1H), 7.08 (ddd, $J = 8.5, 4.3, 2.4$ Hz, 2H).

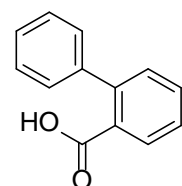
methyl [1,1'-biphenyl]-2-carboxylate [21]



Title compound was prepared from methyl-2-iodobenzoate (400 mg, 1.53 mmol) and phenyl boronic acid (560 mg, 4.6 mmol) according to General Procedure I as a yellow oil (98%).

^1H NMR (400 MHz, CDCl_3) δ 7.83 (dd, $J = 7.7, 1.1$ Hz, 1H), 7.53 (td, $J = 7.5, 1.3$ Hz, 1H), 7.40 (m, 5H), 7.34 – 7.29 (m, 2H), 3.64 (s, 3H).

[1,1'-biphenyl]-2-carboxylic acid [22]

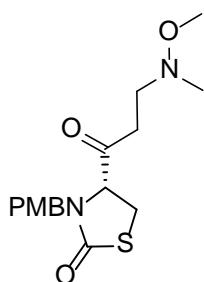


To methyl [1,1'-biphenyl]-2-carboxylate (198 mg, 0.76 mmol) in EtOH (1 mL) was added KOH (128 mg, 2.28 mmol) and stirred for 8 h. The reaction mixture was then diluted with diethyl ether and washed with saturated sodium bicarbonate solution. The aqueous layer was then acidified with 6 M aq. HCl and extracted repeatedly with EtOAc. The combined organic layer was dried with magnesium sulphate and evaporated to dryness to yield the product as a white solid (95%).

^1H NMR (400 MHz, CDCl_3) δ 7.95 (dd, $J = 7.8, 1.2$ Hz, 1H), 7.57 (td, $J = 7.6, 1.4$ Hz, 1H), 7.47 – 7.31 (m, 7H).

(R)-4-(3-(methoxy(methyl)amino)propanoyl)-3-(4-methoxybenzyl)thiazolidin-2-one (4.016)

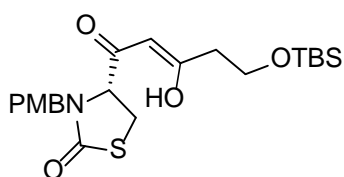
To *N*-methoxy-3-(4-methoxybenzyl)-*N*-methyl-2-oxothiazolidine-4-carboxamide (4.74 g, 15.3 mmol) in THF (51 mL) at 0°C, 1.5 M vinylmagnesium bromide (30.5 mmol) was added drop wise and stirred for 12 h. After completion of the reaction, 2 M HCl was added and then extracted with



DCM (x 3). The combined organic layer was washed with saturated sodium bicarbonate solution, dried with sodium sulphate and evaporated to dryness. Flash chromatography, eluting with a gradient from 10% EtOAc/petroleum spirits to 25% EtOAc/petroleum spirits led to the isolation of the product (1.55 g, 30%).

HPLC – rt 5.98 min > 96% purity at 254 nm; LRMS $[M+H]^+$ 339.2 m/z; HRMS $[M+H]^+$ 339.1373 m/z, found 339.1373 m/z; 1H NMR (400 MHz, $CDCl_3$) δ 7.13 (d, J = 8.5 Hz, 2H), 6.85 (d, J = 8.7 Hz, 2H), 5.06 (d, J = 14.8 Hz, 1H), 4.18 (dd, J = 9.3, 4.0 Hz, 1H), 3.86 (d, J = 14.8 Hz, 1H), 3.80 (s, 3H), 3.53 – 3.45 (dd, J = 11.4, 9.3 Hz, 1H), 3.42 (s, 3H), 3.17 (dd, J = 11.4, 4.0 Hz, 1H), 2.89 (td, J = 6.6, 3.2 Hz, 2H), 2.64 (t, J = 6.4 Hz, 2H), 2.56 (s, 3H); ^{13}C NMR (101 MHz, $CDCl_3$) δ 171.9, 165.8, 159.5, 129.9, 127.4, 114.3, 65.0, 59.9, 55.4, 54.6, 47.4, 44.9, 36.8, 27.7.

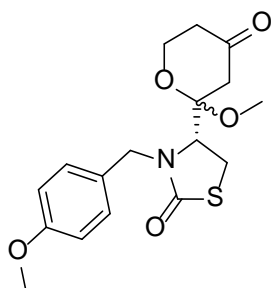
(R,Z)-4-(5-((tert-butyldimethylsilyl)oxy)-3-hydroxypent-2-enoyl)-3-(4-methoxybenzyl)thiazolidin-2-one (4.052a)



(4R)-4-(5-((tert-butyldimethylsilyl)oxy)-3-hydroxypentanoyl)-3-(4-methoxybenzyl)thiazolidin-2-one (71.7 mg, 0.16 mmol) was dissolved in DCM (1.8 mL) and *tert*-butanol (0.2 mL). To this, DMP (100 mg, 0.24 mmol) was added and stirred for 30 min. The reaction was quenched with 1:1 mixture of saturated potassium thiosulphate and saturated sodiumbicarbonate solution and stirred for 30 mins. It was then extracted with DCM (x 3) and dried using sodium sulphate and evaporated *in vacuo*. Flash chromatography, eluting with 15% EtOAc/petroleum spirits yielded the product (28 mg, 38%).

HPLC – rt 5.68 min > 71% purity at 254 nm; LRMS $[M+Na]^+$ 474.1 m/z; HRMS $[M+H]^+$ 452.1921 m/z, found 452.1911 m/z; 1H NMR (400 MHz, $CDCl_3$) δ 7.19 – 7.07 (m, 2H), 6.93 – 6.77 (m, 2H), 5.65 (s, 1H), 5.09 (d, J = 14.8 Hz, 1H), 4.07 (dd, J = 9.0, 3.9 Hz, 1H), 3.91 (t, J = 6.1 Hz, 2H), 3.84 – 3.72 (m, 4H), 3.47 (dd, J = 11.4, 9.0 Hz, 1H), 3.20 (dd, J = 11.4, 3.9 Hz, 1H), 2.54 (t, J = 6.1 Hz, 2H), 0.87 (s, 9H), 0.05 (s, 6H); ^{13}C NMR (101 MHz, $CDCl_3$) δ 193.1, 190.7, 171.2, 159.5, 130.0, 127.6, 114.4, 98.4, 62.2, 59.5, 55.5, 47.3, 41.8, 36.0, 29.7, 26.0.

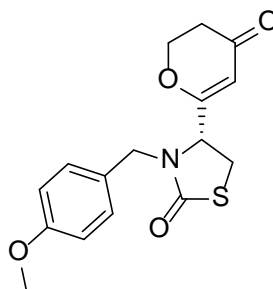
4-(2-methoxy-4-oxotetrahydro-2H-pyran-2-yl)-3-(4-methoxybenzyl)thiazolidin-2-one (4.053)



4-(4-hydroxy-2-methoxytetrahydro-2H-pyran-2-yl)-3-(4-methoxybenzyl)thiazolidin-2-one (30 mg, 0.085 mmol) was dissolved in DCM (1 mL) and DMP (36 mg, 0.085 mmol) was added and stirred for 12 h. The reaction was quenched with 1:1 mixture of saturated potassium thiosulphate solution and saturated sodium bicarbonate solution and stirred for 30 mins. It was then extracted with DCM (x 3), dried using sodium sulphate and evaporated *in vacuo*. Flash chromatography, eluting with 25% EtOAc/petroleum spirits yielded the product as a mixture of two diastereomers; A and B in 1:1 ratio respectively (20.3 mg, 68%).

HPLC – rt 6.90 min > 95% purity at 254 nm; LRMS $[M+H]^+$ 352.2 m/z; HRMS $[M+H]^+$ 352.1213 m/z, found 352.1220 m/z; ^1H NMR (400 MHz, CDCl_3) δ 7.28 – 7.22 (m, 2H), 7.13 (m, 2H), 6.87 (m, 4H), 5.21 (d, $J = 15.6$ Hz, 1H), 4.99 (d, $J = 14.4$ Hz, 1H), 4.43 (d, $J = 14.4$ Hz, 1H), 4.18 – 4.07 (m, 3H), 4.05 (m, 1H), 3.97 (m, 1H), 3.94 – 3.86 (m, 1H), 3.84 (m, 1H), 3.80 (s, 3H), 3.79 (s, 3H), 3.51 – 3.42 (m, 2H), 3.31 (dd, $J = 11.8, 9.9$ Hz, 1H), 3.18 (dd, $J = 11.8, 2.2$ Hz, 1H), 3.14 (s, 3H), 3.06 (s, 3H), 2.89 (d, $J = 14.8$ Hz, 1H), 2.76 – 2.51 (m, 4H), 2.48 – 2.26 (m, 3H); ^{13}C NMR (101 MHz, CDCl_3) δ 203.9, 203.6, 173.0, 172.9, 159.3, 159.3, 130.1, 129.0, 128.5, 128.4, 114.4, 114.2, 105.6, 104.1, 60.5, 60.5, 59.4, 56.6, 55.4, 48.3, 48.2, 48.2, 46.8, 45.8, 45.3, 40.9, 40.7, 26.4, 25.3.

3-(4-methoxybenzyl)-4-(4-oxo-3,4-dihydro-2H-pyran-6-yl)thiazolidin-2-one (4.054)

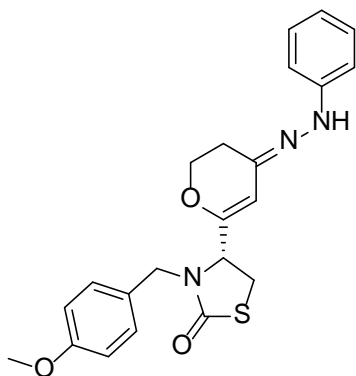


To 4-(2-methoxy-4-oxotetrahydro-2H-pyran-2-yl)-3-(4-methoxybenzyl)thiazolidin-2-one (32.8 mg, 0.093 mmol) in MeOH (1.5 mL) was added *tert*-butyl hydrazine hydrochloride (12.5 mg, 0.1 mmol) and Dowex® resin (acidic) (180 mg) and the reaction mixture refluxed for 8 h. The Dowex® resin was then filtered off and washed repeatedly with hot MeOH. The filtrate was then evaporated to dryness. Flash chromatography, eluting with 50% EtOAc/petroleum spirits yielded the product (20%).

HPLC – rt 6.69 min > 99% purity at 254 nm; LRMS $[M+H]^+$ 390.2 m/z; HRMS $[M+H]^+$ 320.0951 m/z, found 320.0957 m/z; ^1H NMR (400 MHz, CDCl_3) δ 7.15 (m, 2H), 6.85 (m, 2H), 5.43 (s, 1H), 4.90 (d, $J = 14.9$ Hz, 1H), 4.54 (ddd, $J = 11.6, 7.0, 5.4$ Hz, 1H), 4.34 (ddd, $J = 11.5, 10.4, 4.7$ Hz, 1H), 4.14 (dd, $J = 8.8, 4.5$ Hz, 1H), 3.87 (d, $J = 14.9$ Hz, 1H), 3.79 (s, 3H), 3.46 (dd, $J = 11.3, 8.8$ Hz, 1H), 3.24 (dd, $J = 11.3, 4.5$ Hz, 1H), 2.62 (ddd, $J = 17.1, 10.3, 5.4$ Hz, 1H), 2.50 (ddd, $J = 17.0,$

6.8, 4.9 Hz, 1H); ^{13}C NMR (101 MHz, CDCl_3) δ 191.6, 172.0, 171.3, 159.6, 129.9, 127.5, 114.3, 105.7, 68.8, 60.2, 55.5, 47.1, 36.0, 29.3; $[\alpha]_D^{20} = +130.2^\circ$ (*c* 0.65, MeOH).

3-(4-methoxybenzyl)-4-(4-(2-phenylhydrazono)-3,4-dihydro-2H-pyran-6-yl)thiazolidin-2-one (4.056)

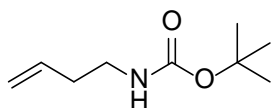


To 3-(4-methoxybenzyl)-4-(4-oxo-3,4-dihydro-2H-pyran-6-yl)thiazolidin-2-one (150 mg, 0.47 mmol) in MeOH (8 mL) was added phenyl hydrazine (25 μL , 0.25 mmol) and Dowex® resin (acidic) (230 mg) and the reaction mixture refluxed for 8 h. The Dowex® resin was then filtered off and washed repeatedly with hot MeOH. The filtrate was then evaporated to dryness. Flash chromatography, eluting with a gradient from 10% to 50% EtOAc/petroleum spirits gave the product (5%).

HPLC – rt 6.23 min > 99% purity at 254 nm; LRMS $[\text{M}+\text{H}]^+$ 410.10 m/z; HRMS $[\text{M}+\text{H}]^+$ 410.1533 m/z, found 410.1543 m/z; ^1H NMR (400 MHz, CDCl_3) δ 7.42 – 7.34 (m, 3H), 7.12 – 7.04 (m, 2H), 6.88 (m, 2H), 6.76 – 6.67 (m, 2H), 6.37 (s, 1H), 5.00 (d, *J* = 14.7 Hz, 1H), 4.71 (dd, *J* = 8.0, 5.3 Hz, 1H), 3.97 (t, *J* = 5.9 Hz, 2H), 3.76 (s, 3H), 3.69 (d, *J* = 14.7 Hz, 1H), 3.45 (dd, *J* = 11.0, 8.0 Hz, 1H), 3.13 (dd, *J* = 11.0, 5.3 Hz, 1H), 2.94 (t, *J* = 5.9 Hz, 2H); ^{13}C NMR (101 MHz, CDCl_3) δ 159.5, 152.1, 141.4, 138.6, 129.8, 129.6, 128.9, 127.4, 125.5, 114.3, 105.6, 61.7, 55.4, 53.9, 46.7, 32.7, 31.3; $[\alpha]_D^{20} = -31.5^\circ$ (*c* 0.37, MeOH).

7.5 Chapter 5 compounds

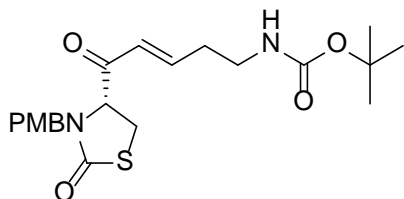
***tert*-butyl but-3-en-1-ylcarbamate (5.004) [23]**



3-buten-1-amine (100 mg, 0.77 mmol) was dissolved in DCM (7 mL) and triethylamine (0.4 mL) was added and cooled to 0°C. di-*tert*-butylcarbamate (336 mg, 1.54 mmol) was then added portion wise and stirred at room temperature for 12 h. At the completion of reaction as indicated by TLC analysis, the solvent was removed and then subjected to flash chromatography, eluting with 10% EtOAc/petroleum spirits to obtain the product as a clear oil (238 mg, 99%).

^1H NMR (400 MHz, CDCl_3) δ 5.75 (ddt, *J* = 17.1, 10.2, 6.8 Hz, 1H), 5.15 – 5.01 (m, 2H), 4.54 (s, 1H), 3.19 (dd, *J* = 12.3, 6.1 Hz, 2H), 2.24 (q, *J* = 6.8 Hz, 2H), 1.44 (s, 9H).

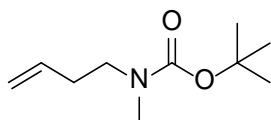
***tert*-butyl (*E*)-(5-(3-(4-methoxybenzyl)-2-oxothiazolidin-4-yl)-5-oxopent-3-en-1-yl)carbamate (5.005)**



To 4-acryloyl-3-(4-methoxybenzyl)thiazolidin-2-one (861.4 mg, 3.8 mmol) dissolved in DCE (9 mL) was added *tert*-butyl but-3-en-1-ylcarbamate (273 g, 1.6 mmol) and catalytic Hoveyda-Grubbs' II catalyst (100 mg, 0.16 mmol). The reaction was then heated to 50°C for 12 h. Upon completion of the reaction, as indicated by TLC analysis, the reaction mixture was filtered through celite to remove the catalyst and then subjected to flash chromatography, eluting with 15% EtOAc/petroleum spirits to obtain the product as a clear oil (256 mg, 38%).

HPLC – rt 6.70 min > 91% purity at 254 nm; LRMS no mass ion was detected; HRMS no mass ion was detected; ¹H NMR (400 MHz, CDCl₃) δ 7.11 (d, *J* = 8.6 Hz, 2H), 6.89 (m, 1H), 6.85 (dd, *J* = 6.4, 4.3 Hz, 2H), 6.23 (dt, *J* = 15.7, 1.4 Hz, 1H), 5.03 (d, *J* = 14.7 Hz, 1H), 4.59 (s, 1H), 4.28 (dd, *J* = 9.2, 4.2 Hz, 1H), 3.83 (d, *J* = 14.8 Hz, 1H), 3.79 (s, 3H), 3.49 (dd, *J* = 11.5, 9.3 Hz, 1H), 3.24 (t, *J* = 9.8 Hz, 2H), 3.13 (dd, *J* = 11.5, 4.5 Hz, 1H), 2.42 (dd, *J* = 12.6, 6.8 Hz, 2H), 1.43 (s, 9H); ¹³C NMR (101 MHz, CDCl₃) δ 194.8, 172.0, 159.4, 147.7, 130.1, 127.3, 114.2, 77.2, 55.3, 47.3, 38.6, 33.6, 31.0, 28.4, 28.0.

***tert*-butyl but-3-en-1-yl(methyl)carbamate (5.011) [24]**

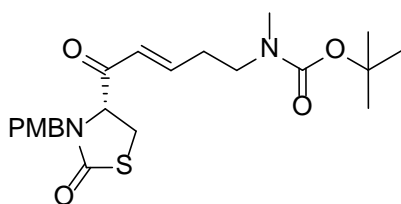


To *tert*-butyl but-3-en-1-ylcarbamate (214 mg, 1.25 mmol) in THF (4 mL) at 0°C was added NaH (126 mg, 3.75 mmol) slowly and stirred at room temperature for 1 h. Iodomethane (0.16 mL, 2.5 mmol) was then added and refluxed for 18 h. The reaction mixture was then allowed to cool to room temperature and ice was added before extracting with EtOAc. The organic layer was then washed with brine before drying with sodium sulphate and evaporating to dryness. Flash chromatography, eluting with 5% EtOAc/petroleum spirits yielded the product (212.8 mg, 92%).

¹H NMR (400 MHz, CDCl₃) δ 5.77 (ddt, *J* = 17.1, 10.2, 6.9 Hz, 1H), 5.15 – 4.93 (m, 2H), 3.26 (t, *J* = 7.2 Hz, 2H), 2.84 (s, 3H), 2.32 – 2.12 (m, 2H), 1.44 (d, *J* = 4.2 Hz, 9H).

***tert*-butyl (*R,E*)-(5-(3-(4-methoxybenzyl)-2-oxothiazolidin-4-yl)-5-oxopent-3-en-1-yl)(methyl)carbamate (5.012)**

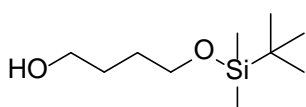
To 4-acryloyl-3-(4-methoxybenzyl)thiazolidin-2-one (780 mg, 3.43 mmol) dissolved in DCE (6 mL) was added *tert*-butyl but-3-en-1-yl(methyl)carbamate (212 g, 1.14 mmol) and catalytic



Hoveyda-Grubbs' II catalyst (71 mg, 0.114 mmol). The reaction was then heated to 50°C for 12 h. Upon completion of the reaction, as indicated by TLC analysis, the reaction mixture was filtered through celite to remove the catalyst and then subjected to flash chromatography, eluting with gradient from 15% to 25% EtOAc/petroleum spirits to obtain the product as a brown oil (252.8 mg, 51%).

HPLC – rt 7.37 min > 83% purity at 254 nm; LRMS $[M+Na]^+$ 457.2 m/z; HRMS $[M+Na]^+$ 457.1768 m/z, found 457.1772 m/z; 1H NMR (400 MHz, $CDCl_3$) δ 7.12 (m, 2H), 6.94 – 6.78 (m, 3H), 6.22 (d, J = 15.6 Hz, 1H), 5.05 (d, J = 14.7 Hz, 1H), 4.40 – 4.17 (m, 1H), 3.88 – 3.73 (m, 4H), 3.48 (dd, J = 11.4, 9.4 Hz, 1H), 3.33 (m, 2H), 3.12 (m, 1H), 2.84 (s, 3H), 2.44 (q, J = 6.5 Hz, 2H), 1.44 (s, 9H); ^{13}C NMR (101 MHz, $CDCl_3$) δ 194.8, 159.7, 148.2, 130.1, 127.5, 114.4, 71.8, 55.4, 48.4, 47.4, 36.9, 31.7, 29.8, 28.5.

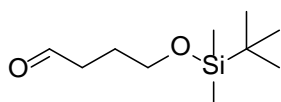
4-((*tert*-butyldimethylsilyl)oxy)butan-1-ol (5.021) [25]



Sodium hydride (186.5 mg, 5.55 mmol) was suspended in THF (11 mL), to which 1,4-butanediol (0.5 mL, 5.55 mmol) was added and stirred for 45 min when a large amount of white precipitate was formed. This was followed by the addition of TBSCl (837 mg, 5.55 mmol) portion wise. The reaction was allowed to stir for 4 h and then diluted with diethyl ether. The reaction mixture was washed with 10% aq. potassium carbonate solution and brine before being dried with sodium sulphate and evaporated to dryness. Flash chromatography, eluting with 20% EtOAc/petroleum spirits yielded the product contaminated with TBSOH (~5%) which was directly used for the next step without further purification.

1H NMR (400 MHz, $CDCl_3$) δ 3.65 (m, 4H), 1.69 – 1.60 (m, 4H), 0.90 (s, 9H), 0.07 (s, 6H).

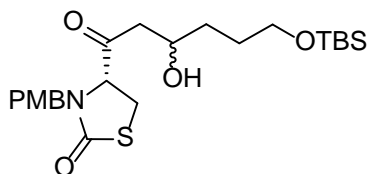
4-((*tert*-butyldimethylsilyl)oxy)butanal (5.022) [25]



Title compound was prepared from 4-((*tert*-butyldimethylsilyl)oxy)butan-1-ol (515 mg, 2.5 mmol) according to General Procedure A as a clear oil (91.4 mg, 24%).

1H NMR (400 MHz, $CDCl_3$) δ 9.77 – 9.74 (m, 1H), 3.62 (t, J = 5.9 Hz, 2H), 2.47 (t, J = 7.1 Hz, 2H), 1.82 (qd, J = 6.6, 3.4 Hz, 2H), 0.85 (s, 9H), 0.01 (s, 6H).

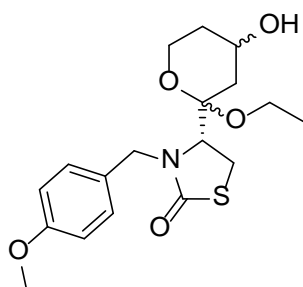
(4R)-4-(6-((*tert*-butyldimethylsilyl)oxy)-3-hydroxyhexanoyl)-3-(4-methoxybenzyl)thiazolidin-2-one (5.023)



Title compound was prepared from (*R*)-4-acetyl-3-(4-methoxybenzyl)thiazolidin-2-one (179 mg, 0.67 mmol) and 4-((*tert*-butyldimethylsilyl)oxy)butanal (91 mg, 0.45 mmol) according to General Procedure D as a mixture of three diastereomers, in 1: 0.2: 0.2 ratios (74 mg, 35%).

HPLC – rt 4.94 min > 95% purity at 254 nm; LRMS (only mass ion of the TBS-deprotected fragment was observed) [(M+Na)-C₆H₁₅Si₁]⁺ 376.1 m/z; HRMS no mass ion could be detected; ¹H NMR (400 MHz, CDCl₃) δ 7.14 – 7.09 (m, 2.8H), 6.87 – 6.82 (m, 2.8H), 5.09 – 4.92 (m, 1.4H), 4.45 – 4.01 (m, 2.8H), 3.95 – 3.86 (m, 1.4H), 3.83 (m, 4.2H), 3.72 – 3.60 (m, 2.8H), 3.42 – 3.55 (m, 1.4H), 3.10 – 3.35 (m, 1.4H), 2.65 – 2.55 (m, 1.4H), 2.45 – 2.30 (m, 1.4H), 1.70 – 1.41 (m, 5.6H), 0.89 (s, 12.6H), 0.07 (d, *J* = 1.4 Hz, 8.4H).

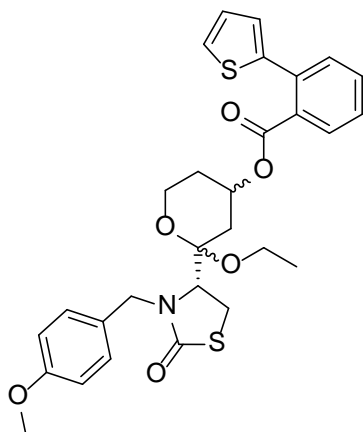
4-(2-ethoxy-4-hydroxytetrahydro-2H-pyran-2-yl)-3-(4-methoxybenzyl)thiazolidin-2-one (5.025)



Title compound was prepared according to General Procedure F using 4-(2,4-dihydroxytetrahydro-2H-pyran-2-yl)-3-(4-methoxybenzyl)thiazolidin-2-one (100 mg, 0.3 mmol) and EtOH (2 mL) as a milky oil and a mixture of two diastereomers; A and B in 1:0.44 ratio respectively (47.2 mg, 42%).

HPLC – rt (diastereomer A) 6.46 min (64%), (diastereomer B) 6.41 min (24%), collectively > 88% purity at 254 nm; LRMS [M+Na]⁺ 390.20 m/z; HRMS [M+Na]⁺ 390.1346 m/z, found 390.1341 m/z; ¹H NMR (400 MHz, CDCl₃) δ 7.20 (m, 2H), 7.10 (d, *J* = 8.5 Hz, 1H), 6.85 (m, 3H), 5.19 (d, *J* = 15.6 Hz, 0.5H), 5.01 (d, *J* = 14.3 Hz, 1H), 4.26 (m, 1.5H), 4.16 – 4.01 (m, 2H), 4.01 – 3.89 (m, 1H), 3.91 – 3.65 (m, 7.5H), 3.65 – 3.55 (m, 1H), 3.55 – 3.03 (m, 6.5H), 2.21 (ddd, *J* = 12.5, 4.6, 1.8 Hz, 1H), 2.10 (ddd, *J* = 12.8, 4.7, 1.7 Hz, 0.5H), 1.98 – 1.31 (m, 4.5H), 1.14 (dt, *J* = 14.1, 7.0 Hz, 4.5H); ¹³C NMR (101 MHz, CDCl₃) δ 173.6, 173.0, 159.2, 159.1, 130.2, 129.9, 129.7, 129.0, 128.8, 128.1, 114.3, 114.2, 114.2, 114.0, 103.3, 102.4, 64.5, 60.4, 60.3, 59.7, 57.6, 55.4, 55.4, 55.2, 54.8, 47.4, 46.7, 38.1, 37.4, 34.8, 34.6, 26.3, 25.5, 15.4, 15.1.

2-ethoxy-2-(3-(4-methoxybenzyl)-2-oxothiazolidin-4-yl)tetrahydro-2H-pyran-4-yl 2-(thiophen-2-yl)benzoate (5.034)

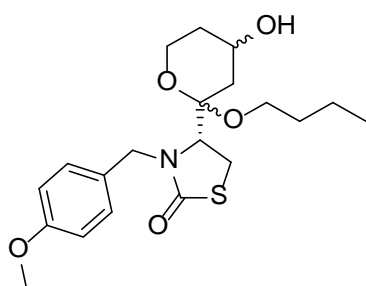


Title compound was prepared using 4-(2-ethoxy-4-hydroxytetrahydro-2H-pyran-2-yl)-3-(4-methoxybenzyl)thiazolidin-2-one (19.5 mg, 0.053 mmol) and 2-(thiophen-2-yl)benzoic acid (33 mg, 0.16 mmol) according to General Procedure G as a clear oil and a mixture of two diastereomers; A and B in 1:0.5 ratio respectively (80%).

HPLC – rt 9.21 min > 97% purity at 254 nm; LRMS $[M+Na]^+$ 576.2 m/z; HRMS $[M+Na]^+$ 576.1485 m/z, found 576.1501 m/z;

1H NMR (400 MHz, $CDCl_3$) δ 7.81 – 7.73 (m, 1.5H), 7.54 – 7.35 (m, 6H), 7.21 (d, J = 8.6 Hz, 2H), 7.09 (ddd, J = 8.7, 8.0, 6.0 Hz, 2.5H), 6.99 (dt, J = 3.5, 1.1 Hz, 1.5H), 6.91 – 6.80 (m, 3H), 5.29 – 5.17 (m, 2H), 5.01 (d, J = 14.4 Hz, 1H), 4.22 (dd, J = 15.0, 9.9 Hz, 1.5H), 3.96 (dd, J = 8.9, 4.0 Hz, 0.5H), 3.86 – 3.69 (m, 7H), 3.68 – 3.59 (m, 1H), 3.58 – 3.49 (m, 0.5H), 3.49 – 3.02 (m, 6H), 2.09 (ddd, J = 12.5, 4.7, 1.7 Hz, 2H), 1.89 (dddd, J = 9.6, 7.2, 4.6, 2.8 Hz, 1H), 1.56 – 1.25 (m, 3H), 1.16 (dt, J = 15.6, 7.0 Hz, 4.5H); ^{13}C NMR (101 MHz, $CDCl_3$) δ 172.8, 168.1, 168.0, 159.2, 142.2, 134.7, 132.3, 132.2, 131.6, 131.5, 131.2, 131.2, 130.2, 129.8, 129.7, 129.0, 128.8, 128.1, 128.0, 127.3, 126.6, 126.2, 126.0, 114.3, 114.1, 103.2, 102.3, 68.3, 59.9, 59.7, 57.2, 55.4, 55.4, 55.4, 54.9, 47.4, 46.6, 33.7, 33.2, 30.9, 30.8, 27.0, 26.2, 25.3, 15.4, 15.1.

4-(2-butoxy-4-hydroxytetrahydro-2H-pyran-2-yl)-3-(4-methoxybenzyl)thiazolidin-2-one (5.026)

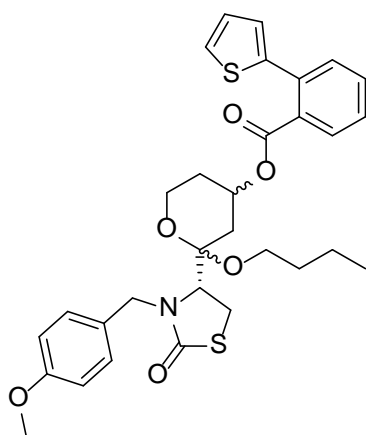


Title compound was prepared according to General Procedure F using 4-(2,4-dihydroxytetrahydro-2H-pyran-2-yl)-3-(4-methoxybenzyl)thiazolidin-2-one (112 mg, 0.33 mmol) and *n*-butanol (4 mL) as a clear oil and a mixture of two diastereomers; A and B in 1:0.4 ratio respectively (57.3 mg, 44%).

HPLC – rt (diastereomer A) 7.45 min (70%), (diastereomer B) 7.33 (23%), collectively > 93% purity at 254 nm; LRMS (only mass ion for the fragment obtained after elimination of water and methanol was observed) $[M-(H_2O + MeOH)]^+$ 304.1 m/z; HRMS $[M+H]^+$ 396.1839 m/z, found 396.1849 m/z; 1H NMR (**diastereomers A**) (400 MHz, $CDCl_3$) δ 7.22 (m, 2H), 6.85 (m, 2H), 5.01 (d, J = 14.4 Hz, 1H), 4.29 (d, J = 14.4 Hz, 1H), 4.15 – 4.01 (m, 1H), 3.90 – 3.81 (m, 2H), 3.79 (s, 3H), 3.66 – 3.57 (m, 1H), 3.44 – 3.34 (m, 1H), 3.31 – 3.20 (m, 2H), 3.07 (m, 1H), 2.21 (ddd, J = 12.4, 4.6, 1.8 Hz, 1H), 1.98 – 1.87 (m, 1H), 1.60 – 1.43 (m, 4H), 1.43 – 1.23 (m, 2H), 0.91 (m, 3H);

¹H NMR (**diastereomers B**) (400 MHz, CDCl₃) δ 7.10 (m, 2H), 6.85 (m, 2H), 5.20 (d, *J* = 15.6 Hz, 1H), 4.23 (d, *J* = 15.6 Hz, 1H), 4.15 – 4.01 (m, 1H), 3.99 (dd, *J* = 8.0, 5.0 Hz, 1H), 3.82 – 3.73 (m, 4H), 3.57 – 3.48 (m, 1H), 3.44 – 3.34 (m, 2H), 3.31 – 3.20 (m, 1H), 3.07 (m, 1H), 2.10 (ddd, *J* = 12.7, 4.7, 1.8 Hz, 1H), 1.98 – 1.87 (m, 1H), 1.66 (dd, *J* = 12.6, 10.9 Hz, 1H), 1.60 – 1.43 (m, 3H), 1.43 – 1.23 (m, 2H), 0.91 (m, 3H); ¹³C NMR (101 MHz, CDCl₃) δ 173.5, 173.0, 159.2, 159.1, 130.2, 130.0, 129.1, 128.8, 128.2, 114.3, 114.0, 103.2, 102.4, 64.5, 60.3, 60.2, 59.7, 59.4, 59.2, 57.4, 55.4, 55.4, 47.5, 46.6, 38.2, 37.5, 34.8, 34.6, 32.0, 26.3, 25.5, 19.7, 19.7, 14.3, 14.1.

2-butoxy-2-((*R*)-3-(4-methoxybenzyl)-2-oxothiazolidin-4-yl)tetrahydro-2H-pyran-4-yl 2-(thiophen-2-yl)benzoate (5.035)

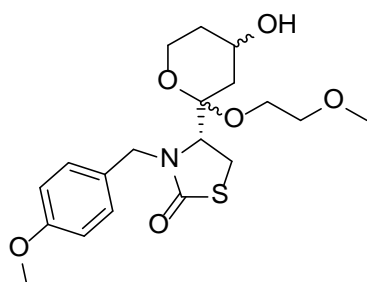


Title compound was prepared using 4-(2-butoxy-4-hydroxytetrahydro-2H-pyran-2-yl)-3-(4-methoxybenzyl)thiazolidin-2-one (51.3 mg, 0.13 mmol) and 2-(thiophen-2-yl)benzoic acid (79 mg, 0.39 mmol) according to General Procedure G as a clear oil and a mixture of two diastereomers; A and B in 1:0.5 ratio respectively (38.7 mg, 51%).

HPLC – rt 9.79 min > 99% purity at 254 nm; LRMS [M+Na]⁺ 604.2 m/z; HRMS [M+H]⁺ 582.1979 m/z, found 582.1991 m/z; ¹H NMR (400 MHz, CDCl₃) δ 7.77 (m, 1.5H), 7.54 – 7.37 (m, 6H), 7.21 (m, 2H), 7.13 – 7.06 (m, 2.5H), 6.98 (m, 1.5H), 6.90 – 6.82 (m, 3H), 5.26 – 5.15 (m, 2H), 5.00 (d, *J* = 14.4 Hz, 1H), 4.24 (d, *J* = 14.2 Hz, 1H), 4.21 (d, *J* = 14.9 Hz, 0.5H), 3.98 (dd, *J* = 8.9, 4.0 Hz, 0.5H), 3.86 – 3.81 (m, 1.5H), 3.79 (s, 4.5H), 3.78 – 3.68 (m, 1H), 3.68 – 3.60 (m, 1H), 3.59 – 3.50 (m, 0.5H), 3.43 – 3.17 (m, 4.5H), 3.12 – 2.98 (m, 1.5H), 2.09 (ddd, *J* = 12.5, 4.7, 1.7 Hz, 1H), 1.97 – 1.82 (m, 2H), 1.60 – 1.24 (m, 9H), 0.92 (m, 4.5H); ¹³C NMR (101 MHz, CDCl₃) δ 173.2, 172.8, 168.0, 167.9, 159.2, 159.1, 142.2, 134.7, 134.5, 132.3, 132.2, 131.6, 131.5, 131.2, 131.1, 130.2, 129.8, 129.7, 129.0, 128.8, 128.1, 128.0, 127.3, 126.6, 126.1, 126.0, 114.3, 114.0, 103.1, 102.2, 68.3, 59.74, 59.66, 59.56, 59.32, 57.13, 55.40, 55.36, 47.42, 46.50, 33.70, 33.17, 31.95, 30.84, 30.7, 27.0, 26.2, 25.3, 19.7, 19.6, 14.3, 14.0.

4-(4-hydroxy-2-(2-methoxyethoxy)tetrahydro-2H-pyran-2-yl)-3-(4-methoxybenzyl)thiazolidin-2-one (5.028)

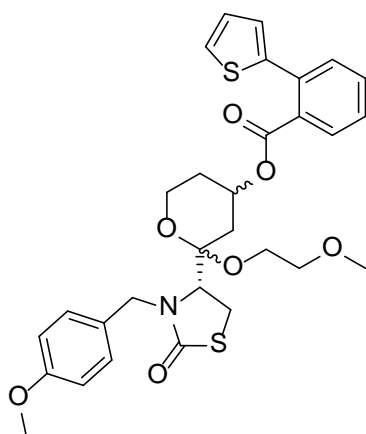
Title compound was prepared according to General Procedure F using 4-(2,4-dihydroxytetrahydro-2H-pyran-2-yl)-3-(4-methoxybenzyl)thiazolidin-2-one (112 mg, 0.329 mmol) and 2-



methoxyethanol (10 mL) as a clear oil and a mixture of two diastereomers; A and B in 1:1 ratio respectively (43 mg, 32%).

HPLC – rt 5.4 min > 87% purity at 254 nm; LRMS $[M+Na]^+$ 420.2 m/z; HRMS $[M+H]^+$ 398.1632 m/z, found 398.1625 m/z; 1H NMR (400 MHz, $CDCl_3$) δ 7.22 (d, J = 8.7 Hz, 2H), 7.14 – 7.08 (m, 2H), 6.89 – 6.80 (m, 4H), 5.03 (dd, J = 14.6, 1.9 Hz, 2H), 4.31 – 4.24 (m, 2H), 4.15 – 4.05 (m, 2H), 3.86 (m, 2H), 3.83 – 3.74 (m, 11H), 3.70 (m, 1H), 3.63 (m, 1H), 3.59 – 3.20 (m, 15H), 2.26 (ddd, J = 12.6, 4.6, 2.0 Hz, 1H), 1.95 (m, 2H), 1.67 (m, 1H), 1.56 – 1.40 (m, 4H); ^{13}C NMR (101 MHz, $CDCl_3$) δ 173.0, 130.2, 130.1, 129.0, 127.5, 114.4, 114.3, 114.2, 114.1, 71.8, 64.5, 64.1, 60.9, 60.6, 60.4, 59.7, 59.5, 59.3, 55.5, 55.4, 47.5, 47.5, 37.4, 35.9, 34.7, 28.1, 25.6.

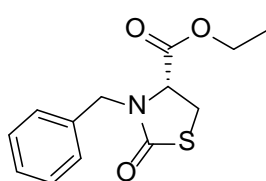
2-((R)-3-(4-methoxybenzyl)-2-oxothiazolidin-4-yl)-2-(2-methoxyethoxy)tetrahydro-2H-pyran-4-yl 2-(thiophen-2-yl)benzoate (5.036)



Title compound was prepared using 4-(4-hydroxy-2-(2-methoxyethoxy)tetrahydro-2H-pyran-2-yl)-3-(4-methoxybenzyl)thiazolidin-2-one (40 mg, 0.1 mmol) and 2-(thiophen-2-yl)benzoic acid (62 mg, 0.3 mmol) according to General Procedure G as a clear oil (10.4 mg, 18%).

HPLC – rt 8.82 min > 99% purity at 254 nm; LRMS $[M+Na]^+$ 606.2 m/z; HRMS $[M+Na]^+$ 606.1591 m/z, found 606.1608 m/z; 1H NMR (400 MHz, $CDCl_3$) δ 7.77 (dd, J = 7.6, 0.9 Hz, 1H), 7.55 – 7.35 (m, 4H), 7.20 (m, 2H), 7.09 (dd, J = 5.1, 3.5 Hz, 1H), 6.98 (dd, J = 3.5, 1.1 Hz, 1H), 6.85 (m, 2H), 5.30 – 5.14 (m, 1H), 5.01 (d, J = 14.4 Hz, 1H), 4.23 (d, J = 14.4 Hz, 1H), 3.80 (m, 5H), 3.77 – 3.67 (m, 1H), 3.57 – 3.50 (m, 1H), 3.49 – 3.41 (m, 2H), 3.33 (s, 3H), 3.31 – 3.20 (m, 3H), 2.13 (ddd, J = 12.6, 4.7, 1.6 Hz, 1H), 1.89 (m, 1H), 1.50 – 1.28 (m, 2H); ^{13}C NMR (101 MHz, $CDCl_3$) δ 172.9, 167.9, 159.2, 142.2, 134.7, 132.2, 131.6, 131.2, 130.2, 129.9, 129.0, 128.0, 127.4, 126.6, 126.0, 114.1, 103.4, 71.7, 68.2, 59.9, 59.7, 59.7, 59.3, 55.4, 47.5, 33.0, 30.7, 25.4.

ethyl 3-benzyl-2-oxothiazolidine-4-carboxylate (5.040) [26]

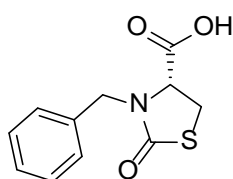


To a stirred suspension of (*R*)-ethyl 2-oxothiazolidine-4-carboxylate (500 g, 2.85 mmol), DMF (13 mL), potassium carbonate (591 g, 4.3 mmol) and catalytic amount of sodium iodide (21 mg, 0.14 mmol), benzylbromide (0.7 mL, 5.7 mmol) was added drop-wise. The reaction was stirred

overnight at room temperature. After the completion of the reaction, diethyl ether was then added and the suspension washed with brine (x 3). The organic layer was dried with magnesium sulphate, filtered and evaporated to dryness. Flash chromatography, eluting with 5% EtOAc/petroleum spirits yielded the product as a clear oil (446 mg, 62%).

^1H NMR (400 MHz, CDCl_3) δ 7.39 – 7.29 (m, 3H), 7.26 – 7.21 (m, 2H), 5.16 (d, J = 15.0 Hz, 1H), 4.24 (q, J = 7.1 Hz, 2H), 4.14 (dd, J = 8.6, 3.0 Hz, 1H), 4.05 (d, J = 15.0 Hz, 1H), 3.51 (dd, J = 11.4, 8.5 Hz, 1H), 3.35 (dd, J = 11.4, 3.0 Hz, 1H), 1.30 (t, J = 7.1 Hz, 3H).

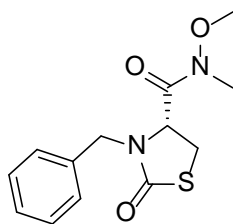
3-benzyl-2-oxothiazolidine-4-carboxylic acid (5.042)



Title compound was prepared from ethyl 3-benzyl-2-oxothiazolidine-4-carboxylate (6.8 g, 27 mmol) using General Procedure C as a white solid (5.5 g, 85%).

HPLC – rt 5.30 min > 99% purity at 254 nm; LRMS $[\text{M}+\text{H}]^+$ 238.0 m/z; HRMS $[\text{M}+\text{H}]^+$ 238.0532 m/z, found 238.0531 m/z; ^1H NMR (400 MHz, CDCl_3) δ 7.40 – 7.29 (m, 3H), 7.28 – 7.24 (m, 2H), 5.23 (d, J = 15.0 Hz, 1H), 4.21 (dd, J = 8.6, 2.5 Hz, 1H), 4.05 (d, J = 15.0 Hz, 1H), 3.56 (dd, J = 11.5, 8.6 Hz, 1H), 3.42 (dd, J = 11.5, 2.5 Hz, 1H); ^{13}C NMR (101 MHz, CDCl_3) δ 173.4, 172.9, 135.5, 129.1, 128.4, 128.3, 59.4, 47.9, 29.3.

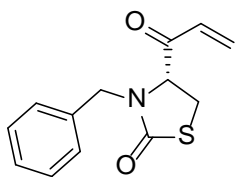
3-benzyl-N-methoxy-N-methyl-2-oxothiazolidine-4-carboxamide (5.044)



Title compound was prepared from 3-benzyl-2-oxothiazolidine-4-carboxylic acid (1 g, 4.2 mmol) according to General Procedure H as a white solid (1.1 g, 93%).

HPLC – rt 5.86 min > 99% purity at 254 nm; LRMS $[\text{M}+\text{H}]^+$ 281.1 m/z; HRMS $[\text{M}+\text{H}]^+$ 281.0954 m/z, found 281.0951 m/z; ^1H NMR (400 MHz, CDCl_3) δ 7.39 – 7.20 (m, 5H), 5.23 (d, J = 14.8 Hz, 1H), 4.40 (dd, J = 8.7, 5.2 Hz, 1H), 3.90 (d, J = 14.8 Hz, 1H), 3.47 (dd, J = 11.3, 8.7 Hz, 1H), 3.32 (s, 3H), 3.20 (s, 3H), 3.16 (dd, J = 11.3, 5.2 Hz, 1H); ^{13}C NMR (101 MHz, CDCl_3) δ 172.6, 169.2, 135.8, 129.0, 128.8, 128.2, 61.3, 57.6, 47.7, 32.6, 28.2.

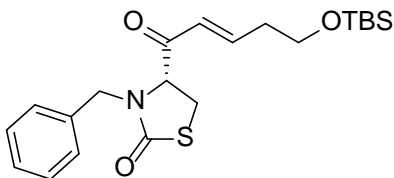
4-acryloyl-3-benzylthiazolidin-2-one (5.046)



To 3-benzyl-*N*-methoxy-*N*-methyl-2-oxothiazolidine-4-carboxamide (704 mg, 2.5 mmol) in THF (8mL) at 0°C, 1.5 M vinylmagnesium bromide (6.8 mL) was added drop wise and stirred overnight. After completion of the reaction, 2 M aq. HCl solution was added and then extracted with DCM (x 3). The combined organic layer was washed with saturated sodium bicarbonate solution, dried with sodium sulphate and evaporated to dryness. Flash chromatography, eluting with a gradient from 10% EtOAc/petroleum spirits to 50% EtOAc/petroleum spirits led to the isolation of the product (589 mg, 95%).

HPLC – rt 6.70 min > 92% purity at 254 nm; LRMS $[M+H]^+$ 248.2 m/z; HRMS $[M+H]^+$ 248.0740 m/z, found 248.0742m/z; 1H NMR (400 MHz, $CDCl_3$) δ 7.38 – 7.26 (m, 3H), 7.19 (dd, J = 7.3, 1.8 Hz, 2H), 6.48 (dd, J = 17.4, 10.4 Hz, 1H), 6.36 (dd, J = 17.4, 1.3 Hz, 1H), 5.91 (dd, J = 10.4, 1.3 Hz, 1H), 5.16 (d, J = 14.9 Hz, 1H), 4.35 (dd, J = 9.4, 4.3 Hz, 1H), 3.85 (d, J = 14.9 Hz, 1H), 3.53 (dd, J = 11.5, 9.4 Hz, 1H), 3.15 (dd, J = 11.5, 4.3 Hz, 1H); ^{13}C NMR (101 MHz, $CDCl_3$) δ 195.3, 172.1, 135.5, 131.9, 131.4, 129.1, 128.7, 128.3, 63.7, 48.0, 27.9.

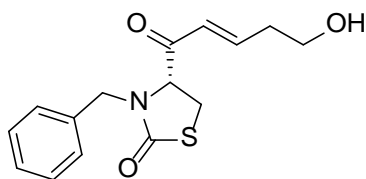
(*E*)-3-benzyl-4-(5-((*tert*-butyldimethylsilyl)oxy)pent-2-enoyl)thiazolidin-2-one (5.048)



To of 4-acryloyl-3-benzylthiazolidin-2-one (560 mg, 2.26 mmol) dissolved in DCE (12 mL) was added (but-3-en-1-yloxy)(*tert*-butyl)dimethylsilane (1.27 g, 6.8 mmol) and catalytic Hoveyda-Grubbs' II catalyst (142 mg, 0.23 mmol). The reaction was then heated to 50°C for 12 h. Upon completion of the reaction, as indicated by TLC analysis, the reaction mixture was filtered through celite to remove the catalyst and then subjected to flash chromatography, eluting with 15% EtOAc/petroleum spirits to obtain the product (150 mg, 67%).

HPLC – rt 9.46 min > 81% purity at 254 nm; LRMS $[M+H]^+$ 406.2 m/z; HRMS $[M+H]^+$ 406.1867m/z, found 406.1856m/z; 1H NMR (400 MHz, $CDCl_3$) δ 7.35 – 7.27 (m, J = 7.1, 3.6 Hz, 3H), 7.22 – 7.15 (m, 2H), 7.00 (dt, J = 15.6, 7.0 Hz, 1H), 6.25 (dt, J = 15.7, 1.5 Hz, 1H), 5.14 (d, J = 15.0 Hz, 1H), 4.29 (dd, J = 9.3, 4.4 Hz, 1H), 3.83 (d, J = 14.9 Hz, 1H), 3.72 (t, J = 6.1 Hz, 2H), 3.49 (dd, J = 11.4, 9.4 Hz, 1H), 3.13 (dd, J = 11.4, 4.4 Hz, 1H), 2.46 – 2.37 (m, J = 7.4, 1.3 Hz, 2H), 0.87 (s, 9H), 0.04 (s, 6H); ^{13}C NMR (101 MHz, $CDCl_3$) δ 194.7, 172.2, 148.9, 135.5, 129.0, 128.6, 128.2, 126.3, 63.8, 61.2, 47.9, 36.3, 28.1, 26.0, -5.2.

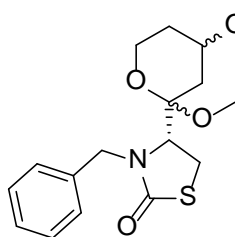
(E)-3-benzyl-4-(5-hydroxypent-2-enoyl)thiazolidin-2-one (5.015)



Title compound was prepared from (*E*)-3-benzyl-4-(5-((*tert*-butyldimethylsilyl)oxy)pent-2-enoyl)thiazolidin-2-one (29 mg, 0.07 mmol) according to General Procedure E (13.3 mg, 86%).

HPLC – rt 6.30 min > 99% purity at 254 nm; LRMS $[M+H]^+$ 292.2 m/z; HRMS $[M+H]^+$ 292.1002 m/z, found 292.1002 m/z; 1H NMR (400 MHz, $CDCl_3$) δ 7.37 – 7.28 (m, 3H), 7.24 – 7.17 (m, 2H), 7.07 – 6.95 (m, 1H), 6.30 (dt, J = 15.7, 1.5 Hz, 1H), 5.13 (d, J = 14.9 Hz, 1H), 4.30 (dd, J = 9.3, 4.4 Hz, 1H), 3.88 (d, J = 14.9 Hz, 1H), 3.79 (t, J = 6.2 Hz, 2H), 3.52 (dd, J = 11.4, 9.3 Hz, 1H), 3.16 (dd, J = 11.5, 4.4 Hz, 1H), 2.49 (ddd, J = 13.2, 6.2, 1.5 Hz, 2H); ^{13}C NMR (101 MHz, $CDCl_3$) δ 194.8, 172.4, 148.1, 135.5, 129.0, 128.7, 128.2, 126.7, 64.0, 60.8, 48.0, 36.0, 28.2.

3-benzyl-4-(4-hydroxy-2-methoxytetrahydro-2H-pyran-2-yl)thiazolidin-2-one (5.037)

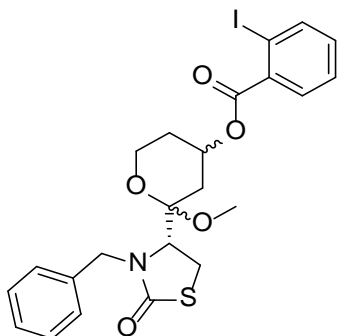


Title compound was prepared in two steps. In the first step, the starting material, (*E*)-3-benzyl-4-(5-((*tert*-butyldimethylsilyl)oxy)pent-2-enoyl)thiazolidin-2-one (391.6 mg, 0.965 mmol) was converted to the hemiacetal 3-benzyl-4-(2,4-dihydroxytetrahydro-2H-pyran-2-yl)thiazolidin-2-one according to General Procedure E (262.7 mg, 88%).

The product obtained was treated with MeOH according to General Procedure F to obtain the title compound as two diastereomers A and B in 1: 0.6 ratios respectively (157.3 mg, 57%).

1H NMR (400 MHz, $CDCl_3$) δ 7.41 – 7.17 (m, 8H), 5.29 (d, J = 15.8 Hz, 0.6H), 5.06 (d, J = 14.5 Hz, 1H), 4.39 (d, J = 14.6 Hz, 1H), 4.29 (d, J = 15.8 Hz, 0.6H), 4.10 – 3.99 (m, 1.6H), 3.96 (dd, J = 8.8, 4.0 Hz, 0.6H), 3.86 (m, 1.6H), 3.83 – 3.76 (m, 1H), 3.60 (ddd, J = 13.7, 11.4, 2.4 Hz, 1H), 3.56 – 3.48 (m, 0.6H), 3.44 – 3.15 (m, 3.2H), 3.08 (s, 3H), 2.98 (s, 1.8H), 2.21 (ddd, J = 12.5, 4.7, 2.0 Hz, 1H), 2.12 (ddd, J = 12.6, 4.7, 1.9 Hz, 0.6H), 1.98 – 1.86 (m, 1.6H), 1.69 (dd, J = 12.8, 10.9 Hz, 1H), 1.61 – 1.30 (m, 2.2H).

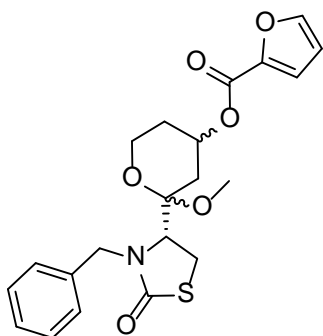
2-(3-benzyl-2-oxothiazolidin-4-yl)-2-methoxytetrahydro-2H-pyran-4-yl 2-iodobenzoate (5.053)



Title compound was prepared from 3-benzyl-4-(4-hydroxy-2-methoxytetrahydro-2H-pyran-2-yl)thiazolidin-2-one (100 mg, 0.31 mmol) and 2-iodobenzoic acid (230 mg, 0.93 mmol) according to the General Procedure G as a clear oil and a mixture of two diastereomers; A and B in 1:0.7 ratio respectively (153.6 mg, 89%).

HPLC – rt 8.75 min > 99% purity at 254 nm; LRMS $[M+H]^+$ 554.0 m/z; HRMS $[M+H]^+$ 554.0493 m/z, found 554.0519 m/z; 1H NMR (400 MHz, $CDCl_3$) δ 7.99 (m, 1.7H), 7.79 (m, 1.7H), 7.42 (m, 1.7H), 7.39 – 7.27 (m, 7.5H), 7.22 (m, 1H), 7.16 (m, 1.7H), 5.43 (m, 1.7H), 5.30 (d, J = 15.9 Hz, 0.7H), 5.08 (d, J = 14.6 Hz, 1H), 4.42 (d, J = 14.6 Hz, 1H), 4.31 (d, J = 15.8 Hz, 0.7H), 4.00 (dd, J = 7.6, 5.2 Hz, 0.7H), 3.96 – 3.82 (m, 2.7H), 3.79 – 3.70 (m, 1H), 3.66 (dd, J = 18.1, 6.5 Hz, 0.7H), 3.46 – 3.23 (m, 3.4H), 3.13 (s, 3H), 3.03 (s, 2.1H), 2.38 (ddd, J = 12.4, 4.8, 1.9 Hz, 1H), 2.28 (ddd, J = 12.6, 4.7, 1.8 Hz, 0.7H), 2.24 – 2.17 (m, 0.7H), 2.17 – 2.08 (m, 1H), 2.00 (dd, J = 12.7, 11.3 Hz, 0.7H), 1.87 – 1.79 (m, 1H), 1.80 – 1.58 (m, 1.7H); ^{13}C NMR (101 MHz, $CDCl_3$) δ 173.2, 166.0, 141.5, 141.4, 137.0, 136.7, 135.0, 132.9, 132.8, 131.2, 131.1, 129.0, 128.8, 128.7, 128.1, 127.8, 127.7, 127.2, 103.3, 102.5, 94.3, 94.2, 69.1, 69.0, 60.1, 59.9, 59.7, 56.9, 48.4, 47.8, 47.7, 47.4, 34.3, 33.7, 31.2, 31.1, 26.3, 25.4.

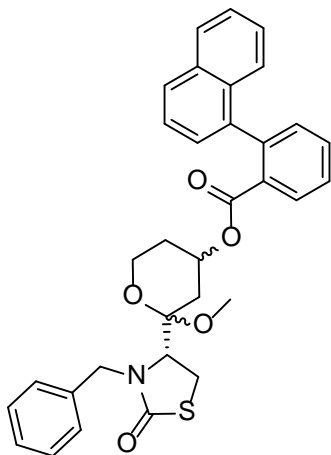
2-((R)-3-benzyl-2-oxothiazolidin-4-yl)-2-methoxytetrahydro-2H-pyran-4-yl furan-2-carboxylate (5.052)



Title compound was prepared from 3-benzyl-4-(4-hydroxy-2-methoxytetrahydro-2H-pyran-2-yl)thiazolidin-2-one (50 mg, 0.15 mmol) and 2-furoic acid (52 mg, 0.46 mmol) according to the General Procedure G as a clear oil and a mixture of two diastereomers; A and B in 1:0.6 ratio respectively (62.5 mg, 99%).

HPLC – rt 7.87 min > 95% purity at 254 nm; LRMS $[M+Na]^+$ 440.10 m/z; HRMS $[M+H]^+$ 418.1319 m/z, found 418.1325 m/z; 1H NMR (400 MHz, $CDCl_3$) δ 7.54 – 6.40 (m, 12.8H), 5.40 – 5.27 (m, 1.6H), 5.24 (m, 0.6H), 5.06 (d, J = 14.6 Hz, 1H), 4.35 (d, J = 14.5 Hz, 1H), 4.24 (d, J = 15.7 Hz, 0.6H), 3.95 – 3.83 (m, 3.2H), 3.64 (m, 1.6H), 3.37 – 3.26 (m, 3.2H), 3.07 (s, 3H), 2.97 (s, 1.8H), 2.26 (m, 1H), 2.18 (m, 0.6H), 2.04 (m, 1.6H), 1.91 (m, 0.6H), 1.76 (m, 1H), 1.72 – 1.41 (m, 1.6H); ^{13}C NMR (101 MHz, $CDCl_3$) δ 146.6, 129.0, 128.8, 128.7, 127.8, 127.7, 127.2, 118.4, 118.3, 112.0, 68.1, 68.0, 60.0, 59.9, 59.6, 56.8, 48.3, 47.7, 47.3, 34.3, 33.7, 31.3, 31.2, 26.2, 25.4.

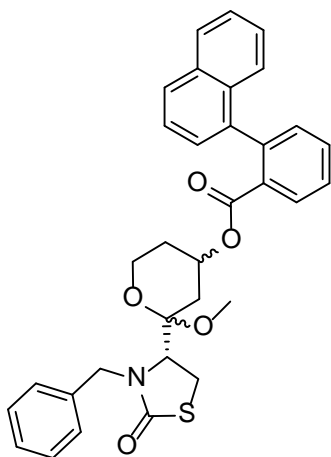
2-((*R*)-3-benzyl-2-oxothiazolidin-4-yl)-2-methoxytetrahydro-2H-pyran-4-yl 2-(naphthalen-1-yl)benzoate (5.054a)



Title compound was prepared from 2-(3-benzyl-2-oxothiazolidin-4-yl)-2-methoxytetrahydro-2H-pyran-4-yl 2-iodobenzoate (87.3 mg, 0.16 mmol) and 1-naphthalene boronic acid (32.6 mg, 0.19 mmol) according to the General Procedure I as a white semisolid as a mixture of two diastereomers with a combined yield of 50%. Diastereomer A was isolated in 27% yield. The proton and carbon NMR spectrum show peak splitting due to axial chirality (1:0.76 ratio).

HPLC – rt 4.59 min > 96% purity at 254 nm; LRMS $[M+H]^+$ 554.20 m/z; HRMS $[M+H]^+$ 554.1996 m/z, found 554.2007 m/z; 1H NMR (400 MHz, $CDCl_3$) δ 8.07 – 8.04 (m, 1.76H), 8.00 – 7.91 (m, 3.52H), 7.63 (m, 1.76H), 7.58 – 7.13 (m, 21.12H), 5.23 (d, J = 14.6 Hz, 1H), 5.19 (d, J = 14.6 Hz, 0.76H), 4.87 – 4.75 (m, 1.76H), 4.15 – 4.02 (m, 1.76H), 3.69 – 3.71 (m, 2.52H), 3.53 – 3.43 (m, 1H), 2.98 – 2.93 (m, 1.76H), 3.22 – 3.16 (m, 3.52H), 2.98 – 2.74 (m, 5.28H), 1.63 – 1.50 (m, 1.76H), 1.49 – 1.40 (m, 1H), 1.37 – 1.23 (m, 0.76H), 0.97 – 0.80 (m, 1.76H), 0.76 – 0.51 (m, 1.76H); ^{13}C NMR (101 MHz, $CDCl_3$) δ 173.5, 173.4, 167.2, 167.2, 141.3, 141.3, 140.2, 140.1, 136.5, 136.5, 133.3, 133.2, 132.5, 132.4, 132.1, 131.9, 131.8, 131.8, 131.7, 130.5, 130.5, 128.9, 128.5, 128.3, 127.8, 127.8, 127.6, 127.6, 127.1, 126.3, 126.1, 126.0, 125.9, 125.9, 125.9, 125.6, 125.4, 125.3, 102.1, 102.0, 67.4, 67.3, 59.7, 59.6, 56.7, 56.6, 47.5, 47.2, 41.0, 32.8, 32.3, 30.4, 29.9, 26.1, 24.0, 22.8, 20.9.

2-((*R*)-3-benzyl-2-oxothiazolidin-4-yl)-2-methoxytetrahydro-2H-pyran-4-yl 2-(naphthalen-1-yl)benzoate (5.054b)

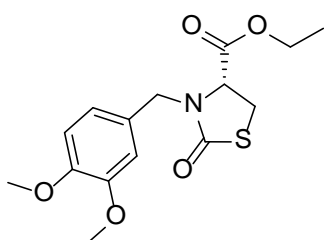


Title compound was prepared from 2-(3-benzyl-2-oxothiazolidin-4-yl)-2-methoxytetrahydro-2H-pyran-4-yl 2-iodobenzoate and 1-naphthalene boronic acid according to the General Procedure I as a white semisolid in 50% yield as a mixture of two diastereomers. Diastereomer B was isolated in 21% yield. The proton and carbon NMR spectrum show the peak splitting due to axial chirality (1:0.76 ratio).

HPLC – rt 4.24 min > 99% purity at 254 nm; LRMS $[M+K]^+$ 592.2 m/z; HRMS $[M+Na]^+$ 576.1815 m/z, found 576.1824 m/z; 1H NMR (400 MHz, $CDCl_3$) δ 8.11 – 8.04 (m, 1.76H), 8.00 – 7.89 (m, 3.52H), 7.63 (m, 1.76H), 7.58 – 7.19

(m, 21.12H), 5.07 (d, $J = 14.6$ Hz, 1H), 4.99 (d, $J = 14.6$ Hz, 0.76H), 4.87 – 4.75 (m, 1.76H), 4.12 (m, 1.76H), 3.69 (m, 1.76H), 3.65 – 3.57 (m, 0.76H), 3.56 – 3.48 (m, 1H), 3.45 – 3.30 (m, 1.76H), 3.22 – 2.76 (m, 3.52H), 2.95 – 2.93 (m, 5.28H), 1.63 – 1.23 (m, 3.52H), 0.97 – 0.51 (m, 3.52H); ^{13}C NMR (101 MHz, CDCl_3) δ 173.0, 172.8, 167.1, 167.0, 141.5, 141.4, 140.2, 140.1, 136.8, 133.3, 133.2, 132.5, 132.4, 132.2, 132.0, 132.0, 131.8, 131.8, 131.7, 131.6, 130.6, 130.4, 128.9, 128.7, 128.7, 128.6, 128.5, 128.4, 128.3, 127.9, 127.8, 127.8, 127.7, 127.7, 127.1, 126.3, 126.1, 126.0, 126.0, 125.9, 125.8, 125.7, 125.7, 125.6, 125.3, 125.1, 102.7, 102.6, 67.3, 67.2, 59.6, 59.6, 59.5, 59.2, 48.0, 47.9, 47.5, 47.5, 32.5, 32.2, 30.26, 29.6, 24.9, 24.9.

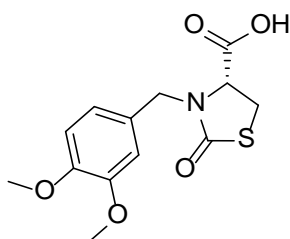
ethyl 3-(3,4-dimethoxybenzyl)-2-oxothiazolidine-4-carboxylate (5.041)



To a stirred suspension of (*R*)-ethyl 2-oxothiazolidine-4-carboxylate (138 mg, 0.72 mmol), DMF (3 mL), potassium carbonate (169 mg, 1.2 mmol) and catalytic amount of sodium iodide (6 mg, 0.036 mmol), 3,4-dimethoxy benzylchloride (220 mg, 1.16 mmol) was added dropwise. The reaction was stirred overnight at room temperature. After the completion of the reaction, diethyl ether was added and the suspension washed with brine (x 3). The organic layer was dried with magnesium sulphate, filtered and evaporated. Flash chromatography, eluting with 25% EtOAc/petroleum spirits yielded the product as a clear oil (175 mg, 75%).

HPLC – rt 6.17 min > 99% purity at 254 nm; LRMS $[\text{M}+\text{Na}]^+$ 348.1 m/z; HRMS $[\text{M}+\text{Na}]^+$ 348.0876 m/z, found 348.0881 m/z; ^1H NMR (400 MHz, CDCl_3) δ 6.77 (m, 3H), 5.08 (d, $J = 14.7$ Hz, 1H), 4.25 (q, $J = 7.1$ Hz, 2H), 4.13 (dd, $J = 8.5, 3.2$ Hz, 1H), 3.99 (d, $J = 14.7$ Hz, 1H), 3.87 (d, $J = 2.9$ Hz, 6H), 3.48 (dd, $J = 11.4, 8.5$ Hz, 1H), 3.34 (dd, $J = 11.4, 3.2$ Hz, 1H), 1.31 (t, $J = 7.1$ Hz, 3H); ^{13}C NMR (101 MHz, CDCl_3) δ 171.8, 170.1, 149.5, 149.1, 128.2, 121.1, 111.7, 111.3, 62.3, 59.5, 56.1, 56.1, 47.9, 29.2, 14.3.

3-(3,4-dimethoxybenzyl)-2-oxothiazolidine-4-carboxylic acid (5.043)

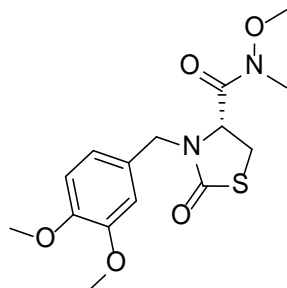


Title compound was prepared from ethyl 3-(3,4-dimethoxybenzyl)-2-oxothiazolidine-4-carboxylate (1.92 g, 5.9 mmol) according to General Procedure C as a yellow oil (1.58 g, 90%).

HPLC – rt 4.65 min > 99% purity at 254 nm; LRMS $[\text{M}+\text{Na}]^+$ 320.0 m/z; HRMS $[\text{M}+\text{H}]^+$ 298.0744 m/z, found 298.0758 m/z; ^1H NMR (400 MHz, CDCl_3) δ 6.85 – 6.75 (m, 3H), 5.13 (d, $J = 14.8$ Hz, 1H), 4.20 (dd, $J = 8.6, 2.7$ Hz, 1H), 4.01 (d, $J = 14.8$ Hz, 1H), 3.87

(d, $J = 1.2$ Hz, 6H), 3.53 (dd, $J = 11.5, 8.6$ Hz, 1H), 3.41 (dd, $J = 11.5, 2.7$ Hz, 1H); ^{13}C NMR (101 MHz, CDCl_3) δ 173.6, 171.9, 149.6, 149.2, 128.0, 121.2, 111.7, 111.3, 58.9, 56.2, 56.1, 47.9, 29.2.

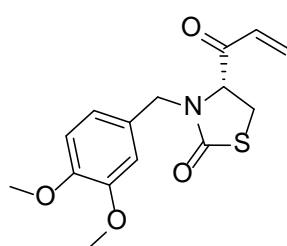
3-(3,4-dimethoxybenzyl)-N-methoxy-N-methyl-2-oxothiazolidine-4-carboxamide (5.045)



Title compound was prepared from 3-(3,4-dimethoxybenzyl)-2-oxothiazolidine-4-carboxylic acid (1.58 g, 5.3 mmol) according to General Procedure H (1.26 g, 70%).

HPLC – rt 5.32 min > 99% purity at 254 nm; LRMS $[\text{M}+\text{Na}]^+$ 363.0 m/z; HRMS $[\text{M}+\text{Na}]^+$ 363.0985 m/z, found 363.1002 m/z; ^1H NMR (400 MHz, CDCl_3) δ 6.77 (m, 3H), 5.14 (d, $J = 14.6$ Hz, 1H), 4.39 (dd, $J = 8.8, 5.1$ Hz, 1H), 3.84 (m, 7H), 3.47 (dd, $J = 11.3, 8.8$ Hz, 1H), 3.39 (s, 3H), 3.22 (s, 3H), 3.16 (dd, $J = 11.3, 5.1$ Hz, 1H); ^{13}C NMR (101 MHz, CDCl_3) δ 172.5, 171.3, 149.5, 149.0, 128.3, 121.4, 112.0, 111.1, 61.4, 57.7, 56.2, 56.1, 47.6, 32.7, 28.3.

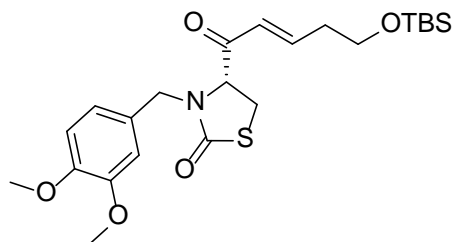
4-acryloyl-3-(3,4-dimethoxybenzyl)thiazolidin-2-one (5.047)



To 3-(3,4-dimethoxybenzyl)-N-methoxy-N-methyl-2-oxothiazolidine-4-carboxamide (1.26 g, 3.7 mmol) in THF (25 mL) at -30°C , 1.5 M vinylmagnesium bromide (13 mL) was added drop wise and stirred overnight. After completion of the reaction, 2 M aq. HCl solution was added and then extracted with DCM (x 3). The combined organic layer was washed with saturated sodium bicarbonate solution, dried with sodium sulphate and evaporated to dryness. Flash chromatography, eluting with a gradient from 20% to 50% EtOAc/petroleum spirits led to the isolation of the product (530 mg, 48%).

HPLC – rt 5.74 min > 99% purity at 254 nm; LRMS $[\text{M}+\text{Na}]^+$ 330.1 m/z; HRMS no mass ion was detected; ^1H NMR (400 MHz, CDCl_3) δ 6.82 – 6.65 (m, 3H), 6.47 (dd, $J = 17.4, 10.3$ Hz, 1H), 6.35 (dd, $J = 17.4, 1.3$ Hz, 1H), 5.90 (dd, $J = 10.3, 1.3$ Hz, 1H), 5.05 (d, $J = 14.6$ Hz, 1H), 4.34 (dd, $J = 9.4, 4.6$ Hz, 1H), 3.84 (m, 7H), 3.50 (dd, $J = 11.5, 9.4$ Hz, 1H), 3.13 (dd, $J = 11.5, 4.6$ Hz, 1H); ^{13}C NMR (101 MHz, CDCl_3) δ 195.3, 172.1, 149.5, 149.1, 131.8, 131.4, 127.8, 121.4, 111.8, 111.2, 63.7, 56.1, 56.1, 47.9, 27.9.

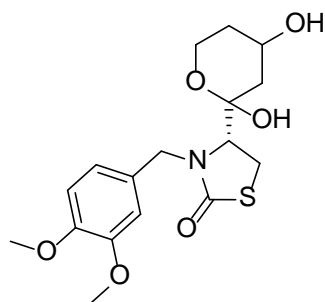
(*E*)-4-(5-((*tert*-butyldimethylsilyl)oxy)pent-2-enoyl)-3-(3,4-dimethoxybenzyl)thiazolidin-2-one (5.049)



To 4-acryloyl-3-(3,4-dimethoxybenzyl)thiazolidin-2-one (530 mg, 1.7 mmol) dissolved in DCE (9 mL) was added (but-3-en-1-yloxy)(*tert*-butyl)dimethylsilane (643 mg, 3.45 mmol) and catalytic Hoveyda-Grubbs' II catalyst (53 mg, 0.085 mmol). The reaction was then heated to 50°C for 12 h. Upon completion of the reaction, as indicated by TLC analysis, the reaction mixture was filtered through celite to remove the catalyst and then subjected to flash chromatography, eluting with 15% EtOAc/petroleum spirits to obtain the product (389 mg, 49%).

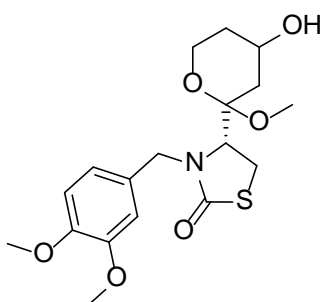
HPLC – rt 8.83 min > 95% purity at 254 nm; LRMS $[M+Na]^+$ 488.2 m/z; HRMS $[M+Na]^+$ 488.1897 m/z, found 488.1916 m/z; 1H NMR (400 MHz, $CDCl_3$) δ 7.03 (dt, $J = 15.7, 7.0$ Hz, 1H), 6.78 (d, $J = 8.1$ Hz, 1H), 6.76 – 6.66 (m, 2H), 6.27 (dt, $J = 15.7, 1.5$ Hz, 1H), 5.07 (d, $J = 14.7$ Hz, 1H), 4.27 (dd, $J = 9.3, 4.7$ Hz, 1H), 3.85 (d, $J = 5.7$ Hz, 6H), 3.80 (d, $J = 14.7$ Hz, 1H), 3.73 (t, $J = 6.1$ Hz, 2H), 3.47 (dd, $J = 11.4, 9.3$ Hz, 1H), 3.13 (dd, $J = 11.4, 4.7$ Hz, 1H), 2.43 (qd, $J = 6.2, 1.4$ Hz, 2H), 0.87 (s, 9H), 0.04 (d, $J = 0.5$ Hz, 6H); ^{13}C NMR (101 MHz, $CDCl_3$) δ 194.9, 172.2, 149.5, 149.1, 148.8, 128.0, 126.3, 121.3, 111.9, 111.2, 64.1, 61.3, 56.1, 56.1, 47.9, 36.4, 28.1, 26.0, -5.2.

4-(2,4-dihydroxytetrahydro-2H-pyran-2-yl)-3-(3,4-dimethoxybenzyl)thiazolidin-2-one (5.051)



Title compound was prepared from (*E*)-4-(5-((*tert*-butyldimethylsilyl)oxy)pent-2-enoyl)-3-(3,4-dimethoxybenzyl)thiazolidin-2-one (389 mg, 0.835 mmol) according to the General Procedure E. The crude was directly used for the next step of acetal formation.

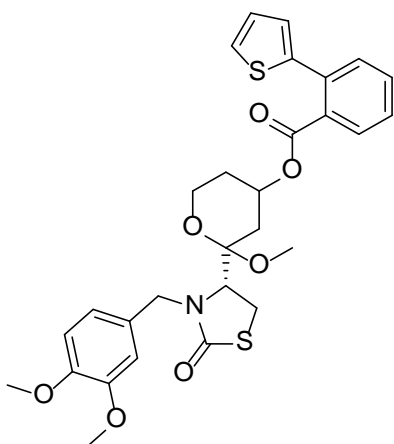
3-(3,4-dimethoxybenzyl)-4-(4-hydroxy-2-methoxytetrahydro-2H-pyran-2-yl)thiazolidin-2-one (5.038)



Title compound was prepared from 4-(2,4-dihydroxytetrahydro-2H-pyran-2-yl)-3-(3,4-dimethoxybenzyl)thiazolidin-2-one (531 mg, 1.44 mmol) and MeOH (15 mL) according to General Procedure F as a pale yellow oil and a mixture of two diastereomers; A and B in 1:0.7 ratios respectively over 2 steps (138 mg, 43%).

HPLC – rt 5.47 min > 90% purity at 254 nm; LRMS $[M+Na]^+$ 406.1 m/z; HRMS $[M+H]^+$ 384.1475 m/z, found 384.1489 m/z; 1H NMR (400 MHz, $CDCl_3$) δ 6.93 – 6.66 (m, 5.1H), 5.21 (d, J = 15.4 Hz, 0.7H), 5.03 (d, J = 14.3 Hz, 1H), 4.26 (d, J = 14.3 Hz, 1H), 4.19 (d, J = 15.4 Hz, 0.7H), 4.09 – 3.98 (m, 1.7H), 3.96 (dd, J = 7.3, 5.6 Hz, 0.7H), 3.93 – 3.83 (m, 11.9H), 3.83 – 3.74 (m, 1H), 3.62 (ddd, J = 13.4, 11.5, 2.3 Hz, 1H), 3.57 – 3.47 (m, 0.7H), 3.39 – 3.18 (m, 3.4H), 3.09 (s, 3H), 3.02 (s, 2.1H), 2.24 – 2.17 (m, 1H), 2.09 (m, 0.7H), 1.99 – 1.85 (m, 2.4H), 1.80 (d, J = 5.3 Hz, 1H), 1.66 (dd, J = 12.8, 10.9 Hz, 0.7H), 1.59 – 1.38 (m, 2.7H); ^{13}C NMR (101 MHz, $CDCl_3$) δ 149.4, 149.2, 148.7, 129.4, 129.2, 121.4, 119.6, 112.0, 112.0, 111.2, 111.1, 110.5, 103.2, 102.5, 64.5, 64.4, 60.5, 60.3, 59.2, 56.9, 56.0, 56.0, 56.0, 47.8, 47.8, 47.6, 47.1, 37.9, 37.3, 34.7, 34.5, 32.5, 31.6, 26.3, 25.4.

2-(3-(3,4-dimethoxybenzyl)-2-oxothiazolidin-4-yl)-2-methoxytetrahydro-2H-pyran-4-yl 2-(thiophen-2-yl)benzoate (5.055)

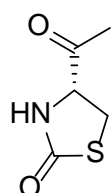


Title compound was prepared from 3-(3,4-dimethoxybenzyl)-4-(4-hydroxy-2-methoxytetrahydro-2H-pyran-2-yl)thiazolidin-2-one (138 mg, 0.36 mmol) and 2-(thiophen-2-yl)benzoic acid (221 mg, 1.08 mmol) according to the General procedure G as a mixture of two diastereomers; A and B in 1:1 ratio respectively (5.6 mg, 3%).

HPLC – rt (diastereomer A) 8.52 min (50%), (diastereomer B) 8.60 min (40%), collectively > 90% purity at 254 nm; LRMS $[M+Na]^+$ 592.1 m/z; HRMS $[M+Na]^+$ 592.1434 m/z, found 592.1442 m/z; 1H NMR (400 MHz, $CDCl_3$) δ 7.76 (ddd, J = 7.6, 4.0, 1.3 Hz, 2H), 7.54 – 7.31 (m, 8H), 7.11 – 7.02 (m, 2H), 6.98 (dd, J = 3.5, 1.1 Hz, 2H), 6.86 – 6.78 (m, 4H), 6.75 (dd, J = 4.2, 2.3 Hz, 2H), 5.29 – 5.12 (m, 3H), 5.03 (d, J = 14.3 Hz, 1H), 4.20 (d, J = 14.1 Hz, 1H), 4.17 (d, J = 15.1 Hz, 1H), 4.00 – 3.71 (m, 16H), 3.71 – 3.59 (m, 1H), 3.60 – 3.50 (m, 1H), 3.41 – 3.15 (m, 4H), 3.09 (s, 3H), 3.01 (s, 3H), 2.12 – 2.02 (m, 1H), 1.93 – 1.74 (m, 3H), 1.68 – 1.28 (m, 4H); ^{13}C NMR (101

MHz, CDCl₃) δ 168.2, 168.1, 149.4, 149.2, 148.7, 148.6, 142.2, 134.6, 134.5, 132.4, 132.2, 131.5, 131.2, 129.8, 129.7, 129.3, 129.2, 128.0, 127.4, 126.6, 126.0, 121.4, 119.6, 112.1, 111.3, 111.1, 110.6, 103.2, 102.4, 68.2, 60.0, 59.9, 59.2, 56.7, 56.1, 56.0, 47.8, 47.7, 47.6, 47.1, 33.5, 33.1, 30.8, 30.7, 26.1, 25.2.

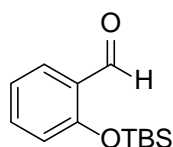
(R)-4-acetylthiazolidin-2-one [27]



To (R)-4-acetyl-3-(4-methoxybenzyl)thiazolidin-2-one (42.6 mg, 0.16 mmol) dissolved in 2:1 mixture of acetonitrile and water (0.33 mL), was added CAN (219 mg, 0.4 mmol) and stirred for 12 h. The reaction mixture was then extracted with DCM, dried using sodium sulphate and evaporated to dryness. Flash chromatography eluting with 50% ethyl acetate/petroleum spirits yielded the desired product as a yellow oil (5.3 mg, 23%).

¹H NMR (400 MHz, CDCl₃) δ 6.72 (s, 1H), 4.37 (ddd, J = 8.4, 6.2, 1.1 Hz, 1H), 3.70 (dd, J = 11.2, 8.5 Hz, 1H), 3.50 (dd, J = 11.2, 6.2 Hz, 1H), 2.29 (s, 3H).

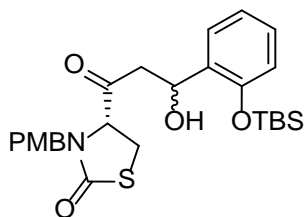
2-((tert-butyldimethylsilyl)oxy)benzaldehyde(5.060) [28]



Salicylaldehyde (146.5 mg, 1.2 mmol), triethylamine (0.2 mL, 1.44 mmol) and DMAP (2.4 mg, 0.02 mmol) were dissolved in DCM (9.6 mL) and the solution was cooled to 0°C. To this cooled solution TBSCl (217 mg, 1.44 mmol) in DCM (4.8 mL) was added dropwise and the reaction mixture was stirred for 4 h. The reaction was then quenched with saturated sodium bicarbonate solution and extracted with DCM (x 3). The combined organic layer was washed with brine and dried with magnesium sulphate and evaporated *in vacuo* to obtain the product (280 mg, 99%).

¹H NMR (400 MHz, CDCl₃) δ 10.47 (d, J = 0.8 Hz, 1H), 7.81 (dd, J = 7.8, 1.8 Hz, 1H), 7.46 (ddd, J = 8.3, 7.3, 1.9 Hz, 1H), 7.07 – 7.00 (m, 1H), 6.88 (dd, J = 8.3, 0.7 Hz, 1H), 1.02 (s, 9H), 0.28 (s, 6H).

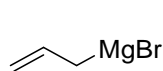
4-(3-(2-((*tert*-butyldimethylsilyl)oxy)phenyl)-3-hydroxypropanoyl)-3-(4-methoxybenzyl)thiazolidin-2-one (5.061)



Title compound was prepared from (*R*)-4-acetyl-3-(4-methoxybenzyl)thiazolidin-2-one (156 mg, 0.59 mmol) and 2-((*tert*-butyldimethylsilyl)oxy)benzaldehyde (132 mg, 0.5 mmol) according to General Procedure D as a yellow oil as a single diastereomer (34 mg, 13%).

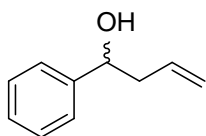
LRMS $[M+Na]^+$ 524.1 m/z; HRMS $[M+H]^+$ 524.1897 m/z, found 524.1896 m/z; 1H NMR (400 MHz, $CDCl_3$) δ 7.41 (dd, $J = 7.6, 1.7$ Hz, 1H), 7.16 (td, $J = 8.1, 1.7$ Hz, 1H), 7.12 – 7.05 (m, 2H), 6.98 (t, $J = 7.5$ Hz, 1H), 6.86 – 6.81 (m, 2H), 6.81 – 6.75 (m, 1H), 5.51 (dt, $J = 8.3, 4.0$ Hz, 1H), 5.06 (d, $J = 14.8$ Hz, 1H), 4.10 (dd, $J = 9.4, 3.7$ Hz, 1H), 3.86 – 3.72 (m, 4H), 3.43 (dd, $J = 11.5, 9.4$ Hz, 1H), 3.17 (dd, $J = 11.5, 3.6$ Hz, 1H), 2.99 (dd, $J = 11.6, 4.6$ Hz, 1H), 2.87 – 2.74 (m, 2H), 1.01 (s, 9H), 0.27 (d, $J = 11.8$ Hz, 6H); ^{13}C NMR (101 MHz, $CDCl_3$) δ 172.0, 159.5, 151.9, 133.0, 129.9, 128.6, 127.5, 126.5, 121.6, 118.3, 114.4, 114.4, 65.5, 65.3, 55.4, 47.3, 46.1, 27.1, 25.9, 18.3, -3.8, -4.2.

allylmagnesium bromide (5.064)



Magnesium (321 mg, 13.2 mmol) and catalytic iodine were added to diethyl ether (20 mL). The reaction mixture was warmed gently before adding allyl bromide (1.04 mL, 6.1 mmol) dropwise. The reaction turns exothermic and was cooled in an ice bath. After the addition of 1-bromopropane was complete, the reaction was stirred for 1 h to obtain the Grignard reagent.

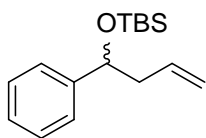
1-phenylbut-3-en-1-ol (5.065) [29]



To benzaldehyde (0.20 mL, 2 mmol) in THF (20 mL) at 0°C was added dropwise 0.6 M allylmagnesium bromide in diethyl ether (4 mmol). The reaction was allowed to slowly warm up to room temperature and left stirring for 8 h. Saturated ammonium chloride solution was used to quench the reaction, followed by extraction with diethyl ether (x 3). The organic layer was then washed with brine, dried with sodium sulphate and evaporated to dryness to obtain the product (290 mg, 99%).

1H NMR (400 MHz, $CDCl_3$) δ 7.39 – 7.33 (m, 4H), 7.32 – 7.26 (m, 1H), 5.89 – 5.74 (m, 1H), 5.21 – 5.12 (m, 2H), 4.74 (dd, $J = 7.6, 5.3$ Hz, 1H), 2.59 – 2.45 (m, 2H), 2.08 (s, 1H).

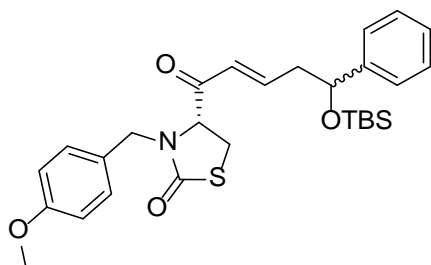
***tert*-butyldimethyl((1-phenylbut-3-en-1-yl)oxy)silane (5.066)** [30]



Title compound was prepared from 1-phenylbut-3-en-1-ol (368 mg, 2.48 mmol) according to the General Procedure B. Flash chromatography, eluting with 100% petroleum spirits afforded the product (500 mg, 76%).

^1H NMR (400 MHz, CDCl_3) δ 7.34 – 7.27 (m, 4H), 7.22 (m, 1H), 5.78 (m, 1H), 5.08 – 4.94 (m, 2H), 4.68 (dd, J = 7.3, 5.2 Hz, 1H), 2.54 – 2.31 (m, 2H), 0.88 (s, 9H), 0.03 (s, 3H), -0.13 (s, 3H).

(*E*)-4-(5-((*tert*-butyldimethylsilyl)oxy)-5-phenylpent-2-en-1-yl)-3-(4-methoxybenzyl)thiazolidin-2-one (5.067)

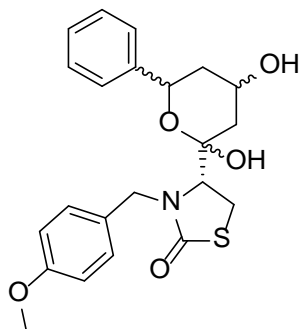


To 4-acryloyl-3-(4-methoxybenzyl)thiazolidin-2-one (743 mg, 3.8 mmol) dissolved in DCE (10 mL) was added *tert*-butyldimethyl((1-phenylbut-3-en-1-yl)oxy)silane (500 g, 1.9 mmol) and catalytic Hoveyda-Grubbs' II catalyst (60 mg, 0.095 mmol). The reaction was then heated to 50°C for 12 h. Upon completion of the reaction, as indicated by TLC

analysis, the reaction mixture was filtered through celite to remove the catalyst and then subjected to flash chromatography, eluting with 25% EtOAc/petroleum spirits to obtain the product as a mixture of two diastereomers; A and B in 1:1 ratio respectively (340 mg, 35%).

HPLC – rt 4.52 min > 96% purity at 254 nm; LRMS $[\text{M}+\text{Na}]^+$ 534.0 m/z; HRMS $[\text{M}+\text{Na}]^+$ 534.2105 m/z, found 534.2114 m/z; ^1H NMR (400 MHz, CDCl_3) δ 7.35 – 7.20 (m, 10H), 7.07 (m, 4H), 6.96 (m, 2H), 6.87 – 6.77 (m, 4H), 6.11 (m, 2H), 5.04 (m, 2H), 4.82 (m, 2H), 4.19 (m, 2H), 3.79 (s, 6H), 3.75 – 3.62 (m, 2H), 3.44 – 3.33 (m, 2H), 3.05 – 2.96 (m, 2H), 2.67 – 2.49 (m, 4H), 0.87 (d, J = 3.5 Hz, 18H), 0.01 (d, J = 7.0 Hz, 6H), -0.13 (d, J = 3.3 Hz, 6H); ^{13}C NMR (101 MHz, CDCl_3) δ 194.8, 194.7, 159.5, 147.8, 147.7, 144.0, 130.1, 128.4, 127.6, 127.6, 127.5, 127.5, 127.1, 127.0, 125.8, 125.8, 114.3, 73.8, 63.9, 63.8, 55.4, 47.3, 47.3, 44.3, 44.3, 31.1, 28.0, 28.0, 25.9, 25.9, -4.6, -4.9.

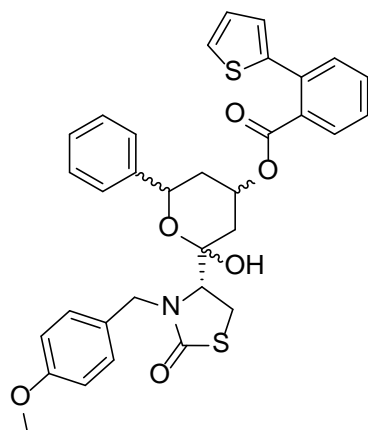
(4R)-4-((2S)-2,4-dihydroxy-6-phenyltetrahydro-2H-pyran-2-yl)-3-(4-methoxybenzyl)thiazolidin-2-one (5.068)



Title compound was prepared using (*E*)-4-(5-((*tert*-butyldimethylsilyl)oxy)-5-phenylpent-2-enoyl)-3-(4-methoxybenzyl)thiazolidin-2-one (340 mg, 0.66 mmol) according to the General Procedure E as a clear oil and a mixture of two diastereomers; A and B in 1:1 ratio respectively (75 mg, 26%).

HPLC – rt (diastereomer A) 6.36 min (46%), (diastereomer B) 6.27 min (38%), collectively > 84% purity at 254 nm; LRMS $[M+Na]^+$ 438.1 m/z; HRMS $[M+H]^+$ 416.1526 m/z, found 416.1532 m/z; 1H NMR (400 MHz, $CDCl_3$) δ 7.42 – 7.27 (m, 10H), 6.98 (dd, J = 8.5, 6.3 Hz, 4H), 6.80 – 6.75 (m, 2H), 6.74 – 6.67 (m, 2H), 5.13 (d, J = 14.5 Hz, 1H), 4.99 – 4.91 (m, 2H), 4.91 – 4.78 (m, 1H), 4.38 (d, J = 12.9 Hz, 1H), 4.34 (d, J = 12.8 Hz, 1H), 4.31 – 4.22 (m, 2H), 3.76 – 3.72 (m, 8H), 3.59 (dd, J = 9.4, 1.5 Hz, 1H), 3.41 (dd, J = 11.9, 1.6 Hz, 1H), 3.36 – 3.23 (m, 2H), 3.06 (dd, J = 40.2, 2.4 Hz, 2H), 2.38 – 2.12 (m, 4H), 1.68 – 1.59 (m, 4H), 1.32 – 0.80 (m, 2H); ^{13}C NMR (101 MHz, $CDCl_3$) δ 174.3, 173.2, 159.1, 159.0, 141.1, 140.8, 129.7, 129.5, 128.6, 128.5, 128.1, 128.0, 126.7, 126.3, 114.1, 114.0, 101.4, 100.4, 72.4, 71.8, 64.9, 64.8, 64.6, 64.1, 55.3, 55.3, 48.3, 47.6, 42.7, 41.9, 38.3, 37.1, 27.7, 26.9, 26.5, 22.6.

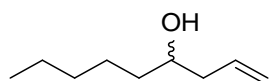
2-hydroxy-2-(3-(4-methoxybenzyl)-2-oxothiazolidin-4-yl)-6-phenyltetrahydro-2H-pyran-4-yl 2-(thiophen-2-yl)benzoate (5.074)



Title compound was prepared using (4R)-4-((2S)-2,4-dihydroxy-6-phenyltetrahydro-2H-pyran-2-yl)-3-(4-methoxybenzyl)thiazolidin-2-one (50 mg, 0.12 mmol) and 2-(thiophen-2-yl)benzoic acid (72 mg, 0.35 mmol) according to the General Procedure G as an off white solid (4.3 mg, 5%).

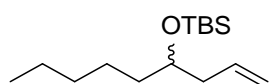
HPLC – rt 8.93 min > 65% purity at 254 nm; LRMS $[M-H]^+$ 600.1 m/z; HRMS $[M+H]^+$ 602.1666 m/z, found 602.1656 m/z; 1H NMR (400 MHz, $CDCl_3$) δ 7.76 (dd, J = 7.7, 0.9 Hz, 1H), 7.54 – 7.31 (m, 10H), 7.07 (dd, J = 5.1, 3.5 Hz, 1H), 7.01 – 6.93 (m, 3H), 6.72 (dd, J = 9.1, 2.4 Hz, 2H), 5.42 (m, 1H), 5.16 (d, J = 14.5 Hz, 1H), 5.01 (dd, J = 12.0, 1.9 Hz, 1H), 4.29 (d, J = 14.5 Hz, 1H), 3.74 (s, 3H), 3.54 (dd, J = 9.3, 1.8 Hz, 1H), 3.34 (m, 2H), 2.27 – 2.17 (m, 2H), 1.54 (m, 2H); ^{13}C NMR (101 MHz, $CDCl_3$) δ 172.8, 168.1, 159.3, 142.3, 140.4, 134.7, 132.2, 131.6, 131.3, 129.9, 129.8, 128.8, 128.6, 128.4, 128.1, 127.4, 126.8, 126.7, 126.1, 114.2, 101.6, 72.3, 68.5, 64.3, 55.4, 47.7, 37.8, 33.0, 26.8.

non-1-en-4-ol (5.070) [31]



To hexanal (0.25 mL, 2 mmol) in THF (20 mL) at 0°C was added dropwise 0.6 M allylmagnesium bromide in diethyl ether (7 mL, 4 mmol). The reaction was allowed to slowly warm to room temperature and left stirring for 8 h. Saturated ammonium chloride solution was used to quench the reaction, followed by extraction with diethyl ether (x 3). The organic layer was then washed with brine and dried with sodium sulphate and evaporated to dryness. Flash chromatography, eluting with 10% EtOAc/petroleum spirits afforded the product with minor impurities which was directly used for the next step of TBS-protection.

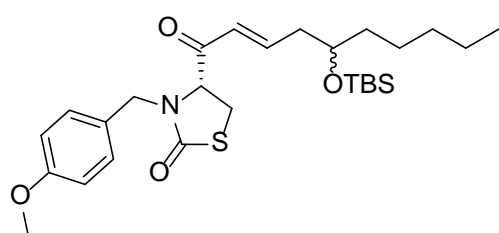
***tert*-butyldimethyl(non-1-en-4-yloxy)silane (5.071) [32]**



Title compound was prepared from non-1-en-4-ol (380 mg, 2.4 mmol) according to the General Procedure B. Flash chromatography, eluting with 100% petroleum spirits afforded the product (303 mg, 44%).

¹H NMR (400 MHz, CDCl₃) δ 5.81 (ddt, *J* = 17.6, 10.4, 7.2 Hz, 1H), 5.09 – 4.94 (m, 2H), 3.67 (q, *J* = 5.8 Hz, 1H), 2.28 – 2.13 (m, 2H), 1.51 – 1.13 (m, 9H), 0.88 (s, 11H), 0.04 (d, *J* = 0.8 Hz, 6H).

(*E*)-4-(5-((*tert*-butyldimethylsilyl)oxy)dec-2-enoyl)-3-(4-methoxybenzyl)thiazolidin-2-one (5.072)

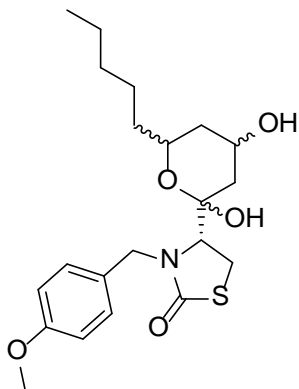


To 4-acryloyl-3-(4-methoxybenzyl)thiazolidin-2-one (484 mg, 2.13 mmol) dissolved in DCE (7 mL) was added *tert*-butyldimethyl(non-1-en-4-yloxy)silane (303.7 g, 1.18 mmol) and catalytic Hoveyda-Grubbs' II catalyst (37 mg, 0.06 mmol). The reaction was then heated to 50°C for 12 h. Upon completion of the reaction, as indicated by TLC analysis, the reaction mixture was filtered through celite to remove the catalyst and then subjected to flash chromatography, eluting with 15% EtOAc/petroleum spirits to obtain the product as a single diastereomer and a clear oil (139.5 mg, 23%).

HPLC – rt 5.95 min > 99% purity at 214 nm; LRMS no mass ion was detected; HRMS [M+H]⁺ 506.2755 m/z, found 506.2759 m/z; ¹H NMR (400 MHz, CDCl₃) δ 7.09 (dd, *J* = 14.4, 5.4 Hz, 2H), 7.04 (dtd, *J* = 9.7, 7.4, 2.3 Hz, 1H), 6.83 (dd, *J* = 8.7, 0.8 Hz, 2H), 6.23 (dd, *J* = 15.6, 1.4 Hz, 1H), 5.08 (d, *J* = 14.8 Hz, 1H), 4.26 (ddd, *J* = 9.3, 4.6, 1.8 Hz, 1H), 3.87 – 3.71 (m, 5H), 3.47 (ddd, *J* = 11.6, 9.3, 2.4 Hz, 1H), 3.11 (ddd, *J* = 11.4, 4.6, 0.8 Hz, 1H), 2.48 – 2.24 (m, 2H), 1.45 – 1.19 (m, 8H), 0.93 – 0.80 (m, 12H), 0.09 – -0.02 (m, 6H); ¹³C NMR (101 MHz, CDCl₃) δ 194.8, 172.1,

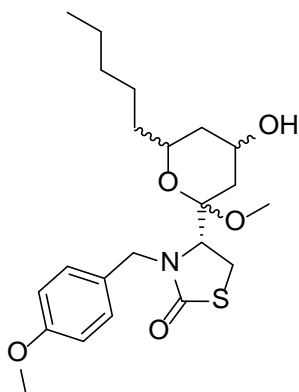
159.6, 149.0, 130.1, 127.5, 126.6, 114.4, 71.2, 63.9, 55.4, 47.4, 40.8, 37.5, 32.0, 28.1, 26.0, 25.1, 22.8, 18.2, 14.2, -4.3.

(4R)-4-(2,4-dihydroxy-6-pentyltetrahydro-2H-pyran-2-yl)-3-(4-methoxybenzyl)thiazolidin-2-one (5.073)



Title compound was prepared using (*E*)-4-(5-((*tert*-butyldimethylsilyl)oxy)dec-2-enoyl)-3-(4-methoxybenzyl)thiazolidin-2-one (139.5 mg, 0.35 mmol) according to the General Procedure E as a clear oil which was directly used for the next step of acetal formation.

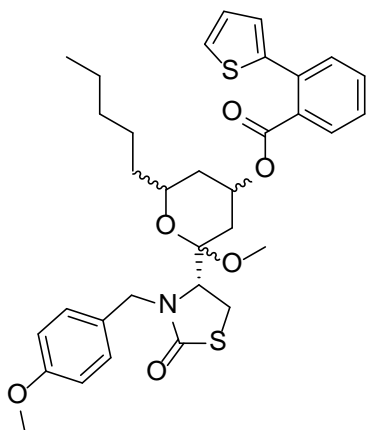
4-(4-hydroxy-2-methoxy-6-pentyltetrahydro-2H-pyran-2-yl)-3-(4-methoxybenzyl)thiazolidin-2-one (5.058)



Title compound was prepared using (4*R*)-4-(2,4-dihydroxy-6-pentyltetrahydro-2H-pyran-2-yl)-3-(4-methoxybenzyl)thiazolidin-2-one (108 mg, 0.26 mmol) and MeOH according to the General Procedure F as a clear oil as a mixture of two diastereomers; A and B in 1:0.8 ratio respectively (30.4 mg, 15% over 2 steps).

HPLC – rt 7.48 min > 53% purity at 254 nm; LRMS $[M+Na]^+$ 446.2 m/z; HRMS $[M+H]^+$ 424.2152 m/z, found 424.2157 m/z; 1H NMR (400 MHz, $CDCl_3$) δ 7.20 – 6.80 (m, 7.2H), 5.20 (d, J = 15.4 Hz, 0.8H), 5.10 (d, J = 14.4 Hz, 1H), 4.27 – 4.21 (m, 1H), 4.25 – 4.18 (m, 0.8H), 4.09 – 4.00 (m, 1.8H), 3.93 (dd, J = 8.5, 4.3 Hz, 0.8H), 3.87 – 3.81 (m, 1H), 3.78 (m, 5.4H), 3.62 – 3.46 (m, 1.8H), 3.40 – 3.13 (m, 3.6H), 3.06 (s, 3H), 3.00 (s, 2.4H), 2.46 – 2.37 (m, 1.8H), 2.32 (ddd, J = 14.8, 8.2, 7.0 Hz, 1H), 2.20 (ddd, J = 12.5, 4.7, 1.7 Hz, 0.8H), 2.13 – 2.05 (m, 1.8H), 2.03 – 0.8 (m, 23.4H); ^{13}C NMR (101 MHz, $CDCl_3$) δ 159.2, 159.1, 130.0, 128.9, 128.7, 128.6, 114.2, 114.1, 103.1, 102.5, 70.4, 70.2, 64.8, 58.9, 57.0, 55.4, 55.4, 53.6, 47.8, 47.6, 47.2, 46.8, 40.6, 40.2, 37.8, 37.1, 36.3, 35.7, 32.0, 32.0, 26.3, 25.6, 25.4, 25.1, 22.8, 22.7, 14.2, 14.1.

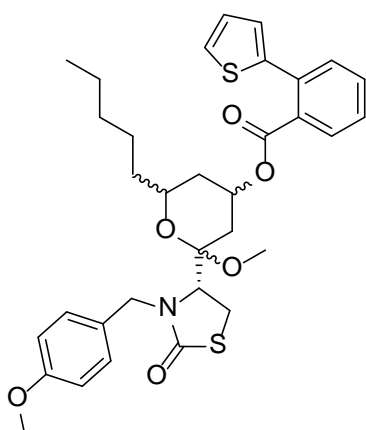
2-methoxy-2-(3-(4-methoxybenzyl)-2-oxothiazolidin-4-yl)-6-pentyltetrahydro-2H-pyran-4-yl 2-(thiophen-2-yl)benzoate (5.075a)



Title compound was prepared using 4-(4-hydroxy-2-methoxy-6-pentyltetrahydro-2H-pyran-2-yl)-3-(4-methoxybenzyl)thiazolidin-2-one (22 mg, 0.05 mmol) and 2-(thiophen-2-yl)benzoic acid (30 mg, 0.15 mmol) according to the General Procedure G (6.3 mg, 20%).

HPLC – rt 7.28 min > 74% purity at 254; LRMS no mass ion was detected; HRMS $[M+H]^+$ 610.2292 m/z, found 610.2284 m/z; 1H NMR (400 MHz, $CDCl_3$) δ 7.74 (dd, J = 7.6, 1.1 Hz, 1H), 7.52 – 7.36 (m, 4H), 7.14 (m, 2H), 7.07 (dd, J = 5.1, 3.5 Hz, 1H), 6.98 (dd, J = 3.5, 1.1 Hz, 1H), 6.91 – 6.83 (m, 2H), 5.28 – 5.12 (m, 2H), 4.19 (d, J = 15.5 Hz, 1H), 3.91 (dd, J = 9.6, 3.3 Hz, 1H), 3.80 (s, 3H), 3.53 (m, 1H), 3.38 – 3.21 (m, 2H), 2.98 (s, 3H), 1.97 – 1.88 (m, 1H), 1.87 – 1.77 (m, 1H), 1.52 – 1.15 (m, 10H), 0.86 (t, J = 6.8 Hz, 3H); ^{13}C NMR (101 MHz, $CDCl_3$) δ 173.2, 168.2, 159.2, 142.2, 134.5, 132.5, 131.4, 131.1, 129.6, 128.7, 128.6, 128.0, 127.4, 126.6, 126.2, 114.3, 102.4, 69.7, 68.6, 56.7, 55.4, 47.7, 46.7, 36.3, 35.5, 33.4, 31.9, 26.2, 25.0, 22.7, 14.1; $[\alpha]_D^{20}$ = -136.8° (c 0.38, MeOH).

2-methoxy-2-(3-(4-methoxybenzyl)-2-oxothiazolidin-4-yl)-6-pentyltetrahydro-2H-pyran-4-yl 2-(thiophen-2-yl)benzoate (5.075b)

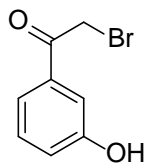


Title compound was prepared using 4-(4-hydroxy-2-methoxy-6-pentyltetrahydro-2H-pyran-2-yl)-3-(4-methoxybenzyl)thiazolidin-2-one (22 mg, 0.05 mmol) and 2-(thiophen-2-yl)benzoic acid (30 mg, 0.15 mmol) according to the General Procedure G (8.8 mg, 29%).

HPLC – rt 8.89 min > 84% purity at 254 nm; LRMS no mass ion was detected; HRMS $[M+H]^+$ 610.2292 m/z, found 610.2232 m/z; 1H NMR (400 MHz, $CDCl_3$) δ 7.76 (dd, J = 7.7, 0.9 Hz, 1H), 7.54 – 7.35 (m, 4H), 7.20 (m, 2H), 7.08 (dd, J = 5.1, 3.5 Hz, 1H), 6.98 (dd, J = 3.5, 1.2 Hz, 1H), 6.89 – 6.83 (m, 2H), 5.26 – 5.14 (m, 1H), 5.09 (d, J = 14.4 Hz, 1H), 4.18 (d, J = 14.4 Hz, 1H), 3.80 (s, 3H), 3.79 (m, 1H), 3.66 – 3.55 (m, 1H), 3.29 – 3.15 (m, 2H), 3.06 (s, 3H), 2.10 – 2.03 (m, 1H), 1.98 – 1.89 (m, 1H), 1.57 – 1.21 (m, 10H), 0.93 (t, J = 6.6 Hz, 3H); ^{13}C NMR (101 MHz, $CDCl_3$) δ 172.8, 168.1, 159.3, 142.2, 134.6, 132.3, 131.5, 131.2, 130.0, 129.8, 128.8, 128.0, 127.4, 126.6,

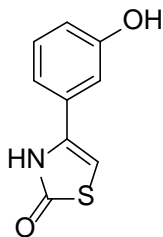
126.0, 114.1, 103.0, 70.0, 68.6, 58.9, 55.4, 47.6, 47.2, 36.4, 36.2, 32.9, 32.0, 25.5, 25.3, 22.8, 14.2;
[α]_D²⁰ = +47.2° (*c* 0.53, MeOH).

2-bromo-1-(3-hydroxyphenyl)ethan-1-one (5.078)



To 3-hydroxy acetophenone (100 mg, 0.73 mmol) in EtOAc (5 mL) was added copper bromide (195.7 mg, 0.88 mmol) and refluxed for 12 h. The reaction mixture was then cooled to room temperature and diluted with EtOAc and washed with brine. The organic layer was then dried with sodium sulphate and evaporated to dryness. Flash chromatography, eluting with 25% EtOAc/petroleum spirits gave a mixture of the product and the starting material in 1:0.5 ratio which was directly used for the next step.

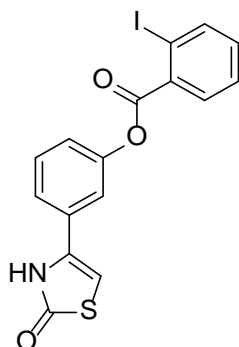
4-(3-hydroxyphenyl)thiazol-2(3H)-one (5.076)



To potassium thiocyanate (68 mg, 0.7 mmol) in acetone (7 mL), was added 2-bromo-1-(3-hydroxyphenyl)ethan-1-one (106.5 mg, 0.5 mmol) and stirred for 10 min. The solvent was then evaporated *in vacuo* and the residue extracted with EtOAc and brine. The organic layer was dried with sodium sulphate and evaporated to dryness. The crude thus obtained was dissolved in acetic acid (3.5 mL) and 50% aq. H₂SO₄ (0.7 mL). The resulting solution was heated to 100°C for 12 h. After cooling the solution to room temperature, EtOAc was added. The organic layer was then washed successively with saturated sodium bicarbonate solution, water and brine. The organic layer was dried with sodium sulphate before evaporating to dryness. Flash chromatography, eluting with 25% EtOAc/petroleum spirits gave the product as an off-white solid (28 mg, 29%).

HPLC – rt 4.5 min > 99% purity at 254 nm; LRMS [$M+H$]⁺ 194.0 m/z; HRMS [$M+H$]⁺ 194.027 m/z, found 194.0274 m/z; ¹H NMR (400 MHz, DMSO) δ 9.63 (s, 1H), 7.21 (t, *J* = 7.9 Hz, 1H), 7.05 (ddd, *J* = 7.7, 1.7, 0.9 Hz, 1H), 7.00 (t, *J* = 2.0 Hz, 1H), 6.77 (ddd, *J* = 8.1, 2.4, 0.9 Hz, 1H), 6.70 (s, 1H); ¹³C NMR (101 MHz, DMSO) δ 172.9, 157.7, 134.1, 131.0, 129.9, 115.8, 115.7, 111.8, 97.9.

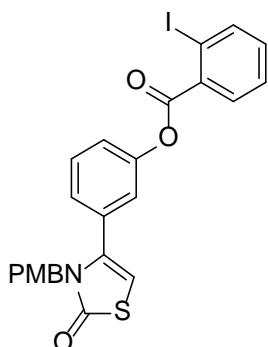
3-(2-oxo-2,3-dihydrothiazol-4-yl)phenyl 2-iodobenzoate (5.079)



Title compound was prepared from 4-(3-hydroxyphenyl)thiazol-2(3H)-one (27.9 mg, 0.144 mmol) according to the General Procedure G as a white solid (27.6 mg, 45%).

HPLC – rt 7.56 min > 99% purity at 254 nm; LRMS $[M+H]^+$ 423.9 m/z; HRMS $[M+H]^+$ 423.9499 m/z, found 423.9500 m/z; 1H NMR (400 MHz, DMSO) δ 8.12 (dd, J = 7.9, 0.9 Hz, 1H), 8.03 (dd, J = 7.8, 1.6 Hz, 1H), 7.68 – 7.60 (m, 3H), 7.55 (t, J = 8.0 Hz, 1H), 7.43 – 7.36 (m, 1H), 7.33 (ddd, J = 8.0, 2.2, 1.0 Hz, 1H), 6.95 (s, 1H); ^{13}C NMR (101 MHz, DMSO) δ 173.3, 165.4, 151.3, 141.5, 134.6, 134.3, 133.3, 131.7, 131.6, 130.7, 129.0, 123.2, 122.4, 118.7, 100.0, 95.6.

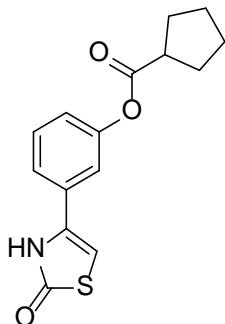
3-(3-(4-methoxybenzyl)-2-oxo-2,3-dihydrothiazol-4-yl)phenyl 2-iodobenzoate (5.080)



To a stirred suspension of 3-(2-oxo-2,3-dihydrothiazol-4-yl)phenyl 2-iodobenzoate (32 mg, 0.076 mmol), DMF (0.4 mL), potassium carbonate (18 mg, 0.13 mmol) and catalytic amount of sodium iodide (0.5 mg, 0.004 mmol), 3-methoxy benzylchloride (12 μ L, 0.1 mmol) was added dropwise. The reaction was stirred overnight at room temperature. After the completion of the reaction, diethyl ether was added and the suspension washed with brine (x 3). The organic layer was dried with magnesium sulphate, filtered and evaporated. Flash chromatography, eluting with 15% EtOAc/petroleum spirits yielded the product as a clear oil (34.5 mg, 83% yield).

HPLC – rt 8.9 min > 99% purity at 254 nm; LRMS $[M-H]^-$ 541.9 m/z; 1H NMR (400 MHz, $CDCl_3$) δ 8.07 (dd, J = 8.0, 1.0 Hz, 1H), 7.98 (dd, J = 7.8, 1.7 Hz, 1H), 7.48 (td, J = 7.6, 1.2 Hz, 1H), 7.42 (t, J = 7.9 Hz, 1H), 7.34 – 7.28 (m, 1H), 7.28 – 7.20 (m, 1H), 7.13 – 7.01 (m, 2H), 6.97 – 6.82 (m, 2H), 6.80 – 6.66 (m, 2H), 6.07 (s, 1H), 4.85 (s, 2H), 3.71 (s, 3H).

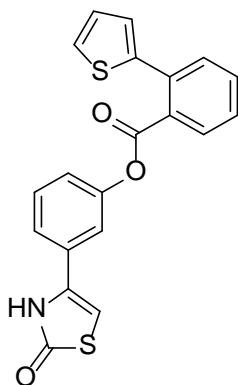
3-(2-oxo-2,3-dihydrothiazol-4-yl)phenyl cyclopentanecarboxylate (5.081)



Title compound was prepared from 4-(3-hydroxyphenyl)thiazol-2(3H)-one (20 mg, 0.104 mmol) and cyclopentane carboxylic acid (34 μ L, 0.31 mmol) according to the General procedure G as a pale yellow solid (75%).

HPLC – rt 7.21 min > 99% purity at 254 nm; LRMS $[M-H]^-$ 288.1 m/z; HRMS $[M+H]^+$ 290.0845 m/z, found 290.0842 m/z; 1H NMR (400 MHz, $CDCl_3$) δ 11.18 (s, 1H), 7.49 – 7.37 (m, 2H), 7.29 (d, J = 1.8 Hz, 1H), 7.07 (dt, J = 7.3, 2.0 Hz, 1H), 6.33 (s, 1H), 3.09 – 2.93 (m, 1H), 2.12 – 1.91 (m, 4H), 1.88 – 1.73 (m, 2H), 1.74 – 1.60 (m, 2H); ^{13}C NMR (101 MHz, $CDCl_3$) δ 176.0, 175.4, 151.6, 133.9, 131.0, 130.3, 122.2, 122.1, 118.4, 99.0, 43.9, 30.2, 26.0.

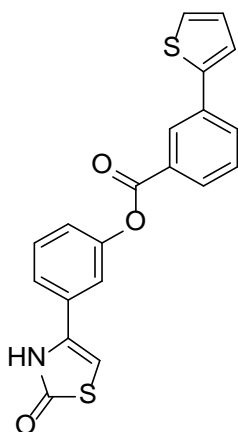
3-(2-oxo-2,3-dihydrothiazol-4-yl)phenyl 2-(thiophen-2-yl)benzoate (5.083)



Title compound was prepared from 4-(3-hydroxyphenyl)thiazol-2(3H)-one (20 mg, 0.08 mmol) and 2-(thiophen-2-yl)benzoic acid (50 mg, 0.24 mmol) according to the General procedure G (29.8 mg, 98%).

HPLC – rt 7.78 min > 99% purity at 254 nm; LRMS $[M+H]^+$ 378.10 m/z; HRMS $[M+H]^+$ 380.041 m/z, found 380.0417 m/z; 1H NMR (400 MHz, $CDCl_3$) δ 9.36 (s, 1H), 7.94 (dd, J = 7.7, 0.9 Hz, 1H), 7.65 – 7.46 (m, 3H), 7.46 – 7.38 (m, 2H), 7.31 (m, 1H), 7.12 (m, 2H), 7.00 (m, 2H), 6.28 (d, J = 1.9 Hz, 1H); ^{13}C NMR (101 MHz, $CDCl_3$) δ 175.6, 167.0, 151.4, 142.0, 134.9, 133.7, 131.9, 131.7, 131.1, 130.9, 130.4, 130.2, 128.2, 127.6, 127.0, 126.3, 122.4, 122.1, 118.1, 99.1.

3-(2-oxo-2,3-dihydrothiazol-4-yl)phenyl 3-(thiophen-2-yl)benzoate (5.084)

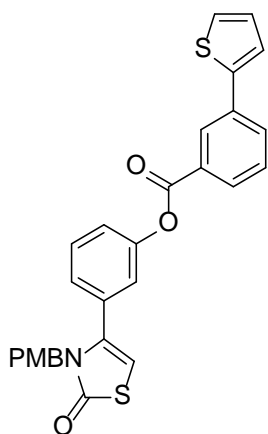


Title compound was prepared from 4-(3-hydroxyphenyl)thiazol-2(3H)-one (50 mg, 0.26 mmol) and 3-(thiophen-2-yl)benzoic acid (100 mg, 0.77 mmol) according to the General procedure G (70.8 mg, 72%).

HPLC – rt 8.16 min > 99% purity at 254 nm; LRMS $[M+H]^+$ 380.0 m/z; HRMS $[M+H]^+$ 380.041 m/z, found 380.0422 m/z; 1H NMR (400 MHz, $CDCl_3$) δ 10.02 (s, 1H), 8.43 (m, 1H), 8.15 – 8.07 (m, 1H), 7.88 (ddd, J = 7.8, 1.9, 1.1 Hz, 1H), 7.59 – 7.49 (m, 2H), 7.47 – 7.39 (m, 3H), 7.35 (dd, J = 5.1, 1.1 Hz, 1H), 7.30 – 7.24 (m, 1H), 7.13 (dd, J = 5.1, 3.6 Hz, 1H), 6.35 (d, J = 1.9 Hz, 1H); ^{13}C NMR (101 MHz, $CDCl_3$) δ 184.7, 176.2, 151.8,

151.7, 135.3, 133.2, 131.3, 131.2, 130.7, 130.0, 129.5, 129.1, 128.4, 127.6, 125.9, 124.2, 122.5, 122.5, 118.6, 99.4.

3-(3-(4-methoxybenzyl)-2-oxo-2,3-dihydrothiazol-4-yl)phenyl 3-(thiophen-2-yl)benzoate (5.085)



To a stirred suspension of 3-(2-oxo-2,3-dihydrothiazol-4-yl)phenyl 3-(thiophen-2-yl)benzoate (50 mg, 0.13 mmol), DMF (3 mL), potassium carbonate (30.5 mg, 0.22 mmol) and catalytic amount of sodium iodide (0.9 mg, 0.0065 mmol), 3-methoxy benzylchloride (21 μ L, 0.17 mmol) was added drop-wise and the reaction stirred for 12 h. After the completion of the reaction, diethyl ether was added and the suspension washed with brine (x 3). The organic layer was dried with magnesium sulphate, filtered and evaporated. Flash chromatography, eluting with 1% EtOAc/cyclohexane yielded the product as a clear oil (75 mg, 70%).

HPLC – rt 9.41 min > 99% purity at 254 nm; LRMS $[M+H]^+$ 500.1 m/z; HRMS $[M+H]^+$ 500.0985 m/z, found 500.0995 m/z; ^1H NMR (400 MHz, CDCl_3) δ 8.41 (t, J = 1.6 Hz, 1H), 8.11 – 8.05 (m, 1H), 7.89 (ddd, J = 7.8, 1.9, 1.1 Hz, 1H), 7.58 – 7.50 (m, 1H), 7.43 (ddd, J = 8.0, 6.2, 2.9 Hz, 2H), 7.35 (dd, J = 5.1, 1.1 Hz, 1H), 7.33 – 7.27 (m, 1H), 7.13 (dd, J = 5.1, 3.6 Hz, 1H), 7.07 (m, 2H), 6.96 – 6.89 (m, 2H), 6.76 – 6.70 (m, 2H), 6.07 (s, 1H), 4.88 (s, 2H), 3.69 (s, 3H); ^{13}C NMR (101 MHz, CDCl_3) δ 172.9, 164.8, 159.1, 150.9, 142.9, 136.8, 135.2, 133.0, 131.2, 129.9, 129.9, 129.4, 129.0, 128.7, 128.7, 128.4, 127.5, 126.8, 125.9, 124.2, 122.9, 122.9, 114.0, 99.7, 55.2, 47.0.

7.6 References

1. Buffet, M.F., et al., Anomeric oxygen to carbon rearrangements of alkynyl tributylstannane derivatives of furanyl (γ)- and pyranyl (δ)-lactols. *Org Biomol Chem*, 2004; 2:1145-1154.
2. Gu, H., Xu, W.M. and Kinstle, T.H., Efficient synthesis of 8,11-dimethylene-bicyclo[5.3.1]undecan-2-one. *Tetrahedron Lett.*, 2005; 46: 6449-6451.
3. Robinson, J.A., et al., Synthesis, characterization, and stereochemistry of bridged intramolecularly alkylated cobaloximes; monomeric and dimeric complexes of different configuration. *Liebigs Ann. Chem.*, 1983; 2: 181-203.
4. Fuerstner, A., et al., Latrunculin analogues with improved biological profiles by "diverted total synthesis": Preparation, evaluation, and computational analysis. *Chem-Eur J*, 2007; 13: 135-149.
5. Fuerstner, A., et al., Total syntheses of the actin-binding macrolides latrunculin A, B, C, M, S and 16-epi-latrunculin B. *Chem-Eur J*, 2007; 13: 115-134.
6. Flahaut, J. and Miginiac, P., Synthèse d'alcools acétyléniques par alkylation d'hydroxy- ω -alkynes-1. *Helvetica Chimica Acta*, 1978; 61: 2275-2285.
7. Fürstner, A., et al., Diverted total synthesis: Preparation of a focused library of latrunculin analogues and evaluation of their actin-binding properties. *P Natl Acad Sci USA*, 2005; 102: 8103-8108.
8. Albrecht, S., Defoin, A. and Tarnus, C., Simple preparation of O-substituted hydroxylamines from alcohols. *Synthesis*, 2006; 10: 1635-1638.
9. Magens, S. and Plietker, B., Nucleophilic Iron Catalysis in Transesterifications: Scope and Limitations. *J. Org. Chem.*, 2010; 75: 3715-3721.
10. Kazemi, F., Massah, A.R. and Javaherian, M., Chemoselective and scalable preparation of alkyl tosylates under solvent-free conditions. *Tetrahedron*, 2007; 63: 5083-5087.
11. Kim, C.H., et al., Site-Specific Incorporation of ϵ -N-Crotonyllysine into Histones. *Angew. Chem., Int. Ed.*, 2012; 51: 7246-7249.
12. Shabtai, J., Ney-Igner, E. and Pines, H., Base-catalyzed reactions of α,β -unsaturated esters and nitriles. 4. Dimerization of β -alkyl-substituted acrylates. *J. Org. Chem.*, 1981; 46: 3795-802.
13. Song, D., Blond, G. and Furstner, A., Study towards bioactive pyrone derivatives from the marine red alga *Phacelocarpus labillardieri*. *Tetrahedron*, 2003; 59: 6899-6904.
14. Zhdankin, V.V., et al., Esters of 2-Iodoxybenzoic Acid: Hypervalent Iodine Oxidizing Reagents with a Pseudobenziodoxole Structure. *J. Org. Chem.*, 2005; 70: 6484-6491.
15. Han, C. and Buchwald, S.L., Negishi Coupling of Secondary Alkylzinc Halides with Aryl Bromides and Chlorides. *J. Am. Chem. Soc.*, 2009; 131: 7532-7533.
16. Ali, S.M. and Tanimoto, S., Reaction of O-silylated enolates of carboxylic esters with benzyne. A convenient route to ortho-alkylbenzoic acids. *J. Chem. Soc., Chem. Commun.*, 1988; 22: 1465-6.
17. Conway, J.C., et al., Palladium mediated spiroketal synthesis: application to pheromone synthesis. *Tetrahedron*, 2005; 61: 11910-11923.
18. Williams, B.D. and Smith, A.B., Total Synthesis of (+)-18-epi-Latrunculol A. *Org Lett*, 2013; 15: 4584-4587.
19. Ghosh, A.K. and Li, J., An Asymmetric Total Synthesis of Brevisamide. *Org. Lett.*, 2009; 11: 4164-4167.
20. Pouchain, L., et al., Quaterthiophenes with Terminal Indeno[1,2-b]thiophene Units as p-Type Organic Semiconductors. *J Org Chem*, 2009; 74: 1054-1064.
21. Desmarests, C., et al., Naphthidine di(radical cation)s-stabilized palladium nanoparticles for efficient catalytic Suzuki-Miyaura cross-coupling reactions. *Tetrahedron*, 2008; 64: 372-381.
22. Mousseau, J.J., et al., Umpolung Direct Arylation Reactions: Facile Process Requiring Only Catalytic Palladium and Substoichiometric Amount of Silver Salts. *J. Am. Chem. Soc.*, 2010; 132: 14412-14414.

23. Pavlyuk, O., Teller, H. and McMills, M.C., An efficient synthesis of nitrogen-containing heterocycles via a tandem carbenoid N-H insertion/ring-closing metathesis sequence. *Tetrahedron Lett.*, 2009; 50: 2716-2718.
24. Dieter, R.K., Gore, V.K. and Chen, N., Regio- and Enantioselective Control in the Reactions of α -(N-Carbamoyl)alkylcuprates with Allylic Phosphates. *Org. Lett.*, 2004; 6: 763-766.
25. Pena-Lopez, M., et al., A Versatile Enantioselective Synthesis of Barrenazines. *Org. Lett.*, 2010; 12: 852-854.
26. Seki, M., et al., A practical synthesis of (+)-biotin from L-cysteine. *Chem-Eur J*, 2004; 10: 6102-6110.
27. White, J.D. and Kawasaki, M., Total synthesis of (+)-latrunculin A. *J Am Chem Soc*, 1990; 112: 4991-3.
28. Goujon, J.-Y., et al., A new approach to 2,2-disubstituted chromenes and tetrahydroquinolines through intramolecular cyclization of chiral 3,4-epoxy alcohols. *Tetrahedron*, 2004; 60: 4037-4049.
29. Lee, C.-H.A. and Loh, T.-P., A highly enantioselective allyl-transfer through suppression of epimerization. *Tetrahedron Lett.*, 2004; 45: 5819-5822.
30. Hiebel, M.-A., Pelotier, B. and Piva, O., Total synthesis of (+/-)-diospongin A via Prins reaction. *Tetrahedron*, 2007; 63: 7874-7878.
31. Schmidt, B., Ruthenium-Catalyzed Olefin Metathesis Double-Bond Isomerization Sequence. *J Org Chem*, 2004; 69: 7672-7687.
32. Harbindu, A. and Kumar, P., Organocatalytic enantioselective approach to the synthesis of verbalactone and (*R*)-massoialactone. *Synthesis*, 2011; 12: 1954-1959.